NOTICE

AVIS

Canada

THE UNIVERSITY OF ALBERTA

AN ELECTROCHEMICAL MODEL FOR REDOX CYCLING

by

JAMES E. NOLAN

A THESIS

SUBMITTED TO THE FACULTY OF GRADUATE STUDIES AND RESEARCH

IN PARTIAL FULFILMENT OF THE REQUIREMENTS FOR THE DEGREE

OF DOCTOR OF PHILOSOPHY

DEPARTMENT OF CHEMISTRY

EDMONTON, ALBERTA

FALL 1988

THE UNIVERSITY OF ALBERTA

RELEASE FORM

NAME OF AUTHOR: JAMES E. NOLAN

TITLE OF THESIS: AN ELECTROCHEMICAL MODEL FOR REDOX CYCLING

DEGREE FOR WHICH THESIS WAS PRESENTED: PH.D.

YEAR THIS DEGREE GRANTED: 1988

    Permission is hereby granted to THE UNIVERSITY OF

ALBERTA LIBRARY to reproduce single copies of this

thesis and to lend or sell such copies for private,

scholarly or scientific research purposes only.

    The author reserves other publication rights, and

neither the thesis nor extensive extracts from it may

be printed or otherwise reproduced without the author's

written permission.

                        James E. Nolan

                        (Signed)

                        PERMANENT ADDRESS:

                        51 Glenhaven Crescent
                        St. Albert, Alberta
                        T8N 1A4
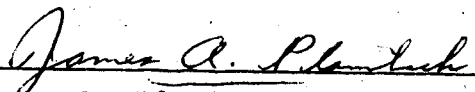
DATED   _September 22, 1988_

THE UNIVERSITY OF ALBERTA

FACULTY OF GRADUATE STUDIES AND RESEARCH

The undersigned certify that they have read, and recommend to the Faculty of Graduate Studies and Research, for acceptance, a thesis entitled AN ELECTROCHEMICAL MODEL FOR REDOX CYCLING.

submitted by JAMES E. NOLAN
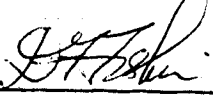
in partial fulfilment of the requirements for the degree of

DOCTOR OF PHILOSOPHY.
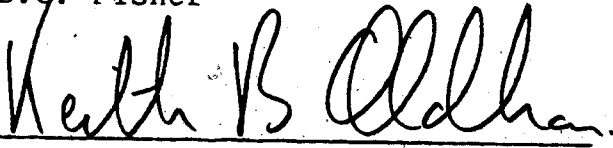
_____
James A. Plambeck, Supervisor

_____
D.J. Harrison

_____
L. Hepler

_____
J.W. Lown

_____
D.G. Fisher

_____
K.B. Oldham, External Examiner

DATE September 16, 1988

TO

S.A.M.

ABSTRACT

Redox cycling is a term used in biochemical pharmacology to denote a certain class of electron-transfer reactions involving NAD(P)H and dioxygen. These reactions are thought to be responsible for the toxic effects of a variety of chemicals and drugs including bipyridinium herbicides and anthracycline antitumor antibiotics. Such compounds function as catalysts of the electron-transfer reactions. The EC-catalytic mechanism provides an electrochemical model for redox cycling, and thus the means to measure the rate of reaction of reduced catalysts with dioxygen. In this work, rate constants for the reaction of electrogenerated bipyridinium cation radicals with dioxygen in acetonitrile and dimethyl-sulfoxide were determined via the second-order EC-catalytic mechanism at the rotating disk electrode (RDE). To evaluate the rate constants, it was necessary to solve the differential equations describing the mechanism. This was done numerically using a polynomial approximation technique. Rate constants for the reaction of dioxygen and cation radicals derived from eighteen doubly quaternized derivatives of 2,2'- and 4,4'-bipyridine and 1,10-phenanthroline were measured. The results obtained ranged from 5.1×10^3 $M^{-1}s^{-1}$ to 2.0×10^8 $M^{-1}s^{-1}$ with an estimated accuracy on the order of

±10%. From the dependence of the rate constants on catalyst half-wave potentials, a value was obtained for the rate constant of the equilibrium exchange reaction between bipyridinium cation radicals and dioxygen in acetonitrile. Rate constants for a number of the cation ███████s showed a strong, negative correlation with published data o██████████cidal activities of the corresponding bipyridinium dications.

The diffusion coefficients of the bipyridinium cation radicals were calculated from mass-transport-limited currents for the two-electron reduction of the dications at the RDE. These calculations required numerical solution of the differential equations describing consecutive electron transfer accompanied by a rapid, irreversible reproportionation reaction. The numerical results were used to derive a modified form of the Levich equation suitable for calculating the diffusion coefficients of the cation radicals. The values obtained were between 30 and 50% larger than those of the corresponding dications. Taking these differences into account increased the estimates of the rate constants for the reaction of the cation radicals and dioxygen by an average of 35%.

ACKNOWLEDGEMENTS

I wish to thank the staff and faculty of the
Chemistry Department for their assistance and support at
various stages of this project. Valuable contributions to
the experimental work were made by the personnel of the
glass shop, the electronics shop, the machine shop, and
the microanalytical laboratory. Thanks are also due Dr.
Pawel Kolodziejczyk for helpful discussions concerning
some of the syntheses. I am especially grateful to Miss
Annabelle Wiseman for agreeing to type the manuscript and
for doing so in an expert fashion. Finally I wish to
thank my thesis supervisor Professor James A. Plambeck for
his patience, advice and encouragement. I sincerely
appreciate the opportunity to follow my own lights, to
make my own mistakes, and so to discover my own
capabilities and limitations.

TABLE OF CONTENTS

*****

LIST OF TABLES

LIST OF FIGURES

CHAPTER I

INTRODUCTION

A. Brief Overview of Redox Cycling

Redox cycling is a term used in biochemical pharmacology and toxicology to denote certain catalyzed electron-transfer reactions that are thought to be responsible for the cytotoxic effects of a number of classes of chemical compounds (1-3). These compounds, or metabolites of these compounds serve as catalysts of electron transfer from cellular reductants such as NADH to dioxygen. The reaction sequence is outlined in Figure 1. As the toxin shuttles electrons from the donor to the acceptor, it is alternately oxidized and reduced, hence the term "redox cycling" (1-3,6-8).

Redox cycling accounts for chemical toxicity at the cellular level in one or more of the following ways (1,3): (1) The unregulated, toxin-mediated reaction of NADH and O_2 may disrupt cellular metabolism by depleting these vital reactants. (2) In a related effect, redox cycling may serve as a serious energy drain. Under normal circumstances, the regulated, cytochrome-mediated reaction of NADH and O_2 yields useful energy in the form of ATP

1

NAD

Donor   e⁻   Red

NADH   Mediator

Ox

O₂

e⁻   Acceptor

O₂⁻˙

Further Reactions of $O_2^{-\bullet}$:

$$O_2^{-\bullet} + H^+ \longrightarrow HO_2^{\bullet}$$

$$O_2^{-\bullet} + HO_2^{\bullet} + H^+ \longrightarrow H_2O_2$$

$$Fe^{2+} + H_2O_2 \longrightarrow Fe^{3+} + OH^- + OH^{\bullet}$$
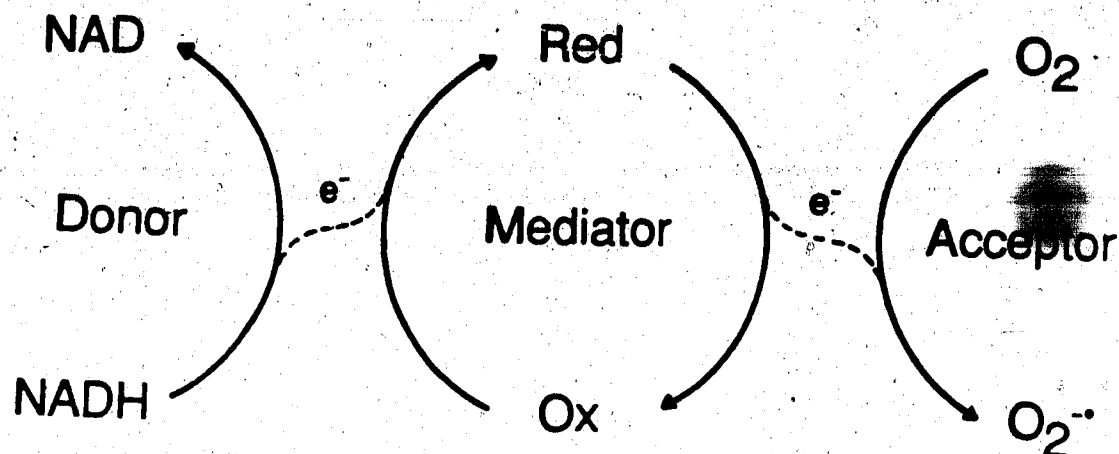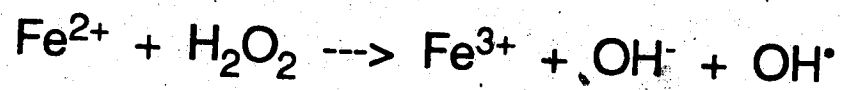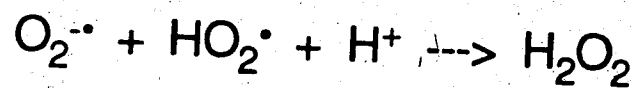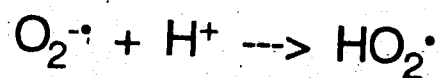
Figure 1.   The Redox Cycling Mechanism and Further Reactions
            of the Superoxide Ion O_2^-.

(3). This energy is denied the cell when electrons are transferred _via_ the toxin-mediated reaction. Finally, reactive oxygen species derived from the superoxide anion radicals produced by redox cycling may damage key cellular components. These species include the perhydroxyl radical $HO_2^\bullet$, the hydroxyl radical $OH^\bullet$ and hydrogen peroxide. The reactions by which these species arise are shown in Figure 1; they are treated in more detail at the end of this chapter.

Examples of cases where the toxic effects of chemical compounds are thought to involve redox cycling include:

1. The mutagenic and possibly carcinogenic effects of quinones and quinone metabolites (5-7).

2. The cytotoxicity, and possibly the antitumor activity, of quinone-containing antitumor agents (6-8).

3. The herbicidal activity of bipyridinium salts such as paraquat and diquat (9).

4. The antimicrobial activity of certain nitro compounds such as metronidazole (3).

5. The hepatotoxicity associated with overdoses of the analgesic acetaminophen (1).

6. The antimalarial activity of drugs such as chloroquine and primaquine (10).

This work is concerned primarily with redox cycles involving mediators of the first three types. Examples of

such mediators may be found in Table 1 and some of the corresponding structures are shown in Figure 2.

B. <u>Redox Cycling and the Cardiotoxicity of Anthracycline Antitumor Antibiotics</u>

One group of compounds which is of particular interest in the context of the present work is the anthracyclines, a class of antitumor antibiotics which include the clinically useful antileukemics adriamycin (doxorubicin) and daunorubicin (7,8). The antitumor activity of these drugs is accompanied by a cardiotoxic side-effect which limits the dosage that can be administered and which thus lowers the therapeutic efficacy of the drugs. The cardiotoxicity is thought to be a consequence of redox cycling (1-3,7,8).

Over the past decade, much work has gone into the preparation and testing of synthetic analogs of the anthracyclines in an effort to obtain a drug which exhibits lessened cardiotoxicity while at the same time possessing equal, or even enhanced, antitumor activity (4,8). A part of this effort has involved the development of chemical and biochemical assays as useful indicators of biological activity. For example, <u>in vitro</u> assays for the production of superoxide ion and hydroxyl radical by

Table 1. Possible Effects of Redox Cycling for Selected Mediators.

Mediator	Biological Activity	Effects of Redox Cycling	References
Adriamycin	Antitumor agent	Cardiotoxicity Mutagenicity	8
Mitomycin C	Antitumor agent	Mutagenicity	8
Benzo[a]pyrene-3,6-dione	-	Mutagenicity Carcinogenicity	5
Menadione (2-Methyl-1,4-naphtho-quinone)	Vitamin K_3	Toxicity Mutagenicity	6,7
Acetaminophen	Analgesic	Hepatotoxicity	1,6
Hydroxynaphtho- and hydroxyanthraquinones	-	Toxicity Mutagenicity	7
Paraquat Diquat	Herbicides	Phytotoxicity	10
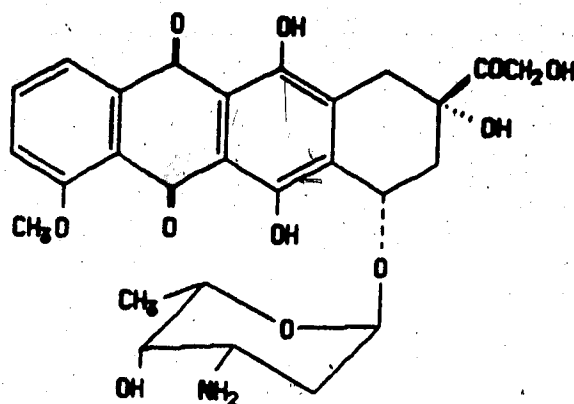
Adriamycin
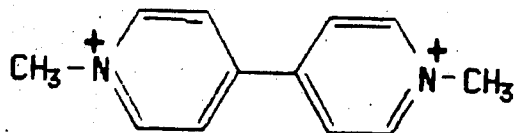
Paraquat
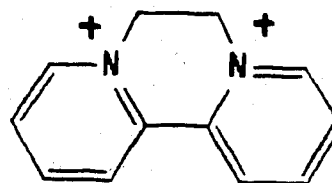
Diquat

Figure 2. Structures of Some Redox Cycling Mediators.

chemically reduced anthracyclines in the presence of
dioxygen have been developed and applied (4,8,11,12). The
results of these assays have been shown to correlate with
various biological properties including cardiotoxicity in
animal models (8,12). In addition to providing a valuable
means of pre-screening potential drug compounds prior to
more elaborate biological studies, these assays are of
some utility in elucidating relationships between
molecular structure and biological activity (4,8,12).

The results of electrochemical studies of anthra-
cyclines have also been found to be of value in predicting
their biological properties (11-14). In particular, the
half-wave potentials of a series of anthracyclines were
measured by d.c. polarography or cyclic voltammetry
(11,12). The results were found to show a significant
correlation with other indicators of biological activity
such as the previously mentioned assays for superoxide ion
and hydroxyl radical production (12).

A chemical property of anthracyclines which has
received very limited attention and yet may be an
important determinant of their biological activity is the
reactivity of anthracycline semiquinones toward
dioxygen. In aqueous solution such reactions are fast and
kinetic studies confined to the technique of pulse
radiolysis (15-17). Thus far, results have been obtained

only for the reaction of adriamycin semiquinone with dioxygen; these are summarized in Table 2. The corresponding reaction of daunorubicin has been studied in DMF by a combination of spectrochemical and electro-chemical techniques (18) but no quantitative rate information was obtained.

To date, there has been no systematic study of the kinetics of the oxidation of anthracycline semiquinones by dioxygen and thus no opportunity to relate the rates of such reactions to indicators of biological activity. Attempts have been made to correlate electrochemical reoxidizability with these indicators(11,12). Electro-chemical reoxidizability was defined as the ratio of anodic to cathodic peak currents as measured by cyclic voltammetry. The work was predicated on the assumption that electrochemical reoxidizability of a semiquinone parallels the reactivity of that semiquinone toward dioxygen. Although electrochemical reoxidizability showed a wide variation amongst the anthracyclines studied, no significant correlations were found to exist between this parameter and indicators of biological activity (12). This finding called into question the assumption that electrochemical reoxidizability parallels chemical reactivity and thus prompted the present work. In this work electrochemical techniques are developed to measure

Table 2. Rate Constants for the Reaction of Some Redox Cycling Mediators with Dioxygen.

Mediator	$k/M^{-1}s^{-1}$	Conditions[a]	Technique[b]	Ref.
(Adriamycin)$^{\bar{\cdot}}$	4.4×10^7	pH 7.0	A	15
	$(3.0\pm0.2) \times 10^8$	pH 7.0	A	16
	$(3.5\pm0.4) \times 10^8$	pH 6.0	A	17
	$(1.7\pm0.2) \times 10^8$	pH 11.5	A	17
(Paraquat)$^{+}$	7.9×10^4	MeOH, -80°C	B	25
	2.2×10^5	MeOH, -50°C	B	25
	3.3×10^6	MeOH	A	27
	1.3×10^6	EtOH, 5% H_2O	A	27
	8.7×10^5	i-PrOH, 5% H_2O	A	27
	3.0×10^6	n-PrOH, 5% H_2O	A	27
	$(2.3\pm0.3) \times 10^5$	DMSO, 1 M HOAc	C	30
	6.0×10^8	H_2O	A	27
	$(8.0\pm0.3) \times 10^8$	pH 6.8, 18°C	A	28
(Diquat)$^{+}$	$(4.4\pm0.4) \times 10^3$	EtOH, -80°C	B	26
	$(4.7\pm0.3) \times 10^8$	pH 6.8, 18°C	A	28

a. Aqueous solution at ambient temperature unless otherwise noted.

b. A = pulse radiolysis, B = stopped-flow spectrophotometry,

   C = cyclic voltammetry.

the rates of the reactions between redox cycling mediators
and dioxygen in solution.

C. <u>Redox Cycling and the Phytotoxicity of Bipyridinium</u>
   <u>Herbicides</u>

The properties of bipyridinium herbicides became of
increasing interest as the work described in this thesis
progressed. The best known member of this class of
compounds is paraquat or 1,1-dimethyl-4,4'-bipyridinium
dichloride (3 in Figure 2). This compound is also
commonly known as methyl viologen. It was first applied
as an oxidation-reduction indicator by Michaelis in his
determinations of the redox potentials of biological
reductants such as NADH (19). He coined the term
"viologen" based on the intense violet color of the cation
radical produced by the one-electron reduction of the
methyl viologen dication. Due to their facile reaction
with components of biological electron transfer systems,
methyl viologen and its 1,1'-dibenzyl analog, benzyl
viologen, have found numerous applications in studies of
such systems (20). As these compounds undergo reversible,
one-electron electrochemical reductions in both aqueous
and organic solvents, they have found widespread use as
model compounds in experimental electrochemistry. The

electrochemistry of methyl viologen and related compounds has been reviewed (21).

The herbicidal activity of bipyridinium salts was first discovered in the 1950s by scientists working for Imperial Chemical Industries Ltd. in Britain (20,22). Two compounds which have found extensive commercial application since that time are paraquat (Gramoxone®, 3 in Figure 2) and diquat (Reglone®, 4 in Figure 2). These compounds are potent, rapid-acting, non-selective, post-emergent herbicides. They find use in orchards, plantations, and tree farms, in pasture rejuvenation, in pre-harvest dessication and in aquatic weed control (20). As they are largely inactivated upon reaching the soil, bipyridinium herbicides possess minimal residual activity. This property makes them valuable for weed control prior to the seeding of crops.

The herbicidal activity of paraquat and diquat is thought to arise from a redox cycling mechanism similar to that postulated for the cardiotoxicity of anthracyclines (10,20). Electrochemical studies have played a prominent role in research into and development of bipyridinium herbicides. Homer et al. found a strong correlation between the herbicidal activity of a number of bipyridinium salts and their standard reduction potentials as measured by potentiometric titration with dithionite

(22). The same authors demonstrated that the presence of dioxygen was essential to the herbicidal activity. White and coworkers at ICI synthesized and tested numerous analogs of diquat and paraquat (21,23). They found polarographic half-wave potentials to be of value in predicting active compounds. Based on measures of herbicidal activity and on <u>in vitro</u> tests, White found that bipyridinium compounds could be separated into three groups with respect to half-wave potential (23):

"A) $E_{1/2}$ more negative than -450 mV (vs NHE): Activity decreased as $E_{1/2}$ increased. Photosynthetic energy is insufficient to allow quantitative radical formation.

B) $E_{1/2}$ more positive than -250 mV: Little or no activity. Electron preferentially transferred to ferredoxin.

C) $E_{1/2}$ -300 to -450 mV: High activity distributed around a Gaussian peak. Differential rates of reoxidation may be responsible for variation in activity."

At the time White's work appeared, no kinetic data were available to support or discount the speculation that reoxidation rates determined herbicidal activity in the third group. Since that time however, a number of studies of the kinetics of the reaction of the paraquat (methyl viologen) cation radical $MeV^{+\cdot}$ or the diquat cation radical $DiQ^{+\cdot}$ with dioxygen have been published. Thornely studied the reaction of $MeV^{+\cdot}$ in aqueous solution by

stopped-flow spectrophotometry (24). He found the
kinetics of the overall reduction of dioxygen to water by
4 $MeV^{+\cdot}$ to be biphasic. The first two electrons were
transfered in less than the mixing time of the instrument
(2 ms) from which it was inferred that $k > 5 \times 10^6$
$M^{-1}s^{-1}$. The rate constant of the subsequent reaction of
$MeV^{+\cdot}$ with H_2O_2 was measured as 2.3×10^3 $M^{-1}s^{-1}$ at
25°C. Evans et al. used the stopped-flow technique to
study the reaction of $MeV^{+\cdot}$ and $DiQ^{+\cdot}$ with dioxygen in
methanol and ethanol respectively (25,26). Useful results
were obtained only in the temperature range -50° to -80°C;
these are presented in Table 2. Patterson et al. studied
the reaction of $MeV^{+\cdot}$ with dioxygen in water and in
alcohols at room temperature by pulse radiolysis (27).
Their results may also be found in Table 2. It is
interesting to note that the rate constants measured in
organic solvents are some two orders of magnitude lower
than that found in water. The value determined in the
latter solvent is in good agreement with the result of
Farrington et al. also obtained by pulse-radiolysis (28).

Most interesting from the vantage point of the
present work are efforts to determine the rate of reaction
of redox cycle mediators with dioxygen by electrochemical
means. Rauwel and Thévenot studied the reaction of
electrogenerated $MeV^{+\cdot}$ with O_2 using Albery's diffusion

layer titration technique at a rotating ring-disk electrode (29). While they were able to confirm the occurrence of a very fast reaction in aqueous solution, experimental complications precluded a quantitative determination of the rate constant. Recently Andrieux et al. obtained a value for the rate constant of the $MeV^{+\cdot}/O_2$ reaction in acidic dimethylsulfoxide (DMSO) by cyclic voltammetry (30). In their experiment, the $MeV^{2+}/MeV^{+\cdot}$ couple catalyzed the reduction of dioxygen according to the EC-catalytic mechanism. Using a numerical solution to the kinetic-diffusion problem, the rate constant for the reaction was found to be $(2.3 \pm 0.3) \times 10^5\ M^{-1}s^{-1}$.

Andrieux et al. chose to study the $MeV^{+\cdot}/O_2$ reaction as an example of a catalytic system wherein the diffusion coefficients of the reactants differed significantly. The diffusion coefficient of dioxygen was found to be 6.3 ± 0.5 times that of $MeV^{+\cdot}$ in DMSO (30). This difference had to be accounted for in the formulation and solution to the kinetic-diffusion problem in order to obtain an estimate of the rate constant.

While a certain amount of data on the rate of reaction of bipyridinium cation radicals with dioxygen has accumulated over the last decade, there has been no attempt to correlate reaction rates with quantitative measures of herbicidal activity to date.

D. Generation of Active Oxygen Species.

The immediate product of the redox cycle, the superoxide ion $O_2^{-\cdot}$, is not sufficiently reactive to cause the sort of cellular damage associated with redox cycling (31). Such damage includes membrane disruption by lipid peroxidation (32), protein damage and enzyme inactivation by amino acid oxidation (3,9) and the cytotoxic and mutagenic events associated with DNA damage (7,8). The oxidants usually invoked to account for these phenomena are the perhydroxyl radical $HO_2^\cdot$, the hydroxyl radical $OH^\cdot$, and hydrogen peroxide (5,7,8).

The perhydroxyl radical is simply the conjugate acid of $O_2^{-\cdot}$; the pK_a of $HO_2^\cdot$ is 4.8 (35). While $HO_2^\cdot$ is a much stronger oxidant than $O_2^{-\cdot}$ (31), it is present as only a very small fraction of $O_2^{-\cdot}$ at physiological pH.

Hydrogen peroxide is the product of the dismutation of superoxide ion. The reaction is catalyzed by superoxide dismutase (SOD) as part of the normal detoxification pathway for oxygen metabolites (8):

$$2O_2^{-\cdot} + 2H^+ \xrightarrow[2.3 \times 10^9 \ M^{-1}s^{-1}]{SOD} H_2O_2 + O_2 \qquad [1]$$

$$2H_2O_2 \xrightarrow[\sim 10^7 \ M^{-1}s^{-1}]{\text{Catalase}} O_2 + 2H_2O \qquad [2]$$
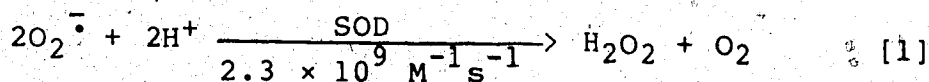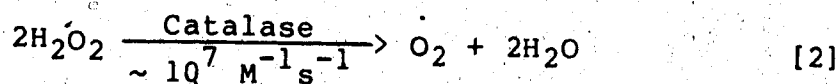
In the absence of transition metal catalysts and at neutral pH, the spontaneous rate of reaction [1] is less than 0.35 $M^{-1}s^{-1}$ (34) and that of reaction [2] is negligible. Thus O_2^{-} and H_2O_2 can accumulate in locations where SOD and catalase activities are low (7,8).

It is the reaction of the superoxide ion and hydrogen peroxide that gives rise to the most reactive of the active oxygen species, the hydroxyl radical OH$^\bullet$. This reaction is of interest in the present work for two reasons. First, the currently accepted mechanism is quite analogous to the redox-cycling mechanism described at the beginning of this chapter. Second, the rate-determining step of the mechanism has been the subject of numerous electrochemical studies of homogeneous reaction kinetics.

The hydroxyl radical is thought to be generated _in vivo_ by an iron-catalyzed one-electron reduction of H_2O_2 by O_2^{-} as depicted in Figure 3 (32-35). The rate-determining step is the oxidation of the Fe^{2+} complex by H_2O_2 (35). The reaction of the aquo complex in aqueous solution

$$Fe^{2+} + H_2O_2 \rightarrow Fe^{3+} + OH^\bullet + OH^-$$

Overall Reaction:

$$O_2^- + H_2O_2 \dashrightarrow O_2 + OH^\bullet + OH^-$$
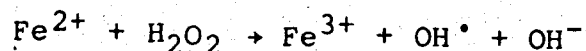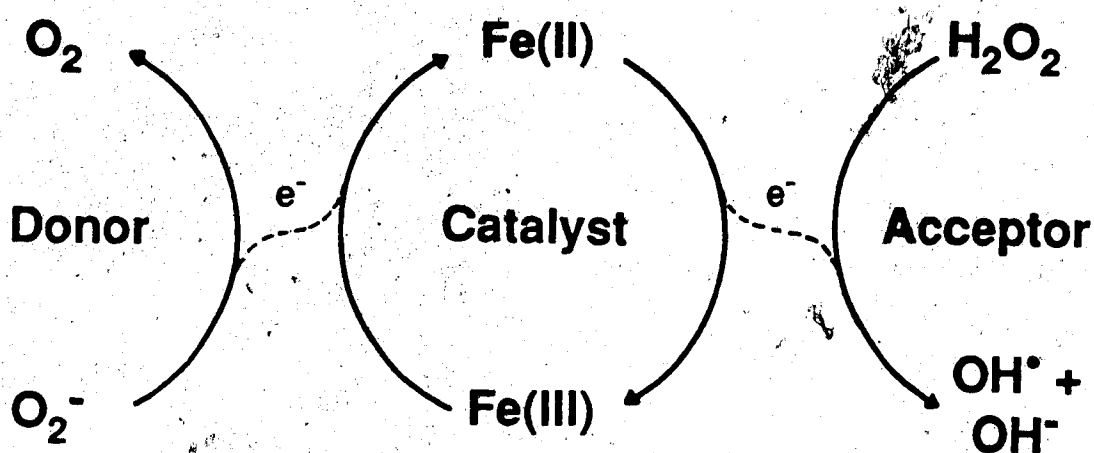
Figure 3. Production of Hydroxyl Radical by the Iron-Catalysed Reduction of Hydrogen Peroxide by the Superoxide Ion. After references 24-28.

is the classic Fenton reaction, a well-known initiator of radical chain reactions (36). The reaction of electro-generated Fe^{2+} with H_2O_2 is the prototypical example of an EC-catalytic mechanism. It is this mechanism which forms the basis for the electrochemical studies of redox cycling which follow.

CHAPTER II

AN ELECTROCHEMICAL APPROACH TO THE KINETICS

OF REDOX CYCLING

A. The EC-Catalytic Mechanism as an Electrochemical Model

for Redox Cycling

The electrochemical analog of redox cycling is the
well-known EC-catalytic mechanism as shown in Figure 4.
The term "EC-catalytic" (41) refers to a mechanism wherein
an electrochemical reaction E is followed by a chemical
reaction C. The adjective "catalytic" describes the
apparent increase in the rate of the electrochemical
reaction that is a consequence of the chemical reaction.
With reference to Figure 4, the reduction of the catalyst
P at an electrode corresponds to the enzyme-catalyzed
reduction of a redox-cycle mediator. The subsequent
reaction of the reduced catalyst Q with substrate A to
regenerate P corresponds to the electron-transfer
reactions that are the focus of the present work.

There are two important features of this
electrochemical model for redox cycling. First, electro-
chemistry provides a convenient method for reactant
generation. It is especially advantageous when dealing

Redox Cycling Mechanism

NAD

Donor

NADH

e^-

Red

Mediator

Ox

e^-

O_2

Acceptor

$O_2^{-\bullet}$

The EC-Catalytic Mechanism

Electrode

e^-

Q

Catalyst

P

e^-

A

Substrate

B
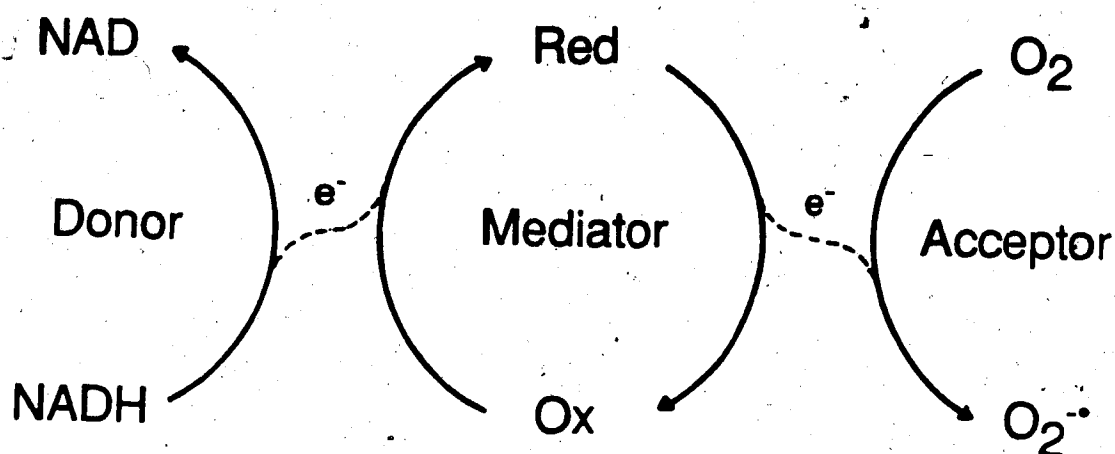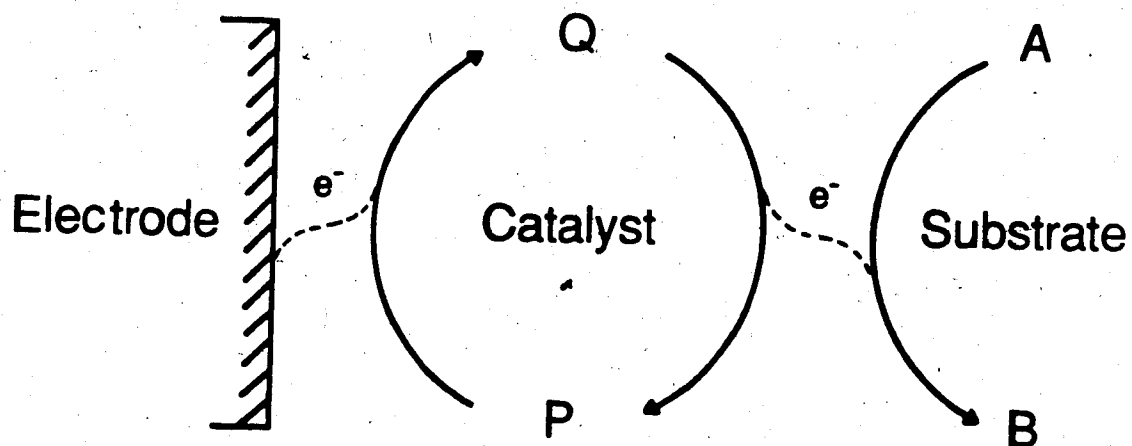
Figure 4.   The EC-Catalytic Mechanism as an Electro-
            chemical Model for Redox Cycling.

with mediator compounds that are reactive toward oxygen,
and thus air-sensitive. Second, under conditions where
the EC-catalytic mechanism applies, the value of the rate
constant for the reaction of catalyst with substrate can
be inferred from the magnitude of the associated catalytic
current.

B. Example of an EC-Catalytic Mechanism

   As mentioned in the Introduction, the classic example
of an EC-catalytic mechanism is the iron-catalyzed
reduction of hydrogen peroxide. The reaction was first
studied polarographically some 35 years ago by Kolthoff
and Parry (40). The reaction scheme in its simplest form
is as follows:

Electrode: $Fe(III) + e^- \rightleftarrows Fe(II)$ [4]

Solution: $Fe(II) + H_2O_2 \xrightarrow{k} Fe(III) + OH^- + OH \cdot$ [5]
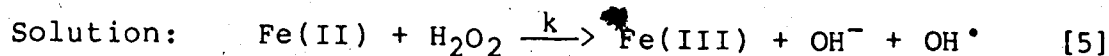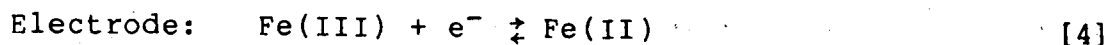
Reaction [5] is the previously encountered Fenton
reaction. An example of the experimental manifestation of
this mechanism is shown in Figure 5. The current observed
for the reduction of $Fe(III)$ in the presence of H_2O_2 is
increased over that observed for $Fe(III)$ alone. The
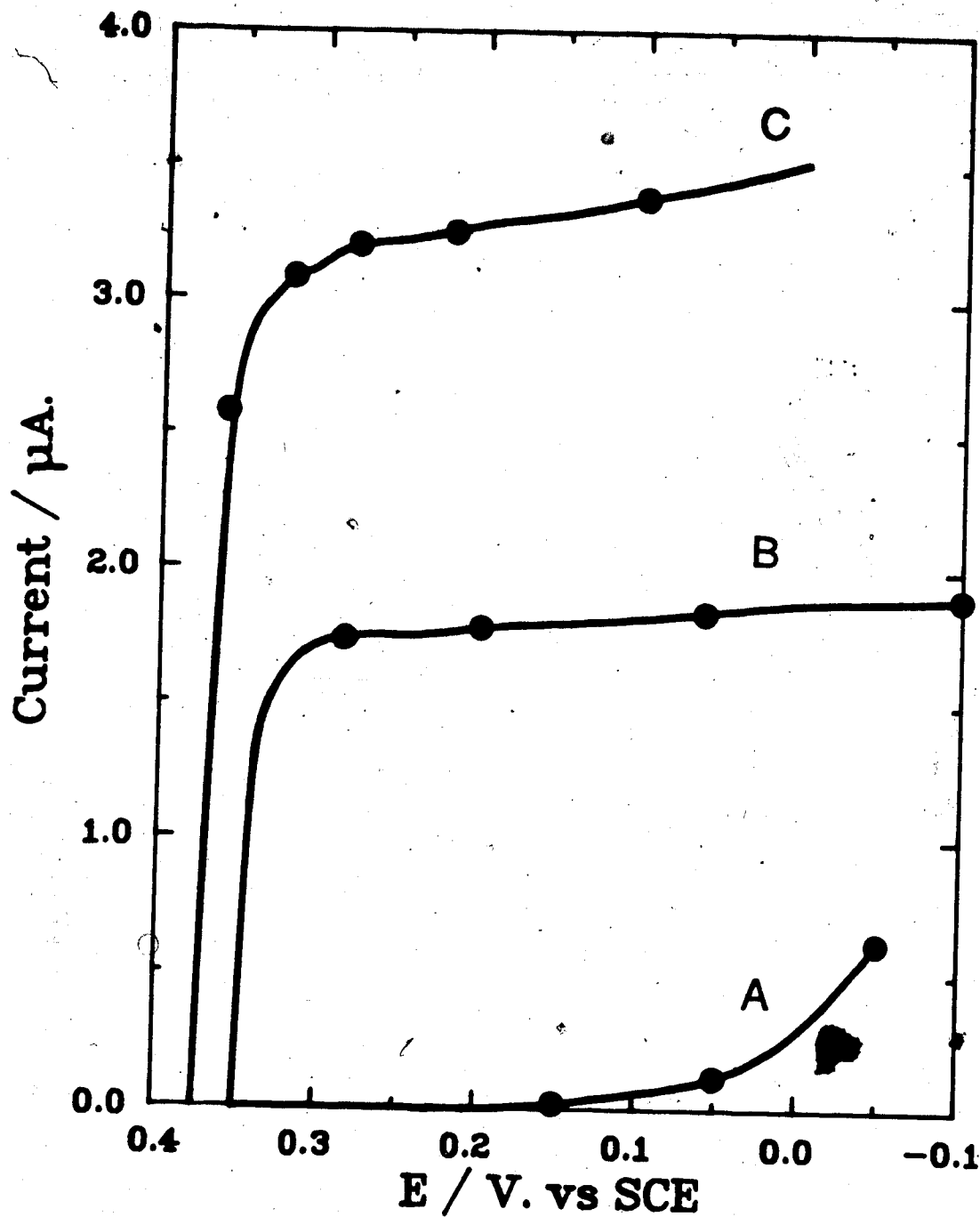
Figure 5. Polarograms for the Reduction of Fe(III) in the
Presence and Absence of Hydrogen Peroxide. From
reference 40. A) 0.147 M H_2O_2, B) 2 x 10^{-4} M
Fe(III), C) 0.0147 M H_2O_2 and 2 x 10^{-4} M Fe(III).
All solutions contained 0.25 M H_2SO_4.

effect of the solution reaction [5] is to oxidize a portion of the product of the electrochemical reaction [4]. The result is an increased flux of Fe(III) to the electrode surface, and thus an increased current. The magnitude of the increase in current is related to the rate of the solution reaction. The nature of this relationship is the subject of the following chapter.

C. Thermodynamic and Kinetic Requirements

The EC-catalytic mechanism is expressed in terms of general electrochemical and chemical reactions in Figure 6. The mechanism is cast in terms of a reduction by analogy with redox cycling, although the general mechanism applies to both oxidation and reduction. Also shown in Figure 6 are the thermodynamic and kinetic requirements for the mechanism (38,41). For the solution reaction to proceed from left to right, the formal potential under the conditions of the experiment $E_A^{O'}$ must be more positive than that of the catalyst couple $E_P^{O'}$. At the same time however, the rate constant $k_{h,A}$ of the electrochemical, or direct, reduction of substrate must be negligible with respect to that of the catalyst, $k_{h,P}$.

Catalytic currents are observed only when there is a kinetic barrier to direct substrate reduction. The

The EC-Catalytic Mechanism

Catalysed Reduction of Substrate:

Electrode: $P + e^- \rightleftharpoons Q$ $\quad k_{h,P}$ $\quad E_P^{o'}$

Solution: $A + Q \rightleftharpoons P + B$ $\quad k_1 \quad k_{-1}$

Overall: $A + e^- \rightleftharpoons B$

Direct Reduction of Substrate:

$A + e^- \rightleftharpoons B$ $\quad k_{h,A}$ $\quad E_A^{o'}$
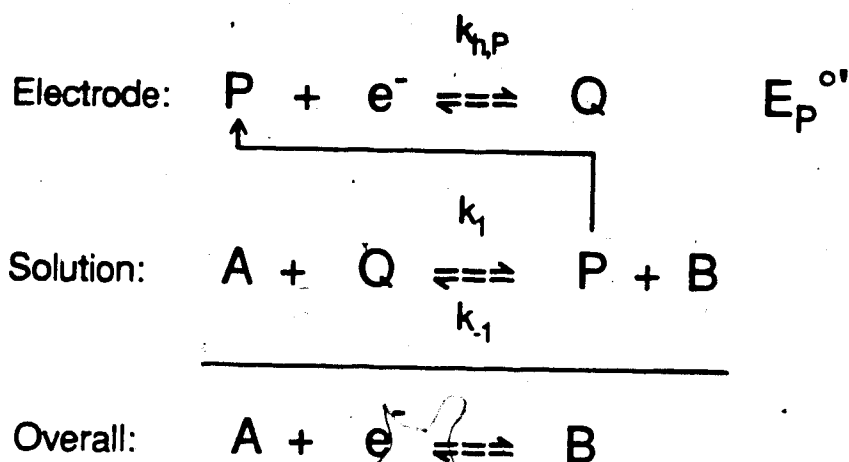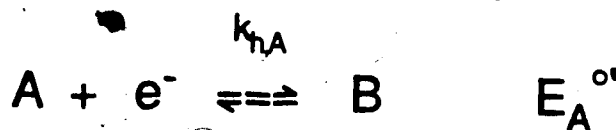
Thermodynamic and Kinetic Requirements:

$$E_A^{o'} > E_P^{o'}; \quad k_{h,A} \ll k_{h,P}$$

Figure 6.   Thermodynamic and Kinetic Requirements for the EC-Catalytic Mechanism. After reference 41. The symbols are defined in the text.

barrier must be large enough that the order of the experimentally observed reduction potentials is the reverse of the corresponding formal potentials. In terms of the Fe(II)/H_2O_2 reaction (Figure 5), a catalytic current is observed because the kinetic barrier for the electrochemical reduction of H_2O_2 is sufficiently large to shift the reduction wave for H_2O_2 negative to that for Fe(III). In the absence of kinetic limitations, the reduction wave for H_2O_2 would precede that for Fe(III). Reaction [5] would still occur under these circumstances, but it would not be manifested as a catalytic current.

D.   Theory for and Applications of the Pseudo-First-Order EC-Catalytic Mechanism

In addition to the thermodynamic and kinetic requirements outlined above, the determination of rate constants for solution reactions from catalytic currents requires a quantitative description of the EC-catalytic mechanism in the context of the experimental technique employed. Analytical solutions to the mathematical problem posed by the EC-catalytic mechanism generally require the assumption that the solution reaction is first-order in catalyst and pseudo-first-order overall (42-59). Thus the experiment must be conducted under

conditions where the substrate is present in large excess over the catalyst. This constitutes the pseudo-first-order EC-catalytic mechanism.

By making suitable approximations, it has been possible to use analytical methods to obtain closed-form expressions relating catalytic currents to pseudo-first-order rate constants for a variety of electrochemical techniques. These techniques are listed in Table 3 together with representative experimental applications. Despite the number of techniques supported by theory, experimental applications of the pseudo-first-order EC-catalytic mechanism are limited in number and in kind. Systems investigated predominantly involve reduced transition metal catalysts such as Fe(II) or Ti(III) reacting with inorganic oxidants such as H_2O_2, ClO_3^-, or NH_2OH. The paucity of applications is partly due to the restrictive assumptions required to make the problem mathematically tractable. In terms of the applications envisaged in the present work, factors such as limited substrate solubility and fast reaction rates frequently preclude use of the pseudo-first-order treatments.

Table 3. Applications of the Pseudo-First-Order EC-Catalytic Mechanism.

Technique	Theory Ref.	Catalyst Couple	Substrate	Rate ($M^{-1} s^{-1}$)	Conditions	Appl'n. Ref.
dc Polarography	42	Fe(III)/Fe(II)	H_2O_2	78±8	0.5 $\underline{M}$ H_2SO_4, 25°C	37
		Fe(III)(EDTA)/Fe(II)(EDTA)	H_2O_2	6.8×10^3	pH 4.7 acetate, 25°C	89
Streaming Hg Electrode	34	Ti(IV)/Ti(III)	ClO_3^-	2.6×10^4	0.1 $\underline{M}$ oxalic acid, 0.2 $\underline{M}$ H_2SO_4, 25°C	91
		Fe(II)(TEA)/Fe(III)(TEA)	H_2O_2	3.2×10^6	1 $\underline{M}$ NaOH, 25°C	91
ac Polarography	43	Ti(IV)/Ti(III)	ClO_3^-	2.6×10^{4a}	0.2 $\underline{M}$ oxalic acid, 25°C	44
Linear sweep voltammetry	33	Fe(III)(EDTA)/Fe(II)(EDTA)	H_2O_2	$(7.2 \pm 0.2) \times 10^3$	pH 4.7 acetate, 25°C	90
		Ti(IV)/Ti(III)	NH_2OH	42.0±1.7	0.2 $\underline{M}$ oxalic acid, 25°C	90
Rotating disk electrode	46	Fe(III)/Fe(II)	H_2O_2	73	1 $\underline{M}$ KCl, 25°C	46
Pulse polarography	47	Fe(III)(EDTA)/Fe(II)(EDTA)	cytochrome c	$(3.1-7.6) \times 10^4$	0.05 $\underline{M}$ Tris, pH 7.3, 24°C	53
Chronocoulometry	48	Ti(IV)/Ti(III)	NH_2OH	43.4±1.1	0.2 $\underline{M}$ oxalic acid, 25°C	55
Rotating ring-disk electrode	49	Fe(III)/Fe(II)	VO_2^+	3.2×10^3	1.0 $\underline{M}$ $HClO_4$, 25°C	49
Tubular electrodes	50	Fe(III)/Fe(II)	H_2O_2	43±2	0.25 $\underline{M}$ H_2SO_4, 25°C	90
Spectroelectrochemistry (SnO₂ OTE)	51	$Fe(CN)_6^{4-}/Fe(CN)_6^{3-}$	ascorbic acid	13.6±0.2	pH 2.2 glycine, 25°C	51

(Cont'd)

Table 3. (Continued)

Technique	Theory Ref.	Catalyst Couple	Substrate	Rate ($M^{-1} s^{-1}$)	Conditions	Appl'n. Ref.
Chronoamperometry	52	phenanthrene	octyl chloride	490±25	0.1 $\underline{M}$ Et$_4$NBr in DMF	52
Second harmonic ac polarography	45	Fe(III) (TEA)/Fe(II) (TEA)	ClO_2^-	8.0×10^3	0.1 $\underline{M}$ NaCl, 0.05 $\underline{M}$ NaOH, 25°C	45
Channel electrode	54	Fe(III)/Fe(II)	H_2O_2	40	0.5 $\underline{M}$ KCl, 25°C	54
Differential pulse polarography	56	Ti(IV)/Ti(III)	ClO_3^-	$(5.6-6.1) \times 10^4$	0.1 $\underline{M}$ oxalic acid, 0.2 $\underline{M}$ H$_2$SO$_4$	56
		Ti(IV)/Ti(III)	NH_2OH	22-46	Same	56
Ring electrodes (turbulent flow)	35	Fe(III) (TEA)/Fe(II) (TEA)	H_2O_2	$(2.0\pm0.5) \times 10^6$	1 $\underline{M}$ NaOH, 20°C	92
		Fe(III)/Fe(II)	H_2O_2	45-48	0.5 $\underline{M}$ HClO$_4$, 20°C	92
Ultramicroelectrodes	57	$Fe(CN)_6^{4-}/Fe(CN)_6^{3-}$	amidopyrine	$(3.0\pm0.6) \times 10^3$	1 $\underline{M}$ KOH	57
Linear sweep voltammetry (RDE)	58	Fe(III)/Fe(II)	H_2O_2	41.7	0.5 $\underline{M}$ KCl	58
Square wave voltammetry	59	Ti(IV)/Ti(III)	NH_2OH	41.2±1.0	0.2 $\underline{M}$ oxalic acid, 25°C	59
		Ti(IV)/Ti(III)	ClO_3^-	$(5.61\pm 0.33) \times 10^4$	0.1 $\underline{M}$ oxalic acid, 0.2 $\underline{M}$ H$_2$SO$_4$, 25°C	59
		Fe(III) (TEA)/Fe(II) (TEA)	NH_2OH	150.8±6.3	0.1 $\underline{M}$ NaOH, 25°C	59

Abbreviations: TEA, triethanolamine; OTE, optically transparent electrode; DMF, N,N'-dimethylformamide; RDE, rotating disk electrode. a. As calculated in Reference 59.

E. Theory for and Applications of the Second-Order

EC-Catalytic Mechanism

The second-order EC-catalytic mechanism refers to the case where the solution reaction is first-order in both catalyst and substrate, and is therefore second-order overall. Unlike the pseudo-first-order case, the second-order EC-catalytic mechanism is not amenable to solution by approximate analytical methods. Instead, recourse to some form of numerical approximation is necessary. Techniques for which numerical solutions have been obtained and experimental applications of the same are summarized in Table 4.

Discussion of the various numerical methods encountered in Table 4 is postponed to the next chapter. Here comments will be confined to experimental applications of the second-order EC-catalytic mechanism. The rates of the reactions in Table 4 encompass the same wide range as those of Table 3. Some six orders of magnitude are spanned with values ranging from the order of 10^1 to 10^6 $M^{-1}s^{-1}$. The applications of the second-order case are somewhat broader in scope, however. For example, some of the reactions in Table 4 possess synthetic utility. Lund and Simonet pioneered this area with their studies of the catalysis of cathodic cleavage

Table 4. Numerical Solutions and Applications of the Second-Order EC-Catalytic Mechanism.

Technique	Numerical Method[a]	Catalyst	Substrate	Rate $(M^{-1} s^{-1})$	Conditions	Ref.
Spectroelectrochemistry	E	$Fe(CN)_6^{3-}$	ascorbic acid	23.6 ± 2.4	pH 2.5, glycine, 25°C	61
	E	tri-p-anisylamine	CN^-	$(2.0 \pm 0.3) \times 10^5$	0.3 $\underline{M}$ TEAP in AN, 25°C	61
Rotating ring-disk electrode	E	Fe(III)	H_2O_2	202 ± 15^{b}	2 $\underline{M}$ HCl, 23°C	62
Chronoabsorptometry	E	methyl viologen	cytochrome c	$(1.0 \pm 0.3) \times 10^6$	pH 7.2, phosphate	63
Chronoamperometry	E	Fe(III) (EDTA)	cytochrome c	2.5×10^4	pH 7.0, phosphate	64
dc Polarography	I	biphenyl	chlorobenzene	1.6×10^4	0.1 $\underline{M}$ Bu_4NI in DMF, 20°C	65
Cyclic voltammetry	I	chrysene	bromobenzene	5×10^3	0.1 $\underline{M}$ Bu_4NI in DMF, 20°C	66
Cyclic voltammetry	E	Fe(III)		2×10^6	0.1 $\underline{M}$ H_2SO_4	41
Rotating disk electrode	E	Co(III) (Cyclam)		3×10^6	0.01 $\underline{M}$ $HClO_4$, 0.49 $\underline{M}$ $NaClO_4$, 22°C	67
Cyclic voltammetry	I	methyl viologen	O_2	2.3×10^5	0.1 $\underline{M}$ Bu_4NI, 1 $\underline{M}$ HOAc in DMSO	30

(Continued)

Table 4. (Continued)

Technique	Numerical Method[a]	Catalyst	Substrate	Rate $(M^{-1} s^{-1})$	Conditions	Ref.
Rotating disk electrode	O	Br^-	allyl alcohol[c]	3.2×10^5	0.5 $\underline{M}$ H_2SO_4, 25°C	69
Rotating ring-disk electrode	H	Fe(III)	H_2O_2	102^e	2 $\underline{M}$ HCl, 23°C	70
Rotating ring-disk electrode	H	Co(III)(Cyclam)[d]	H_2O_2	$(3.0 \pm 0.4) \times 10^3$	0.1 $\underline{M}$ $HClO_4$, 22°C	70

Abbreviations: TEAP, tetraethylammonium perchlorate; AN, acetonitrile; DMF, N,N'-dimethylformamide; DMSO, dimethylsulfoxide.

a. Numerical methods: E, explicit finite-difference; I, implicit finite-difference; H, "hopscotch" finite-difference (Reference 103 and references therein); O, orthogonal collocation.

b. Recalculated value according to Reference 75.

c. Tetrakis(N-methyl-4-pyridyl)porphyrin.

d. 1,4,8,11-Tetraazacyclotetradecane.

e. Calculated from data of Reference 62.

reactions of simple aromatic and aliphatic halides in DMF
(71). Such reactions as catalyzed by anthracene and
diphenylanthracene have been applied to the
electrochemical dechlorination of polychlorinated
biphenyls (72). Similar catalysts have been employed to
aid in the electrochemical removal of protecting groups
such as benzyl ethers (73) and tosyl esters and amides
(73,74).

From the standpoint of redox cycling, reactions
involving dioxygen as substrate are of particular
interest. The work of Andrieux et al. on the reaction of
the paraquat cation radical with dioxygen in DMSO (30) has
already been mentioned. The reactions of the macrocyclic
Fe(II) and Co(II) complexes with dioxygen (41,67) were
studied as part of work directed toward the development of
chemically modified electrodes (CMEs). At these
electrodes, catalysis of the oxidation or reduction of
substrate is effected by a catalyst which is chemically
bound to the electrode surface. As the catalytic reaction
is a heterogeneous process, CMEs represent a kind of
"heterogeneous" redox catalysis (39,41). The EC-catalytic
mechanism, on the other hand, is a kind of "homogeneous"
redox catalysis. The homogeneous case provides a useful
model for the corresponding heterogeneous process and so
the EC-catalytic mechanism has found a role in the
development of CMEs (41).

Homogeneous redox catalysis is also the term applied by Savéant and co-workers to describe their more general analysis of the EC-catalytic mechanism (38,65,93,94). By studying the homogeneously catalyzed reduction of a substrate with a number of catalysts of differing standard potential, these workers have succeeded in determining electrochemical rate and equilibrium parameters for the direct reduction of substrate. The kinetic barrier to the direct reduction renders these parameters inaccessible to standard electrochemical techniques. An example of a reaction studied in this fashion is the reduction of chlorobenzene in DMF as catalyzed by various aromatic compounds such as biphenyl, naphthalene and phenanthrene (65).

CHAPTER III

THE EC-CATALYTIC MECHANISM AT THE ROTATING DISK ELECTRODE:
THEORY

A. The Rotating Disk Electrode as a Tool for the Study of the EC-Catalytic Mechanism

The experimental studies of the EC-catalytic mechanism described in the following chapters were carried out exclusively at rotating disk electrodes (RDEs). Before describing the advantages associated with the RDE in this context, a brief introduction to the electrode system is in order. A cutaway view of a typical RDE is shown in Figure 7. It consists of a disk of the desired electrode material, such as platinum, gold or glassy carbon, mounted on the end of a steel shaft. The lower portion of the shaft is encased in a Teflon shroud. The shroud serves to electrically insulate the shaft and to stabilize the hydrodynamic flow near the edge of the disk. The upper portion of the shaft is mounted in a rotator and electrical contact is made via a carbon brush riding on a slip ring. The experimental apparatus used to perform electrochemical experiments at the RDE is shown in Figure 8. The RDE, a Pt-wire counter electrode and a

Shaft

Alignment
Cone

Electrode
Surface

Teflon
Shroud

r

θ

z

At the Disk
Surface

$r=0$

$z=0$

Below the Disk
Surface
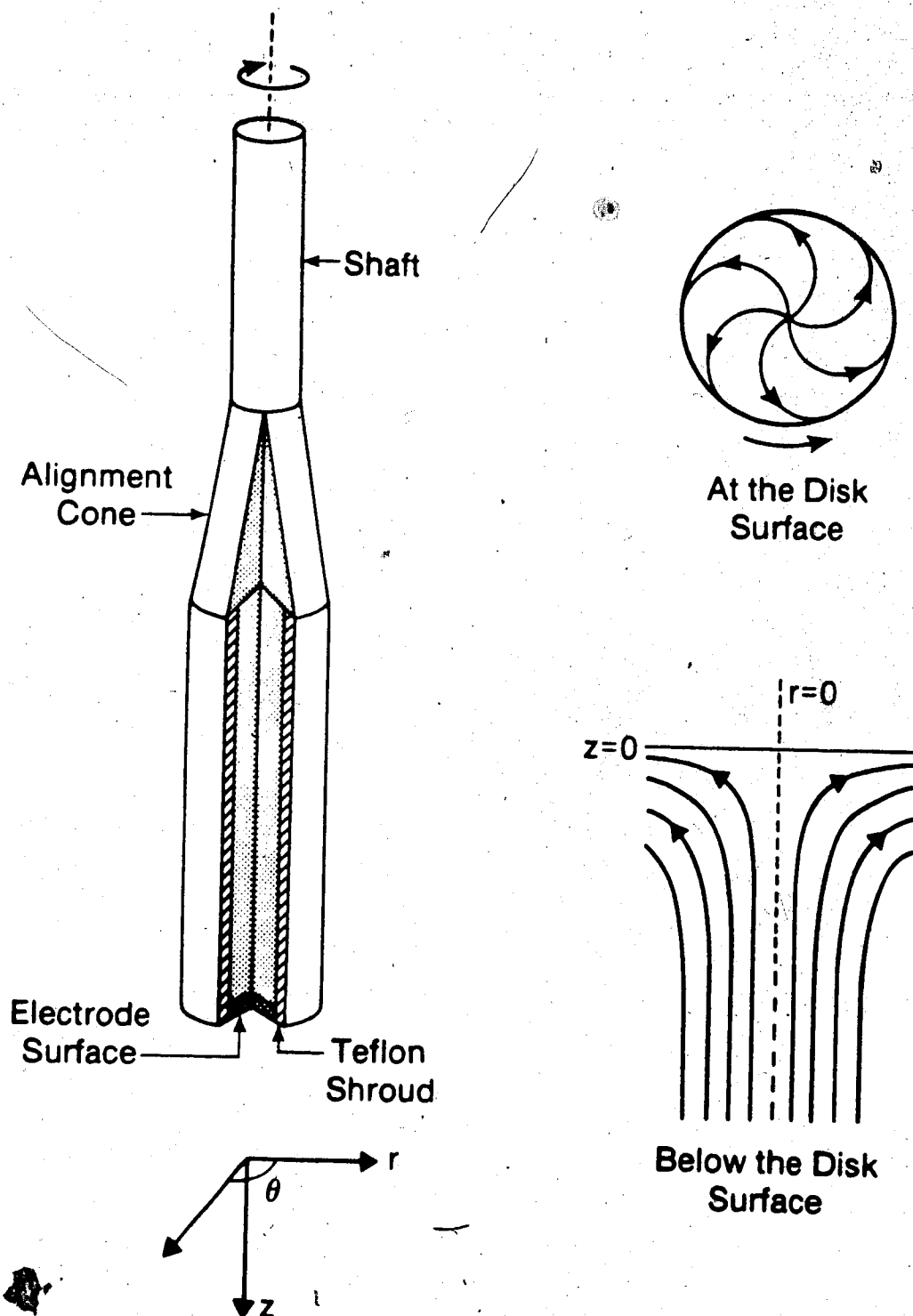
Figure 7.   The Pine Model DT06. Rotating Disk Electrode.
Cutaway view and depiction of the hydrodynamics.
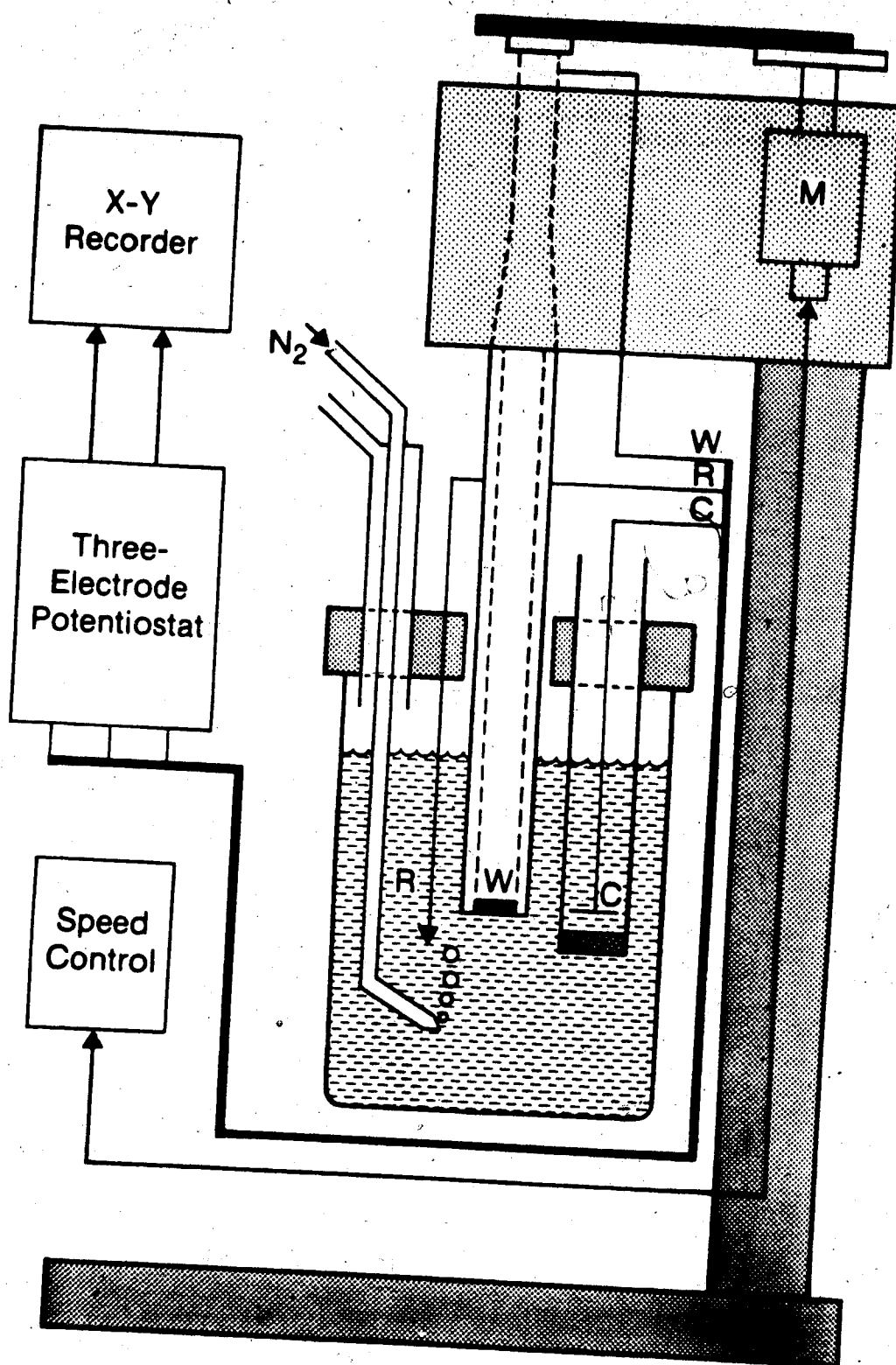
Figure 8. Experimental Apparatus Used for Voltammetry at the Rotating Disk Electrode. W - Working Electrode, R - Reference Electrode, C - Counter Electrode, M - Motor.

saturated calomel reference electrode are connected to a 3-electrode potentiostat. Current flow through the RDE is typically monitored as a function of applied potential at fixed rotation speed or vice versa.

Electrode rotation provides a source of convective mass transport which supplements diffusive mass transport and thus enhances current flow through the electrode. The convective pattern impressed upon the solution below an RDE is depicted by the streamlines in Figure 7. As the electrode rotates, solution near the disk is thrown out radially, and as a consequence of this, solution from below the disk is drawn up axially. The enhanced rate of mass transport due to convection is important analytically as it increases sensitivity. From a kinetic point of view, the chief virtue of the RDE is that mass transport to the electrode can be described in comparatively simple mathematical terms. Such a description is important as mass transport is the baseline upon which kinetic effects at the RDE are superimposed.

The following differential equation describes mass transport to the RDE (76,77,81):

$$\frac{\partial c}{\partial t} = D[\frac{\partial^2 c}{\partial z^2} + \frac{\partial^2 c}{\partial r^2} + \frac{1}{r}\frac{\partial c}{\partial r} + \frac{1}{r^2}\frac{\partial^2 c}{\partial \theta^2}]$$

$$-v_r\frac{\partial c}{\partial r} - \frac{v_\theta}{r}\frac{\partial c}{\partial \theta} - v_z\frac{\partial c}{\partial z} \qquad [6]$$

where   c = concentration of electroactive species

D = diffusion coefficient of same

r, θ, z = cylindrical coordinates

v_r, v_θ, v_z = fluid velocity components

Equation [6] is a special case of the Navier-Stokes equation. It is formulated on the assumption that mass transport by migration is negligible.

The equation describing the mass-transport-limited current at the RDE was provided by Levich (81). He simplified equation [6] by assuming concentrations to be independent of the radial coordinate r. Since derivatives with respect to θ vanish by symmetry, the differential equation governing steady-state mass transport to the RDE can be written as:

$$D \frac{d^2c}{dz^2} = v_z \frac{dc}{dz}$$ [7]

For a mass-transport-limited current, the following boundary conditions apply:

c = c(∞) for z → ∞,

c = 0 at z = 0

where c(∞) is the bulk concentration of the electroactive species. The well-known Levich equation [8] derives from the solution to the above boundary-value problem.

$$i_l = 0.62 \ nFAD^{2/3} \ \nu^{-1/6} \ \omega^{1/2} \ c(\infty) \qquad [8]$$

The terms A, ν and ω in equation [8] denote electrode area (cm^2), kinematic viscosity (cm^2/s) and angular velocity (s^{-1}) respectively. The remaining terms have their usual electrochemical meaning. For a concentration c(∞) in moles/liter, equation [8] gives the limiting current in milliamps. Details concerning the derivation of the Levich equation can be found in Appendix 1.

Rotating disk electrodes have found widespread application in both physical and analytical electro-chemistry. Theory and applications of the RDE have been the subject of several reviews (76,77,78) and books (79,80,81). The RDE possesses a number of advantages over other hydrodynamic techniques and over transient techniques such as cyclic voltammetry. As mentioned above, one of the most attractive features of the RDE is the mathematical simplicity of the differential equation describing steady-state mass transport. Inclusion of kinetic terms is straightforward and the resulting ordinary differential equations are comparatively easy to

solve analytically (80,81) or numerically (82).

Steady-state mass transport also gives rise to some of the experimental advantages associated with the RDE. Measurement of the time-invariant direct currents obtained at the RDE requires no special instrumentation. In addition, steady-state current measurement provides effective discrimination against interfering transient current sources such as charging currents and currents due to surface-limited electrode processes. Electrode rotation speed constitutes a convenient and easily controlled experimental parameter. Finally the RDE can be used in conjunction with a concentric ring electrode (the rotating ring-disk electrode or RRDE). The ring provides an electrochemical means of monitoring species generated by electrochemical reactions at the disk (78,79).

B. Numerical Approaches to the Solution of the Electro-
   chemical Kinetic Problems at the RDE

The earliest application of numerical approximation techniques to the solution of electrochemical kinetic problems is the work of Hale (60). He studied galvanostatic transients at the RDE using the implicit finite-difference method. Widespread application of numerical techniques followed the work of Feldberg (83)

who popularized the "digital simulation" or explicit finite-difference approach. This approach remains popular (see Table 4) in spite of advantages claimed for the implicit method (84,85) and for polynomial approximation methods (86,87).

With the exception of the very recent work of Chapman (69), solutions for the second-order EC-catalytic mechanism at the RDE or the RRDE have been obtained using the explicit finite-difference technique (62,67,70). This technique as applied to the RDE solves the partial differential equation describing the transient response to a potential step:

$$\frac{\partial c}{\partial t} = D \frac{\partial^2 c}{\partial z^2} - v_z \frac{\partial c}{\partial z}$$ [9]

The solution to this equation describes the time-dependent relaxation to steady state. A good approximation to the steady-state solution is obtained at a suitably large value of t. As Eddowes has pointed out, obtaining the solution to equation [7] by repetitive solution of equation [9] a function of time is very inefficient (82). The description of the relaxation of the system to steady-state after the application of a potential step is of little practical value. Indeed, most of the advantages of the RDE enumerated in the preceding section are

predicated on the attainment of steady state.

Given the experimental and computational advantages associated with the steady-state RDE, applications to electrochemical kinetic problems are surprisingly few in number and comparatively recent in origin. The merit in solving for the steady-state case was first suggested by Britz (84) who used the finite-difference method* to solve the basic convective-diffusion equation [7]. Eddowes solved the same equation by finite-difference and by the polynomial-approximation technique of orthogonal collocation (82). In the same work, the latter technique was used to solve a second-order kinetic problem involving multi-step charge transfer in micellar solutions. Chapman has also applied orthogonal collocation to the steady-state RDE (88) including a very recent treatment of the second-order EC-catalytic mechanism (69).

In the present work, the boundary value problems posed by the pseudo-first-order and second-order EC-catalytic mechanisms at the RDE were solved numerically by the technique of orthogonal collocation. An introduction to orthogonal collocation appears in Appendix I. The

---

*The distinction between explicit and implicit techniques does not apply to ordinary, as opposed to partial, differential equations.

mathematical formulation of the boundary-value problems follows that used by Eddowes to describe the mass-transport-limited case (82). The formulation and numerical solution of the latter problem are recounted in Appendix 1. That exercise serves to expose the foundations upon which the solutions to the kinetic problems rest. It also serves to illustrate, in some detail, the application of orthogonal collocation.

C. Numerical Solution for the Pseudo-First-Order EC-Catalytic Mechanism

Although the relationship between the magnitude of the catalytic current and the rate constant of the catalyst/substrate reaction for the pseudo-first-order case is of limited utility, it served as a convenient starting point for the solution of the second-order case. The pseudo-first-order case has been solved independently by at least three different analytical approximations (46,80,95). These solutions provide a useful check on the validity of the numerical solution.

1. Formulation of the Boundary Value Problem

The reaction scheme describing the EC-catalytic mechanism for the case of a reduction is:

$$P + ne^- \rightleftharpoons Q \qquad [10]$$
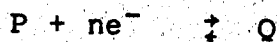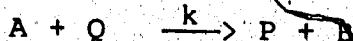
$$A + Q \xrightarrow{k} P + B \qquad [11]$$

The rate of the electrochemical reaction [10] is assumed to be sufficiently fast that the current flow in the absence of substrate is limited only by the rate of transport of P to the electrode surface. The substrate A is taken to be present in large excess so that a pseudo-first-order rate constant, $k' = k[A]$, may be defined for reaction [11].

The formulation of the problem follows the approach outlined in Appendix 1 for the mass-transport-limited case. The differential equations describing the steady-state concentrations of species P and Q as a function of z, the distance normal to the electrode surface, are:

$$D_P \frac{d^2 c_P}{dz^2} - v_z \frac{dc_P}{dz} + k' c_Q = 0 \qquad [12]$$

$$D_Q \frac{d^2 c_Q}{dz^2} - v_z \frac{dc_Q}{dz} - k' c_Q = 0 \qquad [13]$$

where D_P and D_Q are the diffusion coefficients for P and Q, c_P and c_Q are the respective concentrations, and v_z is the axial velocity given by equation A-3 of Appendix 1. The terms in equations [12] and [13] represent mass-

transfer by diffusion, by convection, and by the chemical reaction [11] respectively. The boundary conditions are the same as those given in Appendix 1 for the mass-transport-limited case . At $z = 0$,

$$D_P \frac{dc_P}{dz} + D_Q \frac{dc_Q}{dz} = 0$$

$$c_P(0)/c_Q(0) = \exp(\Psi)$$

where $\Psi = (nF/RT)(E^{\circ\prime} - E)$. At $z = \infty$,

$$c_P(\infty) = \text{the bulk concentration of P.}$$

$$c_Q(\infty) = 0.$$

Equations [12] and [13], when normalized in the fashion described in Appendix 1, become:

$$\bar{D}_P \frac{d^2 C_P}{dz^2} + 23.997\ z^2 \frac{dC_P}{dz} + 13.029\ \bar{k}'\ C_Q = 0 \qquad [14]$$

$$\bar{D}_Q \frac{d^2 C_Q}{dz^2} + 23.997\ z^2 \frac{dC_Q}{dz} - 13.029\ \bar{k}'\ C_Q = 0 \qquad [15]$$

The dimensionless pseudo-first-order kinetic parameter $\bar{k}'$ is defined as

$$\bar{k}' = \left(\frac{\nu}{D_M}\right)^{1/3} \left(\frac{k'}{\omega}\right) \qquad [16]$$

where D_M is the larger of D_P and D_Q. The normalized diffusion coefficients are defined as $\bar{D}_P = D_P/D_M$ and $\bar{D}_Q = D_Q/D_M$.* The boundary conditions become:

$$\text{At } Z = 0, \quad \bar{D}_P \frac{dC_P}{dZ} + \bar{D}_Q \frac{dC_Q}{dZ} = 0 \ ,$$

$$C_P(0)/C_Q(0) = \exp(\psi).$$

$$\text{At } Z = 1, \quad C_P(1) = 1,$$

$$C_Q(1) = 0.$$

2. Numerical Solution by Orthogonal Collocation

Applying the technique of orthogonal collocation as described in Appendix 1 transforms the problem to the following system of simultaneous linear equations:

$$\sum_{j=0}^{N} (\bar{D}_P B_{ij} + 23.997 (z_i)^2 A_{ij}) C_P(z_j)$$

$$+ 13.029 \ \bar{k}' \ C_Q(z_j) =$$

$$- (\bar{D}_P B_{i,N+1} + 23.997 (z_i)^2 A_{i,N+1}) \qquad [17]$$

---

*In many cases the diffusion coefficients of P and Q may be taken as equal, that is $\bar{D}_P = \bar{D}_Q = 1$.

$$\sum_{j=0}^{N} (\bar{D}_Q B_{ij} + 23.997 \ (z_i)^2 A_{ij}) \ C_Q(z_j)$$

$$- 13.029 \ \bar{k}' \ C_Q(z_j) = 0 \hspace{3cm} [18]$$

for i = 1 to N. The boundary conditions at Z = 1 have been included in the above equations. To these 2N equations in 2N+2 unknowns $C_P(z_j)$, $C_Q(z_j)$ must be added the boundary conditions at Z = 0.

$$\sum_{j=0}^{N} A_{0,j} \ (\bar{D}_P C_P(z_j) + \bar{D}_Q C_Q(z_j)) = 0 \hspace{2cm} [19]$$

$$C_P(0)/C_Q(0) = \exp(\psi) \hspace{3cm} [20]$$

For computational purposes, it is convenient to reduce the size of the system of equation by prior elimination of the last two equations. Toward that end the following three functions are defined

$$F_k(i,j) = B_{ij} + 23.997 \ z_i^2 A_{ij}/\bar{D}_k, \text{ where } k = P \text{ or } Q.$$

$$G(i,j) = \frac{A_{1,j} \ \exp(\psi)}{A_{1,1}(\bar{D}_Q + \bar{D}_P \ \exp(\psi))} \ F_P(i,1)$$

$$H(i,j) = \frac{A_{1,j}}{A_{1,1}(\bar{D}_Q + \bar{D}_P \ \exp(\psi))} \ F_Q(i,1)$$

In terms of these functions, the system of equations is expressed as:

$$\sum_{j=1}^{N} [F_P(i,j) - \bar{D}_P G(i,j)] C_P(Z_j)$$

$$- [\bar{D}_Q G(i,j) + 13.029 \, \bar{k}'] C_Q(Z_j)$$

$$= \bar{D}_P G(i, N+2) - F_P(i,N+2), \quad \text{for } i = 1 \text{ to } N \qquad [21]$$

and

$$\sum_{j=1}^{N} [F_Q(i,j) - \bar{D}_Q H(i,j) - 13.029 \, \bar{k}'] C_Q(Z_j)$$

$$- \bar{D}_P H(i,j) C_P(Z_j) = \bar{D}_P H(i,N+2) \quad \text{for } i = 1 \text{ to } N$$

$$[22]$$

The program RDECRI was written to generate and solve the above system of equations as a function of the parameters N, $\bar{k}'$, $\bar{D}_P$, and $\bar{D}_Q$. A listing of the program appears in Appendix II. The solution consists of the concentrations of P and Q at the N collocation points. From these values the concentration gradient for species P and hence the current flow at the electrode can be computed using equations A-14 and A-15 from Appendix I.

It is convenient to present the numerical solution to the problem in the f̶̶̶̶̶̶ working curve such as that shown in Figure 9. ̶̶̶̶̶̶̶̶̶̶less current function R is
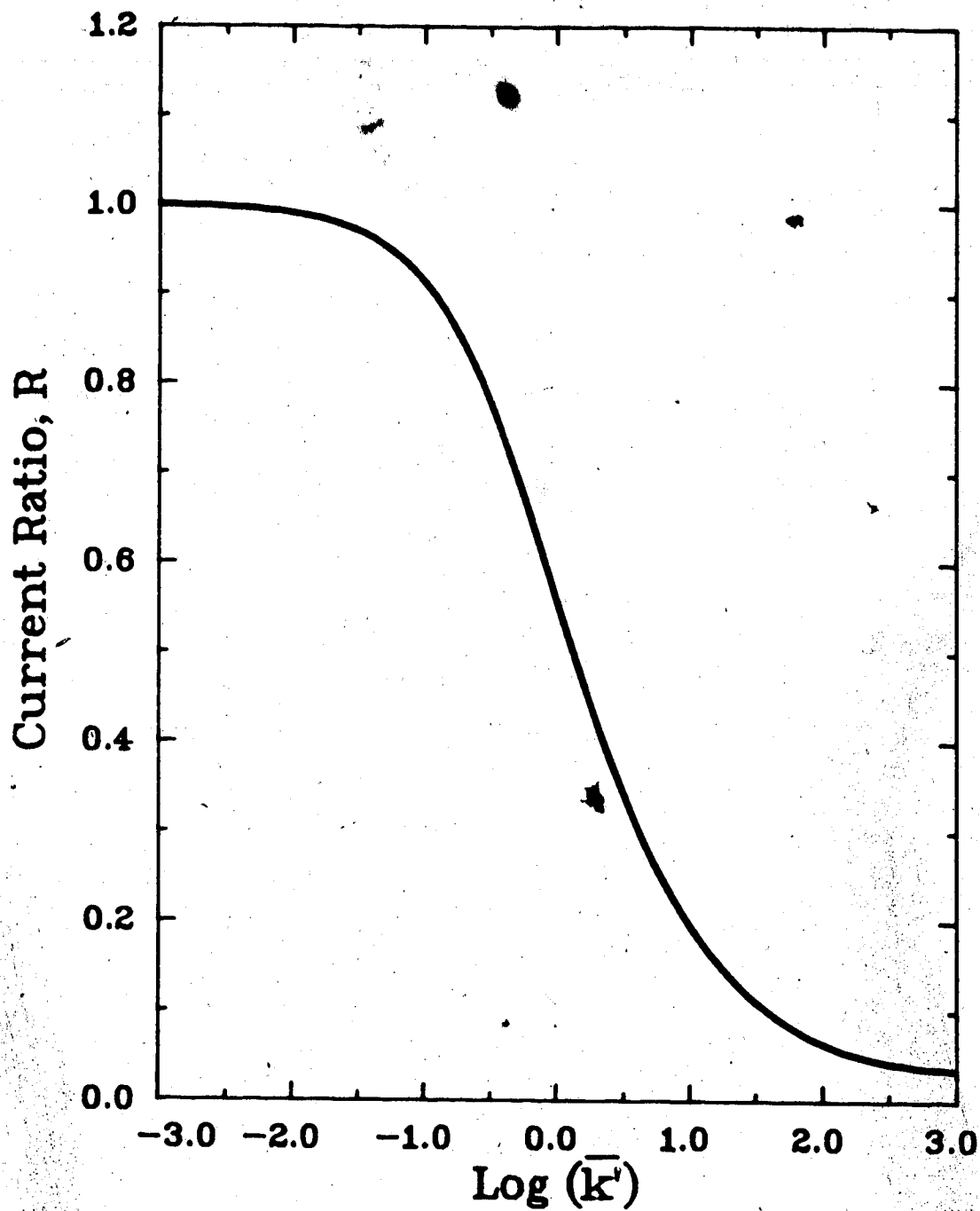
Figure 9. Working Curve for the Pseudo-First-Order EC-Catalytic Mechanism at the Rotating Disk Electrode. $N = 8$, $D_P = D_Q$.

defined as

$$R(\bar{k}') = i_O/i(\bar{k}')$$

where i_O denotes current observed in the absence of
substrate $(\bar{k}' = 0)$. The working curve consists of a plot
of the current function R versus the common logarithm of
the kinetic parameter $\bar{k}'$. The program ECR1WC, which
appears in Appendix II, was used to generate working
curves for the pseudo-first-order EC-catalytic
mechanism. To determine a rate constant experimentally, R
is measured as a function of the angular velocity of the
electrode ω and the corresponding values of $\bar{k}'$ are read
from the appropriate working curve. By plotting $\bar{k}'$ versus
$1/\omega$ according to equation [16], a pseudo-first-order rate
constant for reaction [11] is obtained.

3. Comparison with Approximate Analytical Solutions

The three approximate analytical solutions to the
problem of the pseudo-first-order EC-catalytic mechanism
are listed in Table 5. To facilitate comparison, each of
the equations has been used to generate a working curve of
the sort obtained above. The results, together with the
numerical solution, appear in Figure 10. The numerical
solution is in excellent agreement with the equation of

Table 5. Approximate Analytical Solutions for the Pseudo-First-Order EC-Catalytic Mechanism at the RDE.

Haberland and Landsberg (46)

$$R = \frac{\tanh (1.61 \ (\bar{k}')^{1/2})}{1.61 \ (\bar{k}')^{1/2}}$$

Opekar and Beran (95)[a]

$$R^3 + 1.63 \ \bar{k}' \ R^2 - 1 = 0$$

Pleskov and Filinovskii (78)

$$R = \frac{(3.10 + 1.61^2 \ \bar{k}')^{1/2}}{1.65 + 1.61^2 \ \bar{k}'}$$

a. Equation has been altered to conform to a 1:1 reaction stoichiometry.
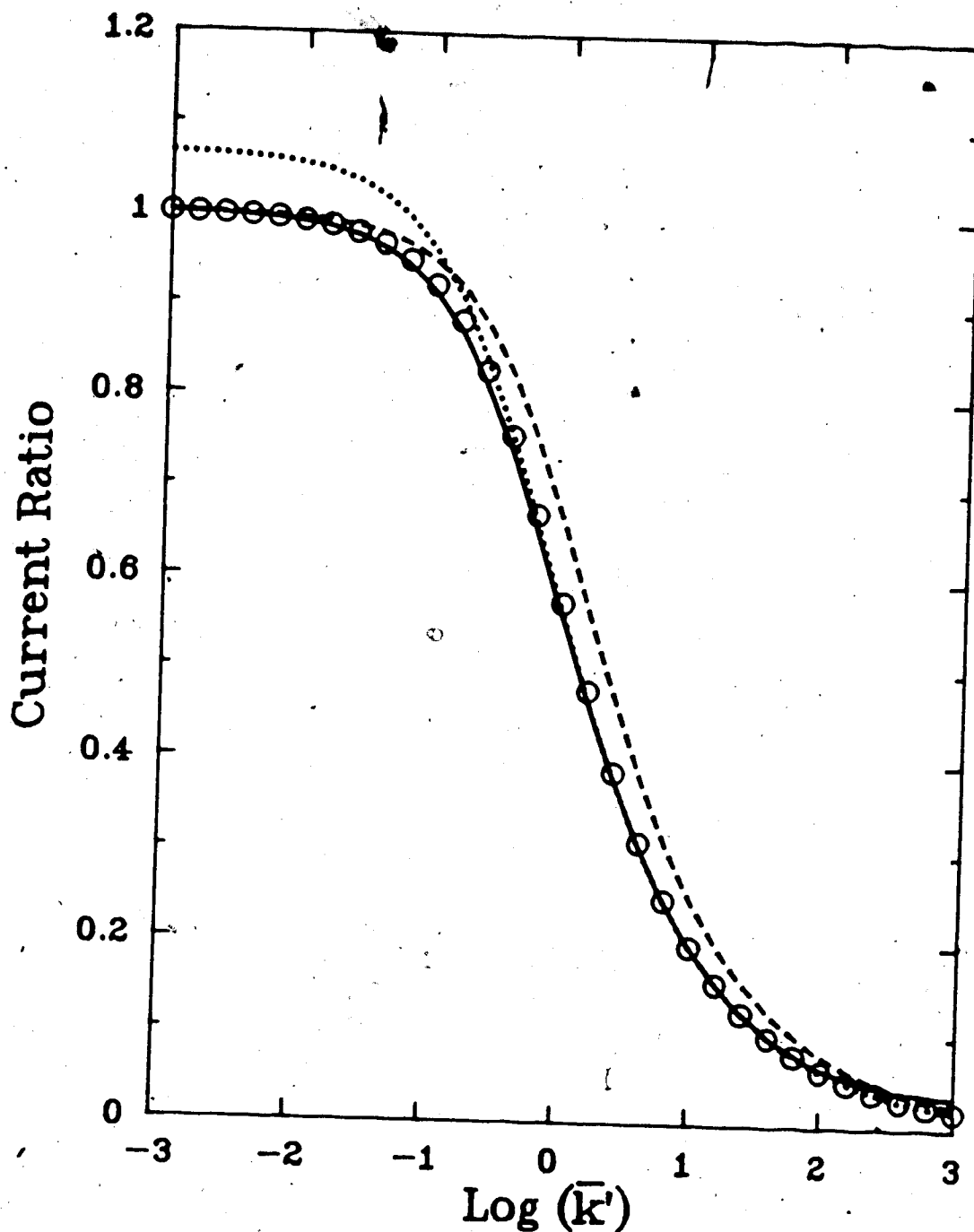
Figure 10. Working Curves for the Pseudo-First-Order EC-Catalytic Mechanism at the Rotating Disk Electrode. Approximate analytical solutions: o o o o o Haberland and Landsberg (46);·········· Pleskov and Filinovskii (78); ————— Opekar and Beran (95); Numerical solution: Orthogonal collocation, N = 8.

Haberland and Landsberg throughout the useful range of the
working curve. Good agreement is also obtained for the
equation of Pleskov and Filinovskii for $\log(\bar{k}') > -1$. The
divergence at low $\bar{k}'$ is not unexpected as the latter
authors report that their approximation yielded a value
for the Levich constant ($\bar{k}' \neq 0$) which was 6% high. Thus
as $\bar{k}'$ approaches 0, R approaches the limit of 1.06
observed in Figure 10.

The working curve obtained using the equation of
Opekar and Beran agrees poorly with the previous
results. The discrepancy is such that rate constants
obtained using this equation are some 50 to 60% larger
than those predicted by the other solutions.

A further test of the validity of the numerical
solution lies in comparison with the analytical solution
for the limiting case of large $\bar{k}'$. For $\bar{k}' > 10$, the
region over which concentrations change appreciably is
confined to Z < 0.1. As a consequence of the parabolic
dependence of axial velocity on distance, the convective
term in equation [12] may be neglected and the resulting
equation solved analytically. The solution was first
obtained by Koutecky and Levich (96):

$$i = nFA\,(D_p\,k')^{1/2}\,c_p(\infty) \qquad\qquad [23]$$

From this equation it follows that:

$$R(\bar{k}') = 0.62048/(\bar{k}')^{1/2} \qquad [24]$$

The logarithmic form of equation [24] is plotted as the solid line in Figure 11. The numerical solution for N = 8 appears as the dashed line in the same figure.

It is apparent from Figure 11 that as log $\bar{k}'$ increases without bound, the value of R obtained numerically approaches a non-zero limit. The source of the problem is revealed by plots of concentration profiles as a function of $\bar{k}'$ (Figure 12). For large values of $\bar{k}'$, the concentration gradient at the electrode surface is so steep that it can no longer be accurately represented by the approximation polynomial. The polynomial still fits the differential equation at the collocation points, but it fails to do so elsewhere.

One solution to the problem of large $\bar{k}'$ is to increase the degree of the approximation polynomial. Such an approach proved unsatisfactory, however. Increasing the degree from 10 to 20 extended the range of accurate representation by only one unit of log($\bar{k}'$) at a cost of a 500% increase in storage required and a 700% increase in execution time. Further, there is an upper limit to the value of N that machine computation can accommodate.
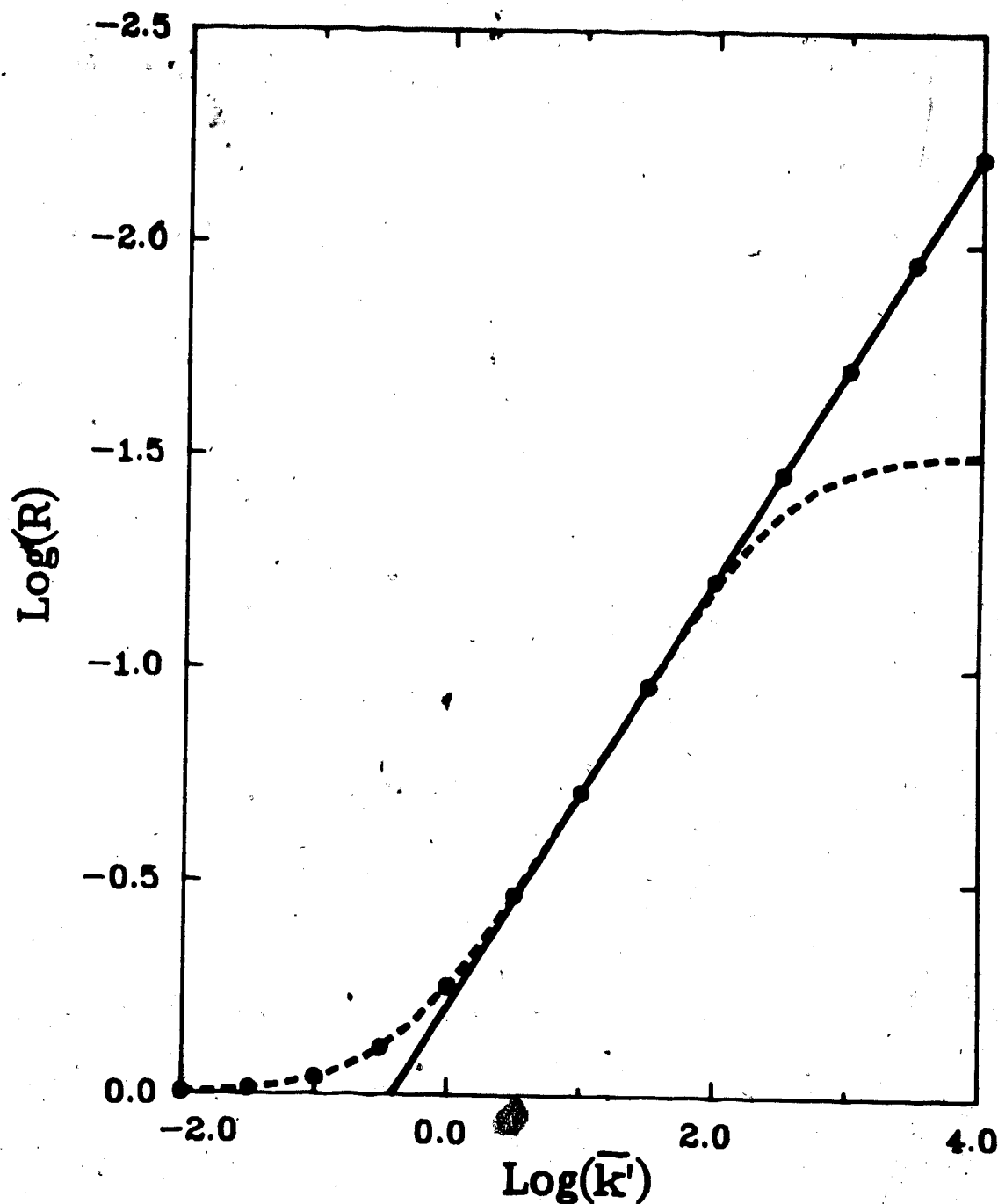
Figure 11. Current Ratio as a Function of the Kinetic Parameter for the Pseudo-First-Order EC-Catalytic Mechanism at the Rotating Disk Electrode. ———— Limiting equation of Koutecky and Levich (96); — — — — Solution by orthogonal collocation, N = 8; • • • • • Solution by orthogonal collocation with variable distance normalization, N = 8.
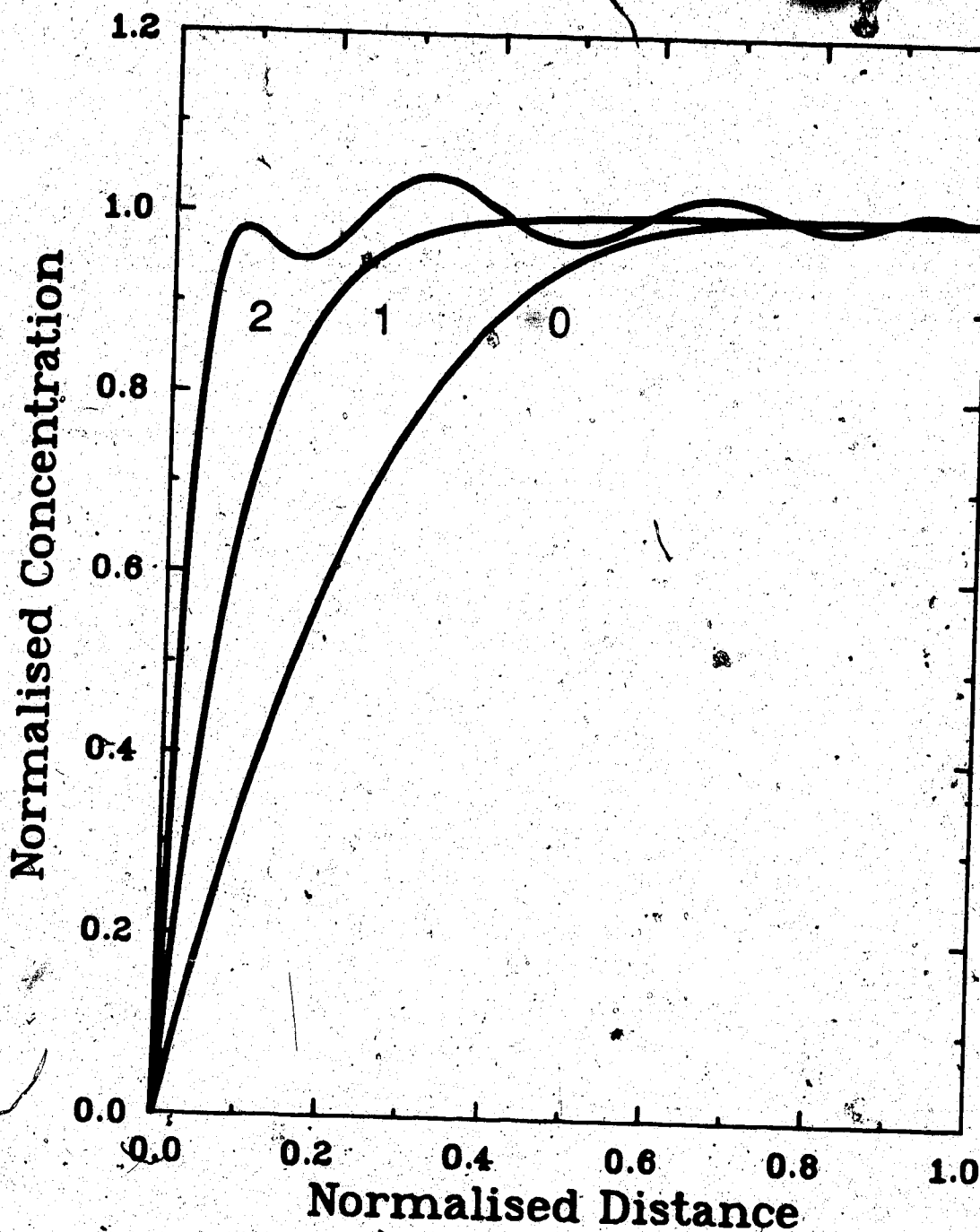
Figure 12. Concentration Profiles of Species P for the
Pseudo-First-Order EC-Catalytic Mechanism as a
Function of the Kinetic Parameter $\bar{k}'$, $D_P = D_Q$,
$N = 8$. The number to the right of each curve
denotes the value of log ($\bar{k}'$).

According to one source, the limit is met for double

precision calculations at about N equals 22 to 24 (86).

. A better approach to the problem of large $\bar{k}'$ consists

of re-definition of the interval over which the solution

is to be approximated. As discussed in Appendix I,

distances were normalized with respect to the transport

boundary layer. The thickness of the layer is given by z_T

$= C_T D^{1/3} \nu^{1/6} \omega^{-1/2}$ where C_T equals 3.61. For large $\bar{k}'$ the

value assigned to C_T is varied according to the value of

$\bar{k}'$. For a given value of $\bar{k}'$, there is a fairly broad

range over which C_T may be varied without significantly

affecting the accuracy of the numerical result. Figure 13

shows that for $\bar{k}' = 1000$, essentially the same value of R

is obtained for $C_T = 1/16$ to 1. Outside this range R

varies greatly, being overestimated when C_T is too large

and underestimated when C_T is too small. Unsuitable

choices for C_T result in oscillatory concentration

profiles if C_T is too large and in significant

concentration gradients at the outer boundary (Z = 1) if

it is too small.

A guideline for defining the thickness of the

transport boundary layer can be derived from equation [23]

which predicts the reaction layer thickness μ as

$\mu = (D/k')^{1/2}$ (96). In terms of the kinetic parameter,

$\bar{k}'$, this becomes $\mu = D^{1/3} \nu^{1/6} \omega^{-1/2}/(\bar{k}')^{1/2}$. If the
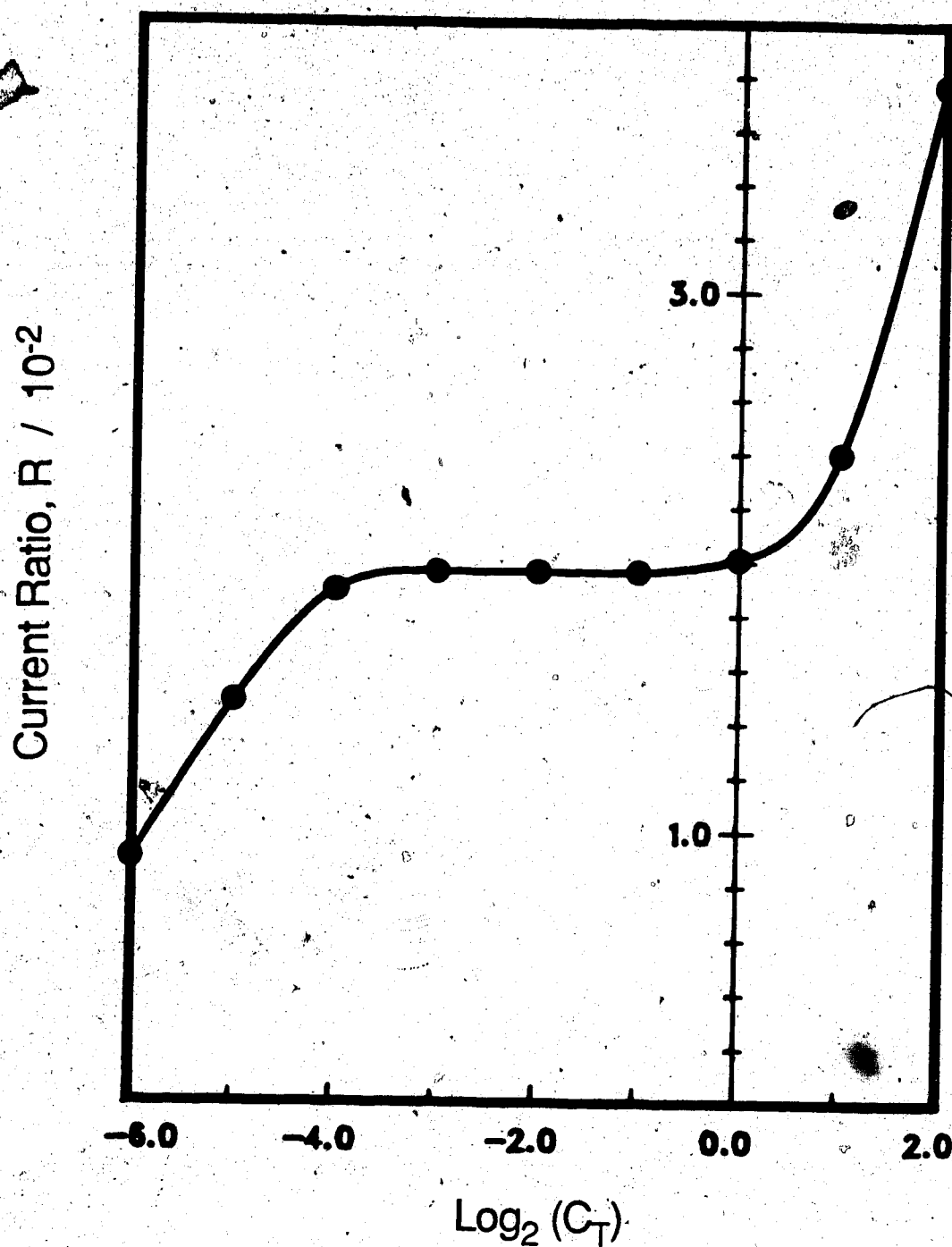
Figure 13. Current Ratio as a Function of the Thickness of the Transport Boundary Layer. $N = 8$, $\log(\bar{k}') = 3$.

transport boundary layer is taken as $2\ \mu$, then $C_T =$ $2/(\bar{k}')^{1/2}$ For $\bar{k}' = 1000$, $\log_2(C_T) = -4$. From Figure 13 it is apparent that 2μ is the minimum acceptable interval. Values up to 32μ serve equally well. Results obtained with $C_T = 8/(\bar{k}')^{1/2}$ are also shown in Figure 11. They are in good agreement with the limiting equation for $\bar{k}' > 5$. This definition of the transport boundary layer thickness is optionally available in the program ECR1WC.

D. Numerical Solution for the Second-Order EC-Catalytic Mechanism

As noted in Chapter II, a number of interesting examples of the EC-catalytic mechanism are not subject to the theoretical treatment for the pseudo-first-order mechanism. In these cases experimental limitations, such as the limit on electrode rotation speed or that on substrate solubility, require reaction [11] to proceed as an overall second-order reaction. The electrochemical determination of rate constants therefore requires a theoretical treatment accommodating the higher reaction order.

The second-order EC-catalytic mechanism differs from the pseudo-first-order case only in that the concentration

of substrate within the transport boundary layer can no longer be considered constant. This has two important consequences. First, a differential equation describing the substrate concentration must be included in the mathematical description of the mechanism. Second, the variability of substrate concentration means the boundary value problem is non-linear and the numerical solution is therefore somewhat more complicated.

1. Formulation of the Boundary Value Problem

The reaction scheme describing the EC-catalytic mechanism is given by equations [10] and [11]. The normalized differential equations describing the second-order mechanism at the RDE are:

$$-D_P \frac{d^2 C_P}{dz^2} + 23.997 \ z^2 \ \frac{dC_P}{dz} + 13.029 \ \bar{k} \ C_A C_Q = 0 \qquad [25]$$

$$-D_Q \frac{d^2 C_Q}{dz^2} + 23.997 \ z^2 \ \frac{dC_Q}{dz} - 13.029 \ \bar{k} \ C_A C_Q = 0 \qquad [26]$$

$$-D_A \frac{d^2 C_A}{dz^2} + 23.997 \ z^2 \ \frac{dC_A}{dz} - 13.029 \ \bar{k} C_A C_Q = 0 \qquad [27]$$

where the second-order kinetic parameter $\bar{k}$ is defined as

$$\bar{k} = (\frac{\nu}{D_M})^{1/3} \frac{k \, c_P(\infty)}{\omega}$$

[28]

As before, D_M denotes the largest of D_P, D_Q and D_A. Note that the definition of $\bar{k}$ includes the bulk concentration of catalyst $c_P(\infty)$ rather than that of substrate as is the case for the pseudo-first-order kinetic parameter $\bar{k}'$ (equation [16])..

boundary conditions for equations [25] and [26] are the same as those described in connection with equations [14] and [15] for the pseudo-first-order case. The boundary conditions for equation [27] describing the substrate are:

At $Z = 0$, $\frac{dC_A}{dZ} = 0$ and

at $Z = 1$, $C_A(1) = c_A(\infty)/c_P(\infty)$.

The former condition corresponds to no direct electrochemical reduction of A at the disk surface. The latter, which is the normalized bulk concentration of substrate, is subject to experimental control.

2. Iterative Numerical Solution by Orthogonal Collocation

The boundary value problem is transformed to a set of 3N algebraic equations in 3N unknown concentrations $C_P(z_j)$, $C_Q(z_j)$ and $C_A(z_j)$, $j = 1$ to N, in the manner described in Appendix 1. The equations are given by:

$$\sum_{j=1}^{N} [F_P(i,j) - \bar{D}_P G(i,j)]C_P(z_j)$$

$$- [\bar{D}_Q G(i,j) - 13.029 \bar{k} C_A(z_j)]C_Q(z_j)$$

$$= \bar{D}_P G(i,N+2) - F(i,N+2), \text{ for } i = 1 \text{ to } N \qquad [29]$$

$$\sum_{j=1}^{N} [F_Q(i,j) - \bar{D}_Q H(i,j) - 13.029 \bar{k} C_A(z_j)]C_Q(z_j)$$

$$- \bar{D}_P H(i,j)C_P(z_j) = \bar{D}_P H(i,N+2), \text{ for } i = 1 \text{ to } N$$

$$[30]$$

$$\sum_{j=1}^{N} [F_A(i,j) - \frac{A_{1,j}}{A_{1,1}} F(i,1) - 13.029 \bar{k} C_Q(z_j)]C_A(z_j)$$

$$= [\frac{A_{1,N+2}}{A_{1,1}} F(i,1) - F(i,N+2)]C_A(1), \text{ for } i = 1 \text{ to } N$$

The functions F, G and H are those defined previously in connection with equations [21] and [22]. Once again the equations describing the boundary conditions have already been eliminated.

The nonlinearity in the kinetic terms of equations [25] through [27] gives rise to a system of algebraic equations which must be solved iteratively. To begin the process, initial estimates are required for the concentrations at the collocation points of the reduced catalyst $C_Q(Z_j)$ and of the substrate $C_A(Z_j)$. Initial values of $C_Q(Z_j)$ are taken to be those obtained for the corresponding mass-transport-limited case ($k = 0$). Initial values of $C_A(Z_j)$ are all set equal to the bulk concentration $C_A(1)$. These values are used to compute the coefficients of the kinetic terms. The system of equations [29] to [31] is then solved and the new values obtained for $C_Q(Z_j)$ and $C_A(Z_j)$ are used to recalculate the coefficients of the kinetic terms. This procedure is repeated until the desired degree of convergence is attained. In practice, iteration was stopped as soon as the sum of the squares of the corrections to the concentrations $C_P(Z_j)$, $C_Q(Z_j)$ and $C_A(Z_j)$ fell below 10^{-8}.

As the iterative procedure was rather time-consuming, a number of steps were taken to optimize the computation procedure and to speed program execution. The system of equations [29] to [31] was initially represented by a 3N by 3N coefficient matrix. However, because the 2N equations describing C_P and C_Q are linked to the N equations describing C_A only through the nonlinear kinetic

term, it was possible to solve the two systems independently and thus, to effect savings in both storage and execution time. This device also had the unforeseen and happy consequence of substantially reducing the number of iterations required to attain convergence.

Further savings in storage and execution time were obtained by carrying out all the calculations using single precision arithmetic. A comparison of representative results obtained by single and double precision programs is given in Table 6. Values for P agree to five places as one might expect given the convergence criterion. In addition to being six times faster, the single precision program could accommodate a larger degree of collocation polynomial (maximum $N = 24$) than the double precision program (maximum $N = 18$).

Another attempt to improve execution times, this time by reducing the number of iterations required for convergence, involved implementation of the Newton-Raphson iteration technique (98). A brief description of this technique follows. Given trial solutions $C_P(z_i)$, $C_Q(z_i)$ and $C_A(z_i)$, $i = 1$ to N:

1. Vectors of residuals L_P, L_Q and L_A are calculated by substituting the trial solution into the left hand side of equations [29] to [31] and subtracting the right hand side.

Table 6. Iterative Solutions of the Second-Order EC-Catalytic
Mechanism at the RDE.

i) Simple Iteration[a]

	Single Precision			Double Precision		
$\bar{k}$	Iterations	Time (s)	R	Iterations	Time (s)	R
0.1	4	8	0.919256	4	49	0.919254
1.0	8	16	0.672226	8	98	0.672223
10.0	16	32	0.517236	16	194	0.517235

ii) Newton-Raphson Iteration

	Damped[b]			Undamped[c]		
$\bar{k}$	Iterations	Time (s)	R	Iterations	Time (s)	R
0.1	10	14	0.919264	9	13	0.919252
1.0	16	22	0.672220	49	65	0.672211
10.0	43	58	0.517213	–	>900	–

a. Program parameters: $N = 8$, $\bar{D}_P = \bar{D}_Q = \bar{D}_A = 1$, $\gamma = 1$, $D/v = 0$.

b. $\alpha = 0.25$.

c. $\alpha = 0.0$.

2. Vectors of correction terms M_P, M_Q and M_A are calculated by dividing the residual vector by the Jacobian matrix for the corresponding system of equations. This is equivalent to solving the following set of equations:

$$\sum_{j=1}^{N} [F_P(i,j) - \bar{D}_P G(i,j)] \, M_P(z_j) = L_P(z_i)$$

$$\sum_{j=1}^{N} [F_Q(i,j) - \bar{D}_Q H(i,j) - 13.029 \, \bar{k} \, C_A(z_j)] \, M_Q(z_j)$$
$$= L_Q(z_i)$$

$$\sum_{j=1}^{N} [F_A(i,j) - A_{1,j} F(i,1)/A_{1,1} - 13.029 \, \bar{k} \, C_Q(z_j)] \, M_A(z_j)$$
$$= L_A(z_i)$$

3. The next approximation to the solution is calculated by subtracting the correction terms from the present trial solution, e.g. $C_P'(z_i) = C_P(z_i) - M_P(z_i)$ and similarly for C_Q and C_A.

4. The procedure is repeated until the desired degree of convergence is attained.

The anticipated benefit of the Newton-Raphson iteration, that is, the reduction of the number of iterations required for convergence, was not realized in practice. The algorithm had an unfortunate tendency to oscillate about the desired solution and, while it did converge, it possessed poorer convergence properties than the simple iteration described previously. Some results are shown in Table 6. It was found that the oscillations could be damped and the convergence properties improved by employing a weighted average in the calculation of the next approximation (82). Step three in the Newton-Raphson procedure becomes

$$C_P'(Z_i) = \alpha\, C_P(Z_i) + (1-\alpha)(C_P(Z_i) - M_P(Z_i))$$

and similarly for C_Q and C_A. The parameter α is chosen empirically; for the problem at hand, $\alpha = 0.25$ was found to give the fastest convergence. Results for the damped Newton-Raphson iteration are shown in Table 6; they remain inferior to those obtained by simple iteration. Employing double precision arithmetic made no difference in the results obtained.

Based on the [illegible] work, it was concluded that simple

iteration and si[illegible] precision arithmetic afforded the

optimum solution [illegible] the problem of the second-order

EC-catalytic me[illegible]nism at the RDE. The program RDECR2 in

Appendix II implements this solution.

Solutions to equations [29] through [31] may be used

to compute current as a function of the kinetic parameter

$\bar{k}$ and thus, to generate working curves of the sort

obtained for the pseudo-first-order case. However, an

additional parameter is required for the second-order

working curve. It is the normalized bulk concentration of

substrate $C_A(1)$, sometimes referred to as the excess

factor and denoted by the symbol γ (93). The solution to

the second-order EC-catalytic mechanism consists of a

family of curves, one for each value of γ. Three such

curves are shown in Figure 14. The program ECR2WC in

Appendix II was used to generate working curves for the

second-order case as a function of N, $\bar{D}_R$, $\bar{D}_Q$, $\bar{D}_A$, and γ.

Rate constants are evaluated using these curves in the way

described for the pseudo-first-order case.

As the substrate is no longer present in large excess

in the second-order case, it is subject to depletion at

large values of $\bar{k}$. So it is that the working curves shown

in Figure 14 approach finite limits with increasing $\bar{k}$.

These limits, whose values depend on γ, correspond to the
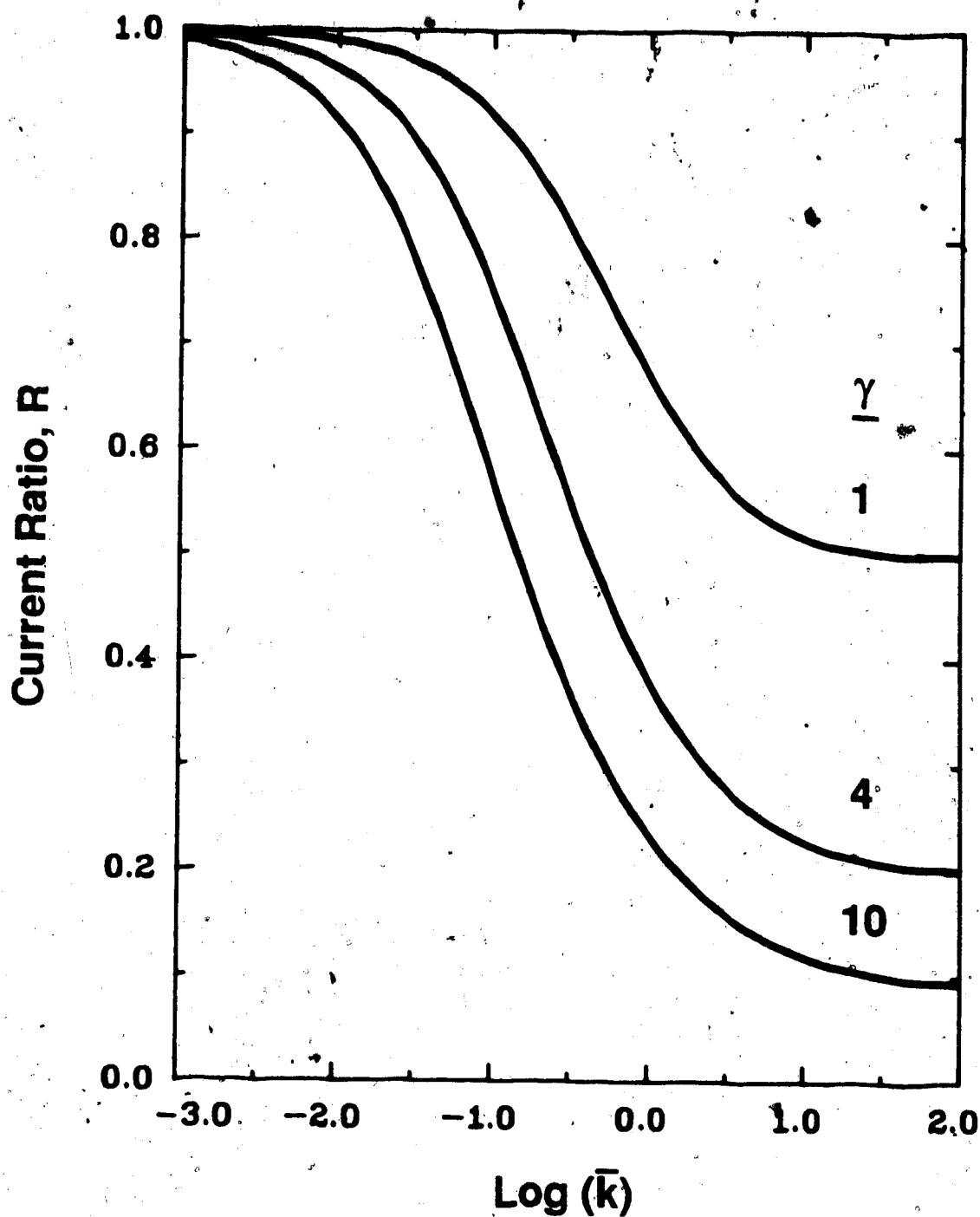
Figure 14. Working Curves for the Second-Order EC-Catalytic
Mechanism at the Rotating Disk Electrode. $D_P = D_Q = D_A$, $N = 8$. γ denotes the normalized bulk
concentration of the substrate.

sum of the mass-transport-limited fluxes of the catalyst

and the substrate.

3. Comparison with Approximate Analytical Solutions

To demonstrate the validity of the numerical solution

for the second-order EC-catalytic mechanism, it was

subjected to a number of tests. The first involved

comparison with results obtained for the pseudo-first-

order case. For this purpose, a second-order working

curve was generated for γ equals 100. It follows from the

definitions of the respective kinetic parameters that, for

$\gamma = 100$, $\bar{k}' = 100 \bar{k}$. Thus the second-order curve for $\gamma =$

100 should be equal to the pseudo-first-oder curve shifted

2 log units left. Such a comparison is shown in Figure

15. Good agreement is obtained throughout the useful

range of the working curves. There is a deviation at

large values of $\bar{k}$, however.

An approximate analytical solution to the second-

order mechanism which is valid for large values of $\bar{k}$ and γ

has been given by Andrieux et al. (93). These authors

defined a dimensionless current function, termed the

catalytic efficiency, as

$$CAT = (1/R - 1)/\gamma$$
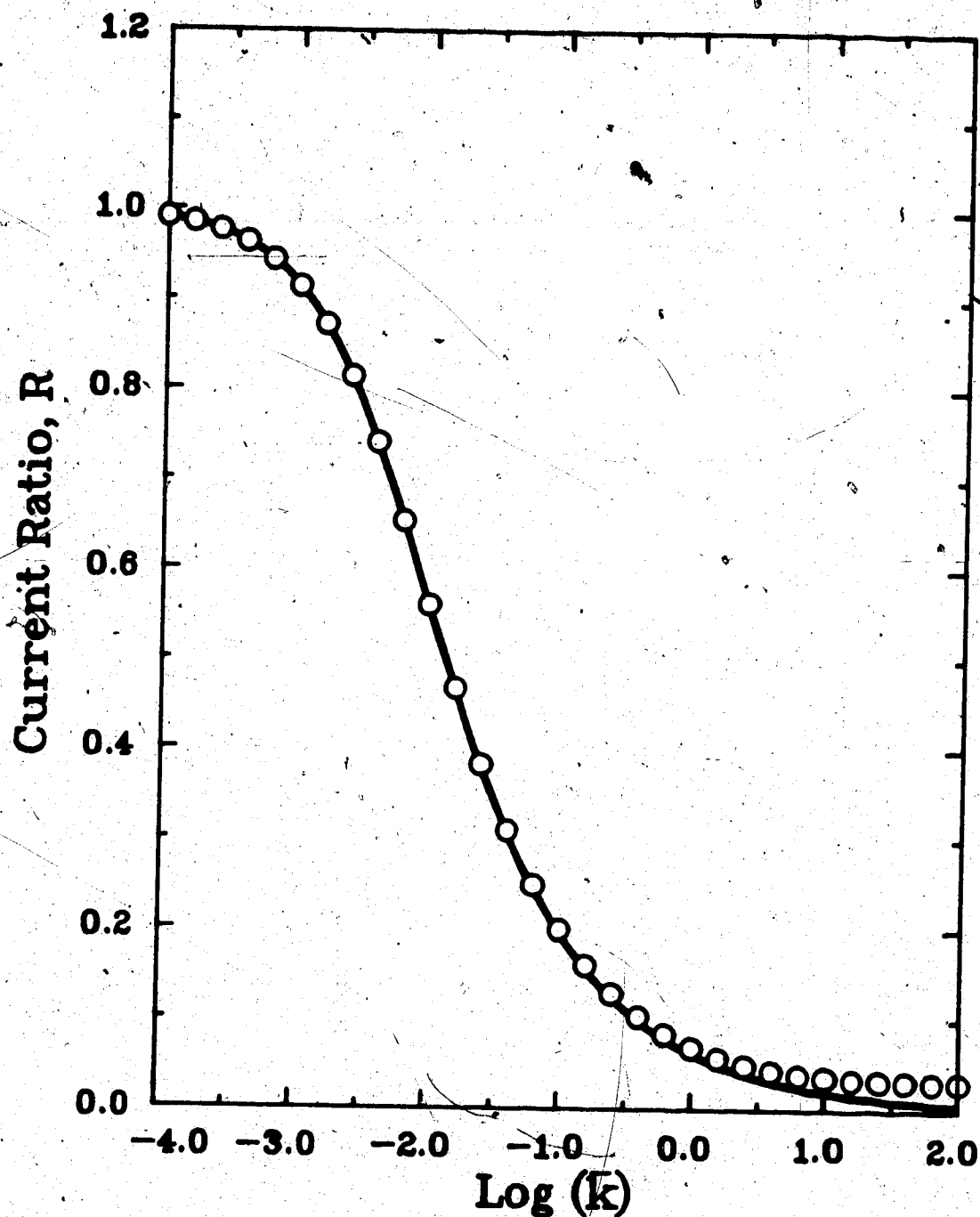
Figure 15. Working Curves for the EC-Catalytic Mechanism in the Presence of a Large Excess of Substrate. o o o o o Solution for the second-order case with $\gamma = 100$, $N = 8$ and $D_P = D_Q = D_A$. ———— Solution for the pseudo-first-order case with $D_P = D_Q$, $N = 8$. The latter curve has been shifted two units left to permit direct comparison.

where R is the current ratio and γ is the excess factor as
defined above. The limiting equation for CAT as a
function of γ and of the kinetic parameter as it is
defined in the present work is given by

$$CAT = \frac{2.59 \ \bar{k}}{2 \ \gamma} \ [(1 + \frac{4(1 + \gamma)}{2.59 \ \bar{k}})^{1/2} - 1] - \frac{1}{\gamma} \qquad [32]$$

This equation has been plotted in Figure 16 along with
corresponding results obtained from the pseudo-first-order
solution for large $\bar{k}'$ and from the second-order solution
for large $\bar{k}$ ($\gamma = 100$). The figure provides a striking
illustration of the limitations of the numerical solutions
when dealing with large values of $\bar{k}$ (or $\bar{k}'$) and γ. Only
the approximate analytical solution correctly predicts a
limiting value for CAT of one.

The deviation of the second-order solution from the
limiting equation [32] at large $\bar{k}\gamma$ results from the
inability of the approximation polynomial to accurately
represent concentration profiles between the collocation
points. This is the same problem encountered by the
pseudo-first-order solution at large $\bar{k}'$ and as before, re-
definition of the transport boundary layer is required.
In the second-order case, the problem is complicated by
presence of the differential equation describing the
substrate concentrations. Figure 17 shows concentration
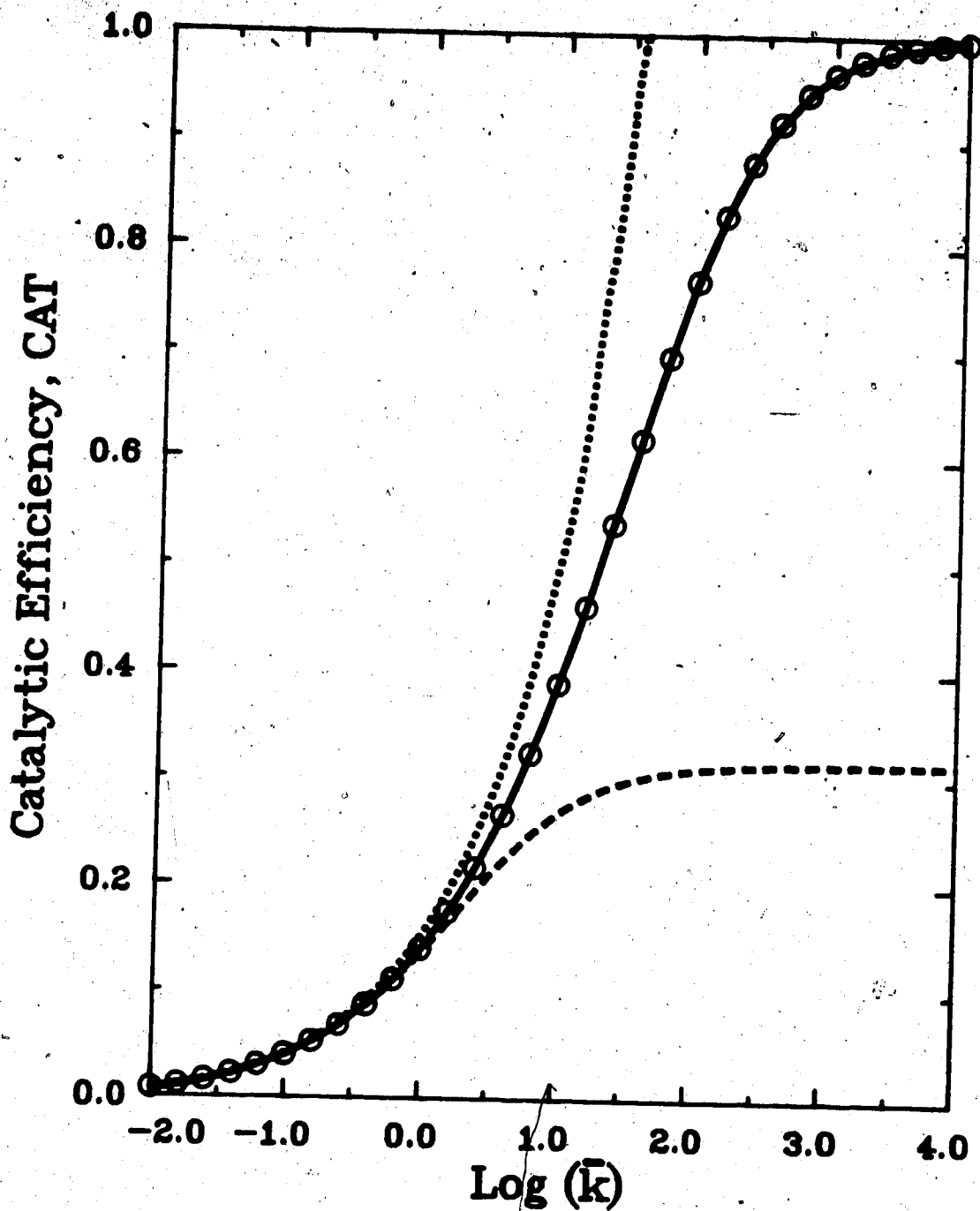
Figure 16. Comparison of Results for the Second-Order EC-
Catalytic Mechanism for the case of Large $k\gamma$.
$D_P = D_Q = D_A$. ———— Limiting equation of
Andrieux et al. (93) for $\gamma = 100$; ••••••••
Numerical solution for the pseudo-first-order
case with variable transport-boundary-layer
thickness, N = 8; ————— Numerical solution
for the second-order case by orthogonal
collocation with $\gamma = 100$, N = 8; o o o o o o
Numerical solution for the second-order case by
spline collocation with $\gamma = 100$, N = 8.
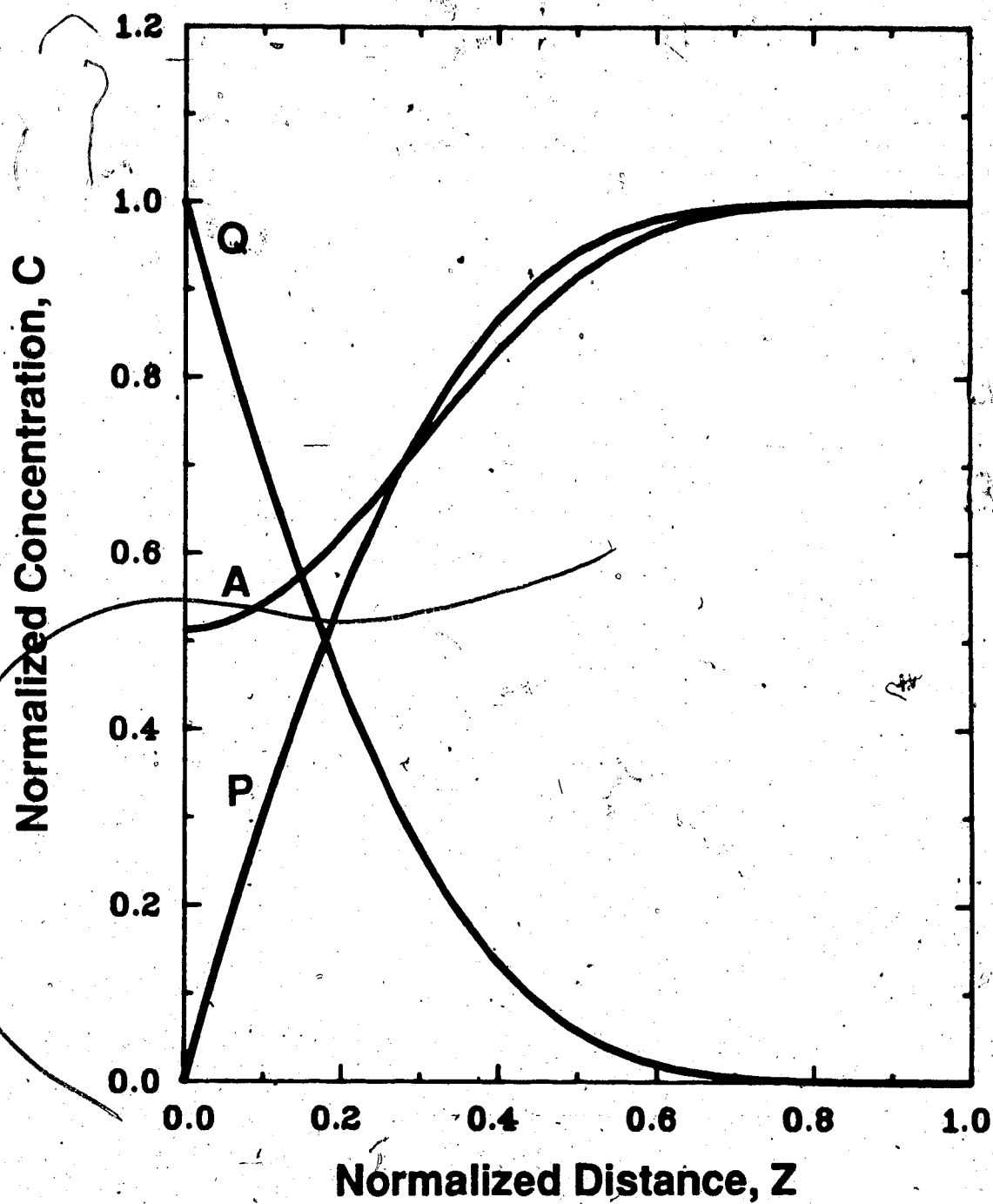
Figure 17. Concentration Profiles for the Species Involved
in the Second-Order EC-Catalytic Mechanism at the
Rotating Disk Electrode. Numerical solution by
orthogonal collocation with $N = 8$, $D_P = D_Q = D_A$,
$k = 1.$, $\gamma = 1$.

profiles of catalyst and substrate calculated for a small
value of the product $\bar{k}\gamma$. While the zone over which the
catalyst concentrations vary retreats toward the disk with
increasing $\bar{k}\gamma$, the same is not true of the zone over which
the substrate concentration varies. To cope with the
problem, it is necessary to define and use two scales of
distance, one for the substrate and one for the catalyst
couple. For the substrate, distance is normalized with
respect to the transport boundary layer as it was
previously defined, that is $Z_{T,S} = 3.61 \, D_M{}^{1/3}v^{1/6}\omega^{-1/2}$.
For the catalyst couple, the definition of the transport
boundary layer depends on the value of $\bar{k}\gamma$. By analogy
with the pseudo-first-order case, the outer boundary for
large values of $\bar{k}\gamma$ is taken as $2/(\bar{k}\gamma)^{1/2}$. For any value
of γ, the transport boundary layer for the catalyst couple
$Z_{T,C}$ is taken as the minimum of $Z_{T,S}$ and $2/(\bar{k}\gamma)^{1/2}$.

Since separate equation systems are maintained for
the catalyst couple and the substrate, the above
modification was readily incorporated in the collocation
solution. However, since the collocation points for the
two systems no longer coincide, it was necessary to solve
for the coefficients of the approximation polynomials for
A and Q and to compute Q concentrations at the A
collocation points and vice versa for each iteration.
While this procedure produced accurate solutions at small

k_γ with only a modest increase in storage requirements and execution time, it suffered from a pronounced tendency to oscillate at large k_γ.. The weighted averaging technique that was successfully applied to the Newton-Raphson iteration failed to ensure convergence in the present case.

4. Application of the Spline Technique to the Problem at Large $\overline{k}_\gamma$

A successful solution of the second-order EC-catalytic mechanism for large $\overline{k}_\gamma$ was obtained by application of the spline technique (98) to the problem. In this technique, a spline point z_s is introduced to divide the interval over which the solution to the differential equations is sought into two sub-intervals. The location of the spline point is chosen in such a way that the first sub-interval is confined to the region over which C_P and C_Q vary appreciably from their bulk values. To implement the spline technique, two new variables U and V are defined to represent normalized distance in the first and second sub-intervals respectively. The following definitions hold:

$$U = z/z_s \qquad\qquad V = (z - z_s)/(1 - z_s)$$
$$dU = dz/z_s \qquad\qquad dV = dz/(1 - z_s)$$

$$d^2U = d^2z/z_S^2 \qquad d^2V = d^2z/(1 - z_S)^2$$

In terms of the new variables, the normalized differential equations for species P become

$$\frac{d^2C_P}{dU^2} + 23.997 \ U^2 \ \frac{z_S^3}{\overline{D}_P} \ \frac{dC_P}{dU} + 13.029 \ z_S^2 \ \overline{k} \ C_A C_Q = 0 \qquad [33]$$

$$\frac{d^2C_P}{dV^2} + 23.997 \ \frac{(1 - z_S)}{\overline{D}_Q} \ [V(1 - z_S) + z_S]^2 \ \frac{dC_P}{dV}$$

$$+ \ 13.029 \ (1 - z_S)^2 \ \overline{k} \ C_A C_Q = 0 \qquad [34]$$

The continuity requirements at the spline point are:

$$\left(\frac{dC_P}{dU}\right)_{U=1} = \frac{z_S}{1 - z_S} \ \left(\frac{dC_P}{dV}\right)_{V=0}$$

$$C_P(U_1) = C_P(V_0)$$

Similar sets of equations can be written for species Q and A with due regard for the sign of the kinetic term.

Application of the orthogonal collocation technique transforms the problem into a set of 6N + 6 equations in 6N + 6 unknowns. The equations are given as follows:

Let $W_k(i,j) = B_{ij} + 23.997 \ U_i^2 Z_S^3 \ A_{ij}/\bar{D}_k$

$X_k(i,j) = B_{ij} + 23.997 \ (1-Z_S)[V_i(1-Z_S) + Z_S]^2 \ A_{ij}/\bar{D}_k$

where $k = P, Q$ or A.

For species P:

$$\sum_{j=0}^{N} W_P(i,j)C_P(U_j) + W_P(i,N+1)C_P(V_0)$$

$$+ 13.029 \ Z_S^2 \ \bar{k} \ C_A(U_i)C_Q(U_i) = 0, \ i = 1 \ \text{to} \ N \quad [35]$$

$$\sum_{j=0}^{N} X_P(i,j) \ C_P(V_j) + 13.029 \ (1-Z_S)^2 \ \bar{k} \ C_A(V_i)C_Q(V_i)$$

$$= -X_P(i,N+1), \ i = 1 \ \text{to} \ N \quad [36]$$

$$\sum_{j=0}^{N} A_{N+1,j} \ C_P(U_j) - A_{0,j} \ Z_S \ C_P(V_j)/(1-Z_S)$$

$$+ A_{N+1,N+1} \ C_P(V_0) = A_{0,N+1} \ Z_S/(1-Z_S) \quad [37]$$

For species Q:

$$\sum_{j=0}^{N} W_Q(i,j) \; C_Q(U_j) + W_Q(i,N+1) \; C_Q(V_0)$$

$$+ \; 13.029 \; z_S^2 \; \bar{k} \; C_A(U_i) \; C_Q(U_i) = 0, \; i = 1 \text{ to } N \quad [38]$$

$$\sum_{j=0}^{N} X_Q(i,j) \; C_Q(V_j) - 13.029 \; (1-z_S)^2 \; \bar{k} \; C_A(V_i) \; C_Q(V_i)$$

$$= 0, \; i = 1 \text{ to } N \quad\quad\quad [39]$$

$$\sum_{j=0}^{N} A_{N+1,j} \; C_Q(U_j) - A_{0,j} \; C_Q(V_j) \; z_S/(1-z_S)$$

$$+ \; A_{N+1,N+1} \; C_Q(V_0) = 0 \quad\quad\quad [40]$$

For species A:

$$\sum_{j=0}^{N} W_A(i,j) \; C_A(U_j) + W_A(i,N+1) \; C_A(V_0)$$

$$- \; 13.029 \; z_S^2 \; \bar{k} \; C_A(U_i) \; C_Q(U_i) = 0, \; i = 1 \text{ to } N \quad [41]$$

$$\sum_{j=0}^{N} X_A(i,j) \; C_A(V_j) - 13.029 \; (1-z_S)^2 \; \bar{k} \; C_A(V_i) \; C_Q(V_i)$$

$$= - X(i,N+1) \; C_A(1), \quad i = 1 \text{ to } N \qquad [42]$$

$$\sum_{j=0}^{N} A_{N+1,j} \; C_A(U_j) - A_{0,j} \; C_A(V_j) \; Z_S/(1-Z_S)$$

$$+ A_{N+1,N+1} \; C_A(V_0) = A_{0,N+1} \; C_A(1) \; Z_S/(1-Z_S) \qquad [43]$$

The boundary conditions at $Z = U = 0$ are:

$$\sum_{j=0}^{N} A_{0,j} \; (\bar{D}_P C_P(U_j) + \bar{D}_Q C_Q(U_j)) +$$

$$A_{0,N+1}(\bar{D}_P C_P(V_0) + \bar{D}_Q C_Q(V_0)) = 0 \qquad [44]$$

$$C_P(U_0) - \exp(\Psi) \; C_Q(U_0) = 0 \qquad [45]$$

$$\sum_{j=0}^{N} A_{0,j} \; C_A(U_j) + A_{0,N+1} \; C_A(V_0) = 0 \qquad [46]$$

To obtain a solution to equations [35] to [46], it is necessary to assign a value to the spline point Z_S. The approximation $Z_S = 2/(\bar{k}\gamma)^{1/2}$ is adequate only when the diffusivities of P, Q and A are equal. For the general case, a satisfactory location for the spline point is given by

$$Z_S = 4/(dC_P/dZ)_{Z=0} \qquad [47]$$

The reciprocal of the surface concentration of species P corresponds to a distance generally known as the thickness of the Nernst diffusion layer and denoted δ_N. At $Z = \delta_N$, a line of slope $(dC_P/dZ)_{Z=0}$ extrapolated from the origin intercepts the line defined by $C_P = 1$. The spline point as defined above is located at $Z = 4 \delta_N$; this interval was found to be quite sufficient to encompass the region over, which C_P and C_Q vary appreciably from their bulk values.

Although the formula for Z_S actually supposes that the solution to the system of equations is already known, this is not a problem in practice. Since the spline technique was used to generate working curves of the sort shown in Figure 14, Z_S for a given value of $\bar{k}$ could be calculated on the basis of the results for the previous point on the working curve. To start the process, Z_S' was initially set to 0.5 and a comparatively small value was selected for the initial value of $\bar{k}$ (less than 10). To avoid problems at small $\bar{k}\gamma$, Z_S was not allowed to exceed 0.5. Since the exact value of Z_S is not critical and since the value of δ_N does not change greatly from one point to the next for a reasonably well-defined working curve, this procedure proved satisfactory. The program,

ECR3WC was written to implement the spline collocation solution. A listing of the program appears in Appendix II. Results obtained with the program are shown in Figure 16; they are in excellent agreement with the limiting equation of Andrieux et al. (93).

The marked deviation observed for the pseudo-first-order solution in Figure 16 is a consequence of the fact that substrate consumption is no longer negligible at large k'. For k' greater than about 100, the pseudo-first-order solution predicts currents which are greatly in excess of those which the rate of substrate transport can sustain. While the pseudo-first-order solution has been made to agree with the limiting equation of Koutecky and Levich for large k' (Figure 11), there is an upper limit to the value of k' for which the assumption of unchanging substrate concentration in the transport boundary layer applies. The range of applicability of the limiting equation can be established by comparison with the results obtained by spline collocation. Such a comparison is shown in Figure 18. It is apparent that for γ equals 100 the limiting equation is only valid over a comparatively narrow range centered on log k' equals 1.
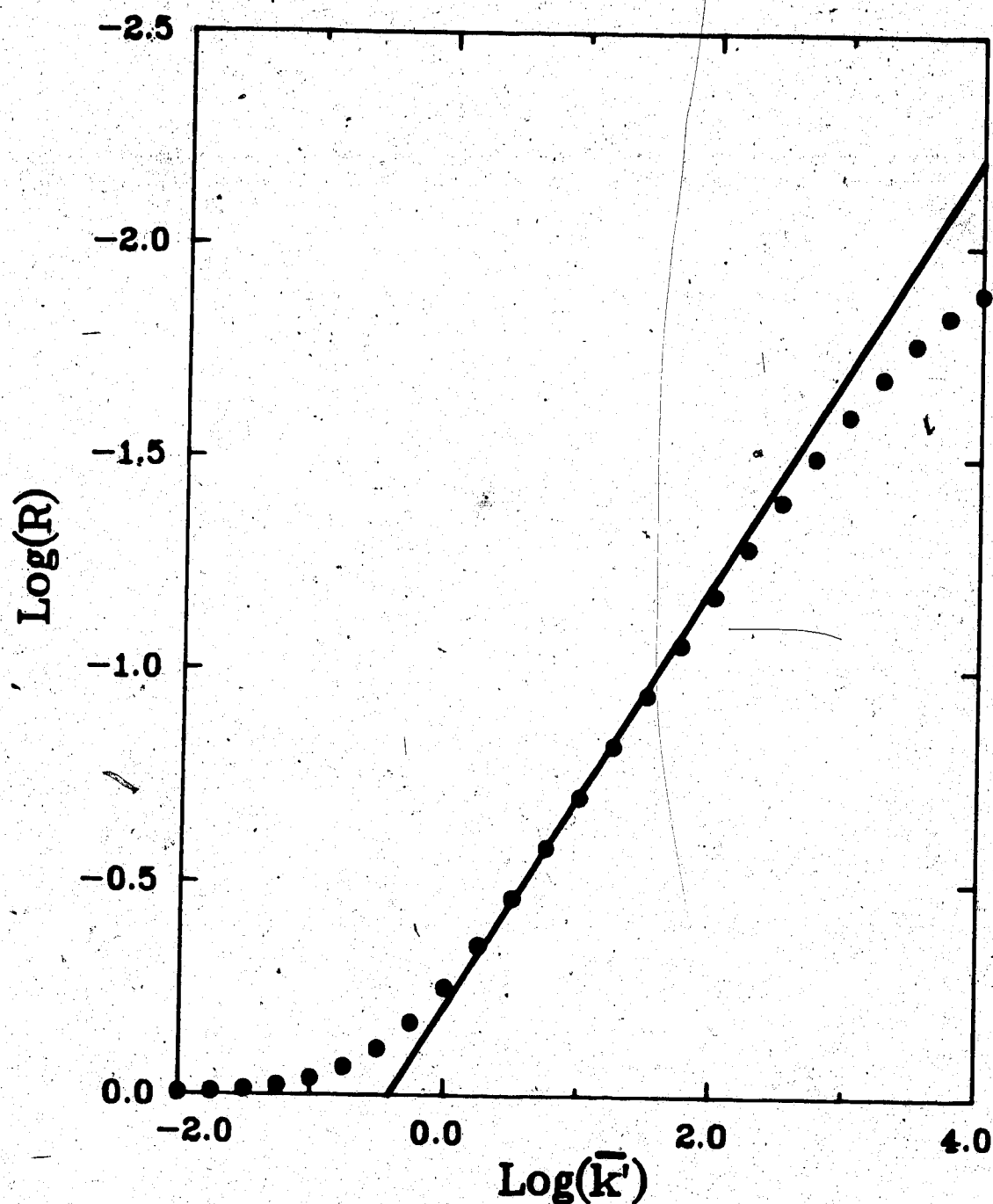
Figure 18. The Range of Applicability of the Limiting
Equation of Koutecky and Levich (96). _____
Limiting equation; • • • • • Numerical
solution by spline collocation with $D_P = D_Q = D_A$,
$N = 8$, $\gamma = 100$.

5. <u>Comparison with Other Numerical Solutions</u>

In 1980, Andrieux <u>et al.</u> published an approximate numerical solution for the second-order EC-catalytic mechanism in the context of steady-state and quasi-steady-state techniques, that is, the RDE and dc polarography (93). The solution was based on the Nernst approximation that concentration profiles are linear over a convective-diffusion layer defined, for the RDE, as $\delta_N = 1.61$ $D^{1/3} v^{1/6} \omega^{-1/2}$. This corresponds to $Z = 0.45$ in the present work. It was further assumed that the diffusion coefficients of all species were equal and that the convection term in the steady-state differential equations could be neglected. Table 7 compares the results obtained by this approximate numerical solution with those of the present work. The excellent agreement confirms the validity of the assumptions made by Andrieux <u>et al.</u>

Recently, working curves for the second-order EC-catalytic mechanism were published by Feldberg <u>et al.</u> (70) and by Machado and Chapman (69). The former authors used the time-dependent explicit finite-difference technique while the latter applied orthogonal collocation to the steady state equations. Samples of the results obtained, as measured from published working curves, are shown in Tables 8 and 9. Agreement among the various approaches is excellent.

Table 7. Comparison of Results for the Second-Order EC-Catalytic

Mechanism with those of Andrieux et al.

γ	Andrieux et al. (93)		This Work	
	$\log \bar{k}_A$ [a]	CAT [b]	$\log \bar{k}$	CAT [b]
1	0	0.27	-0.41	0.27
1	1	0.80	0.59	0.81
4	0	0.23	-0.41	0.24
4	1	0.70	0.59	0.69
10	0	0.19	-0.41	0.19
10	1	0.57	0.59	0.57
10	2	0.91	1.59	0.91

a. The kinetic parameter defined by Andrieux et al., denoted here by

$\bar{k}_A$, equals 2.57 $\bar{k}$.

b. $CAT = (1/R - 1)/\gamma$.

Table 8. Comparison of Results for the Second-Order EC-Catalytic

Mechanism with those of Feldberg et al.

Feldberg et al. (70)		This Work	
log $\bar{k}_F$ [a]	R	log $\bar{k}$	R

$(D_P = D_Q = D_A, \gamma = 1)$

0.0	0.64	-0.3	0.62
0.5	0.46	0.2	0.47
1.0	0.38	0.7	0.38
1.5	0.35	1.2	0.35
2.0	0.34	1.7	0.34

$(D_P = D_Q = 0.3 D_A, \gamma = 1)$

0.0	0.60	-0.3	0.60
0.5	0.41	0.2	0.41
1.0	0.29	0.7	0.29
1.5	0.23	1.2	0.23
2.0	0.20	1.7	0.21

a. The kinetic parameter defined by Feldberg et al., denoted here by

$\bar{k}_F$, equals $2\bar{k}$.

Table 9. Comparison of Results for the Second-Order EC-Catalytic

Mechanism with those of Machado and Chapman.

γ	Machado and Chapman (69)		This Work	
	$\log \bar{k}_M$ [a]	R	$\log \bar{k}$	R
1	0	0.78	-0.51	0.82
1	1	0.54	0.49	0.57
1	2	0.49	1.49	0.50
4	0	0.53	-0.51	0.53
4	1	0.27	0.49	0.28
4	2	0.20	1.49	0.21
10	0	0.35	-0.51	0.37
10	1	0.16	0.49	0.16
10	2	0.10	1.49	0.10

a. The kinetic parameter as defined by Machado and Chapman, denoted

here by $\bar{k}_M$, equals $3.24 \bar{k}$.

6. The Effect of Differing Substrate and Catalyst Diffusivities

A characteristic of the EC-catalytic reactions examined in this work is the marked difference between the diffusion coefficients of the catalyst species and that of the substrate. For example, the diffusion coefficient of oxygen in aqueous solution (2×10^{-5} cm^2/s (77)) is five to ten times that of typical organic catalyst compounds. The effect of such differences on working curves is considerable; some examples are shown in Figure 19. Accounting for such differences is essential to the determination of rate constants of solution reactions via the second-order EC-catalytic mechanism.

7. The Range of Accessible Reaction Rate Constants

Consideration of the working curves for the pseudo-first-order (Figure 9) and second-order (Figure 14) EC-catalytic mechanisms at the RDE allows one to establish the range of reaction rates accessible to the technique. From Figure 14, the upper limit on $\bar{k}$ appears to be approximately 100. Beyond this value the solution reaction is, for practical purposes, infinitely fast. The corresponding second-order rate constant depends on the values of ν, D, $C_p(\infty)$, and ω according to equation [28]. Typical values for ν and D are 10^{-2} cm^2/s and 10^{-5} cm^2/s
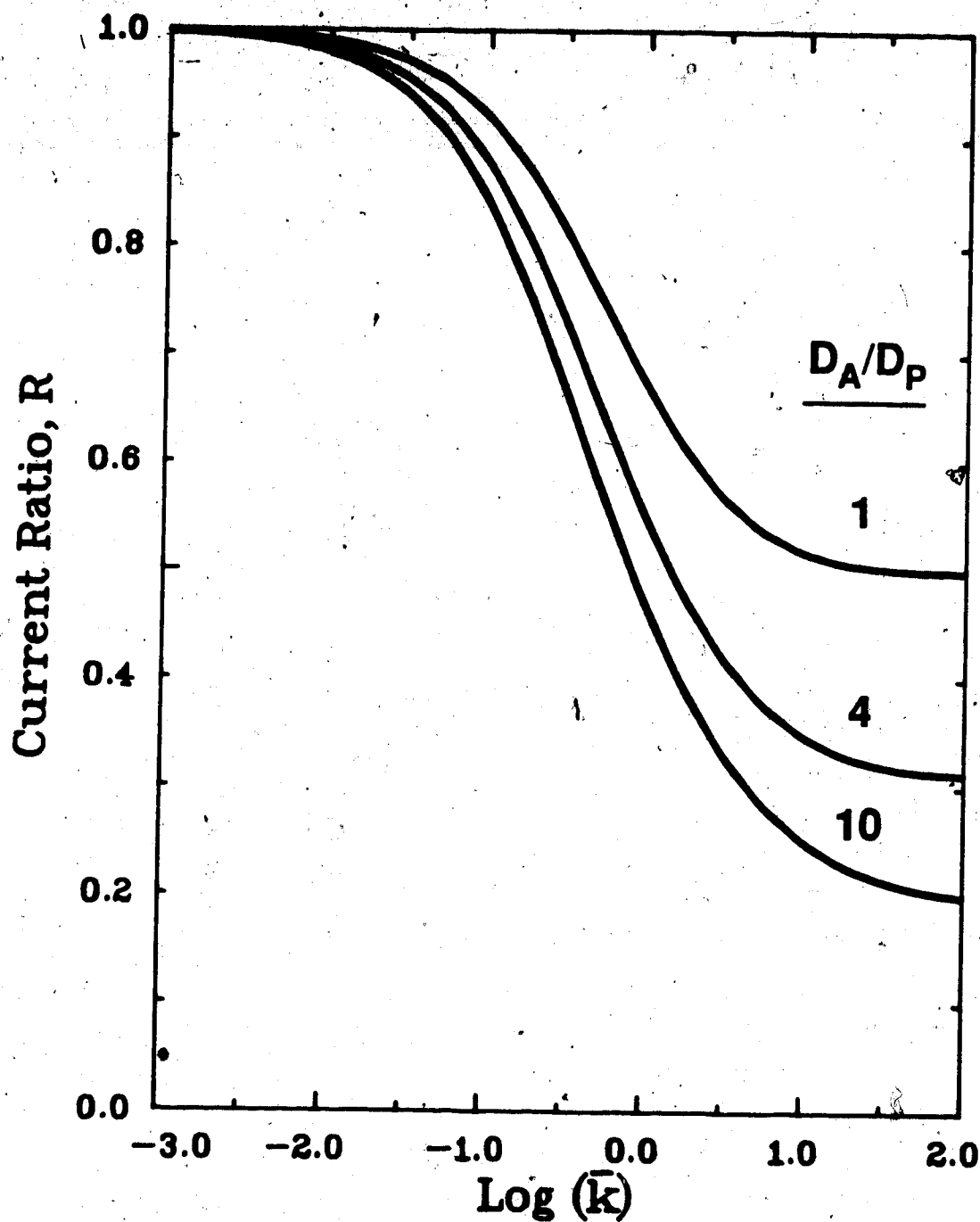
Figure 19. The Effect of Differing Catalyst and Substrate
Diffusivities on Working Curves for the Second-
Order EC-Catalytic Mechanism at the Rotating Disk
Electrode. Numbers above each curve denote the
ratio of the diffusion coefficient of the
substrate A to that of the catalyst P.

respectively. If the lower limit of catalyst concentration $c_p(\infty)$ is taken as 10^{-6} $\underline{M}$ and the upper limit on angular velocity of the electrode is taken as 1000 s^{-1} (9500 rpm), then the largest accessible second-order rate constant (corresponding to $\bar{k}$ equals 100) is 10^{10} $\underline{M}^{-1}s^{-1}$.

Similarly the smallest rate constant can be estimated from the lower limit of the pseudo-first-order working curve. From Figure 9, the smallest value of $\bar{k}$ producing a measurable current ratio (R < 0.95) is approximately 0.1. If the upper limit on substrate concentration is taken as 1 $\underline{M}$ and the lower limit on angular velocity as 10 s^{-1} (95 rpm), then by equation [16] the smallest accessible rate constant is 0.1 $\underline{M}^{-1}s^{-1}$.

Thus the rotating disk electrode used in conjunction with the numerical solutions for the EC-catalytic mechanism has the potential to measure an extraordinarily broad range of rate constants, spanning some eleven orders of magnitude. The upper limit of 10^{10} $\underline{M}^{-1}s^{-1}$ is more than one thousand times that of the best stopped-flow experiments. That a steady-state technique can access such rates is especially remarkable as the study of very fast reactions is generally confined to transient techniques such as temperature jump, flash photolysis and pulse radiolysis experiments.

CHAPTER IV

THE EC-CATALYTIC MECHANISM AT THE ROTATING DISK ELECTRODE. EXPERIMENTAL

A. Electrochemical Apparatus

The apparatus used for the electrochemical experiments is shown in Figure 8. The RDE system consisted of a Pine Model ASR2 Rotator (Pine Instrument Co., Grove City, PA) fitted with Model DT06 ring-disk electrodes. Electrode combinations employed included Pt disk/Pt ring, Au disk/Au ring and glassy carbon disk/Pt ring. (The ring electrodes were not used in any of the experiments described in this work.) Electrode dimensions were measured with a travelling microscope. The results are summarized in Table 10. Electrode rotation speeds were measured with a Cole-Parmer Model 8204-00 photo-tachometer (Cole-Parmer Instrument Co., Chicago, IL).

The electrochemical cell was taken from a Princeton Applied Research (PAR) dropping mercury electrode assembly. The central hole in the cell top was enlarged to accommodate the RDE. The cell bottom was water-jacketed for temperature control. Experiments were conducted at 25.0 $\pm$ 0.1°C unless otherwise noted. A

Table 10. Geometry of the Rotating Ring-Disk Electrodes.

Electrode[a] (Ser. No.)	Radii[b] r_1 (mm)	r_2 (mm)	r_3 (mm)	Disk Area (cm^2)
Pt/Pt (269)	3.8089±0.0016	4.0013±0.0019	4.2470±0.0011	0.45577±0.00038
Au/Au (392)	3.8279±0.0008	3.9857±0.0019	4.2415±0.0009	0.46033±0.00019
GC/Pt (2445)	3.7671±0.0014	3.9893±0.0025	4.2148±0.0018	0.44582±0.00033
Nominal Values[c]	3.82	3.99	4.22	0.4584

a. Disk material/ring material. GC = glassy carbon.

b. r_1, disk radius; r_2, inside ring radius; r_3, outside ring radius.

    Mean ±95% C.I. Values calculated from two pairs of diameter

    measurements made at 90° to each other.

c. "Operating Instructions for RDE 3 Potentiostat", Pine Instrument

    Co., Grove City, PA, p. 46.

30-cm, coiled Pt wire served as the counter electrode. It was kept in a separate compartment which was isolated from the test solution by a sintered glass frit. The reference electrode in all cases was an aqueous saturated calomel electrode (Radiometer Model K401). The input lead was shielded with a braided cable connected to ground.

Current-voltage and current-time curves were obtained using a Pine Model RDE3 bipotentiostat connected to an Omnigraphic Series 2000 X-Y recorder (Houston Instrument Co., Austin, TX). The best signal-to-noise ratio was obtained when the circuit common of the bipotentiostat was tied to earth (chassis) ground.

Before each experiment, the surface of the RDE was polished with an aqueous slurry of 3 μm alumina on a polishing cloth. The electrode was then cleaned ultrasonically, first in alcoholic KOH and then in 6 $\underline{M}$ HNO_3.

B. Control and Measurement of Dioxygen Concentrations

1. Deoxygenation Procedure

An important part of the determination of rate constants described in subsequent chapters involved measurement of mass-transport-limited currents in the absence of dioxygen. Dioxygen was removed from test

solutions by sparging with dinitrogen delivered through a glass tube terminating in a sintered glass frit which was immersed in the solution. After sparging for 15 minutes, dinitrogen flow was redirected so as to purge the cell atmosphere over the test solution. This excluded atmospheric dioxygen from the cell while the electro-chemical measurements were being made.

It was found that deoxygenation procedures adequate for normal polarographic purposes were not sufficient to reduce dioxygen concentrations to levels which were negligible in the context of the present study. Current-voltage curves recorded in acetonitrile were especially sensitive to residual dioxygen. At low concentrations, dioxygen gave rise to a characteristic reduction wave at -0.80 V vs SCE. To reduce dioxygen concentrations to negligible levels, a number of steps were required. First, and most important, was the elimination of dioxygen-permeable materials (in particular, Tygon tubing) from the dinitrogen delivery line. Copper tubing (1/4" o.d.) was used instead. It was connected to the glass fixtures by ground-glass ball-and-socket joints (standard taper 12/5). Copper-to-glass tubing joins were made with very short lengths of Tygon tubing secured with hose clamps. To provide reproducible flow control, a rotameter was installed on the dinitrogen delivery line.

To remove traces of dioxygen from the tank

dinitrogen, the gas was passed in series through two gas-scrubbing bottles each containing vanadous chloride solution in aqueous HCl plus some amalgamated zinc. To improve their efficiency, all gas-scrubbing bottles used were fitted with sintered glass frits. For work in non-aqueous solvents, water vapor was removed from the purified dinitrogen by passing it through a third bottle containing concentrated sulfuric acid. Before entering the electrochemical cell, the gas was passed through yet another gas-scrubbing bottle containing the same electrolyte as the test solution in order to saturate the gas with solvent vapor and thus to minimize evaporative losses from the test solution. This also served to remove any sulfuric acid droplets carried over from the drying bottle.

The vanadous chloride scrubbers were not well suited for use with nonaqueous solvents. At the high gas flow rates which were ultimately found necessary to exclude atmospheric dioxygen (see below), there was significant carryover of solution from one gas-scrubbing bottle to the next. In addition, the pressure required to force gas through four gas-scrubbing bottles caused problems with leakage. For work in nonaqueous solvents, the vanadous chloride dioxygen scrubbers were therefore abandoned in favor of hot copper turnings. A 1 inch by 18 inch glass

tube was packed with copper turnings and placed in a tube furnace at 450°C. Temperature was monitored using an iron-constantan thermocouple placed alongside the tube. The tube was purged with dinitrogen and the copper reduced by passing a stream of hydrogen gas through. When in use, dinitrogen gas at 5 psig flowed past the hot copper, through a rotameter and flow-control valve and then through a single gas-scrubbing tower containing the same electrolyte as the test solution. When not in use, the system remained pressurized and a slow flow of gas was maintained so as to exclude atmospheric dioxygen.

A major point of the entry of atmospheric dioxygen into the electrochemical cell was the port for the RDE, which could not be sealed due to the necessity of rotation. To minimize the flux of dioxygen through the port, a baffle was constructed as shown in Figure 20. It consisted of a liner for the port and a skirt attached to the electrode. Both were fashioned from small Nalgene bottles. To further reduce the clearances, appropriate parts were wrapped with Teflon tape. The arrangement served to greatly lengthen and narrow the diffusion path between the interior of the cell and the outside atmosphere.

Even with the baffle in place, comparatively high sparging and purging flow rates were required. Effective
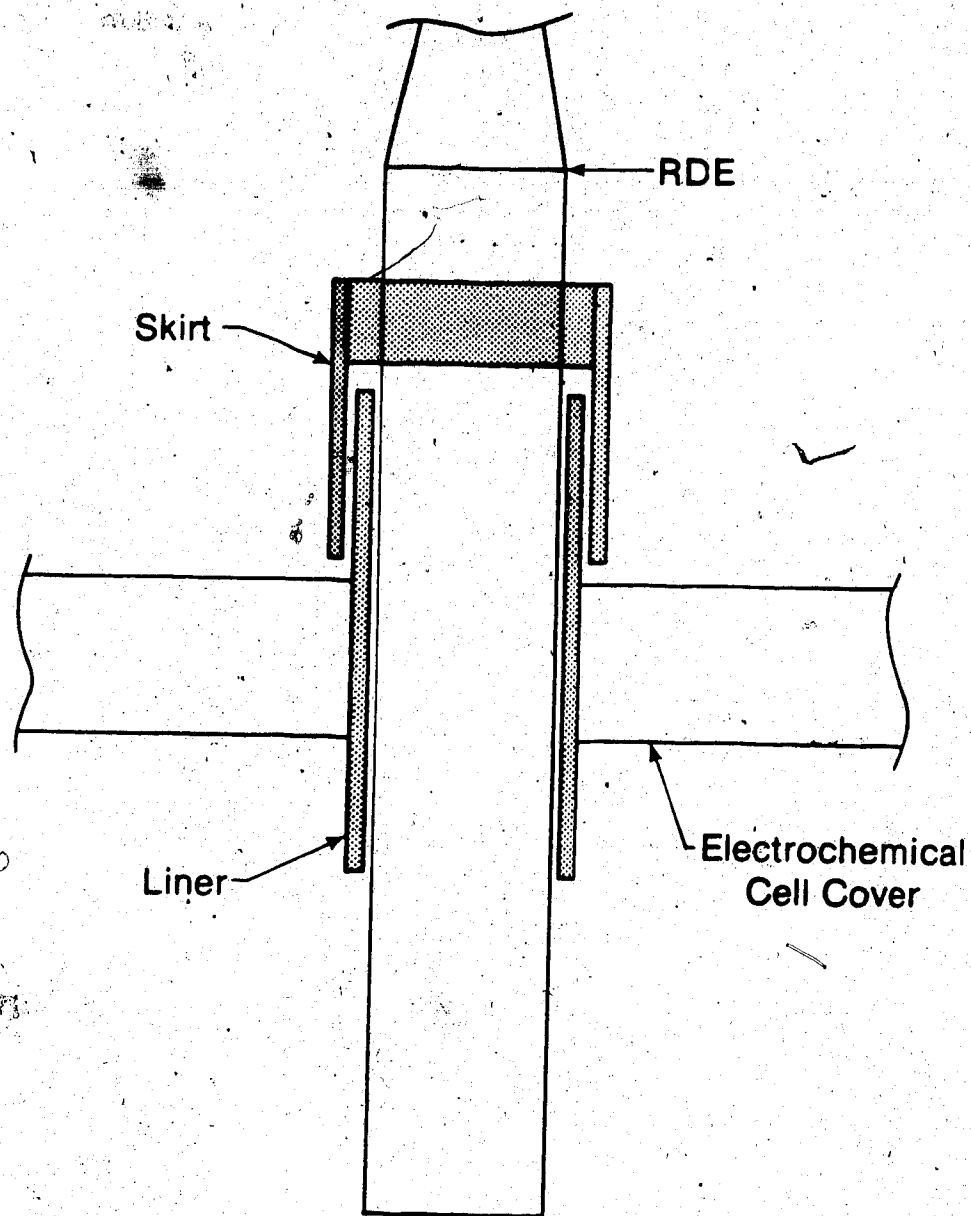
Figure 20. The Baffle Constructed for the RDE Entry Port in the Electrochemical Cell Cover.

exclusion of atmospheric dioxygen from the cell required gas flow rates greater than or equal to 400 mL/min. After sparging for 15 min at this rate, no discernable wave for dioxygen reduction was observed in acetonitrile. Based on data presented in the next chapter, it was concluded that the residual dioxygen level in sparged acetonitrile solutions was less than 5×10^{-7} $\underline{M}$. This concentration is 0.03% of that found in air-saturated solutions. This level could be maintained at electrode rotation speeds up to and including 3600 rpm.

2. The Gas Proportioning System

The dioxygen concentration of test solutions was varied by sparging with mixtures of dioxygen and dinitrogen. A block diagram of the gas control system is shown in Figure 21. Gas flows were metered and mixed with a Matheson R7300 gas proportioner (Matheson Co., East Rutherford, NJ) fitted with No. 600 and No. 601 rotameter tubes and with the corresponding HA1 and HA2 high-accuracy needle valves. To increase the available range of gas flow rates, the glass floats supplied with the rotameter tubes were replaced by stainless steel floats (1/8" stainless steel ball bearings). An essential feature of the gas proportioner design is the location of the flow control valves at the outlet of the rotameter tubes rather
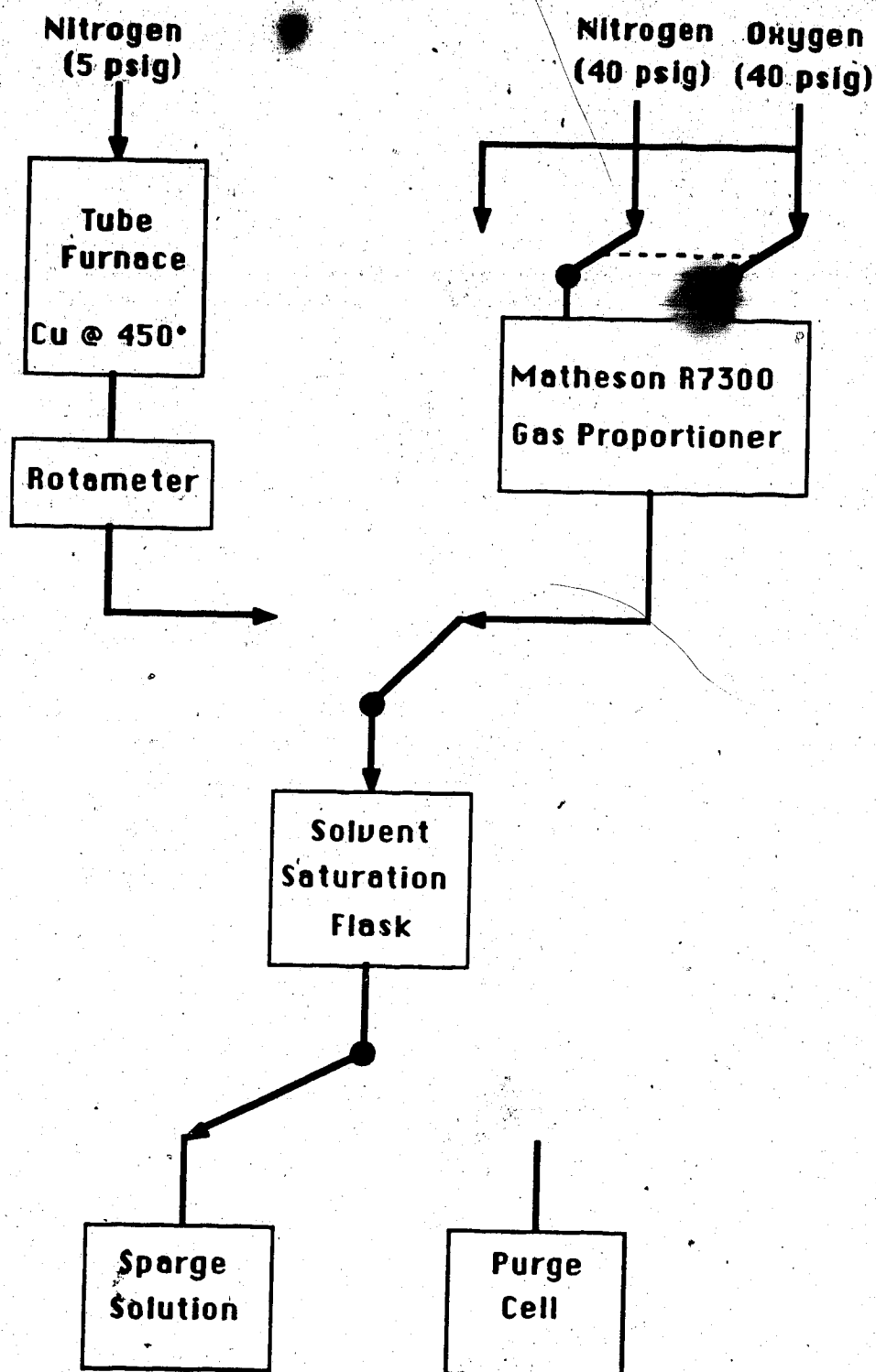
Figure 21. System for the Control of Dioxygen Concentrations in Test Solutions.

than at the inlets as is the usual practice. With the valves at the outlets, measured flow rates are much less sensitive to variations in downstream flow resistance such as that encountered when switching from sparging the solution to purging the cell. With the gas proportioner, only minor adjustments to the gas flows were required when switching between sparging and purging.

Inlet pressures to the gas proportioner were maintained at 40 psig with Matheson Model 8 gas regulators. Quick-connect couplings were used to connect the regulator outlets to the inlet lines; this facilitated exchange of cylinders. Gas mixtures were prepared from dinitrogen and one of dioxygen, air or a mixture of 2.1% dioxygen in dinitrogen. These gases, including the 2.1% mixture were obtained from Union Carbide. For the very lowest dioxygen concentrations, a mixture of 0.107% dioxygen in dinitrogen, obtained from Matheson, was used.

3. Calibration Procedures

The gas proportioning system was calibrated at selected flow ratios in each of the test electrolytes. Dioxygen concentrations were determined amperometrically at an RDE by the method of standard addition. Pure solvents, saturated with dioxygen at 25.0 ± 0.1°C and ambient pressure, served as the standards. In the case of

water at 25°C the concentration of dioxygen in a solution
in equilibrium with the gas at a partial pressure of 1 atm
was taken as 1.27×10^{-3} $\underline{M}$ (104). Some uncertainty exists
over the corresponding value for dimethylsulfoxide. The
IUPAC Solubility Data Series (105) quotes the following
values for the mole fraction of dioxygen in DMSO saturated
with the gas at 25°C and 1 atm: 1.09×10^{-4} (106) and 1.57
$\times 10^{-4}$ (107). The latter value was favored by Battino et
al. in their critical review of dioxygen solubilities
(108). The corresponding molar concentration, 2.2×10^{-3}
$\underline{M}$, is consistent with Sawyer's value of 2.1×10^{-3} $\underline{M}$
determined coulometrically in DMSO containing 0.1 M tetra-
ethylammonium perchlorate (TEAP) (109). Surprisingly,
there are no data in the literature pertaining to the
solubility of dioxygen in pure acetonitrile. Data are
available for solutions of electrolytes in acetonitrile,
however. Using coulometry, Sawyer found the dioxygen
concentration of 0.1 $\underline{M}$ TEAP in acetonitrile saturated with
dioxygen at 1 atm and 25°C to be 8.1×10^{-3} $\underline{M}$ (109). This
value is consistent with the work of Kolthoff and Coetzee
(110). They determined the concentration of dioxygen in
air-saturated acetonitrile containing 0.1 $\underline{M}$ $NaClO_4$ to be
$(1.6 \pm 0.1) \times 10^{-3}$ $\underline{M}$ by titrimetry. Using Sawyer's value
in conjunction with Henry's law, the concentration of
dioxygen in air-saturated 0.1 $\underline{M}$ TEAP in acetonitrile is

expected to be 1.7×10^{-3} M. In the present work, 0.1 M
TEAP in acetonitrile saturated with dioxygen together with
Sawyer's value for the dioxygen concentration was used as
the standard for measurements in acetonitrile solutions.

The actual concentration of dioxygen in the saturated
solvent at the atmospheric pressure prevailing at the time
of the experiment was calculated according to Henry's
law. Atmospheric pressure was measured with a Fortin-type
mercurial barometer (Princo Instruments, Inc.,
Southampton, PA). The partial pressure of dioxygen was
taken as the atmospheric pressure less the vapor pressure
of the solvent at 25°C: for water, 23.8 torr (104); for
dimethylsulfoxide, 0.6 torr (111) and for acetonitrile, 92
torr (112).

To calibrate the gas proportioner at a given flow
ratio, the appropriate gas cylinders were attached to the
inlet lines, the inlet pressures were adjusted to 40 psig
and the flow rates were set. To ensure that the total gas
flow was sufficient to exclude atmospheric dioxygen from
the electrochemical cell, the gas flow rate through the
larger of the two rotameter tubes was fixed at
approximately 400 mL/min (F = 100 on the rotameter
scale). Gas flow through the smaller rotameter tube was
then varied to obtain the desired dioxygen
concentration. After sparging for 15 minutes, the gas

flow was redirected to purge the cell atmosphere and the individual gas flow rates were readjusted if necessary.

Dioxygen concentrations were determined by measuring the mass-transport-limited current for dioxygen reduction at a rotating disk electrode using the method of standard addition. In the case of acetonitrile and dimethyl-sulfoxide electrolytes, a glassy carbon RDE held at a potential of -1.20 V vs SCE was used. As part of the analytical procedure, the limiting current for dioxygen reduction was measured as a function of rotation speed, typically at 100, 400, 900, and 1600 rpm. Current measurements were made by recording current as a function of time using a Houston Instruments X-Y recorder equipped with a Type 6 time-base module on the X-axis. Varying the rotation speed in steps gave rise to the type of i-t trace shown in Figure 22. Having established the rotation speed dependence of the limiting current, the standard addition experiment was performed. The electrode rotation speed was set to 900 or 1600 rpm to ensure thorough and reasonably rapid mixing. Once a steady-state current level was attained, an aliquot of the appropriate standard solution (typically 250 µL to 2 mL) was added via a port in the top of the electrochemical cell. Variable-volume pipets of the Eppendorf type were used to deliver the standard solutions. Significant losses of dioxygen, on
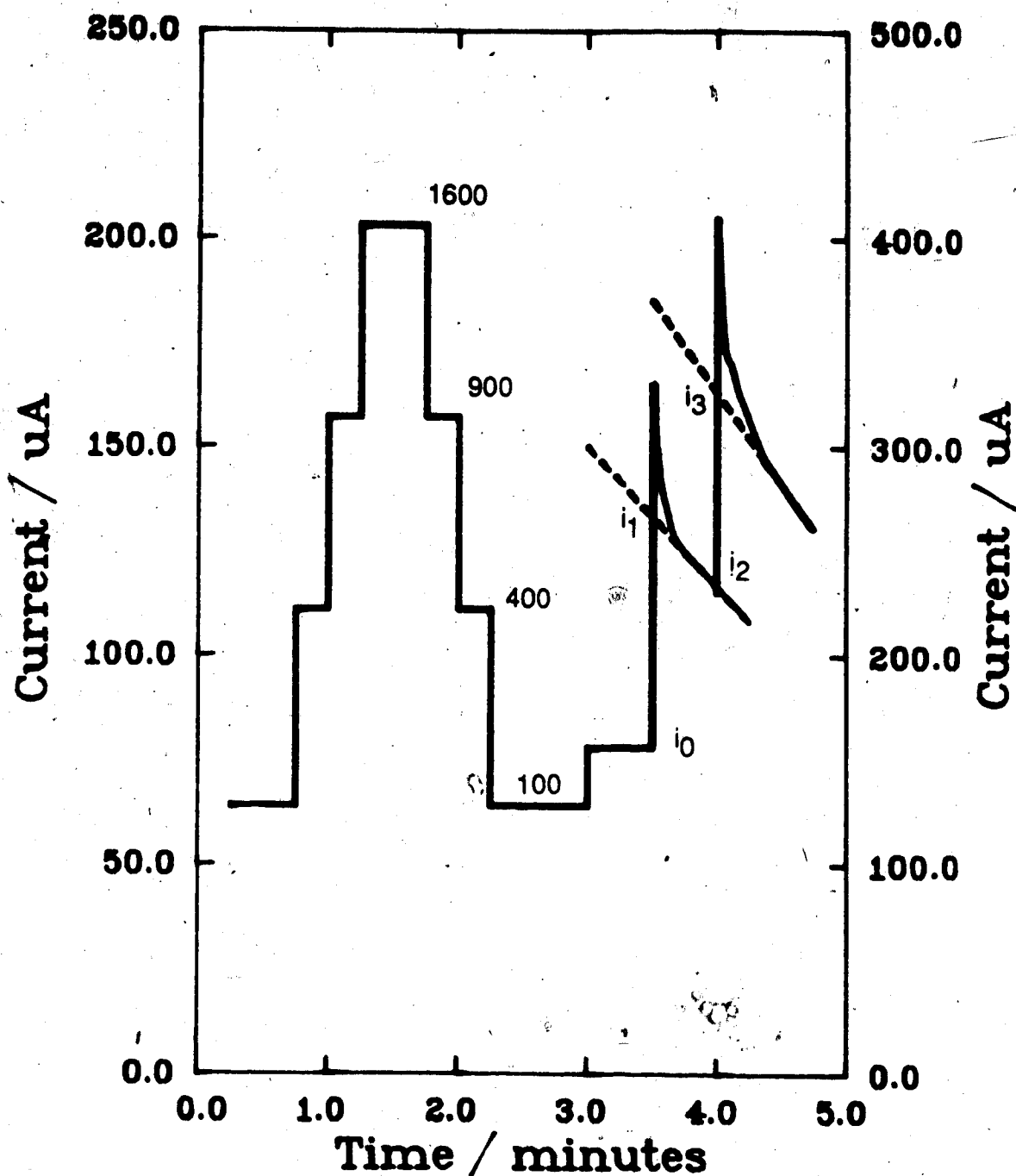
Figure. Reduction Current Recorded as a Function of Time for the Determination of Dioxygen by Standard Addition. 0.1 M TEAP, 1.0 M HOAc in AN at the GC DE, E_D = -1.20 V vs SCE, 500 μL standard additions. Current sensitivity was halved prior to the standard additions. The symbols refer to quantities used in the calculations.

the order of 10 to 15%, were encountered when the usual polypropylene tips were used with dioxygen-saturated standards. The losses were due to the permeability of polypropylene to dioxygen. A Socorex model 831 adjustable pipet (0.5 to 5 mL), which accommodated glass Pasteur pipets was used to counter this problem. For volumes less than 0.5 mL, an adjustable Gilson micropipet was used. Glass tips for the latter were fashioned by press-fitting the lower part of a Pasteur pipet into the upper part of a polypropylene tip. The joint was sealed with Parafilm.

As shown in Figure 22, current increased sharply on the addition of standard. After a 10- to 15-second mixing period, the limiting current decayed in a fairly rapid, linear fashion for the next 30 to 45 seconds as the dioxygen in solution returned to equilibrium with the cell atmosphere. This linear portion of the decay curve was used to extrapolate the limiting current back to the time of addition and thus to compensate for the slow and noisy mixing and for the loss of added dioxygen to the cell atmosphere. A second portion of standard solution was added to the test solution within 45 to 60 seconds of the first, that is, while the decay from the first addition was still reasonably linear. As before, the decay curve resulting from the second standard addition was extrapolated back to the time of the second addition.

To determine the concentration of dioxygen in the test electrolyte, it was necessary to correct the observed currents for the contribution due to processes not dependent on rotation speed. This was done by plotting observed limiting currents versus the square root of angular velocity according to the Levich equation. Such a plot is shown in Figure 23a. (The intercept of this plot gave the background current, i_b. (The slope was used in the calculation of the diffusion coefficient of dioxygen in the test electrolyte as discussed in the next chapter.) Significant background currents were encountered in nonaqueous electrolytes containing large amounts of added acid such as 1 $\underline{M}$ acetic acid. In DMSO these currents were minor (2. to 5% of that for dioxygen reduction) and could have been neglected. In acetonitrile however, background currents were larger by a factor of 10 and could not be ignored. The source of the background current was likely hydrogen ion reduction. Whatever the source, the current-limiting process was chemical or electrochemical in nature, and therefore not dependent on the rotation speed of the electrode.

In addition to the background current i_b, observed currents were also corrected for dilution of the test solution by the added standard according to the following formulas:
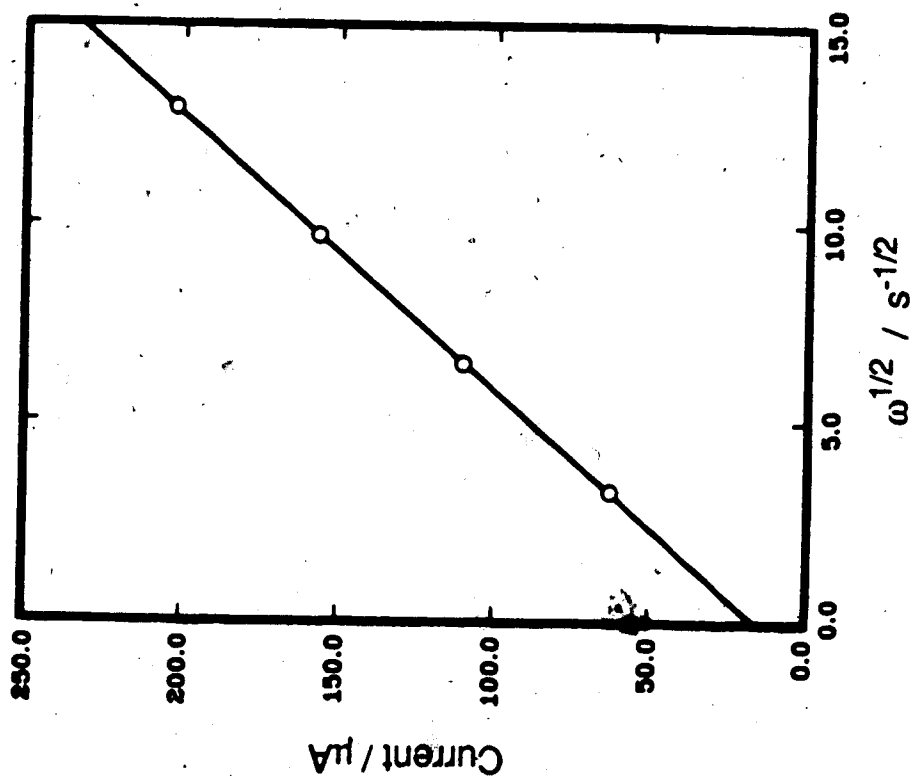
Figure 23a. Levich Plot for Dioxygen Reduction at the GC RDE. Data from Figure 22.
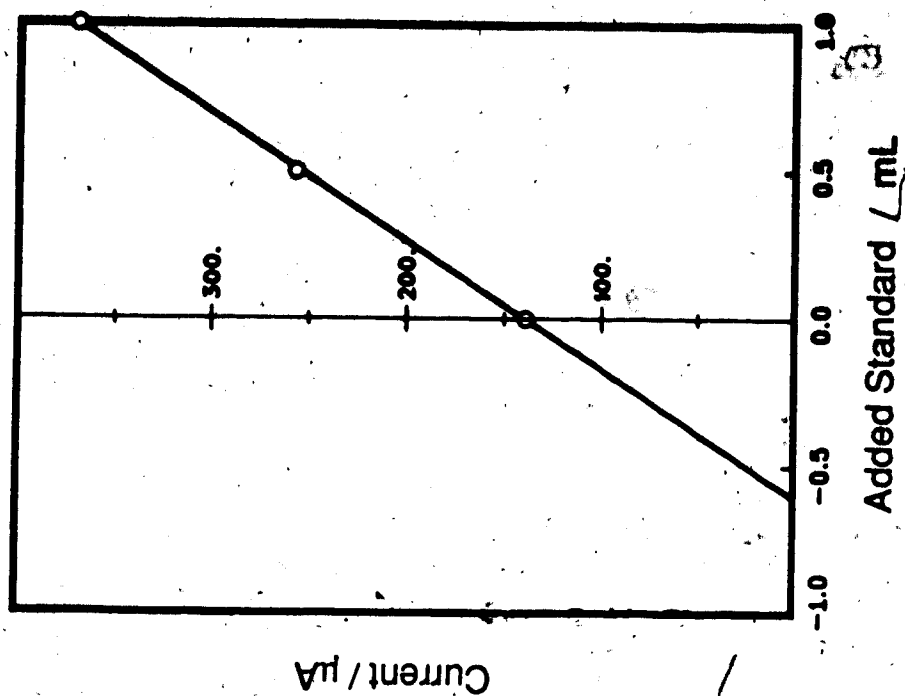
Figure 23b. Standard Addition Plot for the Determination of Dioxygen Concentration. Based on data from Figure 22. $[O_2] = 55.$ µM

Vol. Std. Added	Corrected Current
0	$i_0^* = i_0 - i_b$
V_S	$i_1^* = i_1(V_0+V_S)/V_0 - i_b$
$2V_S$	$i_2^* = i_1^* + (i_3(V_0+2V_S) - i_2(V_0+V_S))/V_0$

V_0 denotes the original volume of the test solution (usually 75 mL) and V_S denotes the volume of added standard. The quantities i_0 to i_3 are defined in Figure 22. By plotting corrected currents versus the volume of added standard, the dioxygen concentration of the test solution could be calculated according to

$$[O_2] = - V_{i=0} [O_2]_{STD}/V_0$$

where $V_{i=0}$ denotes the x-intercept of the standard addition plot, an example of which is shown in Figure 23b.

The standard addition procedure described was validated by determining the concentration of dioxygen in an air-saturated saline solution. A 75-mL portion of a solution containing 10 g Cl^-/L (0.282 $\underline{M}$ NaCl) and 0.01 $\underline{M}$ NaOH was used. The limiting current for dioxygen reduction was measured at a Pt RDE at -0.70 V vs SCE.

1000 μL portions of dioxygen-saturated distilled water served as the added standard. A concentration of 2.16 × 10^{-4} M was found at an atmospheric pressure of 680 torr. This value is in excellent agreement with the literature value of 2.14 × 10^{-4} M (104).

Results obtained for the gas proportioner calibration in test electrolytes are presented in the next chapter in connection with the determination of the diffusion coefficient of dioxygen in these solutions.

C. Synthesis, Purification and Characterization of Bipyridinium Salts

1. Diquaternized Salts of 4,4'-Bipyridine

The structures, designations and formula weights of the diquaternized salts of 4,4'-bipyridine that were used in this work are given in Table 11. These compounds are commonly referred to as "viologens". Of the thirteen listed in Table 11, only three are available commercially. These are methyl, benzyl and heptyl viologens. In this work, the former two were purchased and the remainder were prepared by the reaction of the appropriate organic halide with 4,4'-bipyridine (variants of the Menschutkin reaction).

In the synthesis of the viologens, Michaelis' test

Table 11. Diquaternized Salts of 4,4'-Bipyridine.

$$\left[R-N\overset{+}{=}\hspace{-0.3em}\left\langle\text{pyridyl}\right\rangle\hspace{-0.3em}-\hspace{-0.3em}\left\langle\text{pyridyl}\right\rangle\hspace{-0.3em}\overset{+}{=}N-R \right]^{2+}$$
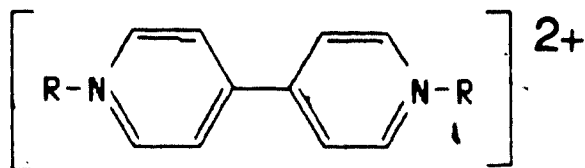
R	Common Name (Abbr.)	X^-	Formula Weight
$-CH_3$	Methyl Viologen	Cl^-	257.16
	(MeV)	ClO_4^-	385.16
$-(CH_2)_2CH_3$	n-Propyl Viologen	Br^-	402.17
	(n-PrV)	ClO_4^-	441.26
$-CH(CH_3)_2$	i-Propyl Viologen	I^-	496.17
	(i-PrV)	ClO_4^-	441.26
$-(CH_2)_3CH_3$	Butyl Viologen	Br^-	430.22
	(BuV)	ClO_4^-	469.32
$-(CH_2)_5CH_3$	Hexyl Viologen	Br^-	486.33
	(HxV)	ClO_4^-	525.42
$-(CH_2)_6CH_3$	Heptyl Viologen	I^-	608.39
	(HpV)	ClO_4^-	553.48

(Continued)

Table 11. (Continued)

R	Common Name (Abbr.)	X⁻	Formula Weight
$-(CH_2)_7CH_3$	Octyl Viologen	Br^-	542.44
	(OcV)	ClO_4^-	581.33
$-CH_2C_6H_5$	Benzyl Viologen	Cl^-	409.36
	(BzV)	ClO_4^-	537.35
$-C_6H_5$	Phenyl Viologen	I^-	564.21
	(PhV)	ClO_4^-	509.30
$-CH_2CH_2OH$	Hydroxyethyl Viologen	Cl^-	317.21
	(HeV)	ClO_4^-	445.21
$-CH_2CH_2COOH$	Carboxyethyl Viologen	Cl^-	373.23
	(CeV)	ClO_4^-	501.23
$-CH_2CO_2C_2H_5$	Carbethoxymethyl Viologen	Cl^-	401.28
	(CxV)	ClO_4^-	529.28
$-CH_2CN$	Cyanomethyl Viologen	I^-	490.08
	(CyV)	ClO_4^-	435.18

for viologens (19) was found indispensable. The test consists of reduction by a solution of sodium dithionite in dilute aqueous ammonia. Doubly-quaternized salts of 4,4'-bipyridine give an intense violet color upon such reduction (blue at lower concentrations). The color disappears on exposure to air for some time and is restored on addition of dithionite. Singly-quaternized salts and 4,4'-bipyridine itself do not give this test. A positive viologen test, reversible toward dioxygen, and a satisfactory elemental analysis were deemed sufficient to establish that the desired compound had, in fact, been prepared.

The paragraphs that follow contain the details concerning the synthesis, purification, and characterization of the compounds listed in Table 11. UV spectral data for these compounds, together with literature values where available, are given in Table 12. The methods referred to as A, B and C in connection with preparation of the perchlorate salts are given at the end of this section.

4,4'-Bipyridine was prepared by the reductive acetylation of pyridine by zinc dust in acetic anhydride according to the procedure of Dimroth and Heene (113) and also that of Bonczos et al. (114). The intermediate 1,1'-diacetyltetrahydro-4,4'-bipyridine was isolated

Table 12. UV Spectral Data for the Diquaternized Salts of 4,4'-Bipyridine.

Cpd	X^-	$\epsilon/10^4$ $M^{-1}cm^{-1}$	λ_{max}[a]	Comments[b]
MeV	Cl^-	2.07	260	aq.
	Cl^-	2.09	260	5% DMSO
	ClO_4^-	2.13	260	2.5% AN
	ClO_4^-	2.10	260	5% AN
	Cl^-	2.10	257	Ref. 120, aq.
	I^-	2.02	257	Ref. 121, aq.
	?	2.36	257	Ref. 23, aq.
n-PrV	ClO_4^-	2.39	262	10% AN
i-PrV	ClO_4^-	2.33	260	10% AN
	I^-	2.32	260	10% AN
	ClO_4^-	2.34	260	Ref. 122, AN
BuV	ClO_4^-	2.45	262	10% AN
HxV	ClO_4^-	2.46	264	10% AN
HpV	ClO_4^-	2.46	264	10% AN
OcV	ClO_4^-	2.49	264	10% AN
	Br^-	2.50	264	aq.
BzV	Cl^-	2.45	260	aq.
	ClO_4^-	2.49	260	5% AN
PhV	I^-	2.10	314	10% AN
	ClO_4^-	2.13	314	10% AN
	ClO_4^-	1.22	250	10% AN
HeV	Cl^-	2.32	266	aq.
	ClO_4^-	2.33	266	5% AN
	ClO_4^-	2.33	266	aq.
	?	2.36	266	Ref. 23, aq.

(Continued)

Table 12. (Continued)

Cpd	X^-	$\varepsilon/10^4$ $M^{-1}cm^{-1}$	λ_{max}[a]	Comments[b]
CeV,	Cl^-	2.14	264	aq.
CxV	ClO_4^-	2.38	264	10% AN
CyV	ClO_4^-	2.16	262	10% AN
	I^-	2.19	262	aq.
	?	2.38	264	Ref. 23, aq.

a. ±2 nm.

b. This work except where noted.

according to Nielsen _et al._ (115). The Dimroth synthesis
gave a 35% yield of the diacetyl compound after 16 h while
the Bonczos procedure gave a 40% yield after only 4 h.
Yields of 25 to 40% are the norm for this reaction
(115). The diacetyl compound was oxidized to
4,4'-bipyridine with dioxygen in glacial acetic acid
(116). After neutralization with 2 _M_ NaOH, the product
was obtained in 60 to 70% yield (20 to 30% overall). It
was recrystallized from water, after treatment with
charcoal, as long, white needles. Drying at 50°C for 16 h
gave anhydrous 4,4'-bipyridine, m.p. 112.5-113°C (lit.
111-112°C (19)).

1,1'-Dimethyl-4,4'-bipyridinium dichloride (methyl
viologen, MeV) was obtained from Sigma as the
trihydrate. It was recrystallized from aqueous acetone
and dried at 50°C _in vacuo_. A portion was converted to
the diperchlorate by Method A as white prisms which turned
blue on exposure to light. Elemental analysis for
MeV·(ClO$_4$)$_2$, C$_{12}$H$_{14}$N$_2$Cl$_2$O$_8$ (% Found/% Expected): C,
37.4/37.4; H, 3.6/3.7; N, 7.2/7.3; Cl, 18.1/18.4; O (by
difference), 33.7/33.2.

1,1'-Bis(phenylmethyl)4,4'-bipyridinium dichloride
(benzyl viologen, BzV) was also obtained from Sigma. It
was recrystallized from methanol/acetone and dried at 50°C
in vacuo. A portion was converted to the diperchlorate by

method A as water-white prisms.

1,1-Dipropyl-4,4'-bipyridinium dibromide (n-propyl viologen, n-PrV) (169,171) was prepared by adding 5 mL of 1-bromopropane to a solution of 0.5 g 4,4'-bipyridine in 15 mL methanol. The solution was refluxed with stirring for 24 h. The yellow solid obtained on evaporation of the solvents was washed twice with acetone and once with diethyl ether. The salt, which gave a positive viologen test, was obtained in 80% yield. It was recrystallized from ethanol/water as waxy, yellow plates which were dried at 110°C for 2 h prior to use. The diperchlorate was prepared by method A as waxy, white plates. Elemental analysis for n-PrV·Br_2, $C_{16}H_{22}Br_2N_2$ (% Found/% Expected): C, 47.5/47.8; H, 5.4/5.5; N, 7.1/7.0; Br (by difference), 40.1/39.8.

1,1'-Dibutyl-4,4'-bipyridinium dibromide (butyl viologen, BuV) (169) was prepared and worked up in the same fashion as the preceding compound except that 1-bromobutane was used. The dibromide was obtained as waxy, yellow plates in 80% yield. The diperchlorate was prepared by Method B as white plates. Elemental analysis for BuV·Br_2, $C_{18}H_{26}Br_2N_2$ (% Found/% Expected): C, 49.8/50.2; H, 6.0/6.1; N, 6.3/6.5; Br (by difference), 37.8/37.2.

1,1'-Dihexyl-4,4'-bipyridinium dibromide (hexyl

viologen, HxV) (169,171) was prepared by adding 5 mL 1-bromohexane to a solution of 0.5 g 4,4'-bipyridine in 15 mL dimethylformamide (DMF). The mixture was heated at 120°C for 6 h. Upon cooling in ice, the product was obtained in better than 90% yield as waxy, yellow crystals. The compound gave a positive viologen test accompanied by formation of a precipitate; both color and precipitate disappeared on exposure to air for some time. After recrystallization from 98% ethanol, the dibromide was dried at 110°C for 2 h. The perchlorate was obtained by method B as finely-divided white crystals. Elemental analysis for HxV·Br$_2$, C$_{22}$H$_{34}$Br$_2$N$_2$ (% Found/% Expected): C, 54.4/54.3; H, 6.7/7.0; N, 5.8/5.8; Br (by difference), 33.1/32.9.

1,1-Dioctyl-4,4'-bipyridinium dibromide (octyl viologen, OcV) (170,171) was prepared in the same fashion as the preceding compound except that 1-bromooctane was used. Other details were identical. Elemental analysis for OcV·Br$_2$, C$_{26}$H$_{42}$Br$_2$N$_2$ (% Found/% Expected): C, 57.8/57.6; H, 7.5/7.8; N, 5.3/5.2; Br (by difference), 29.4/29.5.

1,1-Diheptyl-4,4'-bipyridinium diiodide (heptyl viologen, HpV) (169-171) was prepared in the same fashion as the dihexyl compound except that 1-iodoheptane was used. Use of the iodoalkane rather than the bromoalkane

was prompted by the immediate availability of the

former. The red diiodide salt, which was obtained in 75%

yield, was recrystallized as brick-red prisms from 98%

ethanol. It gave a positive viologen test with

precipitate formation. The diiodide was converted to the

diperchlorate by method B as waxy, yellow plates (in

contrast to all the other n-alkyl viologen diperchlorates

which were white). Elemental analysis for HpV·$(ClO_4)_2$,

$C_{24}H_{38}Cl_2N_2O_8$ (% Found/% Expected): C, 51.9/52.1; H,

6.9/6.9; N, 4.9/5.1.

1,1'-Bis(2-propyl)-4,4'-bipyridinium diiodide

(i-propyl viologen, i-PrV) (122,168) was prepared by

refluxing 0.5 g 4,4'-bipyridine in 15 mL 2-iodopropane

with stirring for 16 h. A reddish-yellow solid was

obtained which gave a positive viologen test with

precipitate formation. An attempt to dissolve the solid

in hot 98%,ethanol resulted in a red solution containing a

yellow solid. On cooling 0.70 g of yellow solid was

obtained. This material also gave a positive viologen

test again with precipitate formation. Elemental analysis

confirmed that ,the yellow salt was the diiodide. (Other

viologen diiodides prepared were all red.) The diiodide,

obtained in 45% yield was dried at 65°C in vacuo. A

portion was converted to the diperchlorate by method C as

pale yellow crystals. Elemental analysis for i-PrV·I_2,

$C_{16}H_{22}I_2N_2$ (% Found/% Expected): C, 38.7/38.7; H, 4.4/4.5; N, 5.6/5.6; I (by difference), 51.4/51.2.

1,1-Bis(2-hydroxyethyl)-4,4'-bipyridinium dichloride (hydroxyethyl viologen, HeV) was prepared by a modification of a procedure given by Kazarinova et al. (117). 5 mL of 2-chloroethanol was added to a solution of 1.0 g 4,4'-bipyridine in 15 mL 2-propanol. The mixture was refluxed with stirring for 20 h after which time the solvents were distilled off. The product, which gave a positive viologen test, was obtained in 70% yield. After washing with acetone and diethyl ether, it was recrystallized from methanol/acetone as white prisms which turned pale blue on exposure to light. The compound was dried at 50°C in vacuo. A portion was converted to the diperchlorate by method A as white needles. Elemental analysis for HeV·Cl$_2$, $C_{14}H_{18}Cl_2N_2O_2$ (% Found/% Expected): C, 53.0/53.0; H, 5.7/5.7; N, 8.8/8.8; Cl, 22.6/22.4; O (by difference), 9.9/10.1.

1,1'-Bis(carboxyethyl)-4,4'-bipyridinium dichloride (carboxyethyl viologen, CeV) (21) was prepared by analogy to Michaelis and Hill's synthesis of the carboxymethyl compound (19). 5.0 g 3-chloropropionic acid was melted in a test tube over a flame. 0.5 g 4,4'-bipyridine was added and the solution boiled briefly (~5 s). The hot solution was carefully added to 75 mL acetone to which 5 drops of concentrated HCl were added. The white precipitate was

filtered off and washed with acetone and diethyl ether.
The product, which gave a positive viologen test, was
obtained in 90% yield. It was recrystallized from
methanol/acetone and dried at 65°C in vacuo. The diper-
chlorate was obtained as white needles by method A.
Elemental analysis for CeV·Cl$_2$, C$_{16}$H$_{18}$Cl$_2$N$_2$O$_4$ (% Found/%
Expected): C, 51.1/51.5; H, 4.8/4.9; N, 7.5/7.5; Cl,
19.8/19.0; O (by difference), 16.7/17.2.

1,1'-Bis(carbethoxymethyl)-4,4'-bipyridinium di-
chloride (carbethoxymethyl viologen, CxV) (21) was
prepared by dissolving 0.25 g 4,4'-bipyridine in 10 mL 98%
ethanol and adding 2.0 g ethyl chloroacetate. The latter
was prepared according to Vogel (118). The solution was
refluxed with stirring for 24 h. The product was
recovered by addition of diethyl ether to precipitate the
salt. It gave a positive viologen test and was obtained
in 90% yield. The diperchlorate salt was prepared by
method B as waxy, white plates. Elemental analysis for
CxV·(ClO$_4$)$_2$, C$_{18}$H$_{22}$N$_2$Cl$_2$O$_{12}$ (% Found/% Expected): C,
40.9/40.8; H, 4.2/4.1; N, 5.3/5.3.

1,1'-Bis(cyanomethyl)-4,4'-bipyridinium diiodide
(cyanomethyl viologen, CyV) (21) was prepared by adding
0.5 g of 4,4'-bipyridine to a solution of iodoacetonitrile
in acetonitrile. The latter was prepared by heating 10 g
chloroacetonitrile plus 20 g KI briefly over a steam
bath. The reddish-brown sludge formed was washed with

small portions of acetonitrile to recover the iodo

compound. The solution containing the 4,4'-bipyridine was

refluxed with stirring for 8 h. On cooling a brick-red

powder was obtained in 50% yield. The material gave a

transient viologen test before forming a permanent

precipitate. After treatment with charcoal, it was

recrystallized from water as red prisms. A portion was

converted to the diperchlorate by method B as olive-green

plates. Elemental analysis for $CyV \cdot I_2$, $C_{12}H_{12}N_4I_2$ (%

Found/% Expected): C, 34.1/34.3; H, 2.3/2.5; N,

11.4/11.4; I (by difference), 52.2/51.8.

1,1'-Diphenyl-4,4'-bipyridinium diiodide (168) was

prepared after Emmert and Roh (119). 1.0 g 4,4'-

bipyridine, 5.0 g 2,4-dinitrochlorobenzene and 10 mL 98%

ethanol were refluxed with stirring for 24 h. A yellow

crystalline solid formed and on cooling 1,1'-bis(2,4-di-

nitrophenyl)-4,4'-bipyridinium dichloride was obtained in

55% yield. It was recrystallized from glacial acetic

acid. This compound did not give a positive viologen

test. A dilute ethanolic solution did turn blue-violet on

addition of aqueous NaOH as per Emmert and Roh (119).

Phenyl viologen was prepared by heating 1.0 g of the 2,4-

dinitro compound in 10 mL 98% ethanol in a water bath at

80°C. 1.4 g of freshly distilled aniline was added. The

solution turned blue-green and then reddish-brown. After

3 h, 10 mL of water was added and the precipitate which

formed was filtered off. The filtrate was treated repeatedly with charcoal to obtain a yellow solution. On addition of saturated aqueous NaI, a red precipitate formed. It was recrystallized from water as red prisms in 20% yield. A portion was converted to the diperchlorate by method C as pale orange leaves. Elemental analysis for PhV·I_2, $C_{22}H_{18}I_2N_2$ (% Found/% Expected: C, 47.0/46.8; H, 3.2/3.2; N, 4.9/5.0; I (by difference), 44.8/45.0.

2. Diquaternized Salts of 2,2'-Bipyridine

The structures, designations and formula weights of the diquaternized salts of 2,2'-bipyridine that were used in this work are given in Table 13. The procedures used to prepare and purify these compounds are set forth in the following paragraphs. UV spectral data for these compounds, together with data from the literature are collected in Table 14. The methods referred to as A, B and C in connection with preparation of the diperchlorate salts are given at the end of this section.

6,7-Dihydrodipyrido[1,2-a:2',1'-c]pyrazinediium dibromide (diquat, DiQ), was prepared by reacting 2,2'-bipyridine (G.F. Smith) with 1,2-dibromoethane according to the procedure of Homer and Tomlinson (123). The salt, which was obtained in 65% yield, was recrystallized from aqueous acetone as pale yellow needles. It was dried at

Table 13. Diquaternized Salts of 2,2'-Bipyridine
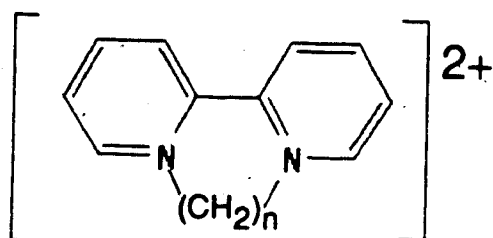
n	Common Name (Abbr.)	X⁻	Formula Weight
2	Diquat (DiQ)	Br^-	344.07
		ClO_4^-	383.16
3	Triquat (TriQ)	Br^-	358.07
		ClO_4^-	397.19
4	Tetraquat (TetQ)	Br^-	372.10
		ClO_4^-	411.20

Table 14. UV Spectral Data for the Diquaternized Salts of 2,2'-Bipyridine.

Cpd	X^-	$\varepsilon/10^4$ $M^{-1}cm^{-1}$	λ_{max}	Comments[b]
DiQ	Br^-	1.92	310	aq.
	ClO_4^-	1.98	310	5% AN
	ClO_4^-	1.96	310	5% AN
	Br^-	1.90	310	Ref. 123, aq.
TriQ	Br^-	1.55	288	aq.
	Br^-	1.51	288	aq.
	Br^-	1.54	288	aq.
	ClO_4^-	1.57	290	10% AN
	Br^-	1.56	287	Ref. 123, aq.
TetQ	ClO_4^-	1.35	276	10% AN
	ClO_4^-	1.36	275	10%
	ClO_4^-	1.38	276	5% AN
	Br^-	1.50[c]	275	Ref. 123, aq.

a. ±2nm.

b. This work except where noted.

c. Elemental analysis corresponded to Cpd·1/3 HBr.

50°C _in vacuo_. A portion was converted to the
diperchlorate by method A as long, white needles.
Elemental analysis for DiQ·Br$_2$, C$_{12}$H$_{12}$Br$_2$N$_2$ (% Found/%
Expected): C, 41.0/41.9; H, 3.6/3.5; N, 7.8/8.1; Br (by
difference), 47.6/46.4. (The anhydrous dibromide is quite
hygroscopic and the sample was observed to gain weight
quickly.) Elemental analysis for DiQ·(ClO$_4$)$_2$,
C$_{12}$H$_{12}$N$_2$Cl$_2$O$_8$ (% Found/% Expected): C, 37.4/37.6; H,
3.1/3.2; N, 7.5/7.3.

7,8-Dihydro-6H-dipyrido[1,2-a:2',1'-c][1,4]diazepine-
diium dibromide (triquat, TriQ) was also prepared
according to Homer and Tomlinson (123) and was obtained in
70% yield. It was recrystallized from methanol/benzene as
a lemon-yellow powder and dried at 50°C _in vacuo_. A
portion was converted to the diperchlorate by method A as
shiny, white needles. Elemental analysis for TriQ·Br$_2$,
C$_{13}$H$_{14}$Br$_2$N$_2$ (% Found/% Expected): C, 42.7/43.6; H,
3.9/4.0; N, 7.5/7.8; Br (by difference), 45.8/44.6.
Elemental analysis for TriQ·(ClO$_4$)$_2$, C$_{13}$H$_{14}$N$_2$Cl$_2$O$_8$
(% Found/% Expected): C, 39.2/39.3; H, 3.5/3.6; N,
7.1/7.2.

6,7,8,9,-Tetrahydrodipyrido[1,2-a:2',1'-c][1,4]-
diazocinediium dibromide (tetraquat, TetQ) was also
prepared according to reference 123. The crude dibromide
was dissolved in water and treated with charcoal. The

diperchlorate salt was recovered by method A as white
needles. Elemental analysis for TetQ·(ClO$_4$)$_2$,
C$_{14}$H$_{16}$N$_2$Cl$_2$O$_8$ (% Found/% Expected): C, 40.8/40.9; H,
3.9/3.9; N, 6.9/6.8.

3. Diquaternized Salts of 1,10-Phenanthroline

The structures, designations and formula weights of
the diquaternized salts of 1,10-phenanthroline that were
used in this work are listed in Table 15. The procedures
used to prepare and purify these compounds are given in
the following paragraphs. As before, the methods referred
to as A, B and C in connection with the preparation of the
diperchlorate salts are explained at the end of this
section.

5,6-Dihydropyrazino[1.2.3.4-lmn]-1,10-phenanthro-
linium dibromide (diphen, DiP) was prepared according to
Summers (125) by the reaction of 1,10-phenanthroline
(Fisher) with 1,2-dibromoethane. It was obtained as a
mustard-yellow solid in 70% yield. After recrystalliza-
tion from methanol/benzene, it was dried at 50°C in
vacuo. The diperchlorate was prepared by method A as
rust-colored needles. Elemental analysis for DiP·Br$_2$,
C$_{14}$H$_{12}$N$_2$Br$_2$ (% Found/% Expected): C, 45.5/45.7; H
3.2/3.3; N, 7.3/7.6; Br (by difference), 44.0/43.4.

5H-6,7-Dihydro-1,4-diazepino[1.2.3.4-lmn]-1,10-phen-

Table 15. Diquaternized Salts of 1,10-Phenanthroline.
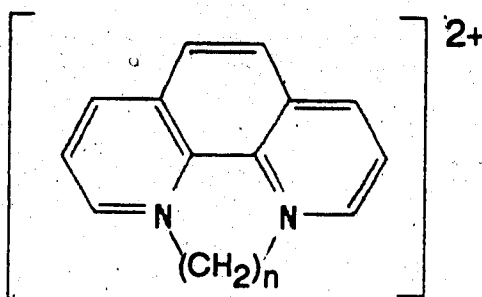
n	Common Name (Abbr.)	X⁻	Formula Weight
2	Diphen (DiP)	Br⁻	368.07
			407.16
3	Triphen (TriP)		382.10
		ClO₄⁻	421.19

anthrolinium dibromide (triphen, TriP) was also prepared
according to Summers (125) in 70% yield. It was
recrystallized from methanol/benzene as bright yellow
crystals which were dried at 50°C _in vacuo_. A portion was
converted to the diperchlorate by method A as white
needles. Elemental analysis for TriP·Br$_2$, C$_{15}$H$_{14}$N$_2$Br$_2$
(% Found/% Expected): C, 47.1/47.2; H, 3.6/3.7; N,
7.3/7.3; Br (by difference), 42.0/41.8.

Both diphen and triphen were found to exhibit
pronounced negative deviations from Beer's law in aqueous
solutions. In an attempt to avoid this problem, molar
absorptivities were determined in acetonitrile. The
results are shown in Table 16 together with comparable
values obtained by Hünig _et al._ (124). Results are in
best agreement for those peaks whose absorptivities
display the least concentration dependence.

4. Conversion of Bipyridinium Dihalides to Diperchlorates

All of the bipyridinium salts used in this work were
initially obtained as dihalides. While these salts were
sufficiently soluble in DMSO, the same was not true in
acetonitrile with the exception of the diiodide salts.
The presence of the iodide ion in the kinetic experiments
was deemed undesirable due to the possible reaction with
dioxygen to produce iodine which would interfere with the

Table 16. UV Spectral Data for the Diquaternized Salts of

1,10-Phenanthroline in Acetonitrile.

Diphen

λ_{max} [a]	This Work		Reference 124	
[DiP]/μM:	54.8	32.9		?
λ_{max} [a]	$\varepsilon/10^4$ M^{-1}cm^{-1}	$\varepsilon/10^4$ M^{-1}cm^{-1}	λ_{max}	$\varepsilon/10^4$ M^{-1}cm^{-1}
212	3.88	4.04	210	0.41[b]
228	2.14	2.14	225s	2.1
282	3.66	3.83	281	3.9
310	1.06	1.10	308	1.2
324	0.60	0.59	321	0.6

Triphen

	This Work		Reference 124	
[TriP]/μM:	49.6	29.8		?
λ_{max} [a]	$\varepsilon/10^4$ M^{-1}cm^{-1}	$\varepsilon/10^4$ M^{-1}cm^{-1}	λ_{max}	$\varepsilon/10^4$ M^{-1}cm^{-1}
216	2.88	2.90	213	3.0
230	2.19	2.20	228	2.3
284	3.54	3.64	283	4.3
312	1.13	1.15	314	0.85
324s	0.58	0.58	325s	0.62

a. ± 2 nm.

b. The factor-of-ten difference between this result and that of the present work may be due to a typographical error in the value of log ε given in reference 124.

electrochemical measurements. To obtain salts that were soluble in acetonitrile, the dihalides were converted to diperchlorates. Three methods were used to accomplish this conversion. Method A, due to Michaelis and Hill (19), involved initial preparation of the dipicrate salt. To a hot aqueous solution of the dihalide, an excess of aqueous picric acid was added. The solution was boiled and, if necessary, water added to dissolve the solid. Upon cooling, the dipicrate was obtained as yellow to orange needles. The diperchlorate was obtained by suspending the dipicrate in acetone and adding a few drops of concentrated $HClO_4$. Ultrasonication hastened the conversion. The diperchlorate salt obtained was dissolved in hot ethanol or ethanol/water, treated with charcoal and filtered while hot. Upon cooling, the diperchlorate was obtained usually as white needles or prisms. The compounds were dried at 65° in vacuo before use.

In the case of viologens with large non-polar substituents, the perchlorate salts were too soluble in acetone to successfully apply method A. In these cases, the dihalide was recrystallized from ethanol or ethanol/water containing a 20-fold excess of $LiClO_4$ (method B) or from water containing a 20-fold excess of $NaClO_4$ (method C). In either case, solutions were treated with charcoal and filtered while hot. The diperchlorate

salt obtained upon cooling was recrystallized from ethanol
or ethanol/water and dried at 65°C <u>in vacuo</u> prior to use.

While the hazards associated with the handling and
use of picric and perchloric acids and their salts are
well known (126,127), no untoward incidents were
encountered with the compounds described in this work.
Potential hazards were minimized by preparing and handling
the compounds in small quantities (<500 mg).

D. <u>Solvent and Miscellaneous Reagent Purification</u>

Reagent grade dimethylsulfoxide (DMSO, sulfinylbis-
[methane]) was vacuum distilled from calcium hydride.
Distilled water was redistilled from alkaline
permanganate. Acetonitrile (AN) (Caledon, non-UV grade)
was purified according to the method of Walter and Ramaley
(128). This procedure involved refluxing with $AlCl_3$
followed by rapid distillation, then refluxing with $KMnO_4$
plus Li_2CO_3 followed again by rapid distillation and
finally refluxing over $KHSO_4$ followed by rapid
distillation. The solvent obtained was then fractionally
distilled from CaH_2 through a 50 cm Vigreux column at 50
mL/h. The fraction boiling from 80 to 81°C (at ambient
atmospheric pressures ranging from 680 to 720 torr) was
retained. Yield for the purification procedure was on the

order of 60%. As the procedure was lengthy and tedious,
it was worthwhile to recover and reuse the solvent.
Discarded test solutions contained tetraethylammonium per-
chlorate (0.1 $\underline{M}$) and usually acetic acid (1.0 $\underline{M}$) plus a
small quantity of the test compound ($\sim 10^{-4}$ $\underline{M}$).
Acetonitrile could be readily separated from the other
components of the recovered solution by fractional
distillation. In carrying out this distillation, it was
imperative that the flask not boil dry as the residue was
potentially explosive. A safe procedure consisted of
first rapidly distilling the acetonitrile from the
recovered solutions using a water bath to heat the still
pot. As a precautionary measure, this distillation was
carried out in an enclosed fume cabinet. The recovered
solvent was purified for re-use by fractional distillation
to remove acetic acid carried over in the rapid
distillation. A second fractional distillation, this time
over CaH_2, produced solvent of a quality similar to that
obtained by purifying the commercial solvent.

UV spectrophotometry provided a convenient means of
monitoring solvent quality. The purified solvent was
transparent down to 220 nm. Absorbance rose below 220 nm
and typically ranged between 0.15 and 0.45 at 200 nm. In
all cases the UV cutoff (defined as the wavelength at
which the absorbance equals 1) was less than 200 nm.

Residual current-voltage curves revealed the presence of a trace of an oxidizable impurity at $E_{1/2}$ = +1.1 V vs SCE. The solvent was otherwise free of electroactive impurities. The useful potential range was ±1.9 V vs SCE.

As DMSO was used in much smaller quantities and as the purification procedure was straightforward, no attempt was made to recover this solvent.

Tetraethylammonium perchlorate (TEAP) was prepared from tetraethylammonium bromide (TEABr) and sodium perchlorate by a modification of the method of Kolthoff and Coetzee (129). To a hot, aqueous solution of 2 $\underline{M}$ TEABr was added an equal amount of 2 $\underline{M}$ $NaClO_4$. Charcoal was added, the solution was heated to dissolve the salt and the mixture was filtered while hot. The white crystals obtained on cooling were filtered off and washed with small portions of ice-cold water until the wash water was free of bromide. The salt was recrystallized once more from water and the washing repeated. It was dried at 65°C <u>in vacuo</u> before use.

The solvent recovery procedure also made it possible to recover the TEAP electrolyte. As bipyridinium salts coprecipitated with the TEAP, simple recrystallization from water did not suffice to purify the latter. To remove the bipyridinium salts, the TEAP was dissolved in hot 0.1 $\underline{M}$ NaOH, boiled for 20 minutes, neutralized and

treated with charcoal. The salt obtained on cooling was recrystallized twice from water and dried at 65°C _in vacuo_. The pure salt was found to be transparent throughout the UV-visible range.

Glacial acetic acid was purified by freezing out portions using a thermoelectric cold plate (Stir-Kool Model SK-12, Thermoelectrics Unlimited, Inc., Wilmington, DE). Sodium perchlorate monohydrate was dried at 110°C before use.

E. Description of the Kinetic Experiments

For the experiments in acetonitrile, a 5×10^{-4} $\underline{M}$ stock solution of the diperchlorate salt of the bi-pyridinium compound was prepared. A five-fold dilution was made and TEAP was added to a final concentration of 0.1 $\underline{M}$. A current-voltage curve for the dilute solution in the absence of dioxygen was recorded at the glassy carbon (GC) RDE (see Figure 24). From this curve, half-wave potentials for the first and second reduction waves were determined. Limiting currents were measured as a function of rotation speed for both waves. From these data, Levich plots were constructed and the diffusion coefficients of the dication and the cation radical were calculated as described in Chapter VI. Once the data for the Levich
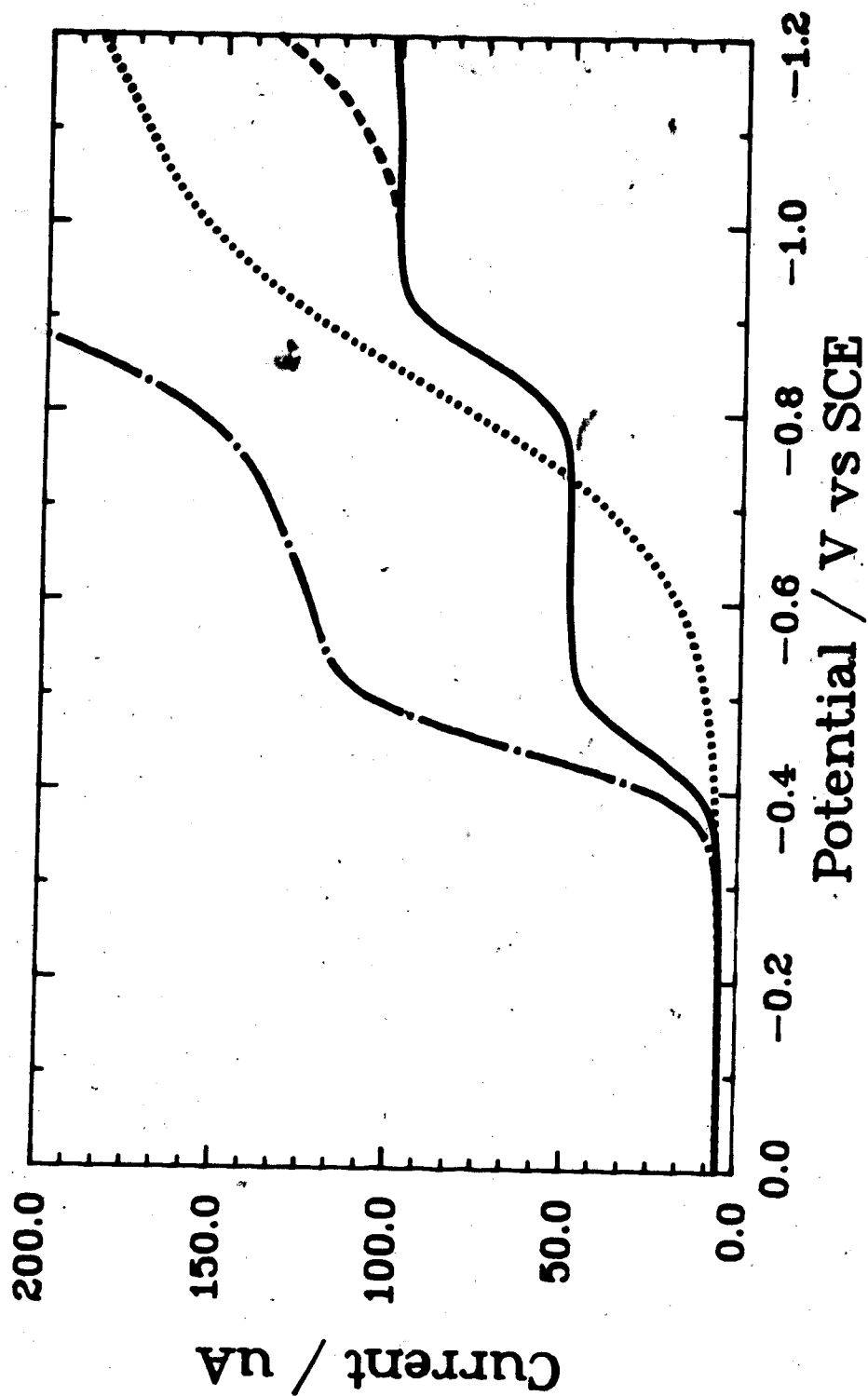
Figure 24. Current-Voltage Curves for Methyl Viologen and Dioxygen in Acetonitrile (0.1 M TEAP). GC RDE @ 900 rpm, scan rate = 0.5 V/min. _____ 125. μM MeV^{2+}; .... 125. μM MeV^{2+}, 1.0 M HOAC; .... 55. μM O$_2$, 1.0 M HOAC; – – – 125. μM MeV^{2+}, 55. μM O$_2$, 1.0 M HOAC; – · – · – · – 125. μM MeV^{2+}, 55. μM O$_2$, 1.0 M HOAC.

plots were collected, glacial acetic acid was added to the
test solution to a final concentration of 1.0 $\underline{M}$. The
solution was deoxygenated and another current-voltage
curve recorded. Finally, dioxygen was admitted to a
concentration of approximately 50 μM and another current-
voltage curve recorded. A typical set of current-voltage
curves, obtained for methyl viologen, is shown in Figure
24. The curve recorded in the presence of dioxygen was
used to select a potential for the kinetic runs. The
choice was governed by the need to measure the limiting
current for catalyst reduction without significant
interference from direct dioxygen reduction. For example,
from the curves recorded for methyl viologen (Figure 24),
-0.60 V vs SCE was selected as the disk potential for the
kinetic measurements.

The kinetic runs were performed at three different
catalyst concentrations, the actual values used depending
on the reaction rate. Catalyst concentrations ranged from
3 to 800 μM with typical values falling between 50 and 100
μM. For each catalyst concentration, the limiting current
for catalyst reduction was measured in the absence of
dioxygen and in the presence of three different dioxygen
concentrations. The latter were selected to be roughly
equal to 0.5 C_p, C_p and 2 C_p where C_p is the bulk catalyst
concentration. Currents were measured at five different

rotation speeds: 400, 900, 1600, 2500, and 3600 rpm. The same solution was used for the four sets of measurements; dioxygen concentrations were adjusted by sparging with the appropriate gas or gas mixture.

The GC RDE, which was used throughout the study, was cleaned and polished at the beginning of each experiment. The procedure used is given in the first section of this chapter. Prior to each series of current measurements, the electrode potential was manually switched between ±2.0 V vs SCE at ~1 Hz for 5 cycles. The electrode potential was then set to the value required for the limiting current measurements. Currents were measured first in the absence and then in the presence of dioxygen. Barometric pressure at the time of the experiment was recorded for use in calculating dioxygen concentrations.

Current measurements were made by recording current as a function of time. To obtain a reliable estimate of the steady-state current, rotation speeds were varied in ascending and then in descending order and the sequence was repeated at least once. A typical current-time trace appears in Figure 25. Current measurements made in the presence of dioxygen exhibited a significant negative drift. The rate of the drift was proportional to the current flow but it was larger than could be accounted for
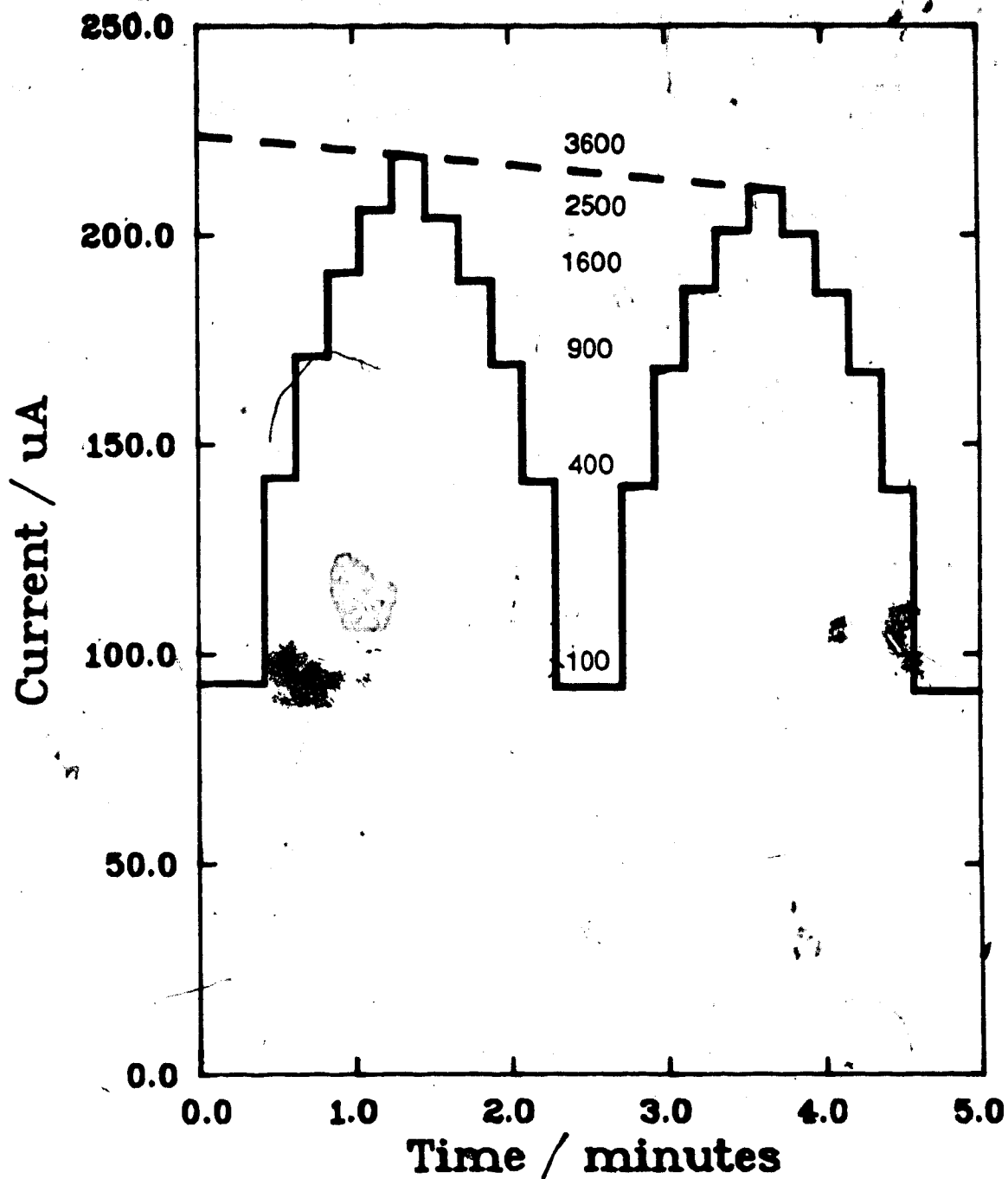
Figure 25. Catalytic Current Recorded as a Function of Time at Selected Rotation Speeds for the Methyl Viologen/Dioxygen Reaction. 84.5 μM MeV^{2+}, 0.1 M TEAP, 1.0 M HOAc in AN at the GC RDE. E_D = -0.60 V vs SCE, 25°. Dashed line is an extrapolation to t = 0.

by consumption of dioxygen. Cycling the electrode potential between ±2.0 V as described above, restored the original current level. This suggested that the source of the drift was some form of electrode passivation. A slight negative drift was associated with current measurements made in the absence of dioxygen but its magnitude was consistent with consumption of the oxidized form of the catalyst. As the observed current drift was fairly linear over the three to five minutes required to record a current-time trace similar to that in Figure 25, the useful expedient of extrapolating back to t = 0 was once again employed. Figure 25 shows how this was done. The calculation of the rate of the solution reaction from the measured currents is described in the next chapter.

F. Determination of Kinematic Viscosities

Kinematic viscosities were determined at 25.0 ± 0.1°C using a calibrated Ubbelohde viscometer (Cannon Instrument Co., State College, PA). Results obtained are given in Table 17. That found for pure DMSO is in good agreement with the literature value.

Table 17. Kinematic Viscosities of Nonaqueous Solutions.

Solution	$\nu/(10^{-2}\ cm^2/s)$
0.1 $\underline{M}$ TEAP in AN	0.480
0.1 $\underline{M}$ TEAP, 1.0 $\underline{M}$ HOAc in AN	0.495
0.1 $\underline{M}$ NaClO$_4$ in DMSO	1.97
0.1 $\underline{M}$ NaClO$_4$, 1.0 $\underline{M}$ HOAc in DMSO	2.03
DMSO	1.85
DMSO (from Ref. 111)[a]	1.81

a. Calculated from the data given for viscosity and density.

G.   Determination of the Diffusion Coefficient of the

Methyl Viologen Cation Radical

The diffusion coefficient of the methyl viologen cation radical was determined by preparing a solution of the radical by bulk electrolysis in the absence of dioxygen. The RDE electrochemical cell with the GC RDE in place was employed for this purpose. The actual working electrode was a 5.1 cm by 1.3 cm bright Pt flag. The counter electrode was an isolated, coiled Pt wire. The reference electrode was an aqueous SCE isolated from the test solution by a salt bridge equipped with a ground glass junction and filled with 0.1 $\underline{M}$ TEAP in acetonitrile. To prepare a solution of the cation radical, 50 mL of ~100 μM MeV^{2+} in acetonitrile containing 0.1 $\underline{M}$ TEAP was introduced into the electrochemical cell. After deoxygenation for 15 minutes, the electrolysis was carried out at -0.65 V vs SCE. Magnetic stirring was used to enhance the rate of mass transport. Current was recorded as a function of time and displayed the expected exponential decay. An estimate of the half-life was made from the decay curve and the electrolysis was continued for 10 half-lives. Total electrolysis time was typically 1.5 h. Upon completion of the electrolysis, limiting currents were measured at the GC RDE at 100, 400, 900, and

1600 rpm. Data were obtained for the reduction of $MeV^{+\cdot}$ (E_D = -1.10 V vs SCE) and for the oxication (E_D = 0.0 V vs SCE). Diffusion coefficients were calculated according to the Levich equation.

CHAPTER V

KINETIC STUDIES OF THE REACTION OF BIPYRIDINIUM CATION RADICALS WITH DIOXYGEN

A. Experimental Realization of Homogeneously Catalyzed Dioxygen Reduction

The general thermodynamic and kinetic requirements for the EC-catalytic mechanism were outlined in Chapter II. The particular case of dioxygen reduction as homogeneously catalyzed by a bipyridinium compound requires conditions under which (i) dioxygen is significantly more difficult to reduce than is the bipyridinium compound and (ii) dioxygen is a sufficiently strong oxidant to drive the solution reaction quantitatively in the desired direction. In aqueous solutions, condition (ii) holds but (i) does not (29) whereas in organic solutions the reverse is usually true (30). Savéant and coworkers found that DMSO containing comparatively large concentrations of added acid (such as 1 $\underline{M}$ acetic or chloroacetic acid) provided a suitable medium for the catalysis of dioxygen reduction by methyl viologen (30). The detailed reaction scheme was given as:

$$MeV^{2+} + e \rightleftharpoons MeV^{+} \cdot \qquad [48]$$

$$MeV^{+} \cdot + O_2 \underset{k_{-1}}{\overset{k_1}{\rightleftharpoons}} MeV^{2+} + O_2^{-} \qquad [49]$$

$$O_2^{-} + HA \overset{k}{\longrightarrow} HO_2 \cdot + A^{-} \qquad [50]$$

$$MeV^{+} \cdot + HO_2 \cdot \rightarrow MeV^{2+} + HO_2^{-} \qquad [51]$$

$$HO_2^{-} + HA \rightarrow H_2O_2 + A^{-} \qquad [52]$$
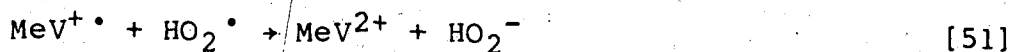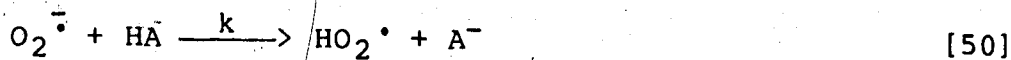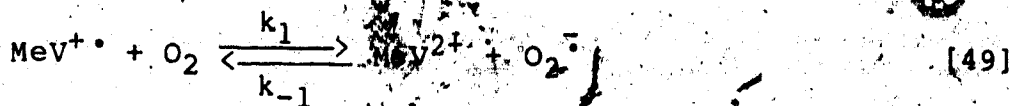
The net solution reaction is given by:

$$2MeV^{+} \cdot + 2HA + O_2 \overset{k_1}{\longrightarrow} 2MeV^{2+} + 2A^{-} + H_2O_2 \qquad [53]$$
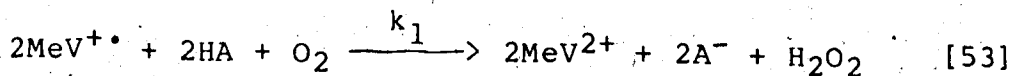
The added acid was required to drive reaction [49] from left to right and thus create a situation in which the magnitude of the catalytic current was controlled by k_1 (30). The large concentration of acid ensures that the rate of reaction [50] exceeds that of the back-reaction [49]. The rate of reaction [51] was assumed to be fast with respect to k_1.

 using cyclic voltammetry at a stationary glassy carbon disk electrode together with a numerical solution of the differential equation describing the mechanism,

Savéant et al. determined k_1 to be $(2.3 \pm 0.3) \times 10^5$ $M^{-1}s^{-1}$. The rate of reaction [49] was of interest to these workers as an example of a case where the diffusivities of catalyst and substrate differed greatly. The ratio $D_{O_2}/D_{MeV^{2+}}$ was found to be 6.3 ± 0.5 in DMSO (30). This difference has a significant effect on the observed catalytic currents and therefore had to be accounted for in formulating and solving the kinetic-diffusion equation. DMSO was chosen as a solvent primarily because of the better solubility of methyl viologen dichloride.

Following Savéant et al., the present work began with studies in DMSO but using amperometry at a RDE rather than cyclic voltammetry. The resolution between catalyst and substrate reduction waves observed in DMSO was found to be rather marginal, however. An example is shown in Figure 26 for the $MeV^{+\cdot}/O_2$ reaction. To successfully apply the EC-catalytic mechanism, it is necessary to be able to measure the limiting current for catalyst reduction without significant interference from direct substrate reduction. This implies sufficient separation of catalyst and substrate waves so that a more or less well-defined limiting-current plateau is observed. For polarographic applications, 175 mV has been suggested as a reasonable lower lim   the difference in half-wave potentials
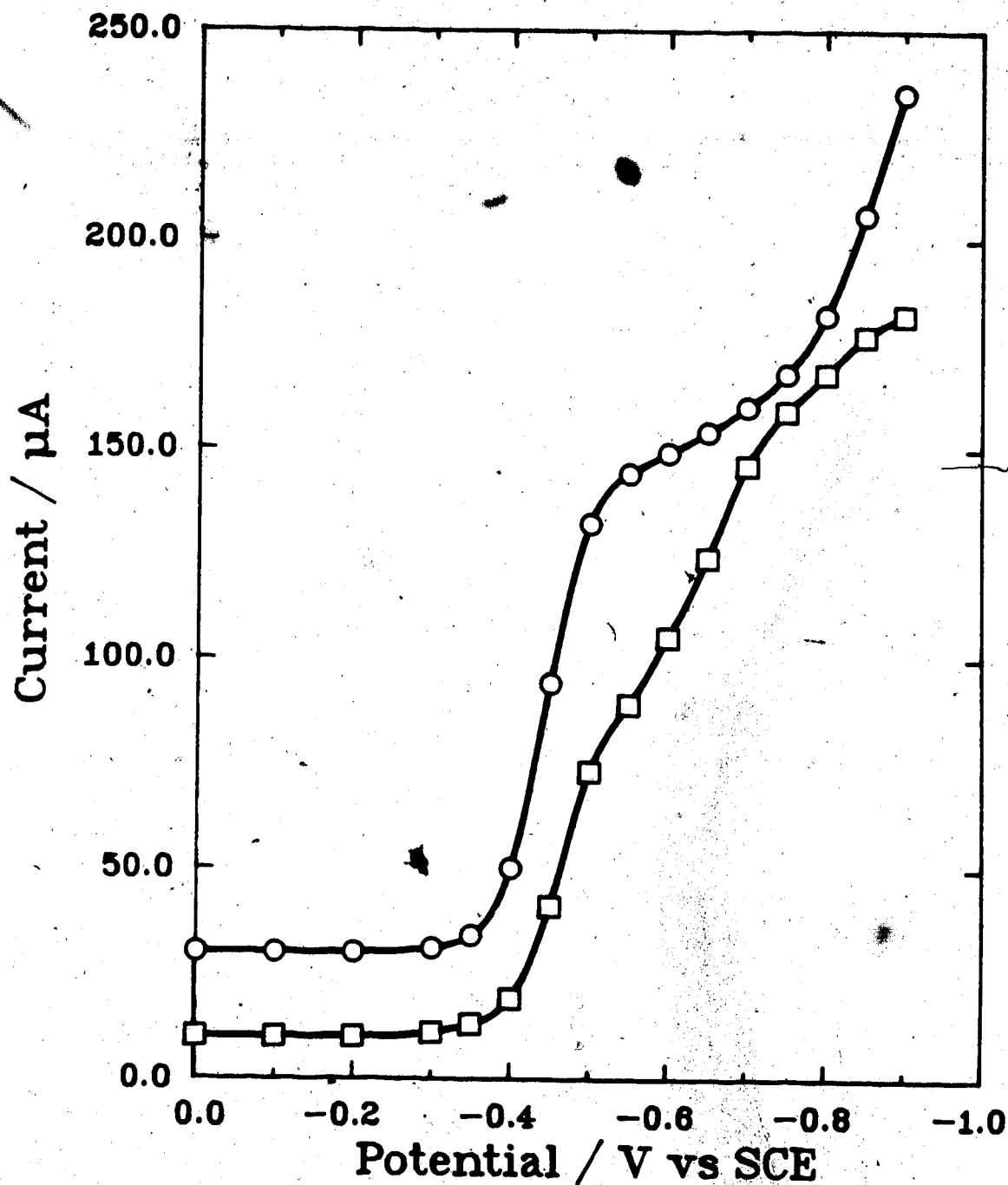
Figure 26. Current-Voltage Curves for Mixtures of Methyl
Viologen and Dioxygen in Acetonitrile and DMSO.
GC RDE @ 900 rpm, scan rate = 0.5 V/min.
○──○──○   125. μM MeV^{2+}, 55. μM O$_2$, 0.1 M
TEAP, 1.0 M HOAc in acetonitrile; □──□──□
103. μM MeV^{2+}, 88. μM O$_2$, 0.1 M NaClO$_4$, 1.0 M HOAc
in DMSO. Baselines have been shifted for
clarity.

(38). The potential separation for the $MeV^{+\cdot}/O_2$ reaction

in acidic DMSO is at this lower limit (Figure 26).

The marginal resolution afforded by DMSO prompted a

search for more suitable experimental conditions. The

search began by considering the reduction of dioxygen.

There exists an extensive literature on this subject that

has been reviewed on a number of occasions (130-133).

From compilations of half-wave potentials for the

polarographic reduction of dioxygen (130,131) it was found

that the most negative potentials are associated with

dipolar aprotic solvents. Values for common solvents,

taken from the literature (130), appear in Table 18. Of

the solvents shown, only DMSO, DMF, acetonitrile, and, to

a lesser extent, pyridine and propylene carbonate find

regular application in electrochemical studies. Sawyer

and coworkers have systematically studied dioxygen

reduction in these solvents (109,136). From cyclic

voltammetry at GC, Pt, Au, and Hg electrodes, values were

obtained for the formal reduction potential for the one-

electron reduction of dioxygen (109); these are given in

Table 18. From Sawyer's results, it is apparent that

dioxygen is significantly more difficult to reduce in DMF,

acetonitrile and pyridine than in DMSO. While the formal

potentials for the former three solvents are very similar,

cathodic peak potentials were generally 100 to 200 mV more

Table 18.   Half-Wave and Formal Potentials for the One-Electron
Reduction of Dioxygen in Various Solvents (from Ref. 130).

Solvent	$E_{1/2}$/V vs aq. SCE
Dimethylsulfoxide	-0.75^a
Propylene carbonate	-0.77
Methylene chloride	-0.79
Acetonitrile	-0.82
Dimethylformamide	-0.84^b
Acetone	-0.88
Pyridine	-0.89
Quinoline	-0.90

Formal Potentials for the O_2/O_2^- Couple[c] (from Ref. 109).

Solvent[d]	$E^{\circ\prime}$/V vs aq. SCE
Dimethylsulfoxide	-0.78
Dimethylformamide	-0.86
Acetonitrile	-0.87
Pyridine	-0.88
Water (pH 7)	-0.41

a.   Average of 4 separate determinations.

b.   Average of 3 separate determinations.

c.   From cyclic voltammetry (average of $E_{p,c}$ and $E_{p,a}$).

d.   Containing 0.1 $\underline{M}$ TEAP as electrolyte.

negative in acetonitrile (depending on electrode
material). From published work, it was concluded that
acetonitrile was worthy of investigation as an alternative
to DMSO.

If the additional potential separation afforded by
acetonitrile was to be useful, it had to be maintained in
the presence of large amounts of acetic acid. The results
obtained for dioxygen reduction in DMSO and acetonitrile
in the presence and absence of 1.0 $\underline{M}$ acetic acid are shown
in Table 19. In the absence of acid, the half-wave
potential was found to be 140 mV more negative in
acetonitrile. Because of differences in the response to
added acid, the potential separation increased to 210 mV
in the presence of 1.0 $\underline{M}$ acetic acid. Observed currents
doubled on addition of acid in both cases as the electro-
chemical process shifted from a one-electron to a two-
electron reduction. The comparative insensitivity of the
dioxygen half-wave potential to added weak acids has been
observed on a number of occasions in dipolar aprotic
solvents (109,134-136).

Results obtained at a Pt RDE are also shown in Table
19. The half-wave potential observed in acetonitrile is
some 200 mV negative to that observed on GC.
Unfortunately, Pt is unsuitable for this application as
the hydrogen peroxide produced by the overall solution

Table 19. Dioxygen Reduction in Acetonitrile and Dimethylsulfoxide Electrolytes.

Solvent	Electrolyte	GC RDE		Pt RDE	
		$E_{1/2}$	i_{lim}	$E_{1/2}$	i_{lim}
DMSO	0.1 M TEAP	-0.80 V	0.16 mA	-0.83 V	0.17 mA
	0.1 M TEAP, 1.0 M HOAc	-0.68	0.35	a	a
AN	0.1 M TEAP	-0.94	1.6	-1.16	1.7
	0.1 M TEAP, 1.0 M HOAc	-0.89	3.1	a	a

Conditions: Air-saturated solutions at 22°C, 700 torr. In AN, $[O_2]$ = 1.5×10^{-3} M; in DMSO, 0.4 mM. Electrode rotation speed 900 rpm. Potentials are referenced to an aqueous SCE.

a. Beyond cathodic limit.

reaction [53] is reducible on Pt. Such is not the case on glassy carbon (133).

The more negative half-wave potential for dioxygen reduction observed in acetonitrile translated into substantially improved resolution between catalyst and substrate waves as shown in Figure 26. An additional advantage associated with acetonitrile is the greater solubility of dioxygen. Acetonitrile saturated with dioxygen at 760 torr and 25°C contains 8.1 mM O_2 whereas DMSO under the same conditions contains 2.1 mM O_2 (109). The bulk of the experimental work described in the pages which follow was performed in acetonitrile. The results of earlier, more limited studies in DMSO have been included for comparison.

B. <u>Determination of the Diffusion Coefficient of Dioxygen in Acetonitrile and Dimethylsulfoxide Solutions</u>

Calculation of the numerical working curves for the kinetic experiments required knowledge of the diffusion coefficients of the chemical species involved. Diffusion coefficients for the catalysts and for dioxygen were determined by measuring limiting currents as a function of electrode rotation speed at the GC RDE and then plotting the results according to the Levich equation. The

diffusion coefficient of dioxygen was determined in
conjunction with the calibration of the gas proportioning
system. The calibration procedure is described in detail
in Chapter IV. Results for the calibration in
acetonitrile solutions appear in Table 20; those for DMSO
solutions in Table 21. Also given are the slopes of the
Levich plots prepared as part of the calibration
procedure. The diffusion coefficient of dioxygen was
calculated by plotting Levich slopes against the measured
dioxygen concentration. The plot obtained from the data
collected in acetonitrile solutions is shown in Figure 27;
that for DMSO solutions in Figure 28. Calculated values
for the diffusion coefficient of dioxygen in these
solutions appear in Table 22.

As the bulk of the experimental work was done in
acetonitrile, a much more extensive calibration was
carried out in this solvent. From the data in Table 20,
it can be seen that the reproducibility of the Levich
slopes is $\pm 1\%$. It can be inferred that the
reproducibility of the dioxygen concentration for a given
flow rate ratio is of the same order. Reproducibility of
the measured dioxygen concentrations was slightly poorer
and, excepting the three lowest concentrations, ranged
from $\pm 1\%$ to $\pm 3\%$.

Concerning the diffusion coefficients for dioxygen in

Table 20. Results for the Gas Proportioner Calibration in
Acetonitrile (0.1 M TEAP, 1.0 M HOAc).

Gas Mixture[a]		Flow Rates[a]		Levich Slope[b]	$[O_2]$[b,c]
600	601	600	601	($\mu A\ s^{1/2}$)	(μM)
N_2	0.1% O_2	100	100	0.88 ± 0.06	2.4 ± 0.3
		0	100	2.13 ± 0.32	5.8 ± 0.8
2.1% O_2	N_2	25	100	4.04 ± 0.05	17.3 ± 1.0
		50	100	7.48 ± 0.06	30.5 ± 0.5
		75	100	11.13 ± 0.12	42.6 ± 1.3
		100	100	14.38 ± 0.14	54.5 ± 1.2
N_2	2.1% O_2	100	100	16.94 ± 0.04	68.3 ± 0.4
		50	100	23.98 ± 0.21	97.7 ± 1.5
		0	100	31.14 ± 0.22	123.8 ± 1.7
Air	N_2	35	100	48.8 ± 1.3	200 ± 6
		50	100	69.0 ± 0.6	280 ± 9
		70	100	97.5 ± 1.0	406 ± 6
		90	100	123.6 ± 1.6	526 ± 7

a. The numbers 600 and 601 refer to the gas proportioner rotameter tubes. Flow rates are given in arbitrary rotameter units.
b. Average ±95% C.I. for 4 determinations.
c. Corrected to 700 torr total pressure.

Table 21. Results for the Gas Proportioner Calibration in Dimethyl-
sulfoxide (0.1 $\underline{M}$ NaClO$_4$, 1.0 $\underline{M}$ HOAc).

Gas Mixture[a]		Flow Rates[a]		Levich Slope	$[O_2]$[b]
600	601	600	601	(μA s$^{1/2}$)	(μM)
Air	N$_2$	50	150	5.0	54
		100	150	10.2	115
		150	150	14.3	169
N$_2$	Air	0	150	35.7	421

a. The numbers 600 and 601 refer to the gas proportioner rotameter
tubes. Flow rates are given in arbitrary rotameter units.

b. Corrected to 700 torr total pressure.
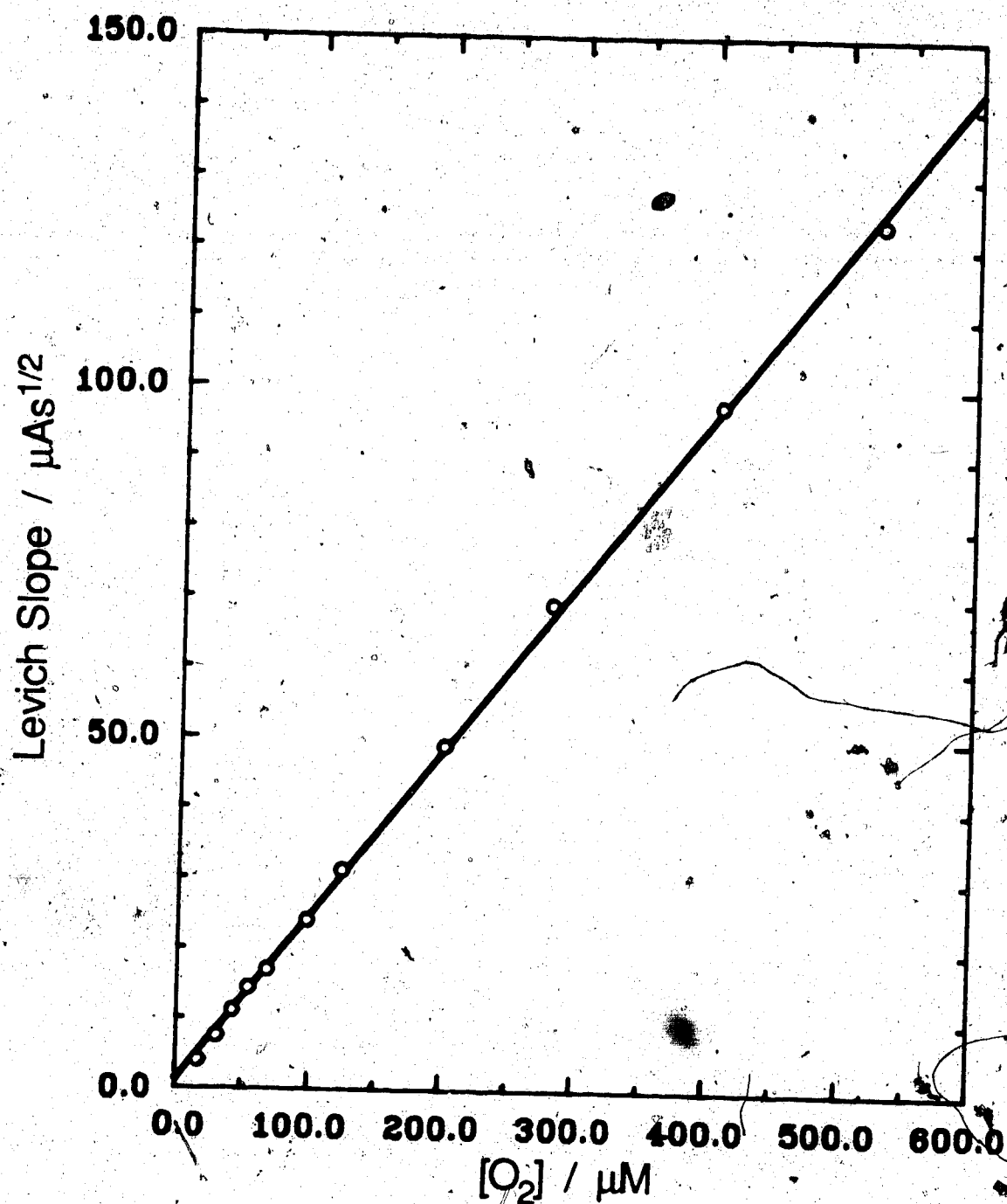
Figure 27. Determination of the Diffusion Coefficient of Dioxygen in Acetonitrile. 0.1 M TEAP, 1.0 M HOAc, 25.0°. Calculated values of the slope, intercept and diffusion coefficient appear in Table 22
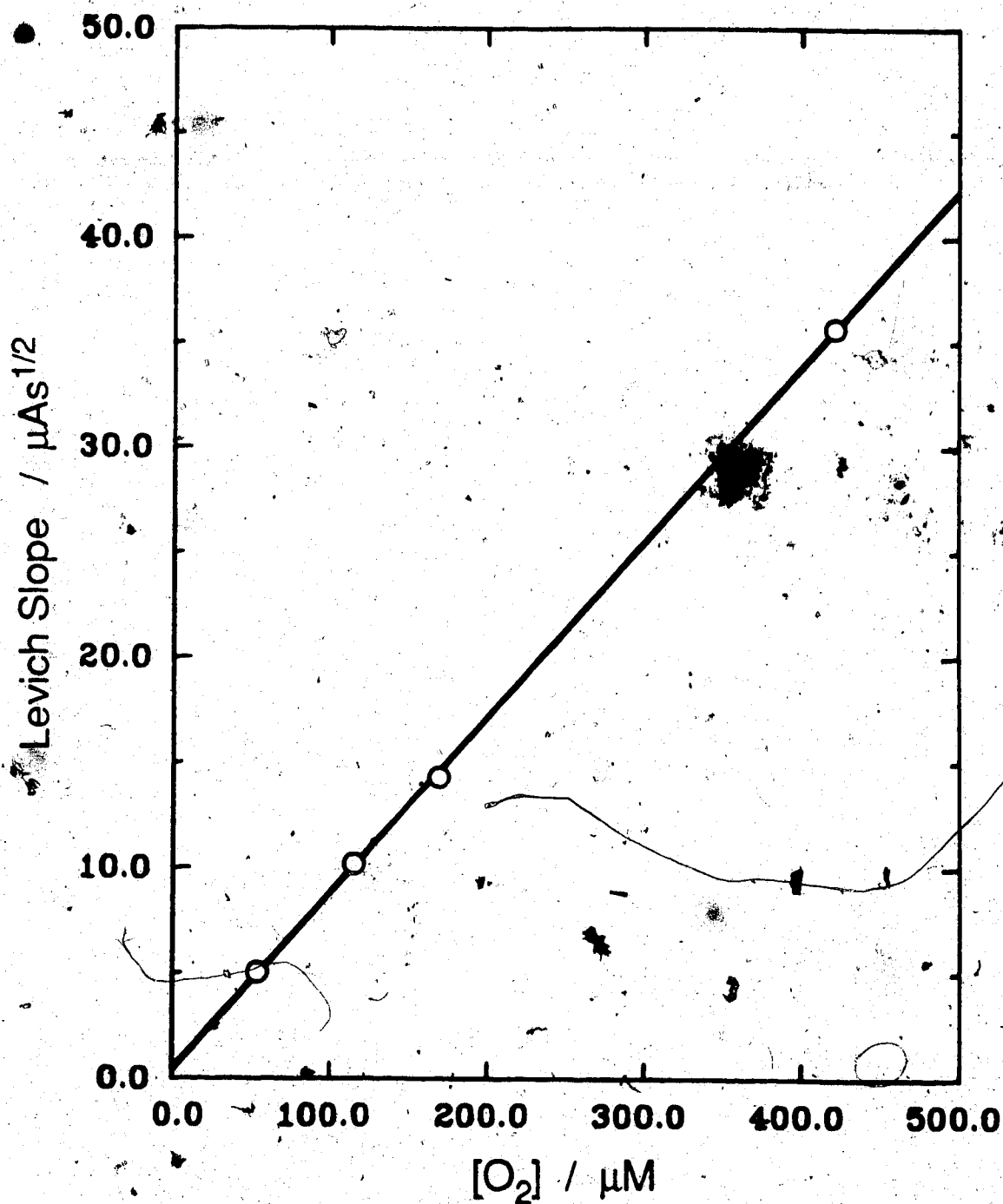
Figure 28. Determination of the Diffusion Coefficient of Dioxygen in DMSO. 0.1 M NaClO$_4$, 1.0 M HOAc, 25.0°. Calculated values of the slope, intercept and diffusion coefficient appear in Table 22.

Table 22. The Diffusion Coefficient of Dioxygen in Acetonitrile and

Dimethylsulfoxide Solutions.

i) Acetonitrile (0.1 $\underline{M}$ TEAP, 1.0 $\underline{M}$ HOAc)

Slope: (0.248 ± 0.005) $\mu A \ s^{1/2}/\mu M$

Intercept: (0.01 ± 0.60) $\mu A \ s^{1/2}$

Correlation: 0.9998

D: (8.40 ± 0.26) $\times 10^{-5} \ cm^2/s$

Results ±95% C.I. from weighted least-squares analysis of data

in Table 20 (plotted in Figure 27). D calculated using n = 2, A

= 0.4458 cm^2, $v = 4.95 \times 10^{-3} \ cm^2/s$.

ii) Dimethylsulfoxide (0.1 $\underline{M}$ NaClO$_4$, 1.0 $\underline{M}$ HC

Slope: (0.084 ± 0.003) $\mu A \ s^{1/2}/\mu M$

Intercept: (0.45 ± 0.80) $\mu A \ s^{1/2}$

Correlation: 0.9999

D: (2.36 ± 0.12) $\times 10^{-5} \ cm^2/s$

Results ±95% C.I. from least-squares analysis of data in Table

21 (plotted in Figure 28). D calculated using n = 2, A = 0.4458

cm^2 and $v = 2.03 \times 10^{-2} \ cm^2/s$.

nonaqueous solvents, very few results are available for
comparison with those obtained in the present work. In
DMSO, Johnson et al. found a value of $(2.8 \pm 0.5) \times 10^{-5}$
cm^2/s using d.c. polarography and the Ilkovic equation
(137). This is in reasonable agreement with the value of
$(2.36 \pm 0.12) \times 10^{-5}$ cm^2/s measured in this work. In
acetonitrile, Kolthoff and Coetzee found that a value of
6.7×10^{-5} cm^2/s was consistent with polarographic results
for dioxygen reduction (110). Their value was arrived at
using the diffusion coefficient measured in aqueous
solution together with the viscosities of water and
acetonitrile. The value obtained in this work, $(8.4 \pm$
$0.3) \times 10^{-5}$ cm^2/s, is not that far removed from their
estimate.

C. Kinetic Studies of the Diquaternized Salts of
    4,4'-Bipyridine in Acetonitrile.

The procedure employed in making the experimental
measurements was described in Chapter IV. From current-
voltage curves, examples of which appear in Figure 24,
half-wave potentials were obtained for the following
reactions:

$$[R-N\text{—}\langle\rangle\text{—}\langle\rangle\text{—}N-R]^{2+} + e^- \rightleftharpoons [R-N\text{—}\langle\rangle\text{—}\langle\rangle\text{—}N-R]^{+} \quad [54]$$

$$[R-N \overset{+ \cdot}{\diagdown} N-R]^{+ \cdot} + e^- \rightleftharpoons [R-N \diagdown N-R]^0 \qquad [55]$$
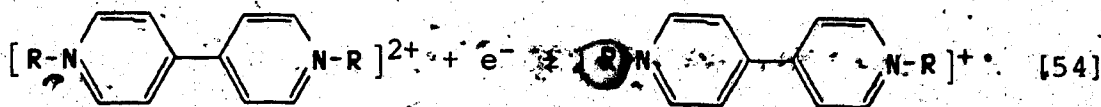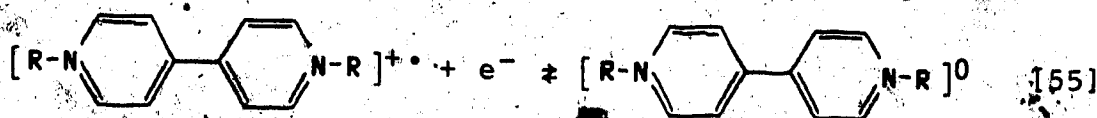
The results for the diquaternized salts of 4,4'-bipyridine are given in Table 23. Where available, literature values have been included for comparison. The results are in good agreement. The half-wave potential for reaction [54] was also measured in the presence of 1 $\underline{M}$ acetic acid; these values also appear in Table 23. Reduction potentials are 10 to 20 mV more negative in the presence of the acid. Half-wave potentials for reaction [55] could not be reliably estimated in the presence of acetic acid as the onset of hydrogen ion reduction obscured the limiting current plateau for the second wave.

The procedure used to calculate the rate constants k_1 for the reaction [49] will be illustrated by considering the results obtained for the reaction of the methyl viologen cation radical $MeV^{+ \cdot}$ with dioxygen. The concentrations of catalyst and substrate used and the experimentally measured limiting currents are given in Table 24. The diffusion coefficient of the catalyst MeV^{2+} was calculated by plotting limiting currents measured in the absence of dioxygen versus the product $[MeV^{2+}] \omega^{1/2}$ as shown in Figure 29. The diffusion coefficient was

Table 23. Half-Wave Potentials for the Diquaternized Salts of 4,4'-Bipyridine in Acetonitrile (0.1 $\underline{M}$ TEAP) vs SCE.

Compound	$-E^1_{1/2}$	$-E^2_{1/2}$	$-E^1_{1/2}$ (1.0 M HOAc)
MeV	0.45 (0.45)[a,b]	0.86 (0.87)[a,b]	0.45
HeV	0.44	0.87	0.45
CeV	$-$[c]	$-$[c]	0.44
BzV	0.37 (0.38)[b]	0.78 (0.79)[b]	0.39
CxV	0.31	0.72	0.32
PhV	0.24 (0.23)[b]	0.55 (0.56)[b]	0.24
CyV	0.18	0.52	0.19
n-PrV	0.44	0.88	0.46
i-PrV	0.45 (0.46)[b]	0.88 (0.87)[b]	0.46
BuV	0.44	0.87	0.46
HxV	0.44	0.87	0.45
HpV	0.44	0.88	0.45
OcV	0.44	0.87	0.45

a. From Reference 140 using E(Ag/AgCl) vs E aq. (SCE) = -0.046 V (cited in Reference 140).

b. From reference 122 using E(Ag/AgCl/Acetonitrile) vs E aq. (SCE) = -0.19 V (calculated using $E^1_{1/2}$ given for methyl viologen in References 122 and 140).

c. Compound not soluble in the absence of HOAc.

Table 24. Experimental Results for the MeV$^{+\cdot}$/O$_2$ Reaction in
Acetonitrile.

Limiting Current for MeV$^{+\cdot}$ Reduction
(GC RDE, E_D = -0.60 V vs SCE)

[MeV] (μM)	[O$_2$] (μM)	Rotation Speed (rpm)				
		400	900	1600	2500	3600
56.3	0	12.7	18.8	24.9	30.9	36.9
	30	41.6	51.8	60.4	67.2	73.6
	54	64.1	77.5	87.0	94.4	100.8
	97	94.5	112.2	125.1	134.9	142.7
84.5	0	20.2	29.7	39.1	48.3	57.4
	43	68.1	87.6	101.3	113.0	125.0
	69	90.1	112.7	129.0	142.2	153.1
	124	141.0	169.6	189.8	204.0	217.9
112.7	0	26.0	38.4	50.8	63.0	75.2
	54	89.6	114.8	134.1	150.4	163.9
	97	129.2	163.2	188.3	207.9	223.7
	198	232.4	286.0	320.8	349.8	372.4
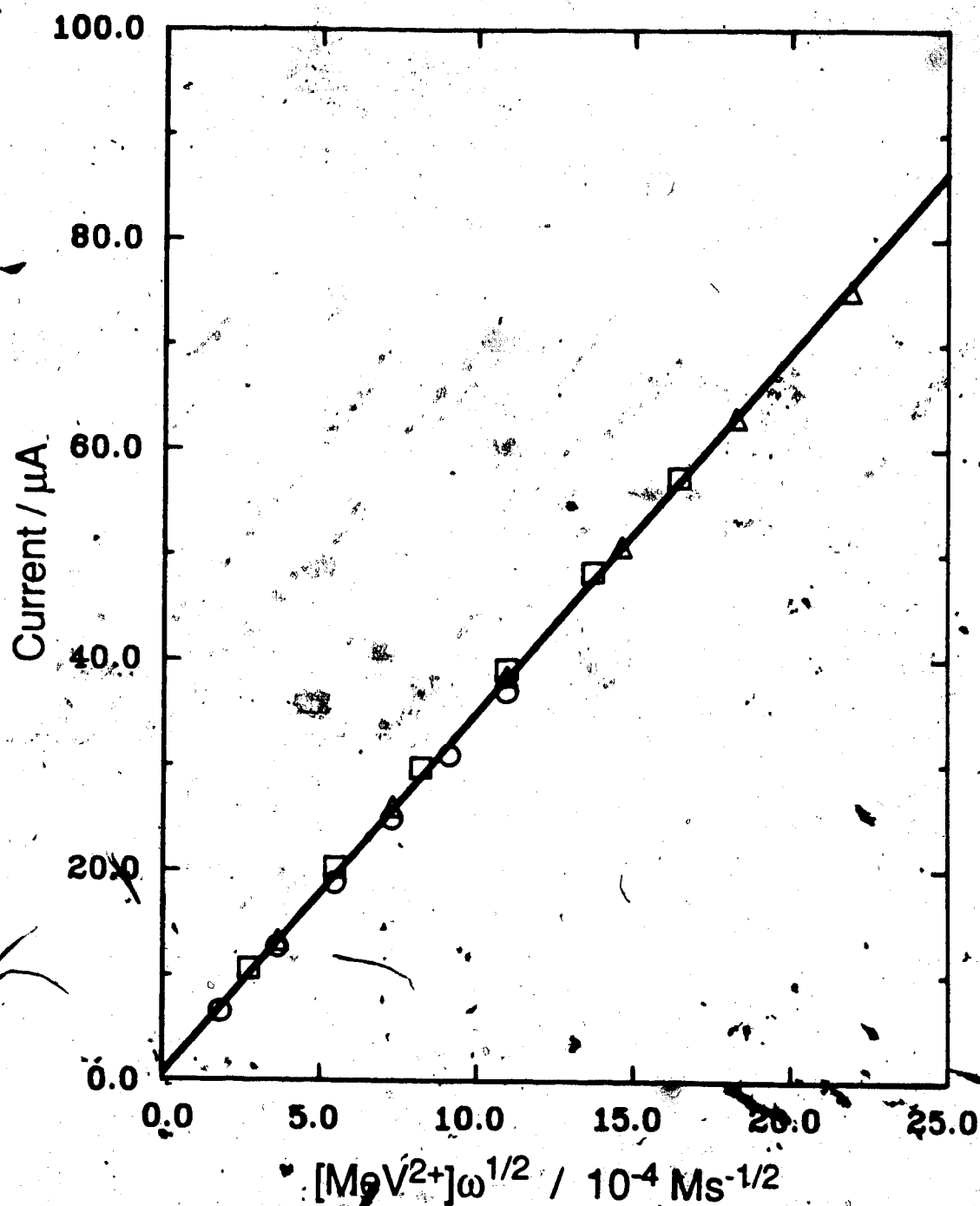
Figure 29. Determination of the Diffusion Coefficient of Methyl Viologen in Acetonitrile. 0.1 M TEAP, 1.0 M HOAc, 25.0°. Data from Table 24 ([O_2] = 0). [MeV^{2+}]: ○ 56.3 μM; □ 84.5 μM; △ 112.7 μM.

calculated from the slope of this plot. Results for
methyl viologen and for the other viologens appear in
Table 25. In the work described in this chapter, it was
assumed that the diffusion coefficients of the reduced
form of the catalysts (the cation radicals) equalled those
measured for the oxidized form (the dications).

The diffusion coefficients for the catalyst species
and for the substrate together with the catalyst and
substrate concentrations used in the kinetic experiment
were used to calculate a set of working curves relating
the current ratio R to the kinetic parameter $\bar{k}$. The
program ECR2WC was used for this purpose; a program
listing and the details associated with the computations
may be found in Appendix II. The program output for a
typical working curve is shown in Figure 30. Collocation
polynomials of degree 8 were used throughout. The time
required to generate the set of nine working curves
required for a complete kinetic experiment was on the
order of an hour. The overall 2:1 MeV$^{+\cdot}$:O_2 stoichiometry
for reaction [53] was accommodated by using twice the
actual substrate concentrations in the calculation of the
working curves (30,94).

Currents measured in the presence and absence of
dioxygen were corrected for the background current (the
intercept of the Levich plot) prior to calculating current

Table 25. Diffusion Coefficients of the Diquaternized Salts of
4,4'-Bipyridine in Acetonitrile (0.1 $\underline{M}$ TEAP, 1.0 $\underline{M}$ HOAc).

Compound	$-E_D$ (V vs SCE)	Slope[a] ($\mu A\ s^{1/2}/mM$)	Intercept[a] (μA)	D ($10^{-5}\ cm^2/s$)
MeV	0.60	34.2±0.6	0.7±0.7	1.22±0.04
HeV	0.60	31.1±0.2	0.6±0.2	1.06±0.01
CeV	0.60	29.7±1.0	2.3±1.5	0.98±0.05
BzV	0.55	29.8±0.3	0.0±0.3	0.99±0.01
CxV	0.45	28.9±0.2	0.2±0.2	0.94±0.01
PhV	0.38	30.2±0.1	1.0±0.5	1.01±0.01
CyV	0.30	28.0±0.1	2.0±0.7	0.90±0.01
n-PrV	0.60	32.3±0.3	1.6±0.4	1.12±0.0
i-PrV	0.60	32.6±0.3	0.7±0.4	1.13±0.0
BuV	0.60	31.8±0.3	0.8±0.4	1.09±0.02
HxV	0.60	30.5±0.3	1.4±0.3	1.03±0.02
HpV	0.60	28.9±0.7	1.4±0.4	0.94±0.04
OcV	0.60	28.9±0.3	0.7±0.2	0.94±0.01

a. Results calculated by weighted linear least-squares regression.
Uncertainties given are 95% confidence limits.

```
***Second-Order EC-Catalytic Mechanism***
        at the Rotating Disk Electrode

    Working Curves by Orthogonal Collocation
```

Ver   01-B   11-AUG-88

Enter degree of collocation polynomial (12).   8

Enter diffusion coefficient for species P.   0.148

Enter diffusion coefficient for species Q.   0.148

Enter diffusion coefficient for species A.   1.000

Enter normalized concentration of species A.   1.073

Enter D/v ratio.   0.000

Enter convergence criterion.   1.000E-08

Log(k)	Current Ratio	Cat. Efficiency	Nits
-1.500000E+00	9.432492E-01	5.607203E-02	3
-1.400000E+00	9.301330E-01	7.000463E-02	3
-1.300000E+00	9.144194E-01	8.722287E-02	3
-1.200000E+00	8.957937E-01	1.084141E-01	3
-1.100000E+00	8.739943E-01	1.343637E-01	3
-1.000000E+00	8.488557E-01	1.659427E-01	3
-9.000000E-01	8.203420E-01	2.041042E-01	3
-8.000000E-01	7.886087E-01	2.498192E-01	4
-7.000000E-01	7.539750E-01	3.041044E-01	4
-6.000000E-01	7.169841E-01	3.678761E-01	4
-5.000000E-01	6.783253E-01	4.419562E-01	5
-4.000000E-01	6.388206E-01	5.269195E-01	5
-3.000000E-01	5.993042E-01	6.231143E-01	5
-1.999999E-01	5.605884E-01	7.305126E-01	6
-1.000000E-01	5.233446E-01	8.488230E-01	6
0.000000E-01	4.881102E-01	9.773698E-01	7
1.000000E-01	4.552892E-01	1.115010E+00	7
2.000000E-01	4.251222E-01	1.260266E+00	8
3.000001E-01	3.976909E-01	1.411478E+00	8
4.000000E-01	3.729858E-01	1.566699E+00	9
5.000000E-01	3.509607E-01	1.723506E+00	9
6.000001E-01	3.315115E-01	1.879298E+00	10
7.000000E-01	3.144222E-01	2.032094E+00	11
8.000000E-01	2.995651E-01	2.179098E+00	11
9.000001E-01	2.867758E-01	2.317843E+00	12
1.000000E+00	2.758034E-01	2.447130E+00	13
1.100000E+00	2.665130E-01	2.564923E+00	13
1.200000E+00	2.587394E-01	2.669984E+00	14
1.300000E+00	2.522587E-01	2.762521E+00	14
1.400000E+00	2.468936E-01	2.842804E+00	15
1.500000E+00	2.425357E-01	2.910628E+00	15

Figure 30. Sample Working Curve for the Methyl Viologen/
            Dioxygen Reaction in Acetonitrile. A listing
            of the program ECR2WC, which was used to compute
            these results, appears in Appendix II.

ratios.   For the $MeV^{+\bullet}/O_2$ reaction, the following background currents were found:

[MeV]	i_b
56.3 μM	0.58 μA
84.5	1.51
112.7	1.16

These values ranged from 0.3% to 7.5% of the observed currents.   For each experimental run, corrected currents together with the appropriate working curves were input to the program KPRCAL (Appendix II). Within the program, current ratios were calculated and the corresponding kinetic parameters were estimated from the working curve by three-point or four-point Lagrangian interpolation. The complete set of results obtained for the $MeV^{+\bullet}/O_2$ reaction is shown in Table 26.

To determine the rate constant k_1, the three values of the kinetic parameter obtained at each rotation speed (one for each dioxygen concentration) were averaged.   The average values were plotted against the quantity $[MeV]/\omega$ according to the definition of the kinetic parameter:

Table 26. Calculated Results for the $MeV^{+\bullet}/O_2$ Reaction in Acetonitrile.

Kinetic Parameter as a Function of Catalyst and Substrate Concentrations and Electrode Rotation Speed.

[MeV]	[O_2]	Rotation Speed (rpm)				
(μM)	(μM)	400	900	1600	2500	3600
56.3	30	6.70	3.00	1.85	1.26	0.94
	54	8.65	3.82	2.22	1.48	1.07
	97	8.80	4.04	2.43	1.65	1.22
	Avg.	8.0	3.62	2.17	1.46	1.08
	s.d.	1.2	0.55	0.29	0.20	0.14
84.5	43	11.30	4.87	2.72	1.83	1.41
	69	9.15	4.31	2.57	1.76	1.30
	124	11.32	5.02	2.95	1.96	1.46
	Avg.	10.6	4.73	2.75	1.85	1.39
	s.d.	1.2	0.37	0.19	0.10	0.08
112.7	54	15.47	5.69	3.18	2.11	1.51
	97	11.55	5.44	3.27	2.21	1.61
	198	18.26	8.05	4.55	3.05	2.22
	Avg.	15.1	6.4	3.67	2.46	1.78
	s.d.	3.4	1.4	0.77	0.52	0.38

$$\bar{k} = (\frac{\nu}{D_A})^{1/3} \frac{c_P(\infty)}{\omega} k$$

The plot appears in Figure 31. The rate constant was calculated from the slope of the plot given that for the acetonitrile solutions $(\nu/D_A)^{1/3} = (4.95 \times 10^{-3}/8.4 \times 10^{-5})^{1/3} = 3.89$. The value obtained for k_1 for the MeV^{+}/O_2 reaction was $(1.40 \pm 0.05) \times 10^6 M^{-1}s^{-1}$.

Though the scatter in the values of $\bar{k}$ shown in Table 26 is considerable, especially at the lower rotation speeds, the mean values as plotted in Figure 31 fall satisfactorily along a straight line. Making measurements at three different substrate concentrations for each catalyst concentration was well worth the additional effort. That the same slope, and therefore the same value of k_1, is observed at each of the three catalyst concentrations employed is evidence of the validity of the mechanism proposed by Savéant et al. (30) which is described by equations [48] to [53].

As the variances associated with the average values of $\bar{k}$ were not constant as a function of rotation speed, a weighted linear least-squares procedure (138,139) was used to calculate the slopes and intercepts of the kinetic parameter plots. In this procedure, a weighted sum of the squares of the residuals given by
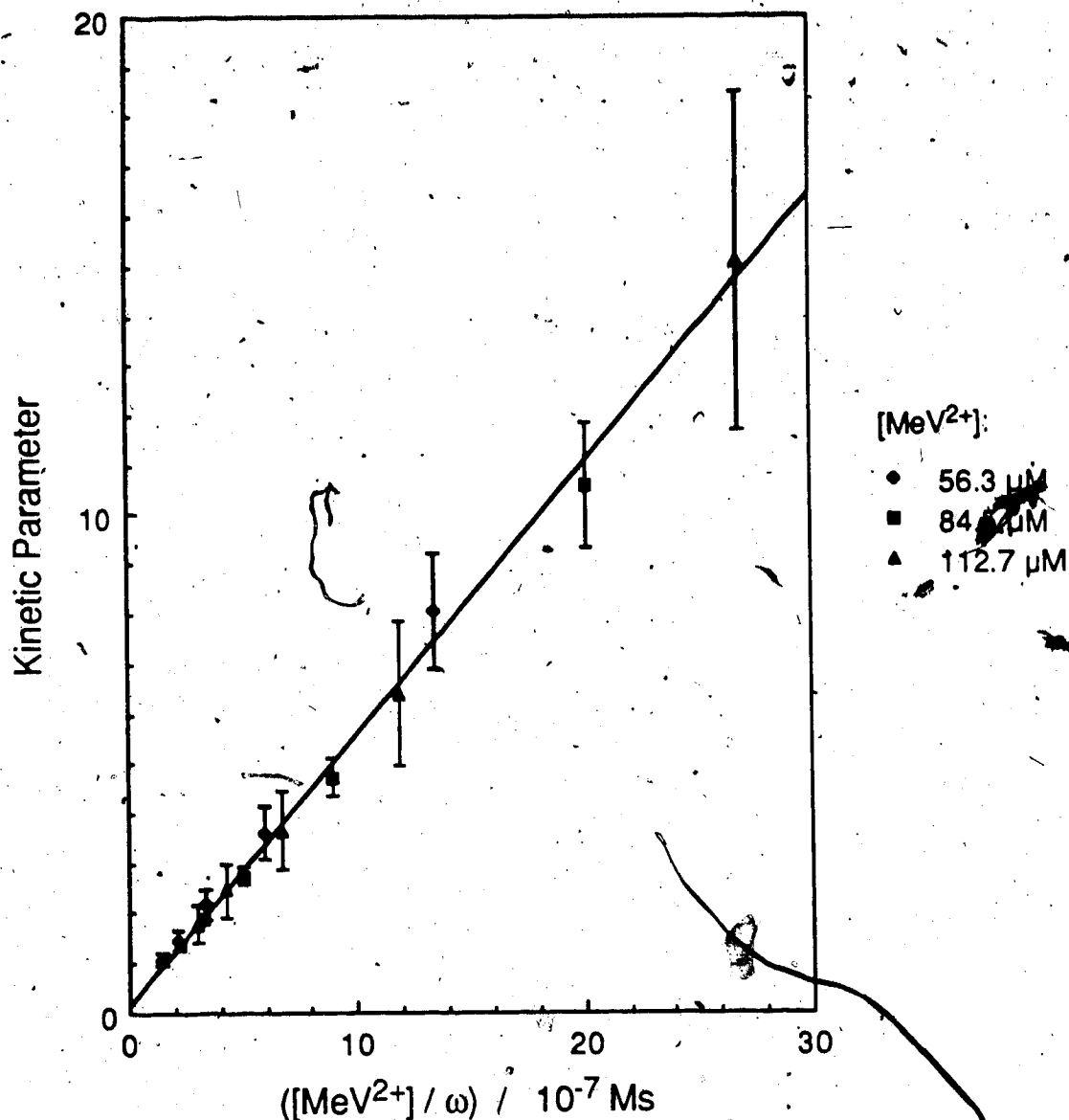
Figure 31. Kinetic Parameter Plot for the Methyl Viologen/
Dioxygen Reaction in Acetonitrile. 0.1 M TEAP,
1.0 M HOAc, 25.0°. Average kinetic parameter ±
standard deviation for 3 determinations.

$$S = \Sigma_i (y_i - a - b \, x_i)^2 / (\sigma_{y_i}^2 \pm b^2 \sigma_{x_i}^2)$$

was minimized. In this formula, x_i and y_i represent the observed data, σ_{x_i} and σ_{y_i} are the associated standard deviations and a and b are the intercept and slope of the fitted line. In the present case, σ_{x_i} was taken to be zero.

Rate constants for the other viologens were determined in the same fashion as described for the $MeV^{+\cdot}/O_2$ reaction. Average values for the kinetic parameters calculated from the experimental data are presented in Table 27. Plots of average kinetic parameter versus $[Catalyst]/\omega$ for each of the compounds appear in Figures 31 to 43. The slopes and intercepts of these plots and the corresponding values obtained for k_1 appear in Table 28.

The uncertainties associated with the rate constants given in Table 28 were calculated from the 95% confidence intervals for the slopes of the kinetic parameter plots. These values do not include the uncertainties associated with the working curves. The latter are due to errors in the diffusion coefficients and dioxygen concentrations used to calculate the working curves. To determine the effect of uncertainties in the dioxygen concentrations on the calculated values for k_1, working curves for the

Table 27. Calculated Results for the Diquaternized Salts of 4,4'-Bipyridine in Acetonitrile.

Average Kinetic Parameters and Their Standard Deviations

Compound	Conc. (μM)	Rotation Speed (rpm)				
		400	900	1600	2500	3600
MeV	56.3	8.0 ±1.2	3.62 0.55	2.17 0.29	1.46 0.20	1.08 0.14
	84.5	10.6 ±1.2	4.73 0.37	2.75 0.19	1.85 0.10	1.39 0.08
	112.7	15.1 ±3.4	6.4 1.4	3.67 0.77	2.46 0.52	1.78 0.38
HeV	51.9	5.9 ±1.0	2.74 0.40	1.61 0.22	1.07 0.13	0.78 0.10
	77.8	8.8 ±1.0	3.78 0.30	2.16 0.16	1.42 0.10	1.02 0.07
	103.8	12.1 ±2.5	5.02 0.66	2.80 0.30	1.81 0.18	1.31 0.13
CeV	68.3	7.4 ±1.3	3.39 0.48	1.99 0.26	1.37 0.16	1.01 0.11
	102.5	13.3 ±2.0	5.73 0.52	3.37 0.32	2.26 0.23	1.66 0.16
	136.6	12.7 ±2.2	5.45 0.52	3.22 0.29	2.17 0.18	1.58 0.14
BzV	60.8	2.15 ±0.24	1.00 0.09	0.60 0.04	0.39 0.03	0.29 0.02
	91.3	3.47 ±0.44	1.56 0.17	0.90 0.10	0.60 0.06	0.43 0.04
	121.7	4.28 ±0.42	1.88 0.12	1.09 0.06	0.71 0.04	0.52 0.02

(Continued)

Table 27: (Continued)

Compound	Conc. (µM)	Rotation Speed (rpm)				
		400	900	1600	2500	3600
CxV	55.4	0.428 ±0.017	0.203 0.004	0.117 0.003	0.079 0.001	0.058 0.001
	110.7	0.764 ±0.065	0.341 0.026	0.196 0.0f6	0.127 0.010	0.094 0.009
	166.1	1.064 ±0.006	0.473 0.006	0.274 0.005	0.179 0.004	0.126 0.005
PhV	99.9	0.216 ±0.011	0.109 0.003	0.067 0.002	0.048 0.001	0.0355 0.0004
	199.9	0.342 ±0.016	0.165 0.006	0.101 0.005	0.071 0.004	0.052 0.003
	399.8	0.586 ±0.017	0.274 0.006	0.161 0.002	0.108 0.001	0.078 0.001
CyV	201.8	0.111 ±0.004	0.051 0.003	0.032 0.004	0.022 0.003	0.017 0.003
	403.6	0.190 ±0.003	0.088 0.002	0.051 0.002	0.035 0.002	0.025 0.001
	807.2	0.356 ±0.034	0.164 0.017	0.096 0.011	0.063 0.007	0.042 0.004
n-PrV	58.0	6.7 ±1.1	3.09 0.38	1.80 0.19	1.19 0.11	0.86 0.07
	87.0	9.4 ±1.2	3.91 0.42	2.21 0.25	1.45 0.18	1.04 0.12
	116.0	17.1 ±5.9	6.53 1.07	3.71 0.44	2.46 0.26	1.72 0.18
i-PrV	59.8	5.7 ±0.8	2.48 0.31	1.43 0.10	0.95 0.10	0.69 0.07
	89.7	8.1 ±1.2	3.37 0.36	1.90 0.19	1.24 0.13	0.88 0.08
	119.7	10.1 ±1.5	4.18 0.33	2.31 0.12	1.51 0.06	1.07 0.03

(Continued)

Table 27. (Continued)

Compound	Conc.	Rotation Speed (rpm)				
	(µM)	400	900	1600	2500	3600
BuV	56.0	9.2 ±2.4	4.17 1.04	2.46 0.59	1.63 0.38	1.17 0.26
	84.1	11.3 ±1.7	4.77 0.44	2.79 0.22	1.86 0.16	1.33 0.10
	112.1	17.4 ±6.3	7.5 1.9	4.2 1.1	2.70 0.66	1.91 0.44
HxV	52.3	13.5 ±2.7	6.0 1.1	3.5 0.6	2.30 0.37	1.65 0.25
	78.5	15.8 ±4.3	7.1 1.9	4.2 1.1	2.75 0.71	2.00 0.52
	104.7	15.3 ±3.3	9.7 2.8	5.3 1.3	3.45 0.79	2.36 0.51
HpV	51.0	10.9 ±2.6	5.0 0.8	2.99 0.40	2.03 0.21	1.47 0.13
	76.4	13.9 ±1.6	6.3 1.0	3.72 0.57	2.53 0.41	1.83 0.30
	101.9	19.1 ±1.3	8.4 1.0	4.79 0.55	3.19 0.37	2.40 0.28
OcV	54.9	13.2 ±1.9	5.7 1.4	3.69 0.50	2.46 0.29	1.77 0.20
	73.0	17.1 ±0.1	7.7 0.8	4.54 0.65	3.02 0.45	2.20 0.32
	97.3	20.6 ±0.9	9.0 1.1	5.23 0.81	3.41 0.59	2.48 0.47

Figure 32. Kinetic Parameter Plot for the Hydroxyethyl
Viologen/Dioxygen Reaction in Acetonitrile.
0.1 M TEAP, 1.0 M HOAc, 25.0°. Average kinetic
parameter ± standard deviation for 3 deter-
minations.
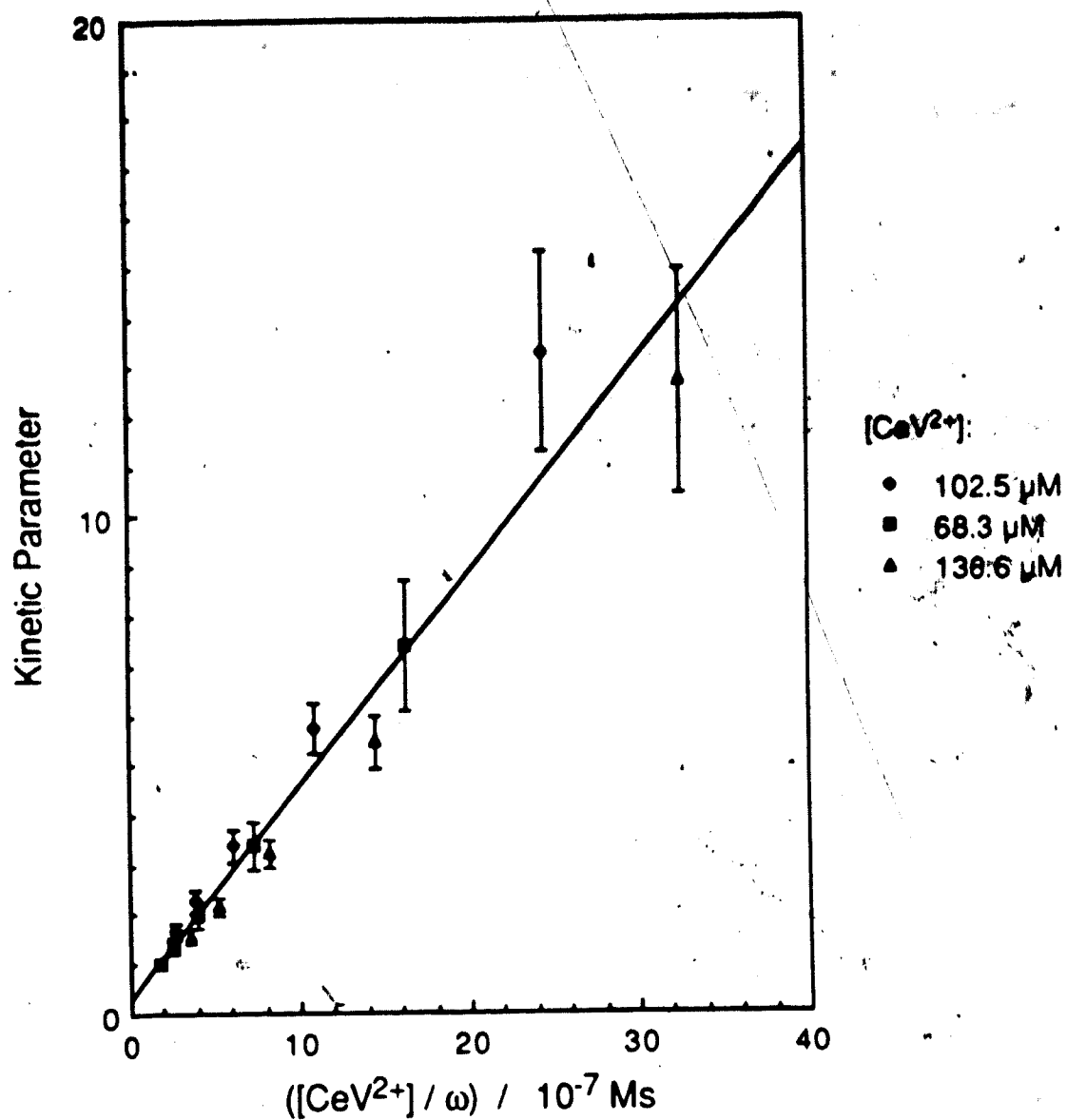
Figure 33. Kinetic Parameter Plot for the Carboxyethyl
Viologen/Dioxygen Reaction in Acetonitrile.
0.1 M TEAP, 1.0 M HOAc, 25.0°. Average kinetic
parameter ± standard deviation for 3 deter-
minations.
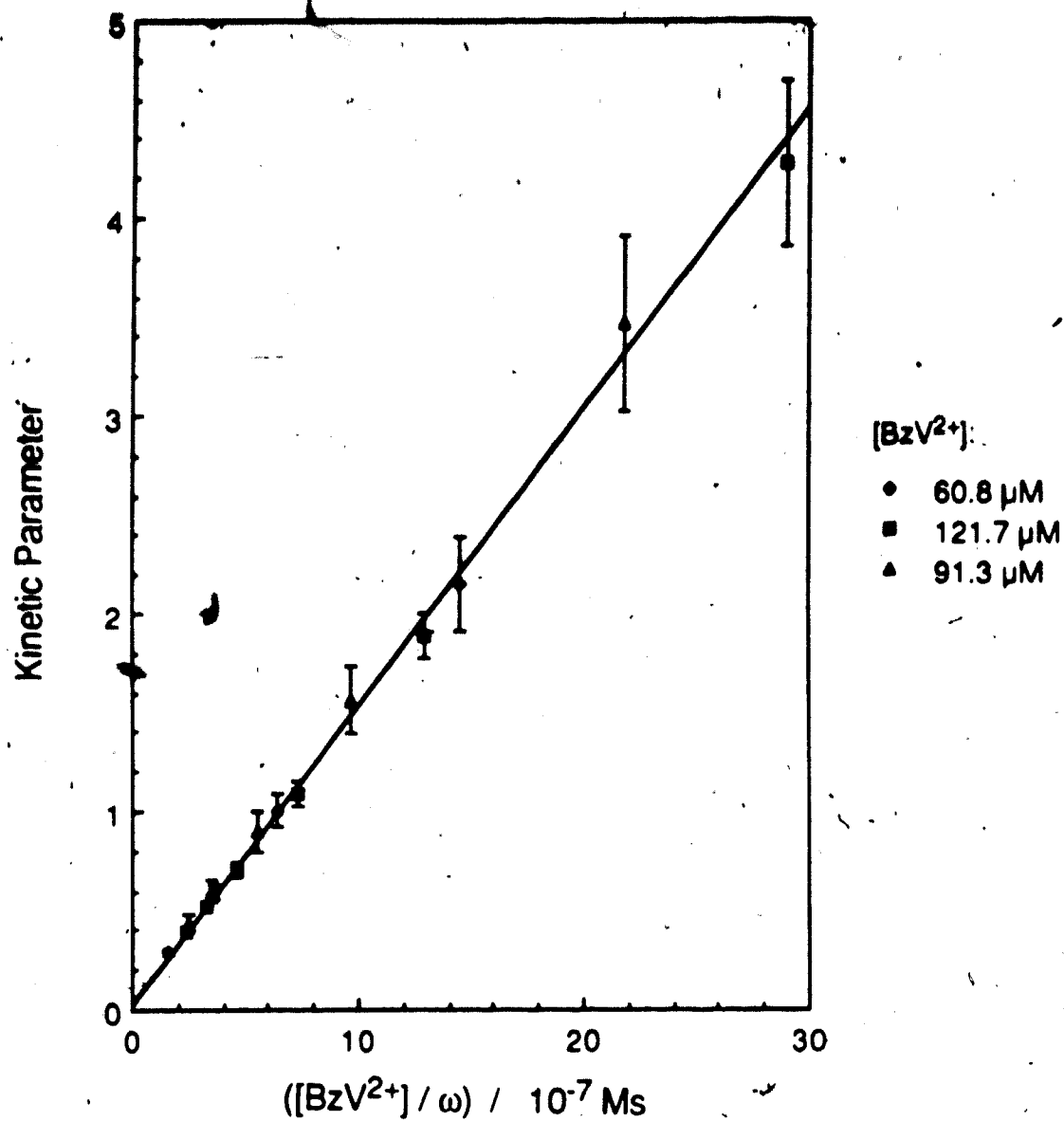
Figure 34. Kinetic Parameter Plot for the Benzyl Viologen/ Dioxygen Reaction in Acetonitrile. 0.1 M TEAP, 1.0 M HOAc, 25.0°. Average kinetic parameter ± standard deviation for 3 determinations.
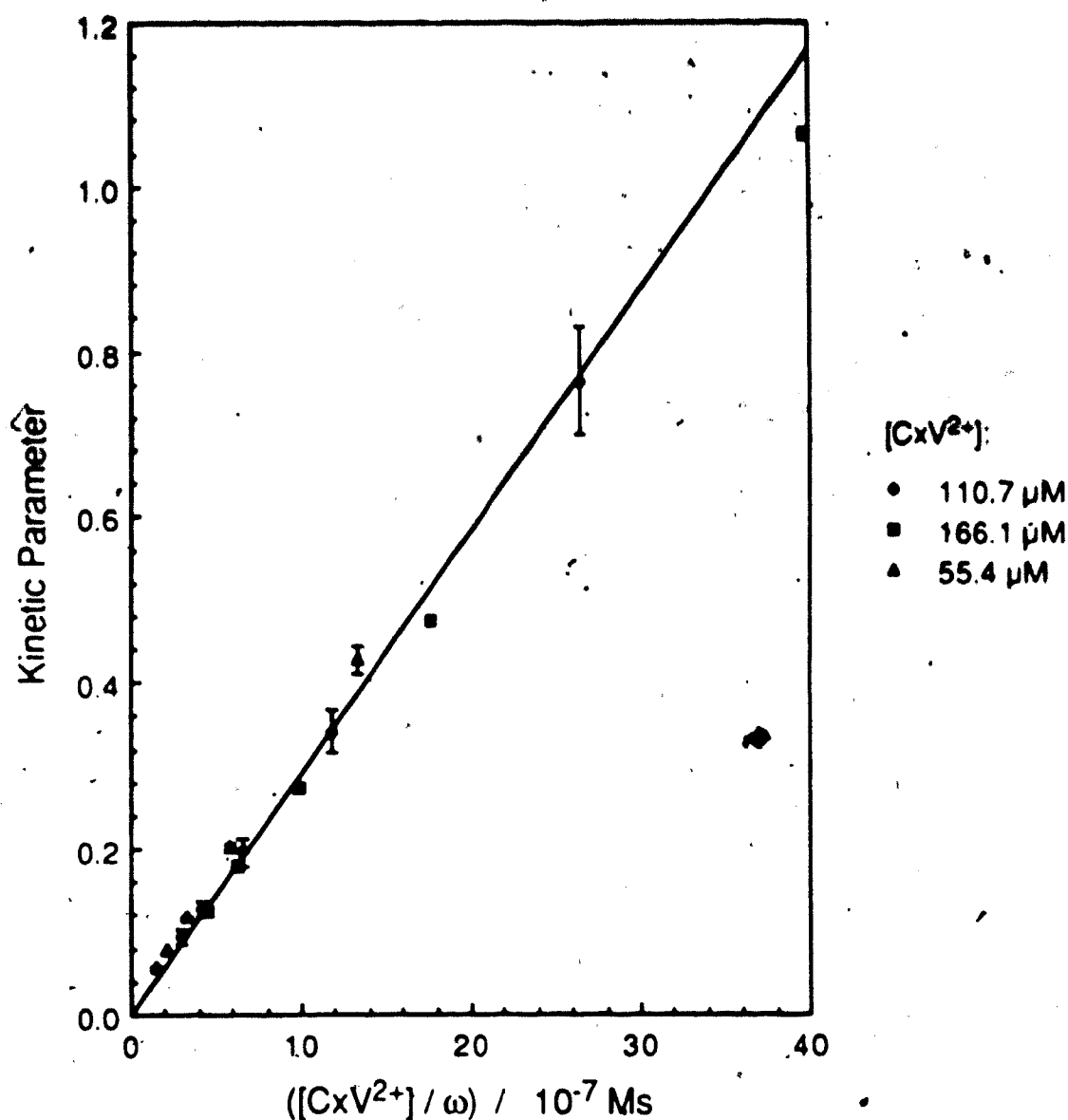
Figure 35. Kinetic Parameter Plot for the Carbethoxyethyl
Viologen Dioxygen Reaction in Acetonitrile. 0.1 M
TEAP, 1.0 M HOAc, 25.0°. Average kinetic parameter
± standard deviation for 3 determinations.
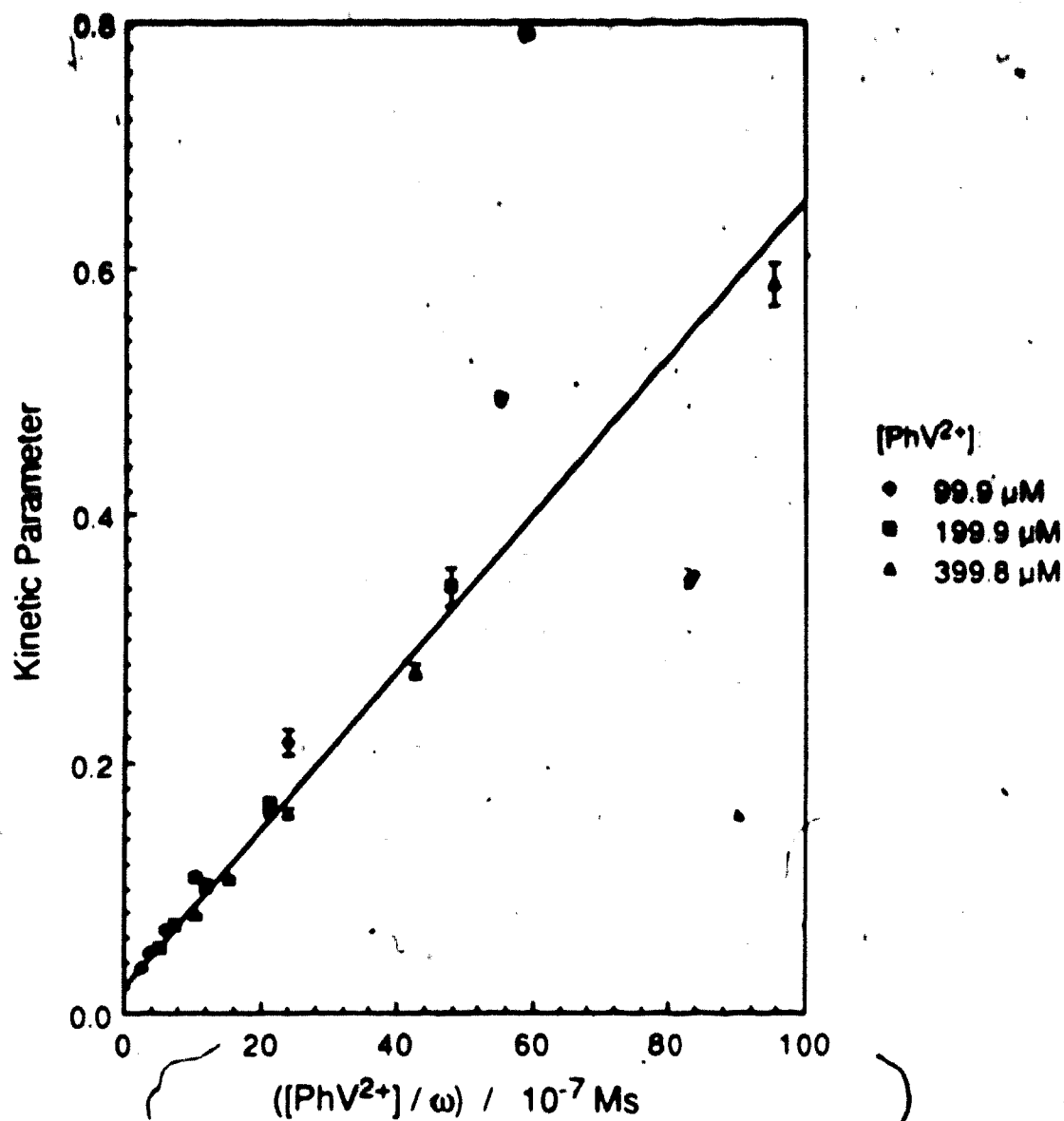
Figure 36. Kinetic Parameter Plot for the Phenyl Viologen/
Dioxygen Reaction in Acetonitrile. 0.1 M TEAP,
1.0 M HOAc, 25.0°. Average kinetic parameter ±
standard deviation for 3 determinations.

Figure 37. Kinetic Parameter Plot for the Cyanomethyl
Viologen/Dioxygen Reaction in Acetonitrile.
0.1 M TEAP, 1.0 M HOAc, 25.0°. Average kinetic
parameter ± standard deviation for 3 deter-
minations.

Figure 38. Kinetic Parameter Plot for the i-Propyl Viologen/
Dioxygen Reaction in Acetonitrile. 0.1 M TEAP,
1.0 M HOAc, 25.0°. Average kinetic parameter ±
standard deviation for 3 determinations.
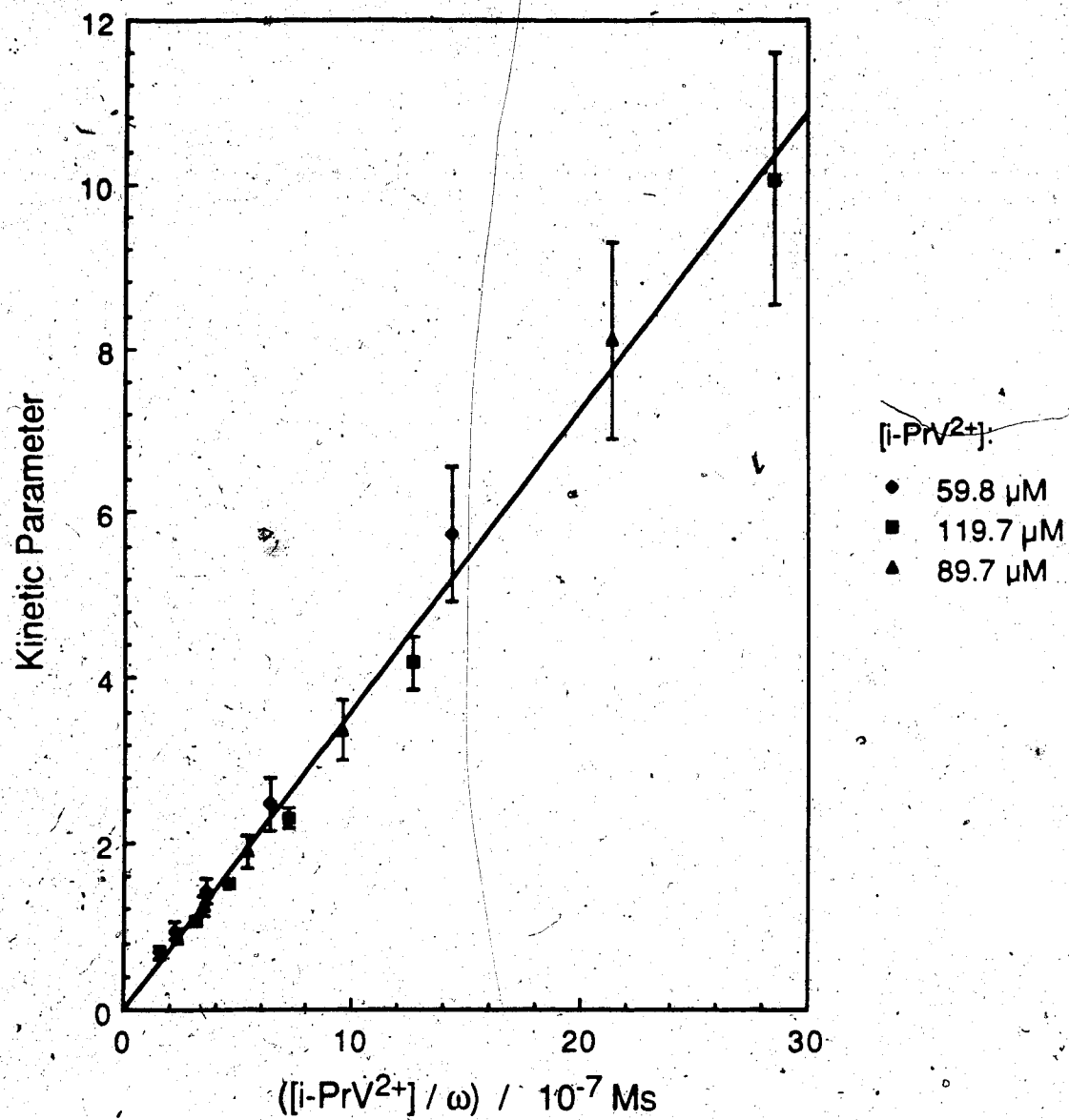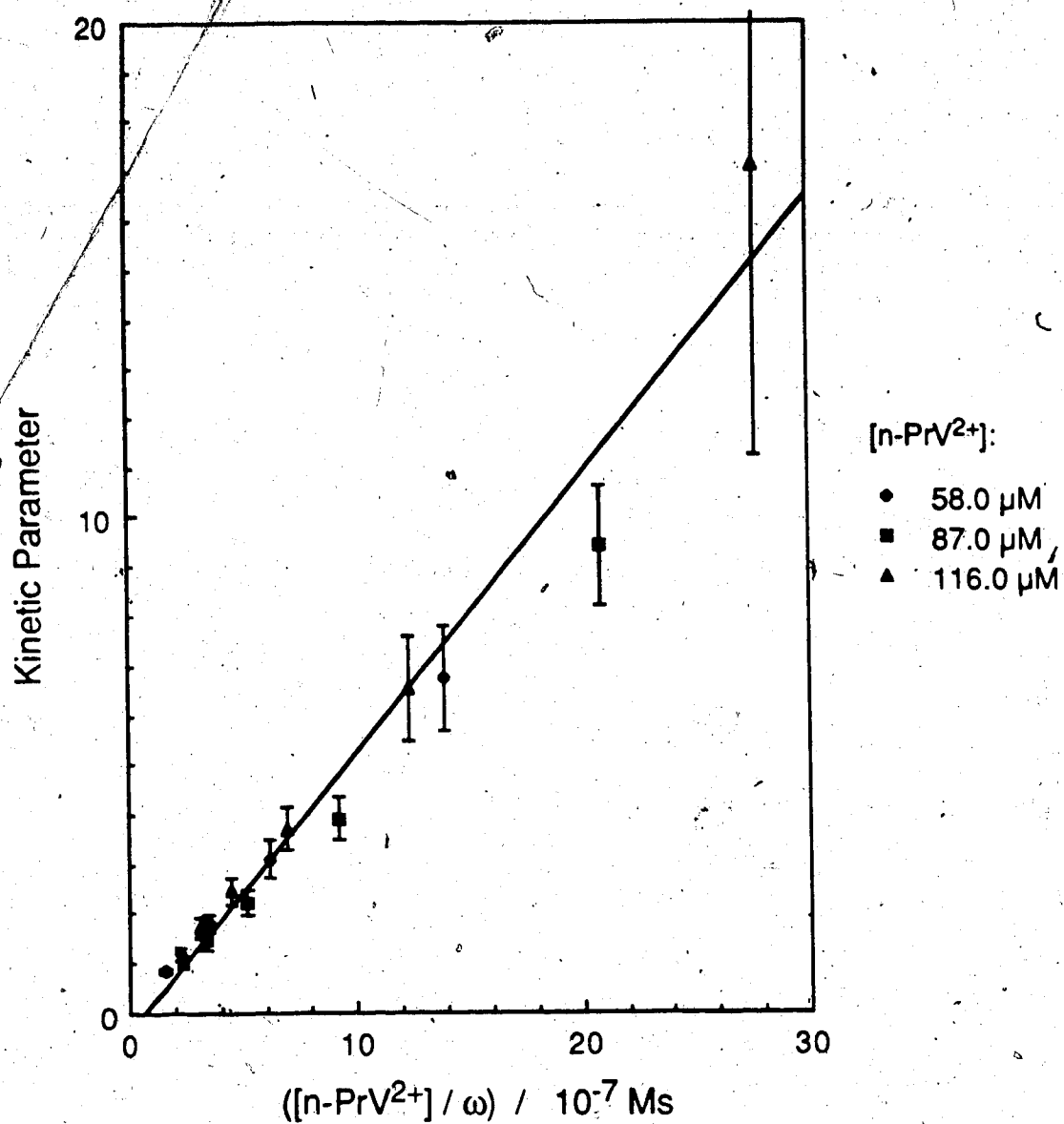
Figure 39. Kinetic Parameter Plot for the n-Propyl Viologen/
Dioxygen Reaction in Acetonitrile. 0.1 M TEAP,
1.0 M HOAc, 25.0°. Average kinetic parameter ±
standard deviation for 3 determinations.

Figure 40. Kinetic Parameter Plot for the Butyl Viologen/
Dioxygen Reaction in Acetonitrile. 0.1 M TEAP,
1.0 M HOAc, 25.0°. Average kinetic parameter ±
standard deviation for 3 determinations.
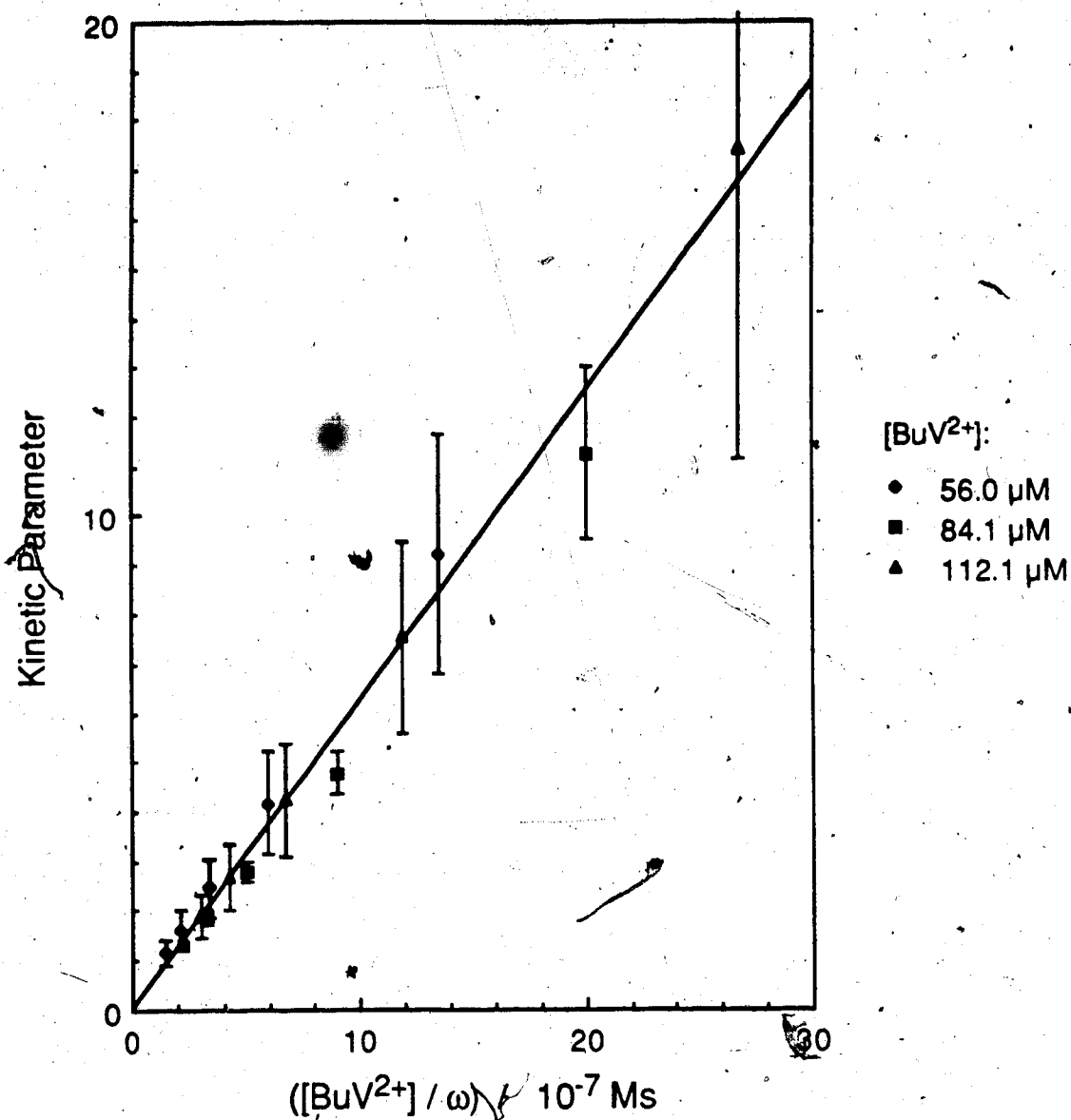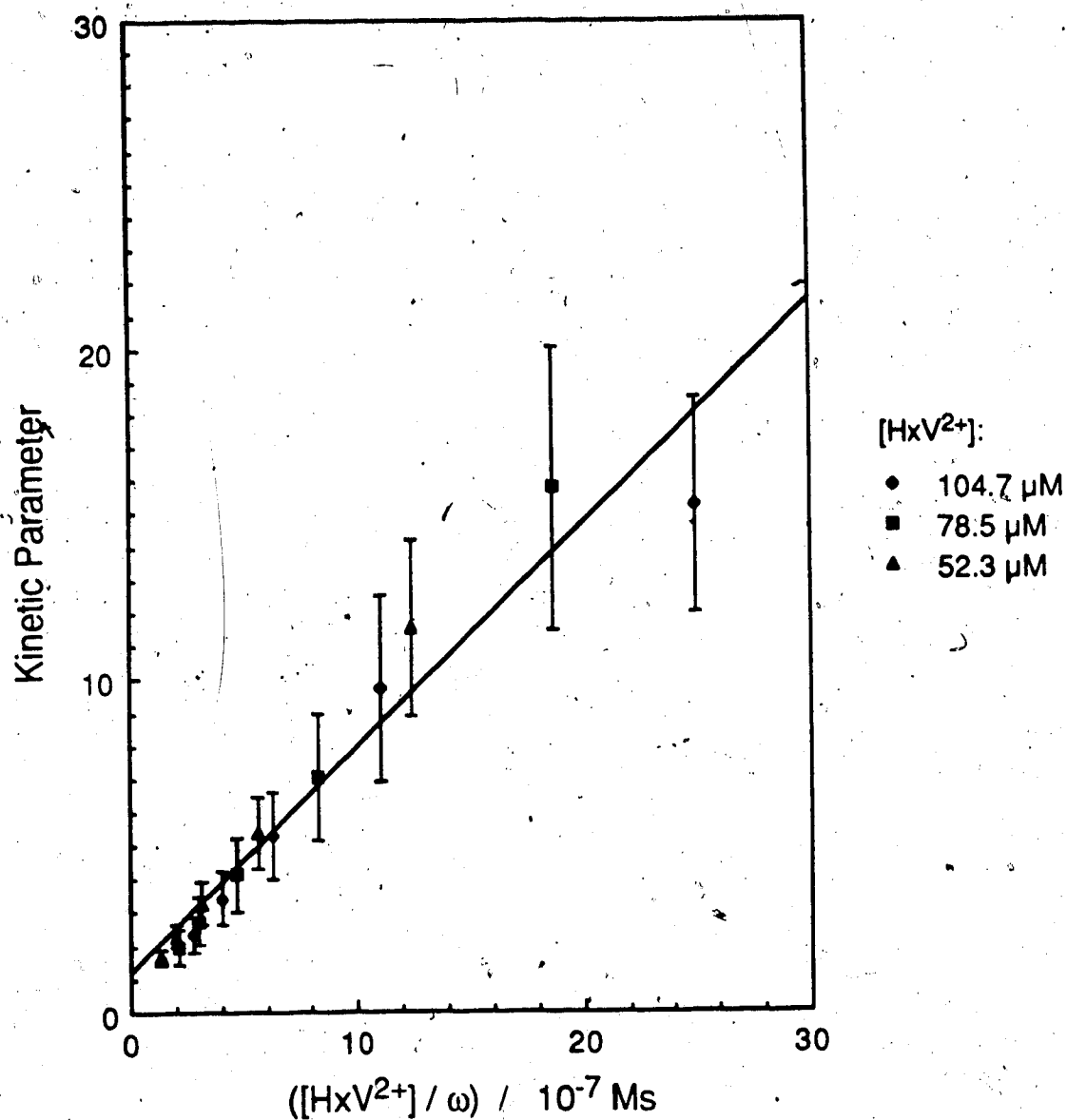
Figure 41. Kinetic Parameter Plot for the Hexyl Viologen/
Dioxygen Reaction in Acetonitrile. 0.1 M TEAP,
1.0 M HOAc, 25.0°. Average kinetic parameter ±
standard deviation for 3 determinations.
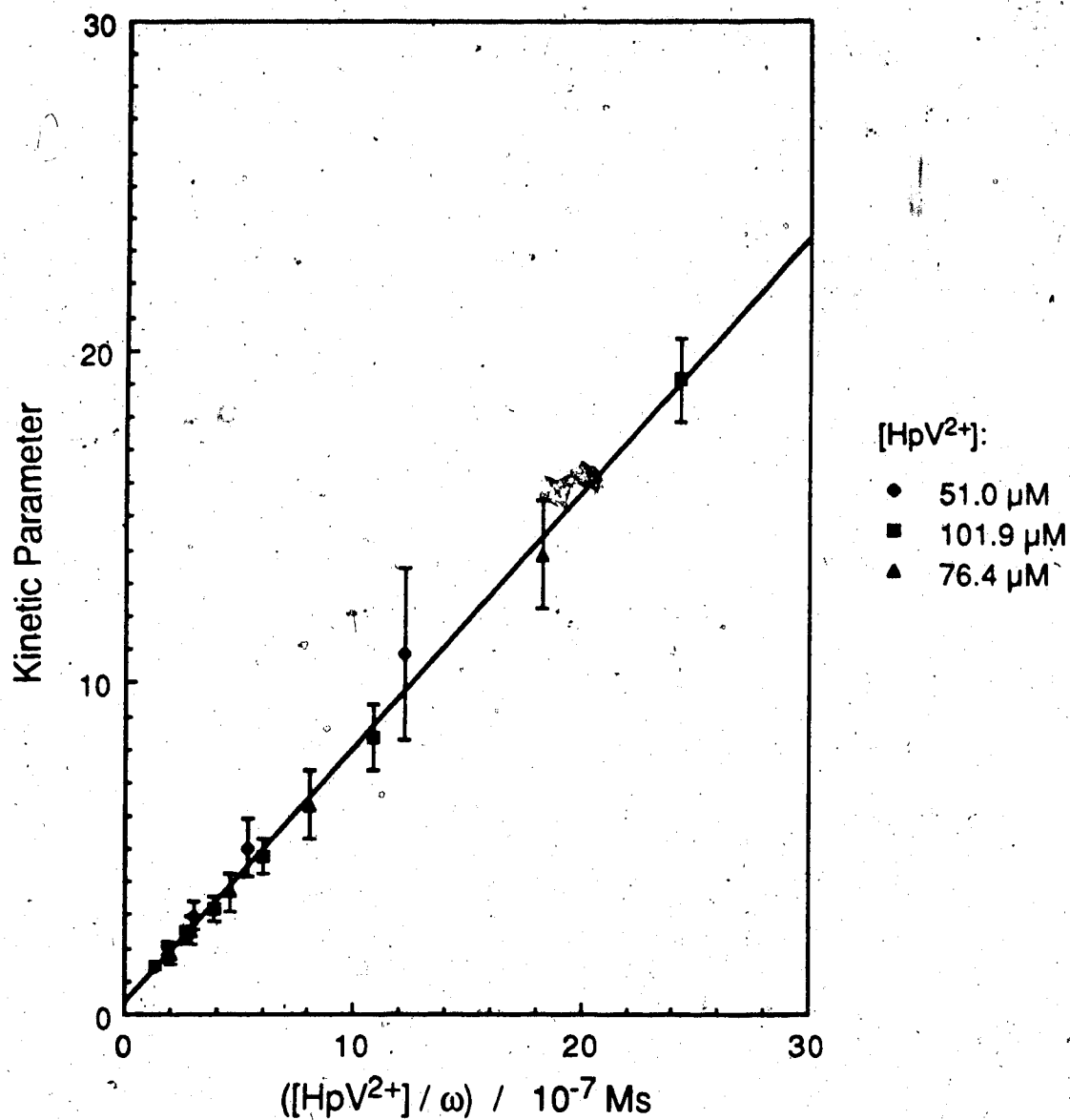
Figure 42. Kinetic Parameter Plot for the Heptyl Viologen/
Dioxygen Reaction in Acetonitrile. 0.1 M TEAP,
1.0 M HOAc, 25.0°. Average kinetic parameter ±
standard deviation for 3 determinations.
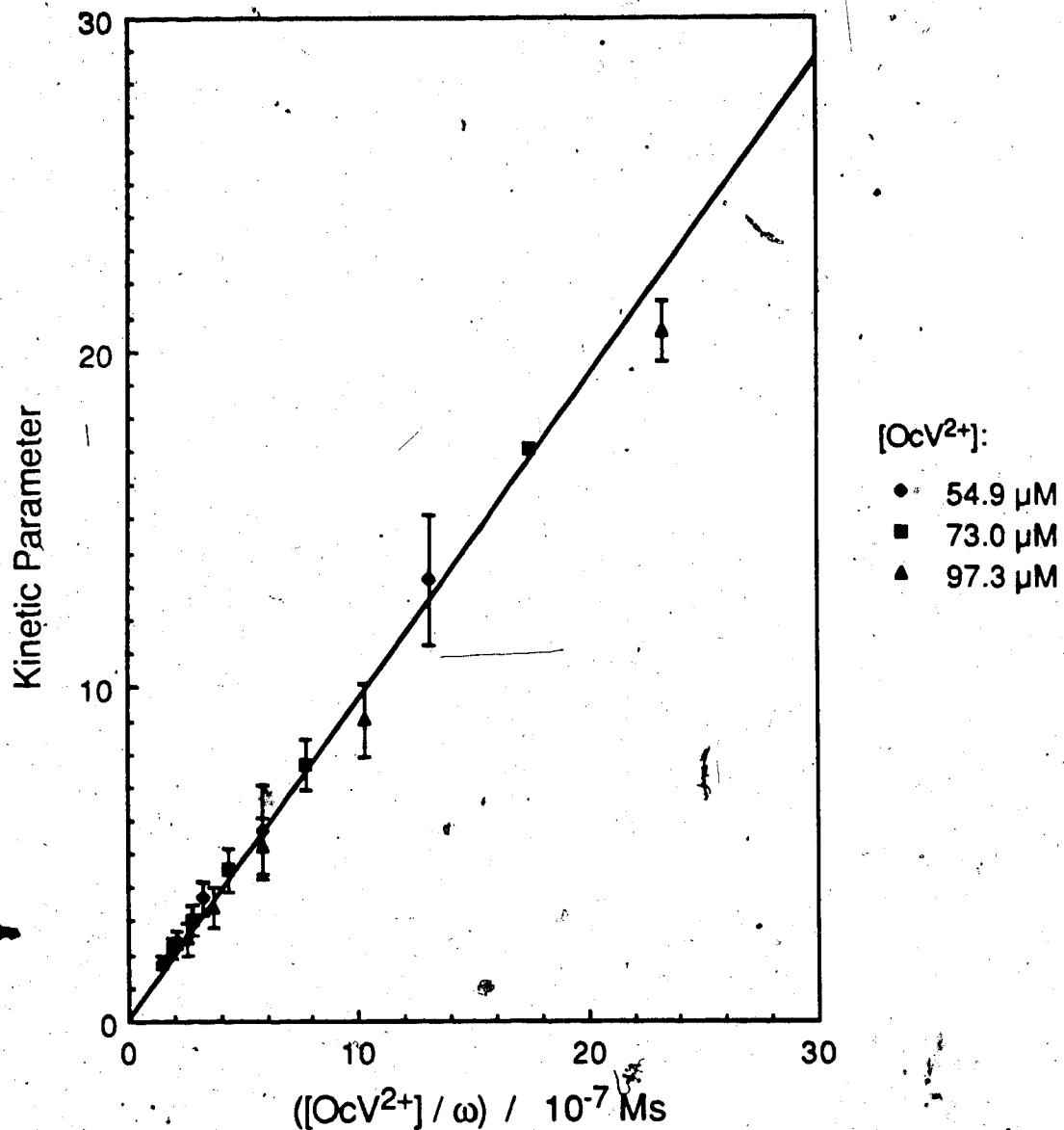
Figure 43. Kinetic Parameter Plot for the Octyl Viologen/ Dioxygen Reaction in Acetonitrile. 0.1 M TEAP, 1.0 M HOAc, 25.0°. Average kinetic parameter ± standard deviation for 3 determinations.

Table 28. Rate Constants for the Reaction of Cation Radicals of the
Diquaternized Salts of 4,4'-Bipyridine with Dioxygen at
25°C.

Compound	Slope $(M^{-1}s^{-1})$	Intercept	k_1 $(M^{-1}s^{-1})$
MeV	$(5.44\pm0.21)\times10^6$	0.16 ± 0.22	$(1.40\pm0.05)\times10^6$
HeV	$(4.81\pm0.11)\times10^6$	0.03 ± 0.10	$(1.24\pm0.03)\times10^6$
CeV	$(4.28\pm0.56)\times10^6$	0.32 ± 0.72	$(1.10\pm0.14)\times10^6$
BzV	$(1.51\pm0.05)\times10^6$	0.03 ± 0.05	$(3.88\pm0.13)\times10^5$
CxV	$(2.92\pm0.17)\times10^5$	0.00 ± 0.02	$(7.51\pm0.44)\times10^4$
PhV	$(6.35\pm0.43)\times10^4$	0.02 ± 0.01	$(1.63\pm0.11)\times10^4$
CyV	$(1.98\pm0.10)\times10^4$	0.00 ± 0.02	$(5.10\pm0.26)\times10^3$
n-PrV	$(5.64\pm0.59)\times10^6$	-0.39 ± 0.65	$(1.45\pm0.15)\times10^6$
i-PrV	$(3.63\pm0.18)\times10^6$	0.00 ± 0.20	$(0.93\pm0.05)\times10^6$
BuV	$(6.24\pm0.42)\times10^6$	0.05 ± 0.44	$(1.60\pm0.11)\times10^6$
HxV	$(6.76\pm0.92)\times10^6$	1.2 ± 0.09	$(1.74\pm0.24)\times10^6$
HpV	$(7.67\pm0.34)\times10^6$	0.40 ± 0.33	$(1.97\pm0.09)\times10^6$
OcV	$(9.55\pm0.52)\times10^6$	0.10 ± 0.49	$(2.46\pm0.13)\times10^6$

NOTE: Results obtained by weighted linear least-squares
regression. Uncertainties given are 95% confidence limits.

$MeV^{+\cdot}/O_2$ reaction were calculated using the upper and then the lower 95% confidence limits for the appropriate dioxygen concentrations in Table 20. The following results were obtained for k_1 (±95% C.I.): low O_2, (1.66 ± 0.07) × 10^6 $M^{-1}s^{-1}$; average O_2, (1.40 ± 0.05); high O_2, (1.22 ± 0.05). Uncertainties of ±2-5% in dioxygen concentrations correspond to variations in k_1 on the order of ±15%. A similar calculation was carried out to ascertain the effect of errors in the diffusion coefficients of MeV^{2+} and O_2 on the value of k_1. For the $MeV^{+\cdot}/O_2$ reaction, $\bar{D}_P = \bar{D}_Q = 0.148 ± 0.007$ based on the appropriate values and their 95% confidence intervals as given in Tables 22 and 25. The following results were obtained for k_1 (±95% C.I.): low $\bar{D}_P$, (1.26 ± 0.05) × 10^6 $M^{-1}s^{-1}$; average $\bar{D}_P$, (1.40 ± 0.05) × 10^6 $M^{-1}s^{-1}$; high $\bar{D}_P$, (1.57 ± 0.07) × 10^6 $M^{-1}s^{-1}$. An uncertainty of ±5% in $\bar{D}_P$ corresponds to variations in k_1 on the order of ±10%. This error estimate and the one preceding are exaggerated in that the calculations fail to take into account the tendency of random errors to cancel. Nevertheless it would seem that the largest source of error in the estimates of k_1 are the uncertainties associated with the dioxygen concentrations and the diffusion coefficients. In lieu of a full-scale error analysis, it is reasonable to suppose that the actual error associated with the

values of k_1 in Table 28 is on the order of ±10%.

D. **Kinetic Studies of the Diquaternized Salts of**

   2,2'-Bipyridine and 1,10-Phenanthroline in

   Acetonitrile

Half-wave potentials and rate constants for the
diquaternized salts of 2,2'-bipyridine and 1,10-phen-
anthroline in acetonitrile were determined according to
procedures described in Chapter IV. Half-wave potentials
measured for the two reduction waves are given in Table
29. The results of Hünig et al. (140,141) obtained by dc
polarography, have been included for comparison. The
values are in good agreement for the salts of
2,2'-bipyridine (diquat and triquat). It was not possible
to determine $E^2_{1/2}$ for the salts of 1,10-phenanthroline
(diphen and triphen) as the electrode was rapidly
passivated at potentials corresponding to the second
wave. The passivation was probably due to precipitation
of the neutral form of the compounds on the electrode
surface. The discrepancy between measured half-wave
potentials for the first one-electron reduction and those
found by Hünig et al. (141) may be related to this
phenomenon.

Diffusion coefficients for the compounds studied are

Table 29. Half-Wave Potentials for the Diquaternized Salts of
2,2'-Bipyridine and 1,10-Phenanthroline in Acetonitrile
(0.1 M TEAP).

Compound	$-E^1_{1/2}$	$-E^2_{1/2}$	$-E^1_{1/2}$ (1 M HOAc)
DiQ	0.38 (0.39)[a]	0.87 (0.87)[a]	0.39
TriQ	0.57 (0.57)[a]	0.89 (0.90)[a]	0.59
TetQ	0.69	0.88	0.70
DiP	0.35 (0.30)[b]	-[c] (0.64)[b]	0.36
TriP	0.34 (0.29)[b]	-[c] (0.58)[b]	0.35

a. From Reference 140 using E(Ag/AgCl) vs E(SCE) = -0.046 V (cited in Ref. 140).

b. From Reference 141 using E(Ag/AgCl) vs E(SCE) = -0.046 V (cited in Ref. 140).

c. Electrode passivated by the product of the second reduction step.

given in Table 30 while the average values of the calculated kinetic parameters appear in Table 31. Plots of average kinetic parameter versus [Catalyst]/ω are shown in Figures 44 to 48. Values for the slope and intercept of these plots together with the corresponding values of k_1 are listed in Table 32. As before the error limits for k_1 were calculated using the 95% confidence limits for the slope of the kinetic parameter plot. For reasons outlined in the preceding section, overall errors in k_1 are on the order of ±10%.

The determination of k_1 for the trimethylene- and tetramethylene-bridged salts of 2,2'-bipyridine (triquat and tetraquat) merited special consideration. Of the compounds studied, these displayed the most negative values of $E_{1/2}$: -0.57 V vs SCE for triquat and -0.69 V for tetraquat. These compounds also possessed the largest values for k_1. The rapid reaction rate meant that the catalyst concentrations had to be kept low in order to observe a measurable dependence of current ratio R on rotation speed. As discussed in Chapter III, if the product of the catalyst concentration and reaction rate is too large relative to accessible rotation speeds, the corresponding kinetic parameter is large and the solution reaction is, in effect, infinitely fast on the time scale of the experiment. In the case of the $TetQ^{+\cdot}/O_2$ reaction,

Table 30. Diffusion Coefficients of the Diquaternized Salts of 2,2'-Bipyridine and 1,10-Phenanthroline in Acetonitrile (0.1 $\underline{M}$ TEAP, 1.0 $\underline{M}$ HOAc).

Compound	$-E_D$ (V vs SCE)	Slope[a] ($\mu A\ s^{1/2}\ mM$)	Intercept[a] (μA)	D ($10^{-5}\ cm^2/s$)
DiQ	0.55	32.3±0.3	0.5±0.4	1.12±0.02
TriQ	0.72	32.5±0.4	1.9±0.3	1.13±0.02
TetQ	0.80	34.7±1.1	1.0±0.2	1.24±0.06[b]
DiP	0.52	32.3±0.2	0.7±0.2	1.12±0.01
TriP	0.50	32.7±0.1	0.5±0.1	1.14±0.01

a. Results obtained by weighted linear least-squares regression. Uncertainties given are 95% confidence limits.

b. Limiting current plateau ill-defined. See Figure 50.

Table 31. Calculated Results for the Diquaternised Salts of

2,2'-Bipyridine and 1,10-Phenanthroline in Acetonitrile.

Average Kinetic Parameters and Their Standard Deviations

Compound	Conc.	Rotation Speed (rpm)				
	(μM)	400	900	1600	2500	3600
DiQ	63.4	2.63	1.18	0.71	0.47	0.34
		±0.20	0.08	0.04	0.02	0.02
	95.1	3.97	1.80	1.04	0.69	0.49
		±0.17	0.04	0.02	0.01	0.01
	126.8	6.22	2.54	1.43	0.95	0.67
		±1.36	0.34	0.16	0.09	0.06
TriQ	27.8	33.	15.7	9.6	6.6	5.0
		±22.	7.8	4.3	2.8	1.9
	55.6	58.	37.	18.9	11.7	8.4
		±8.	20.	6.3	3.4	2.1
	83.5	–	41.	34.	18.7	11.9
		±	4.	20	6.3	2.4
TetQ	3.3	61.	24.	16.	12.	9.4
		±33.	10.	6.	4.	3.2
	5.4	105.	38.	28.	21.	14.
		±69.	12.	16.	10.	6.
	10.8	–	–	108.	58.	44.
		±	–	46.	17.	22.
DiP	50.3	14.9	7.4	4.64	3.23	2.42
		±3.1	1.2	0.58	0.36	0.25
	75.5	22.4	9.7	5.99	4.13	3.05
		±8.1	1.5	0.71	0.48	0.35
	100.7	20.7	12.6	7.3	4.9	3.59
		±2.8	4.3	1.8	1.1	0.76

(Continued)

Table 31. (Continued)

Compound	Conc. (μM)	Rotation Speed (rpm)				
		400	900	1600	2500	3600
TrIP	57.4	6.8	3.39	2.09	1.45	1.08
		±0.9	0.41	0.24	0.18	0.11
	86.2	9.0	4.18	2.63	1.84	1.37
		±2.0	0.57	0.35	0.24	0.15
	114.9	13.2	5.50	3.36	2.28	1.68
		±4.3	1.00	0.55	0.35	0.24
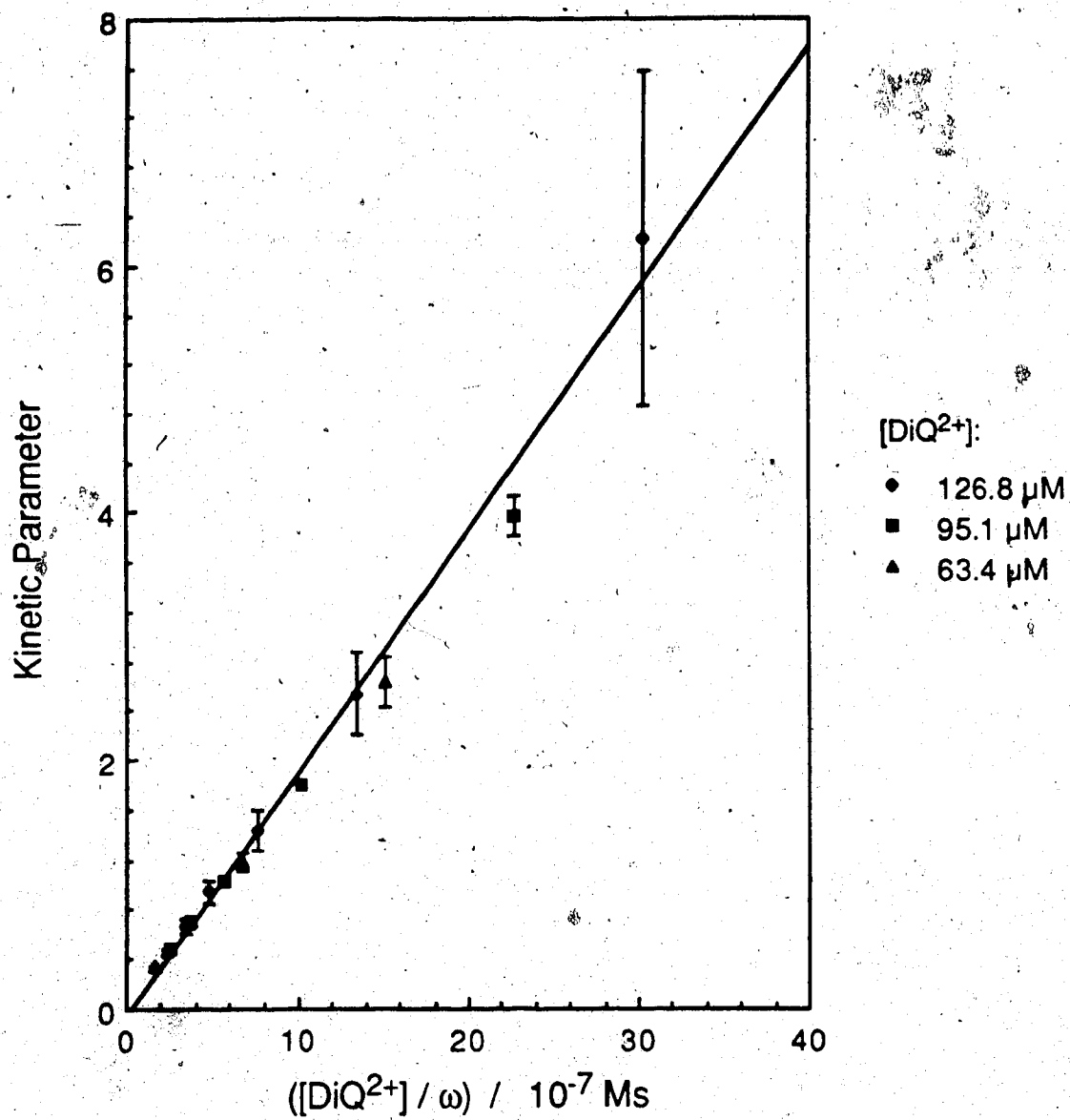
Figure 44. Kinetic Parameter Plot for the Diquat/Dioxygen
Reaction in Acetonitrile. 0.1 M TEAP, 1.0 M HOAc,
25.0°. Average kinetic parameter ±standard
deviation for 3 determinations.
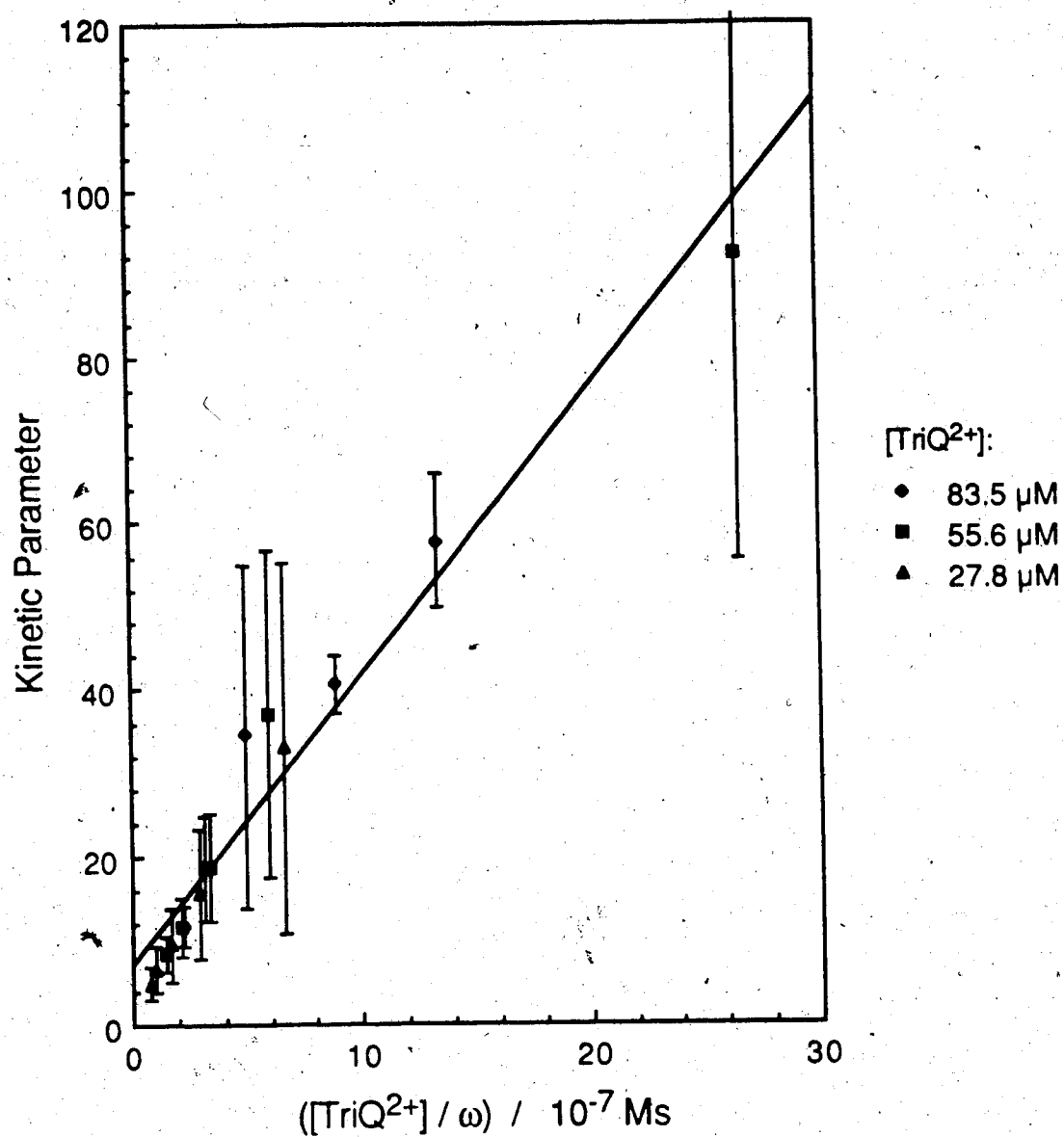
Figure 45. Kinetic Parameter Plot for the Triquat/Dioxygen
Reaction in Acetonitrile. 0.1 M TEAP, 1.0 M HOAc,
25.0°. Average kinetic parameter ±standard
deviation for 3 determinations.
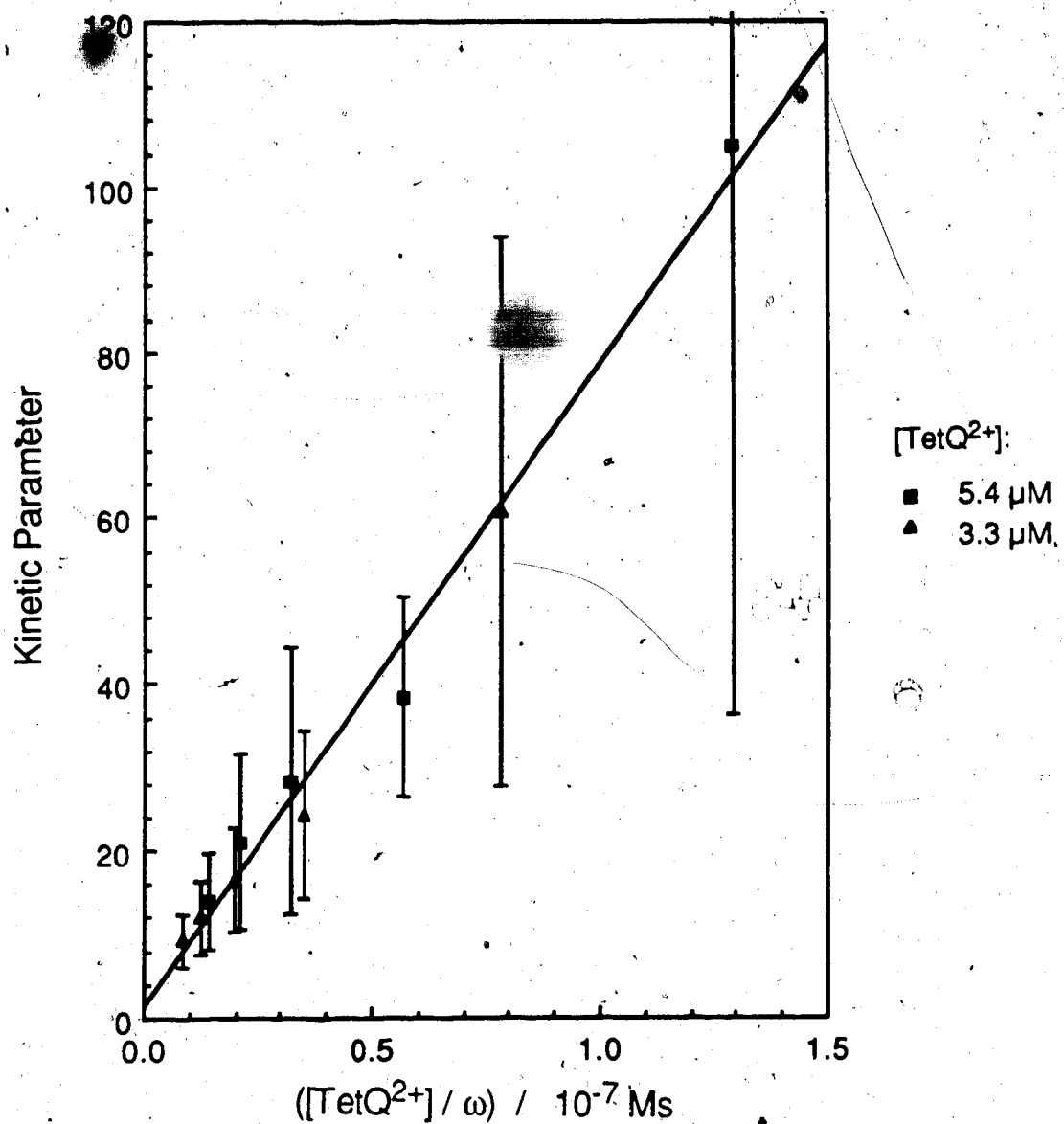
Figure 46. Kinetic Parameter Plot for the Tetraquat/Dioxygen
Reaction in Acetonitrile. 0.1 M TEAP, 1.0 M HOAc,
25.0°. Average kinetic parameter ±standard
deviation for 3 determinations.
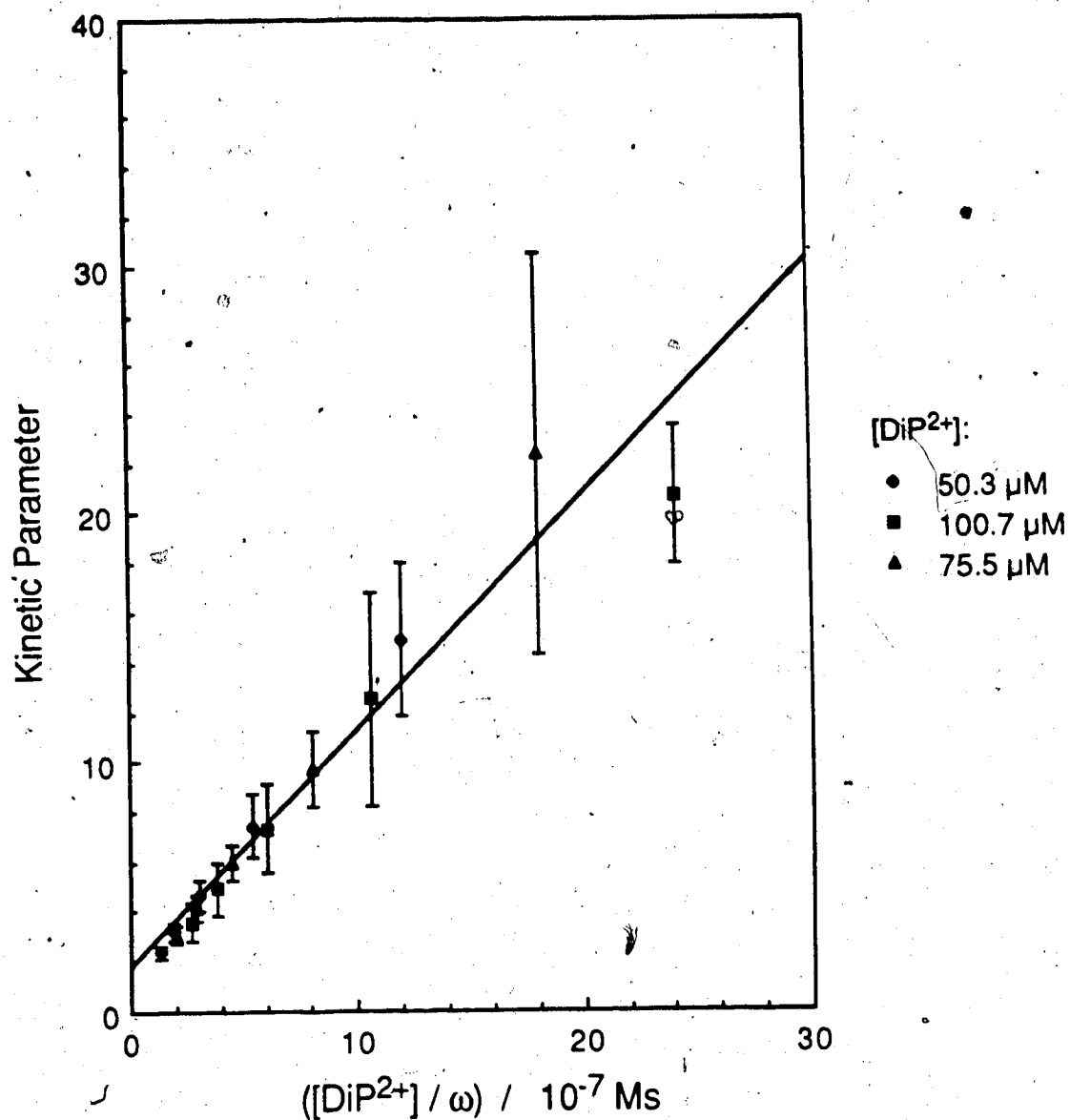
Figure 47. Kinetic Parameter Plot for the Diphen/Dioxygen
Reaction in Acetonitrile. 0.1 M TEAP, 1.0 M HOAc,
25.0°. Average kinetic parameter ±standard
deviation for 3 determinations.
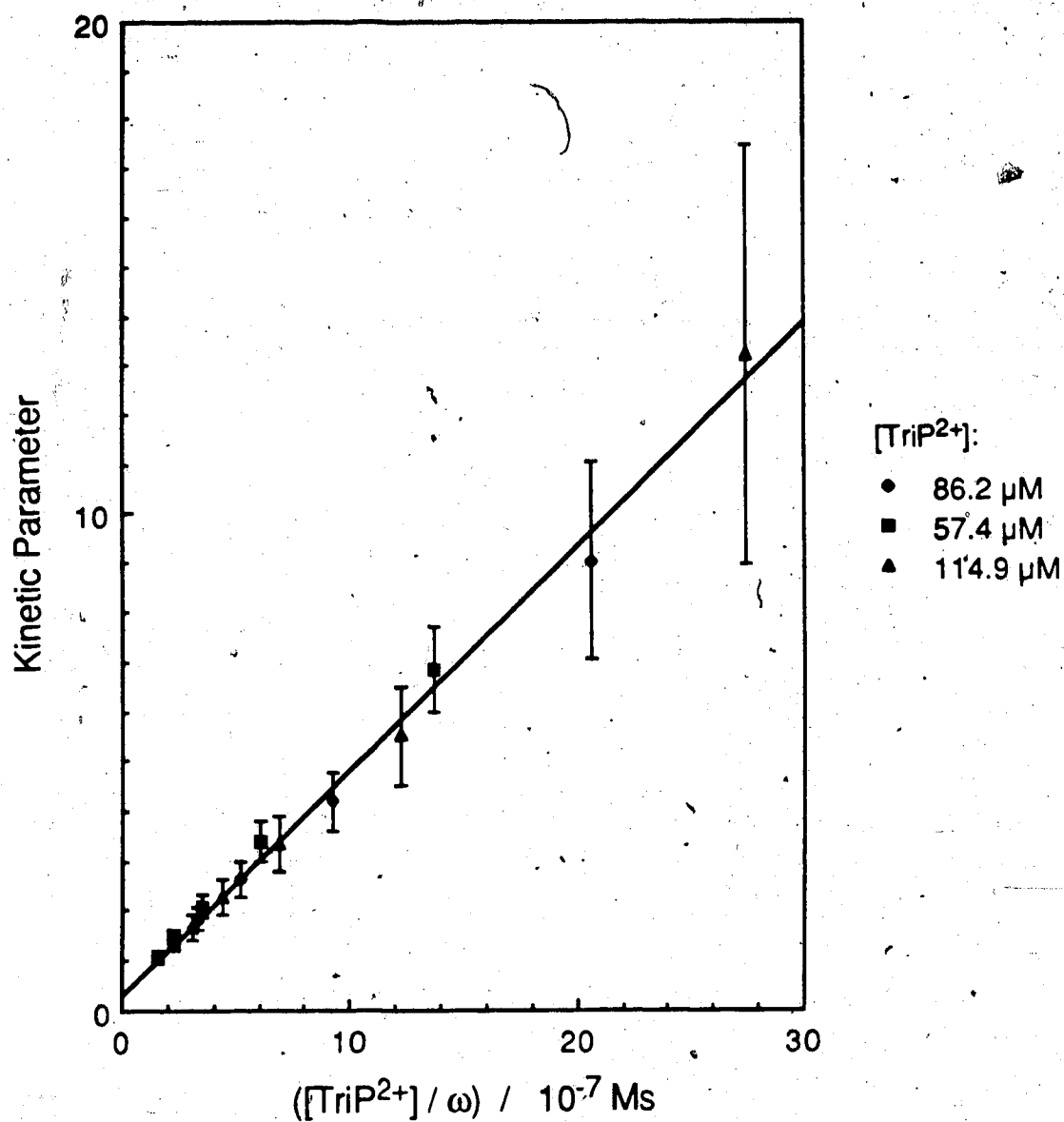
Figure 48. Kinetic Parameter Plot for the Triphen/Dioxygen Reaction in Acetonitrile. 0.1 M TEAP, 1.0 M HOAc, 25.0°. Average kinetic parameter ±standard deviation for 3 determinations.

Table 32. Rate Constants for the Reaction of the Cation Radicals of

the Diquaternized Salts of 2,2'-Bipyridine and

1,10-Phenanthroline with Dioxygen at 25°C.

Compound	Slope $(M^{-1}s^{-1})$	Intercept	k_1 $(M^{-1}s^{-1})$
DiQ	$(1.96\pm0.12)\times10^6$	-0.07 ± 0.14	$(5.04\pm0.31)\times10^5$
TriQ	$(3.46\pm0.42)\times10^7$	7.2 ± 3.6	$(8.9\pm1.1)\times10^6$
TetQ	$(7.72\pm0.64)\times10^8$	1.6 ± 3.4	$(1.98\pm0.16)\times10^8$
DiP	$(9.5\pm1.3)\times10^6$	1.8 ± 1.2	$(2.43\pm0.33)\times10^6$
TriP	$(4.53\pm0.20)\times10^6$	0.3 ± 0.2	$(1.16\pm0.05)\times10^6$

Note: Results obtained by weighted linear least-squares

regression. Uncertainties given are 95% confidence limits.

catalyst concentrations on the order of 3 to 5 μM were required to reliably estimate the rate constant. Larger concentrations were used for the slower $TriQ^{+ \cdot}/O_2$ reaction (25 to 75 μM). Somewhat lower concentrations could have been employed to advantage were it not for the problem of interference by direct substrate reduction (v.i.).

In addition to comparatively low catalyst concentrations, the determination of rate constants for triquat and tetraquat required use of the global spline collocation technique, which was described in Chapter III, to compute working curves. The ordinary orthogonal collocation technique was satisfactory when dealing with kinetic parameters less than 20. For larger values of $\bar{k}$, the ordinary technique underestimates the surface concentration gradient $(dC_P/dZ)_{Z=0}$ and therfore also the catalytic current. When working curves are calculated by ordinary collocation, the current ratios at larger values of $\bar{k}$ are too large leading to nonlinearity in the kinetic parameter plot and an overestimate of the rate constant. Such curves were also frequently observed to predict limiting values of R at large $\bar{k}$ which were in excess of those values actually observed. In these circumstances, no estimate of $\bar{k}$ could be obtained unless the spline technique was used to compute working curves. The program ECR3WC was used for this purpose. A listing of this

program appears in Appendix II. Execution time for the
spline program was a factor of teh larger than that of the
ordinary collocation program ECR2WC. Calculation of the
set of nine working curves required for the complete
kinetic experiment took about ten hours.

As the half-wave potentials for the first reduction
waves of triquat and tetraquat were significantly more
negative than those of any of the other compounds studied,
problems were anticipated due to interference by the
direct reduction of dioxygen at the electrode surface.
Current-voltage curves for the catalyst and the substrate
individually and together are shown in Figure 49 for the
$TriQ^{+\cdot}/O_2$ reaction and in Figure 50 for the $TetQ^{+\cdot}/O_2$
reaction. In the former case, a substantial contribution
from direct dioxygen reduction was expected at the
potential of the kinetic experiments (located by the arrow
in Figure 49). In the latter case, complete overlap
between the catalyst and substrate reduction waves was
observed (Figure 50). Nevertheless, the current-voltage
curve for the mixture of tetraquat and dioxygen displayed
a reasonably well-developed limiting current plateau. The
kinetic parameter plots obtained for the $TriQ^{+\cdot}/O_2$
reaction (Figure 45) and the $TetQ^{+\cdot}/O_2$ reaction (Figure
46) displayed acceptable linearity and intercepts not far
removed from zero. Thus, the anticipated interference by
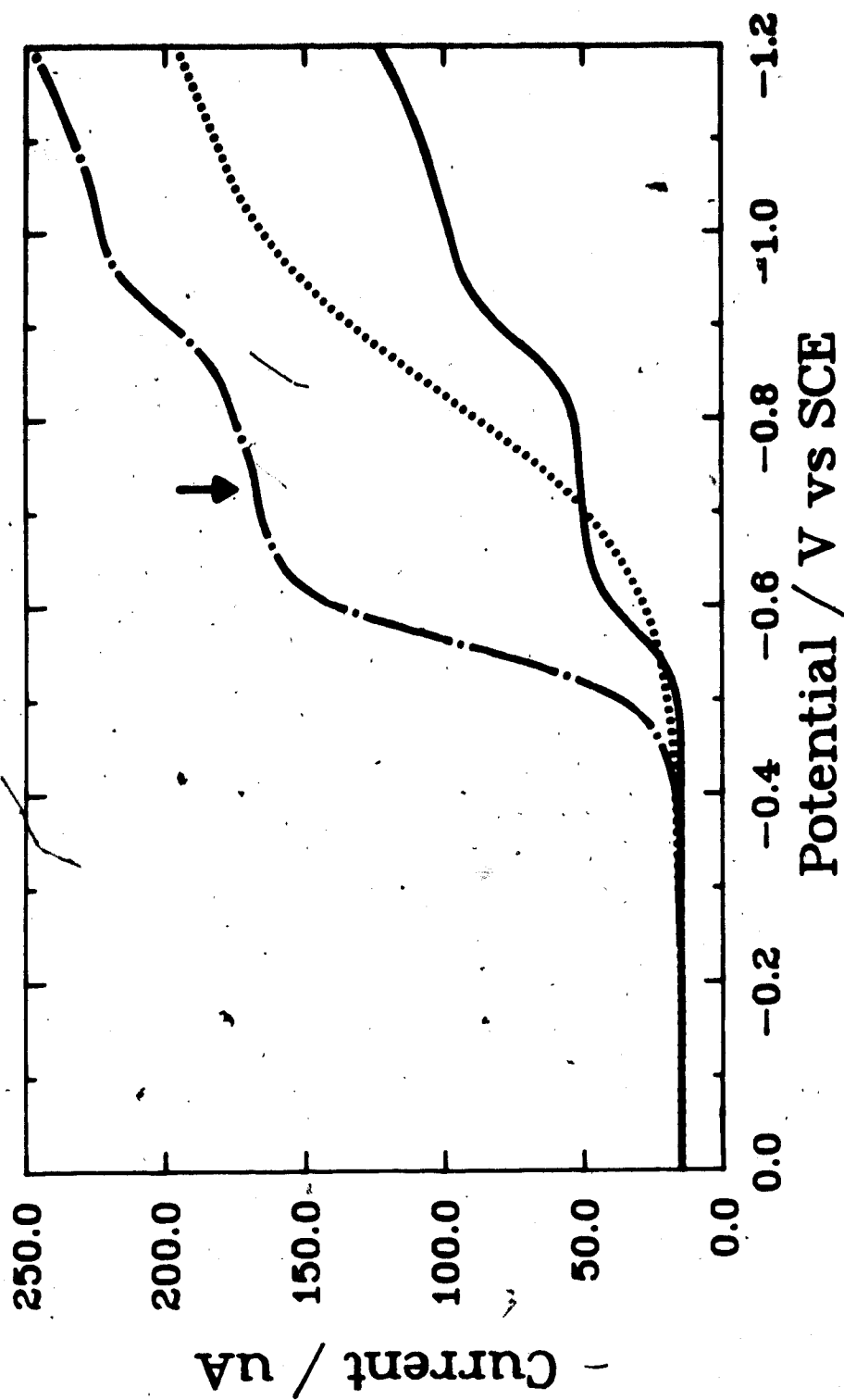
Figure 49. Current-Voltage Curves for the Triquat/Dioxygen
Reaction. 0.1 M TEAP, 1.0 M HOAc in Acetonitrile.
GC RDE @ 900 rpm. ———— 111. μM TriQ^{2+}; ········
55. μM O$_2$; —·—·—·— 111. μM TriQ^{2+}, 55. μM O$_2$. The
arrow marks the electrode potential used for the
kinetic experiments.
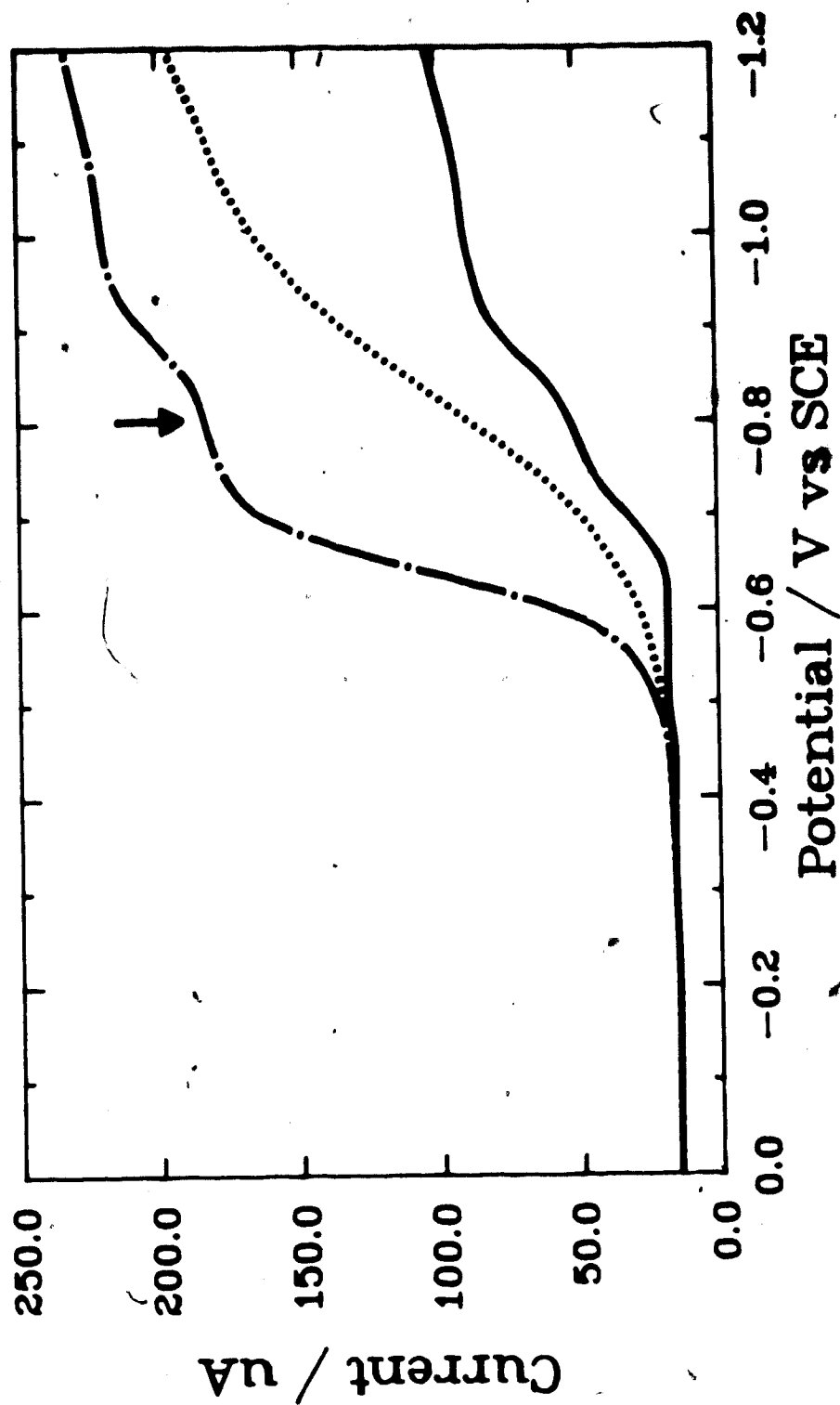
Figure 50. Current-Voltage Curves for the Tetraquat/Dioxygen Reaction. 0.1 M TEAP, 1.0 M HOAc in Acetonitrile. GC RDE @ 900 rpm. ——— 107. μM TetQ^{2+}; ········ 55. μM O$_2$; —·—·—·— 107. μM TetQ^{2+}, 55. μM O$_2$. The arrow marks the electrode potential used for the kinetic experiments.

direct dioxygen reduction failed to materialize.

The success of the kinetic experiment for triquat and tetraquat was a result of the comparatively large values assumed by the kinetic parameter (generally ranging between 10 and 100). Concentration profiles for the catalyst species and the substrate, which were calculated for $\bar{k}$ equals 50, are shown in Figure 51. At larger values of $\bar{k}$, the effect of the solution reaction is to lower the concentration of substrate at the electrode surface to a fraction of its bulk value. The lowered surface concentration means that the contribution of direct substrate reduction to the observed current tends to be negligible.

E.   Kinetic Studies of Diquaternized Bipyridinium Salts in Dimethylsulfoxide

This section contains the results of kinetic experiments performed in DMSO. For reasons described in the beginning of this chapter, DMSO was abandoned in favor of acetonitrile early on in the work. Despite the apparent poor resolution between catalyst and substrate waves (see Figure 26), good experimental results were obtained for the limited number of compounds studied. The compounds studied, the catalyst concentrations used and
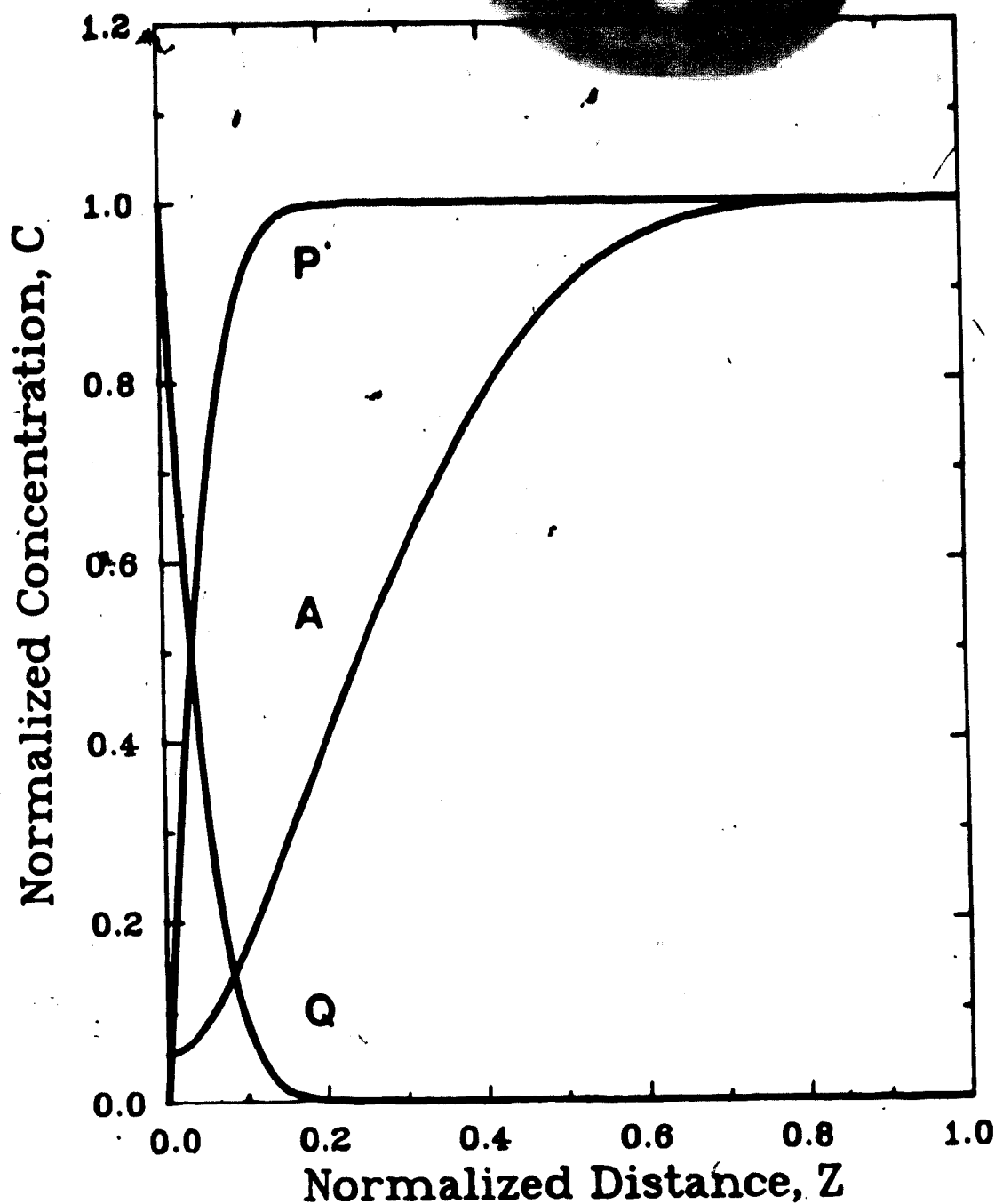
Figure 51. Concentration Profiles for the Second-Order EC-Catalytic Mechanism at the Rotating Disk Electrode for $\bar{k} = 50$, $\gamma = 1$. Computed by spline collocation with $N = 8$, $D_P = D_Q = 0.137 D_A$ and spline point at $Z = 0.22$.

the average values obtained for the kinetic parameter as a function of rotation speed are listed in Table 33. The corresponding kinetic parameter plots appear in Figures 52 to 54 Half-wave potentials, diffusion coefficients and rate constants are summarized in Table 34. The corresponding results obtained in acetonitrile are shown for the sake of comparison. The value found for the $MeV^{+\cdot}/O_2$ reaction in DMSO $(4.0 \pm 0.2) \times 10^5$ $M^{-1}s^{-1}$, is in reasonable agreement with Savéant's value of $(2.3 \pm 0.3) \times 10^5$ $M^{-1}s^{-1}$ (30).

Table 33. Calculated Results for Diquaternised Bipyridinium Salts in
Dimethylsulfoxide.

Average Kinetic Parameters and Their Standard Deviations

Compound	Conc. (μM)	Rotation Speed (rpm)				
		400	900	1600	2500	3600
MeV	103	9.8	4.4	2.5	1.7	-
		±1.6	0.8	0.4	0.3	-
	103	9.0	3.8	2.2	1.4	-
		±0.9	0.3	0.1	0.1	-
HeV	133	13.4	5.47	3.02	1.8	1.25
		±1.0	0.16	0.06	0.08	0.07
	109	13.8	5.13	2.81	1.76	1.27
		±1.0	0.13	0.04	0.05	0.04
	66.5	7.5	2.82	1.56	0.99	0.69
		±0.8	0.27	0.14	0.10	0.07
	54.5	7.6	2.45	1.44	0.92	0.64
		±3.0	0.32	0.10	0.04	0.03
DiQ	104.6	4.97	2.30	1.37	0.91	0.64
		±0.32	0.09	0.05	0.03	0.02
	105.5	4.02	1.87	1.08	0.72	0.50
		±0.21	0.03	0.01	0.01	0.01
	209.2	7.80	3.61	2.12	1.39	0.98
		±0.46	0.27	0.19	0.16	0.12
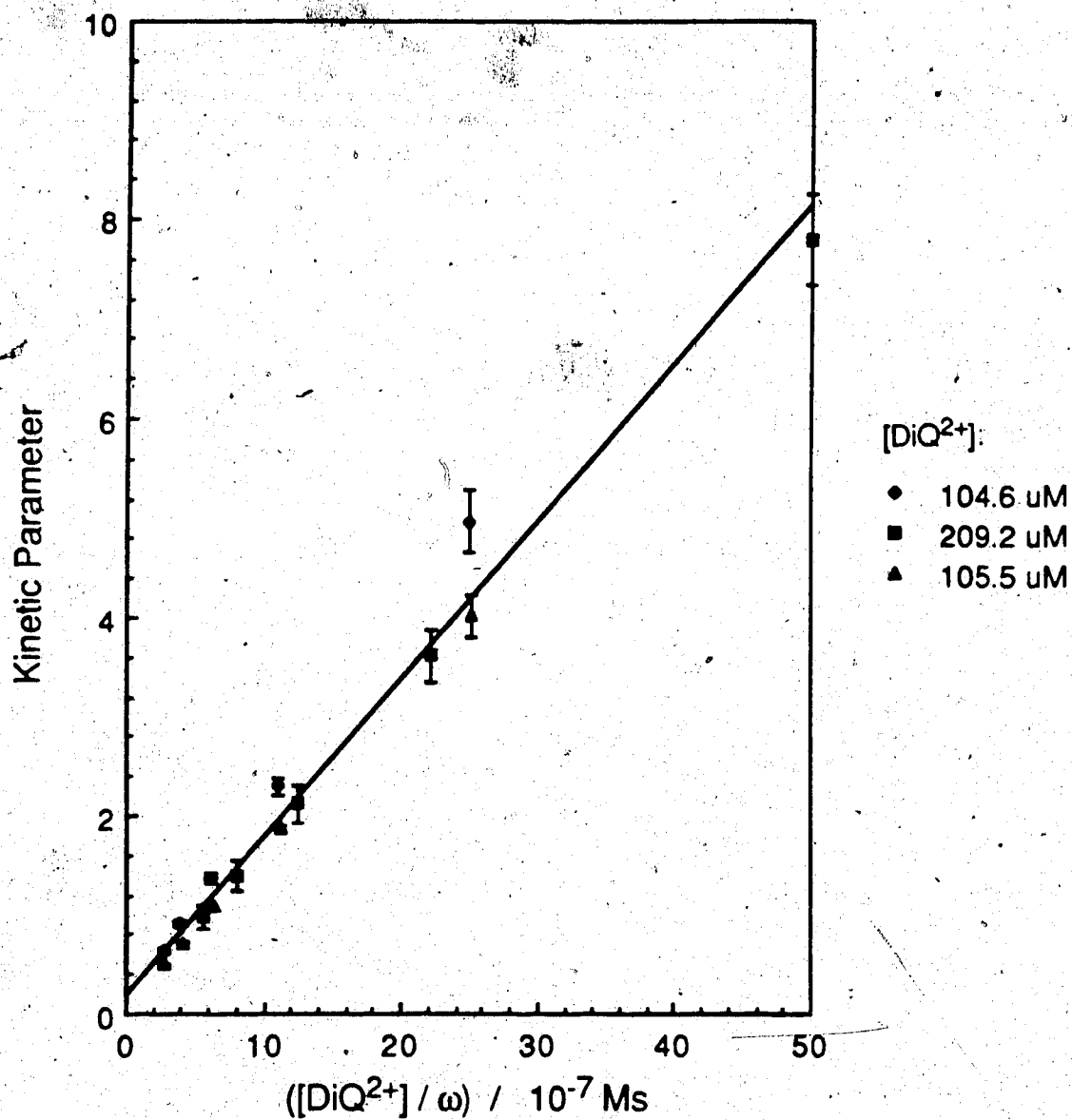
Figure 52. Kinetic Parameter Plot for the Diquat/Dioxygen Reaction in DMSO. 0.1 M NaClO₄, 1.0 M HOAc, 25.0°.
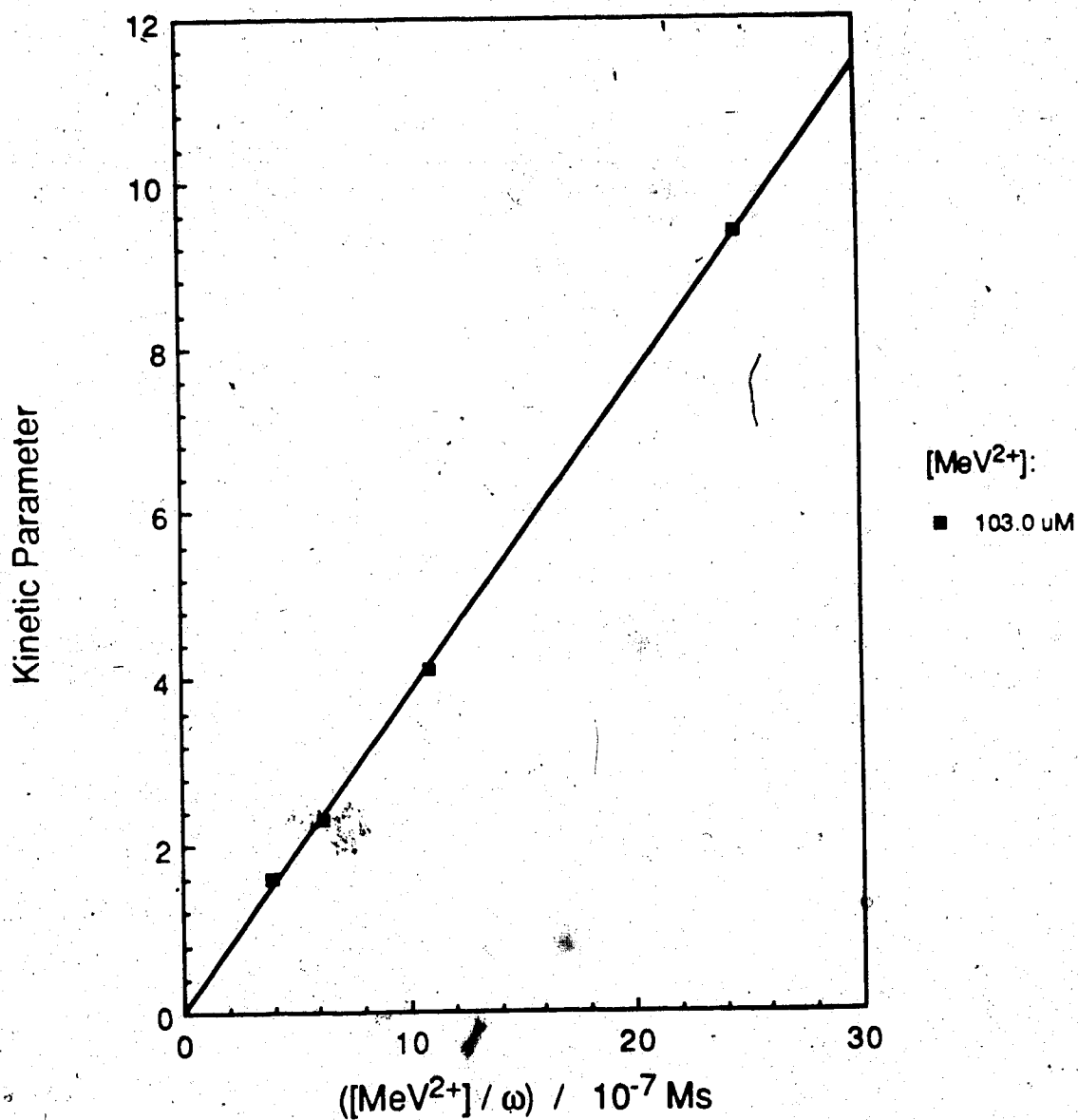
Figure 53. Kinetic Parameter Plot for the Methyl Viologen/
Dioxygen Reaction in DMSO.   0.1 M NaClO$_4$,
1.0 M HOAc, 25.0°.
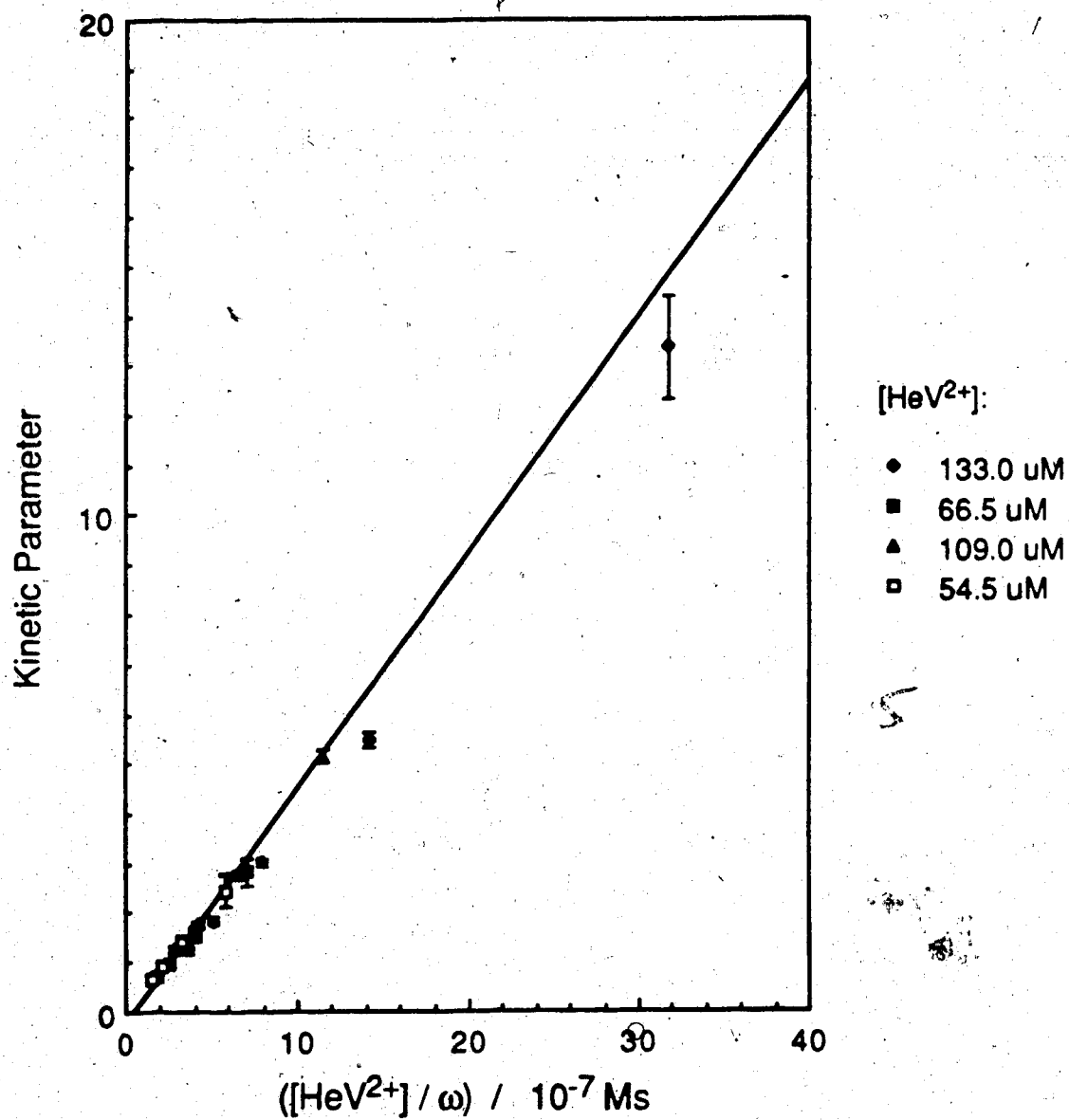
Figure 54. Kinetic Parameter Plot for the Hydroxyethyl
Viologen/Dioxygen Reaction in DMSO. 0.1 M NaClO$_4$,
1.0 M HOAc, 25.0°.

Table 34. Summary of Results Obtained for Diquaternized Bipyridinium Salts in Dimethylsulfoxide.[a]

Compound	$-E^1_{1/2}$ (V vs SCE)	D^c (10^{-6} cm^1/s)	k_1^c (10^5(M^{-1}s^{-1}))
MeV	0.47	2.50±0.10	4.0±0.2
HeV	0.46	1.98±0.04	5.0±0.4
DiQ	0.42	2.17±0.05	1.7±0.1

Comparable Results Obtained in Acetonitrile[b]

Compound	$-E^1_{1/2}$ (V vs SCE)	D^c (10^{-6} cm^2/s)	k_1^c (10^5(M^{-1}s^{-1}))
MeV	0.45	12.2±0.4	14.0±0.5
HeV	0.45	10.6±0.1	12.4±0.3
DiQ	0.39	11.2±0.2	5.0±0.3

a. 0.1 M NaClO$_4$, 1 M HOAc, 25°C.

b. 0.1 M TEAP, 1 M HOAc, 25°C.

c. Uncertainties based on 95% confidence intervals from weighted linear least-squares regression.

DIFFERENCES IN THE DIFFUSIVITIES OF BIPYRIDINIUM DICATIONS

AND CATION RADICALS AND THEIR EFFECT ON THE

CALCULATED RATE CONSTANTS

A. Levich Plots for the One- and Two-Electron Reductions

of Diquaternized Bipyridinium Salts

A characteristic feature of the current-voltage curves obtained for the diquaternized bipyridinium salts was a noticeable difference in the height of the waves due to the first and second one-electron reduction steps (see, for example, Figure 24). Levich plots for the individual one-electron reductions of methyl viologen in acetonitrile are shown in Figure 55. The slope measured for the second wave (5.24 ± 0.06 μA $s^{1/2}$) was some 20% larger than that found for the first wave (4.38 ± 0.03) μA $s^{1/2}$. Similar behavior was observed for all the compounds studied. For a given rotation speed, the limiting current for the overall two-electron reduction was invariably more than twice that observed for the one-electron process. The slopes of Levich plots for the initial one-electron and the overall two-electron reductions are given in Table 35. Ratios of the slopes vary from 2.1 to 2.3.
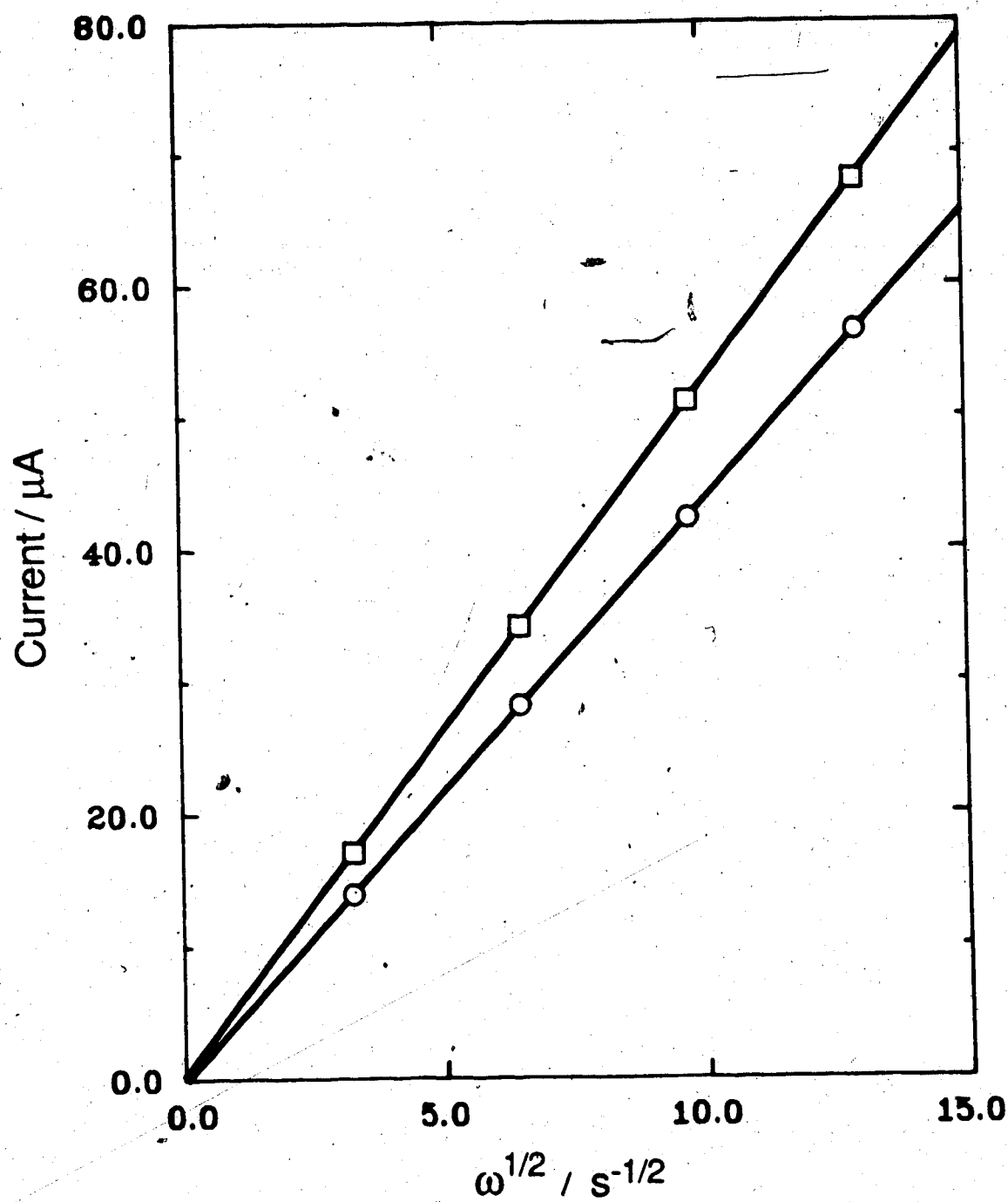
Figure 55. Levich Plots for the Individual One-Electron Reductions of Methyl Viologen. 125. μM MeV^{2+}, 0.1 M TEAP in acetonitrile. o $E_D = -0.65$ V vs SCE; □ $E_D = -1.10$ V vs SCE.

Table 35. Slopes of Levich Plots for the One- and Two-Electron

Reductions of Diquaternized Bipyridinium Salts in

Acetonitrile (0.1 $\underline{M}$ TEAP).

Compound	Concentration (mM)	$\Delta i / \Delta \omega^{1/2}$ n = 1 ($\mu A\ s^{1/2}$)[a]	$\Delta i / \Delta \omega^{1/2}$ n = 2 ($\mu A\ s^{1/2}$)[a]
MeV	0.1246	4.38±0.03	9.62±0.06
HeV	0.2075	6.81±0.03	14.56±0.08
CeV[b]	–	–	–
BzV	0.1078	3.34±0.03	7.58±0.03
CxV	0.1107	3.04±0.02	6.68±0.05
PhV	0.0999	3.17±0.02	6.82±0.05
CyV	0.1089	3.05±0.01	6.96±0.03
n-PrV	0.1160	4.02±0.03	8.58±0.07
i-PrV	0.1196	4.12±0.01	8.91±0.10
BuV	0.1121	3.65±0.05	8.03±0.09
HxV	0.1047	3.28±0.02	7.01±0.04
HpV	0.1019	3.12±0.02	6.60±0.03
OcV	0.0973	2.93±0.01	6.18±0.03
DiQ	0.1289	4.43±0.11	9.83±0.02
TriQ	0.1113	3.92±0.03	8.41±0.02
TetQ	0.1070	3.72±0.04	8.23±0.09
DiP	0.1007	3.06±0.03	–[c]
TriP	0.1149	3.25±0.04	–[c]

a. Uncertainties given are 95% confidence limits.
b. Compound insoluble.
c. Electrode passivated by the product of the two-electron reduction.

The data in Table 35 were collected with the goal of
calculating the diffusion coefficients of the bipyridinium
cation radicals in mind. It was of interest to determine
the magnitude of the differences between the diffusion
coefficients of the bipyridinium dications and cation
radicals and to investigate the effect of such differences
on the computed working curves, and thence on the
estimates of the rate constants. Calculating the value of
the diffusion coefficient of a cation radical from the
slope of the Levich plot for the second reduction step
proved to be rather more complicated than initially
anticipated. It was ultimately necessary to solve another
boundary value problem, this time for a mechanism
involving consecutive electron transfer accompanied by
reproportionation, as described in this chapter.

B. Consecutive Electron Transfer with Reproportionation

1. The Two-Electron Reduction of Methyl Viologen

The following reactions describe the processes
occurring at the level of the second reduction wave of
methyl viologen (21,142). At the electrode:

$$MeV^{2+} + e^- \rightleftharpoons MeV^{+\cdot} \qquad E_{1/2}^1 \qquad [56]$$

$$MeV^{+\bullet} + e^- \rightleftarrows MeV^0 \qquad\qquad E^2_{1/2} \qquad\qquad [57]$$
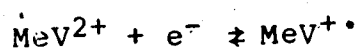
In solution:
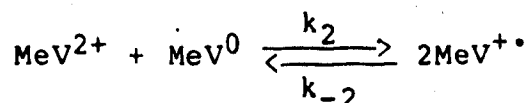
$$MeV^{2+} + MeV^0 \underset{k_{-2}}{\overset{k_2}{\rightleftarrows}} 2MeV^{+\bullet} \qquad\qquad [58]$$

For reaction [58]:

$$K_{eq}' = k_2/k_{-2} = \exp(F(E^1_{1/2} - E^2_{1/2})/RT)$$

Reaction [58] is variously referred to as a conproportion-ation reaction (21) or a reproportionation reaction (142,144). Insofar as the observed half-wave potentials (Tables 23 and 29) possess thermodynamic value, the right hand side of reaction [58] is favored for all the compounds studied in this work. Hünig and coworkers have investigated the polarography of a number of these compounds and have found that both the first and second reductions are electrochemically reversible in acetonitrile (124,140). From the half-wave potentials, equilibrium constants were calculated. These range from a low of 3.9×10^5 for phenyl viologen (124) to a high of 1 $\times 10^8$ for diquat (140). Kuwana and colleagues have shown by spectroelectrochemical techniques that the forward rate

constant for reaction [58] in acetonitrile is in excess of 3×10^9 $M^{-1}s^{-1}$ (142,143).

2. Other Work on Reproportionation Reactions

Although reproportionation reactions in general are thermodynamically favored, they have received very little attention to date. It has been suggested that this is due to the rather minor effects that reproportionation is expected to have on electrochemical measurables (147). It has been shown theoretically that if the diffusion coefficients of the participating species are equal, a reproportionation reaction occurring at any rate has no discernable effect on polarographic waves (145). Ruzic and Smith have considered the effect of reproportionation reactions on a.c. polarograms (146). If both the first and second reduction steps are electrochemically reversible (meaning that the kinetics of the heterogeneous electron transfer reactions are not rate-limiting), then the reproportionation reaction again has no effect. If the second reaction is not reversible however, a facile reproportionation reaction gives rise to an increase in the peak current for the second reduction (146). The effect of differing diffusivities among the species involved was briefly considered in this context.

Experimental studies of reproportionation reactions

are predominantly of the spectroelectrochemical variety.
The work of Kuwana and coworkers has already been
mentioned (142,143). Armstrong <u>et al.</u> determined the rate
of the reproportionation reaction occurring during the
two-electron reduction of p-nitrobenzaldehyde in sulfolane
by spectroelectrochemistry (148). More recently Bewick <u>et</u>
<u>al.</u> examined reproportionation reactions occurring upon
the two-electron oxidation of N-aryl-p-phenylenediamines
also by a spectroelectrochemical technique (144). In this
study, ratios of the limiting current for the second one-
electron oxidation over the first at a Pt RDE ranged from
0.88 to 1,10. No explanation was offered for this
difference. Similarly, Andrieux and Savéant reported
observing decreased wave heights at both the DME and the
RDE for the second reduction step of ene-diamines (145)
but again no attempt was made to explain the phenomenon in
terms of differing diffusivities.

Consecutive electron transfer accompanied by repro-
portionation can be represented by the following general
scheme:

$$P + e^- \rightleftharpoons Q \qquad E^o_{PQ} \qquad\qquad [59]$$

$$Q + e^- \rightleftharpoons R \qquad E^o_{QR} \qquad\qquad [60]$$

$$P + R \xrightleftharpoons[k_{-3}]{k_3} 2Q \qquad\qquad [61]$$

To date, only one study has considered the effect that differing diffusivities of the species P, Q and R might have on mass-transport-limited currents observed for the second wave. Eddowes and Grätzel studied the oxidation of tetrathiafulvalene in aqueous micellar solution (149). The micelles were required to solubilize the test compound. Since the product of the one-electron oxidation bore a positive charge, and thus resided predominantly in the aqueous phase, its diffusivity was observed to be some 12.5 times larger than that of the micelle-bound neutral compound. As a consequence, the limiting current measured at a Pt RDE for the two-electron oxidation step was over five times that for the initial one-electron process (149).

The diffusion coefficient of Q may be calculated from the value of the limiting current for the two-electron reduction (or oxidation) according to the following equation (82,149):

$$\frac{i}{FA} = 2 \ D_P \left(\frac{dc_P}{dz}\right)_{z=0} + D_Q \left(\frac{dc_Q}{dz}\right)_{z=0} \qquad [62]$$

Evaluation of the surface concentration gradients for P and Q requires solution of a set of differential equations not unlike those solved for the EC-catalytic mechanism in Chapter III. Eddowes has formulated the problem on two occasions (82,149) but, as yet, has published a solution only for the case $D_Q/D_P = 12.5$.

3. Independent Electrode Reactions Coupled by a Homogeneous Electron-Transfer Reaction

Before proceeding to the formulation and numerical solution of the boundary value problem corresponding to reactions [59] to [61], some pertinent results obtained for a related mechanism will be briefly discussed. For two independent electrode reactions coupled by a homogeneous electron-transfer reaction, the following scheme can be written:

$$A + n_1 \ e^- \rightleftarrows B \qquad\qquad E^\circ_{AB} \qquad [63a]$$

$$C + n_2 \ e \rightleftarrows D \qquad\qquad E^\circ_{CD} \qquad [63b]$$

$$A + (n_1/n_2)D \underset{k_{-4}}{\overset{k_4}{\rightleftarrows}} B + (n_1/n_2)C \qquad [64]$$
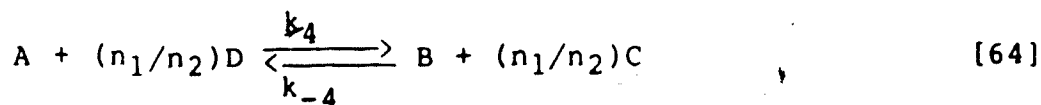
where $E_{CD}^\circ < E_{AB}^\circ$. One of the earliest examples of this mechanism (ca. 1953), due to Miller and Orleman (150), had $Ce(IV)/Ce(III)$ and O_2/H_2O_2 as the A/B and C/D couples respectively. A 14% increase in the polarographic diffusion current for dioxygen reduction was observed in the presence of $Ce(IV)$. A rapid, electron transfer reaction was postulated to occur in the diffusion layer and the non-additivity of the diffusion currents for the reduction of $Ce(IV)$ and O_2 was attributed to the large difference in the diffusion coefficients of $Ce(IV)$ (0.6 × 10^{-5} cm^2/s) and O_2 (2.6 × 10^{-5} cm^2/s) (150). Some thirty years elapsed before a quantitative treatment relating observed current to the rate and equilibrium parameters of reaction [64] and accounting for differing diffusivities appeared (151). In this case, Andrieux et al. solved the mechanism in the context of potential step chronoamperometry and chronocoulometry. The theory was successfully applied to the reduction of a mixture of 4-nitrotoluene and Co(II) tetraphenylporphyrin in DMF (152). From independent measurements, the diffusion coefficient of the former compound was found to be nearly three times that of the latter. Using this ratio and assuming a fast homogeneous electron transfer reaction, Andrieux et al. were able to predict the reduction currents observed in a mixture of the two compounds.

Of relevance to the present work was the finding that the chronoamperometric response observed for most experimental systems could be explained on the basis of two limiting cases (151). Thermodynamically, the limiting cases corresponded to K_{eq} for reaction [64] equals one (self-exchange) or K_{eq} equals ∞ (irreversible cross-exchange). The numerical value of K_{eq} had a significant effect on the predicted electrochemical response only over the interval $2 < K_{eq} < 100$. This corresponds to differences in standard potentials ranging from 18 to 118 mV for $n = 1$. For potential separations greater than 118 mV, reaction [64] may be treated as irreversible (that is, $k_{-4} = 0$). A second finding of Andrieux et al. was also of relevance to the present work. The kinetics of reaction [64] were found to affect the predicted electrochemical response over only a comparatively narrow range of rate constants (151). For potential-step chronoamperometry, a dimensionless kinetic parameter was defined as $\lambda = k_4 c_p(\infty)\theta$ where θ is the total measurement time (151). The rate of reaction [64] has a significant effect on the predicted response only for $0.25 < \lambda < 4$. Below this interval k_4 is effectively zero; above, it is effectively infinite.

C. The Dependence of the Levich Constant on the Diffusion Coefficient Ratio D_P/D_Q

1. Formulation of the Boundary Value Problem

The numerical solution of the differential equations describing consecutive electron transfer with reproportionation (reactions [59] to [61]) was undertaken in order to calculate diffusion coefficients from measured limiting currents. (In the studies already mentioned (149,152), independently measured diffusion coefficients were used to calculate limiting currents.) The formulation of the problem is based on the work of Eddowes (82,149). The problem has been simplified by assuming the reproportionation reaction [61] is "irreversible" ($k_3 \gg k_{-3}$). For all the compounds studied, the difference in half-wave potentials for the first and second reduction steps exceeded the required 118 mV minimum (151). The concentrations of P and Q at the electrode surface were taken to be zero. The electrode potential is therefore assumed to lie on the limiting current plateau for the second reduction step. While the problem is formulated in terms of reduction reactions, the results apply equally to oxidations.

Following the conventions established in Appendix I and used in Chapter III, the normalized differential equations describing consecutive electron transfer with reproportionation are:

$$\bar{D}_P \frac{d^2 C_P}{dz^2} + 23.997 \ z^2 \frac{dC_P}{dz} - 13.029 \ \bar{k} \ C_P C_R = 0 \qquad [65]$$

$$\bar{D}_Q \frac{d^2 C_Q}{dz^2} + 23.997 \ z^2 \frac{dC_Q}{dz} + 2(13.029) \ \bar{k} \ C_P C_R = 0 \qquad [66]$$

$$\bar{D}_R \frac{d^2 C_R}{dz^2} + 23.997 \ z^2 \frac{dC_R}{dz} - 13.029 \ \bar{k} \ C_P C_R = 0 \qquad [67]$$

The boundary conditions are:

At $Z = 0$, $C_P(0) = 0$; $C_Q(0) = 0$

$$\bar{D}_P \frac{dC_P}{dz} + \bar{D}_Q \frac{dC_Q}{dz} + \bar{D}_R \frac{dC_R}{dz} = 0.$$

At $Z = 1$, $C_P(1) = 1$; $C_Q(1) = 0$; $C_R(1) = 0$.

2. Numerical Solution by Orthogonal Collocation.

Application of the orthogonal collocation technique transforms the boundary value problem to the following set of simultaneous equations:

First, define

$$F_k(i,j) = B(i,j) + 23.997 \frac{z_i^2}{D_k} A(i,j)$$

where $k = P$, Q or R.

For species P:

$$\sum_{j=2}^{N+1} F_P(i,j) C_P(z_j) - 13.029 \frac{k}{D_P} C_P(z_i) C_R(z_i) =$$

$$- F_P(i,N+2) \tag{68}$$

For species Q:

$$\sum_{j=2}^{N+1} F_Q(i,j) C_Q(z_j) + 2(13.029) \frac{k}{D_Q} C_P(z_i) C_R(z_i)$$

$$= 0 \tag{69}$$

For species R:

$$\sum_{j=2}^{N+1} F_R(i,j) \, C_R(z_j) - \frac{F_R(i,1) \, A(1,j)}{\overline{D}_R A(1,1)} \times$$

$$(\overline{D}_P C_P(z_j) + \overline{D}_Q C_Q(z_j) + \overline{D}_R C_R(z_j))$$

$$- 13.029 \, \frac{k}{\overline{D}_R} \, C_P(z_i) C_R(z_i) = F_R(i,1) \, \frac{\overline{D}_P \, A(1,N+2)}{\overline{D}_R \, A(1,1)}$$

The boundary conditions at $Z = 0$ and $Z = 1$ have been incorporated into the above set of equations. The equation for species R makes use of the following expression for $C_R(0)$ derived from the boundary conditions at $Z = 0$:

$$C_R(0) = - \frac{\overline{D}_P \, A(1,N+2)}{\overline{D}_R \, A(1,1)} - \sum_{j=2}^{N+1} \frac{A(1,j)}{\overline{D}_R \, A(1,1)} \times$$

$$(\overline{D}_P C_P(z_j) + \overline{D}_Q C_Q(z_j) + \overline{D}_R C_R(z_j))$$

The program CETRP2 was written to solve equations [68] to [70] as a function of $\overline{D}_P$, $\overline{D}_Q$, $\overline{D}_R$, and $\overline{k}$. A listing of the program appears in Appendix II.

3. Validation of the Numerical Solution

To verify operation of the program, the problem was solved for $\bar{D}_P = \bar{D}_Q = \bar{D}_R = 1$. According to Andrieux and Savéant, the solution in this case is simply the Levich equation with n = 2 (145). For N = 24 and $\bar{k}$ = 1000, the following results were obtained:

$$\left(\frac{dC_P}{dZ}\right)_{Z=0} = 1.1 \times 10^{-4}; \qquad \left(\frac{dC_Q}{dZ}\right)_{Z=0} = 4.479$$

The corresponding concentration profiles are shown in Figure 56. In the limit of large $\bar{k}$, the concentration gradient of species P at the electrode surface is effectively zero. The incoming flux of electroactive species at the electrode surface consists entirely of the intermediate Q. The limiting current for the overall two-electron reduction is given by

$$i_l = C_L \, FAD_Q^{2/3} \, \nu^{-1/6} \, \omega^{1/2} \, C_P(\infty) \tag{71}$$

For $D_P = D_Q = D_R$, $C_L = 1.241$ in which case equation [71] corresponds to the Levich equation with n = 2.

As a further check on the validity of the numerical solution, a calculation was carried out for the case solved by Eddowes and Grätzel (149). For $D_Q/D_P = 12.5$, $D_R/D_Q = 1$, $\bar{k} = 1000$, and N = 24, the following surface concentration gradients were found:
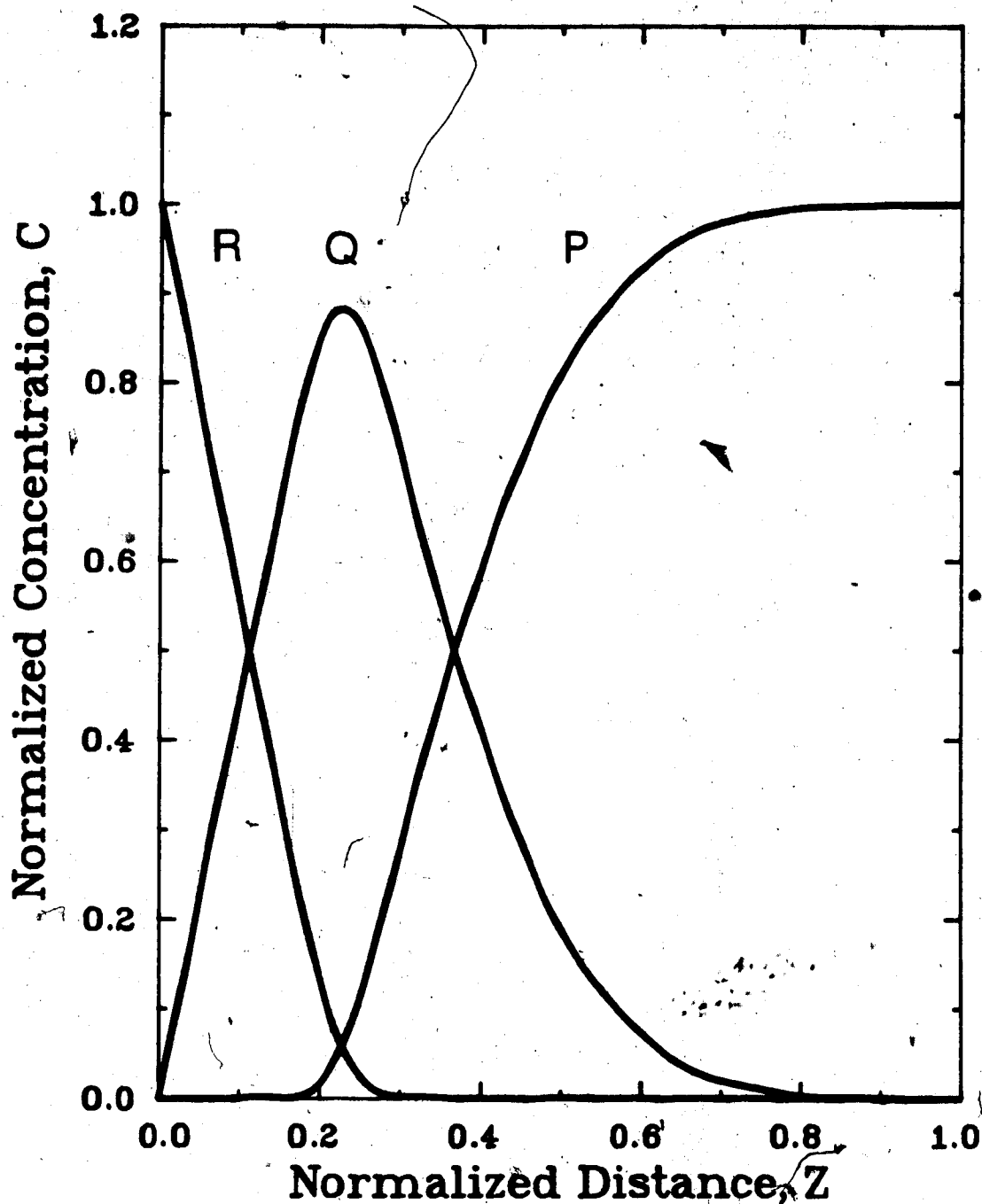
Figure 56. Concentration Profiles for Consecutive Electron Transfer Accompanied by a Rapid Reproportionation Reaction at the Rotating Disk Electrode. Curves computed by orthogonal collocation with $N = 24$, $D_P = D_Q = D_R$, $\bar{k} = 1000$.

$$\left(\frac{dC_P}{dZ}\right)_{Z=0} = 0.066; \qquad \left(\frac{dC_Q}{dZ}\right)_{Z=0} = 1.88$$

Substituting these values into equation [62], expressing D_Q in terms of D_P and reverting to dimensioned variables gave:

$$i_1 = 2.82 \ FAD_P^{2/3} \ \nu^{-1/6} \ \omega^{1/2} \ C_P(\infty)$$

which when converted to rotation speed in Hz was in excellent agreement with the equation given by Eddowes and Grätzel (149). A problem existed with the numerical solution in that the surface concentration gradient for species·P ought to have been zero (and that for species Q correspondingly larger). Increasing the value of $\bar{k}$ used in the calculation only aggravated the problem. It turns out that the case under consideration lies close to the limit of applicability of the orthogonal collocation solution. As a consequence of the large difference in the diffusion coefficients of P and Q, the P concentration profile drops rather abruptly to zero as Z decreases and even a degree 24 polymonial is not quite adequate to the task of representing it. The problem is manifested as a non-zero surface concentration gradient for P and by oscillations on the order of ±1% in the concentration

profile for P. Although it is significant numerically, the error in the collocation solution for $D_Q/D_P = 12.5$ is still minor from an experimental point of view.

The problem encountered at extreme values of D_Q/D_P can be overcome by application of the spline technique as was done in Chapter III for the second-order EC-catalytic mechanism at large $\bar{k}$. Alternatively, Eddowes recommended the following change of variable:

$$U = (1 + \exp(-\alpha\beta))/(1 + \exp(\alpha(Z-\beta)))$$

where α and β are adjustable parameters used to make the transformed function better fit the collocation points (82). A third option uses exponentially weighted orthogonal polynomials to better fit the collocation points to the function (153). None of these solutions was implemented in the present work however. The ordinary collocation technique with $N = 24$ and $\bar{k} = 1000$ gave good results over the modest range of diffusion coefficient ratios examined ($0.5 < D_P/D_Q < 2.0$). The normalized surface concentration gradient for P was less than 5×10^{-4} throughout and oscillations in the concentration profiles never exceeded $\pm 0.01\%$ in amplitude. Although machine accuracy for single precision was not attained, the accuracy of the numerical solution was more than adequate for the purpose of the present work.

4. The Levich Constant as a Function of D_P/D_Q

To determine the diffusion coefficients of the bipyridinium cation radicals from limiting current measurements, it was necessary to solve equations [68] to [70] as a function of D_P/D_Q for $\bar{k}$ equals 1000. This was done over the interval $0.5 < D_P/D_Q < 2.0$ and from the results the coefficient of equation [71] C_L was calculated as a function of D_P/D_Q. The values obtained, which are independent of D_R, are listed in Table 36 for $D_P/D_Q < 1$ and in Table 37 for $D_P/D_Q > 1$. Plots of these data appear in Figures 57 and 58. For each graph, the points can be fitted to a good approximation by two line segments, one for each half of the graph. The equations for these line segments and the intervals over which they apply are given in Tables 36 and 37.

D. Calculation of the Diffusion Coefficients of Bipyridinium Cation Radicals

To illustrate the calculation of diffusion coefficients from limiting current measurements, the case of methyl viologen will be considered in detail. The diffusion coefficient of the dication was calculated using the Levich equation together with the result given in Table 35 for the initial one-electron reduction. Taking A

Table 36. Consecutive Electron Transfer with Reproportionation. The Levich Constant for $0.5 < D_P/D_Q < 1$.

D_P/D_Q	$(dC_Q/dZ)_{Z=0}$	C_L
0.50	3.3246	0.921
0.55	3.4562	0.958
0.60	3.5825	0.992
0.65	3.7049	1.026
0.70	3.8238	1.059
0.75	3.9393	1.091
0.80	4.0523	1.123
0.85	4.1624	1.153
0.90	4.2702	1.183
0.95	4.3755	1.212
1.00	4.4790	1.241

For $0.50 < D_P/D_Q < 0.75$: $C_L = 0.678 (D_P/D_Q) + 0.584$.

For $0.75 < D_P/D_Q < 1.00$: $C_L = 0.598 (D_P/D_Q) + 0.644$.

Table 37. Consecutive Electron Transfer with Reproportionation. The Levich Constant for $1 < D_P/D_Q < 2$.

D_P/D_Q	$(dC_Q/dZ)_{Z=0}$	C_L
1.00	4.4790	1.241
1.10	4.8311	1.338
1.20	5.1795	1.435
1.30	5.5246	1.530
1.40	5.8670	1.625
1.50	6.2068	1.719
1.60	6.5446	1.813
1.70	6.8799	1.906
1.80	7.2135	1.998
1.90	7.5450	2.090
2.00	7.8751	2.182

For $1.0 < D_P/D_Q < 1.5$: $C_L = 0.956 (D_P/D_Q) + 0.286$.

For $1.5 < D_P/D_Q < 2.0$: $C_L = 0.925 (D_P/D_Q) + 0.322$.
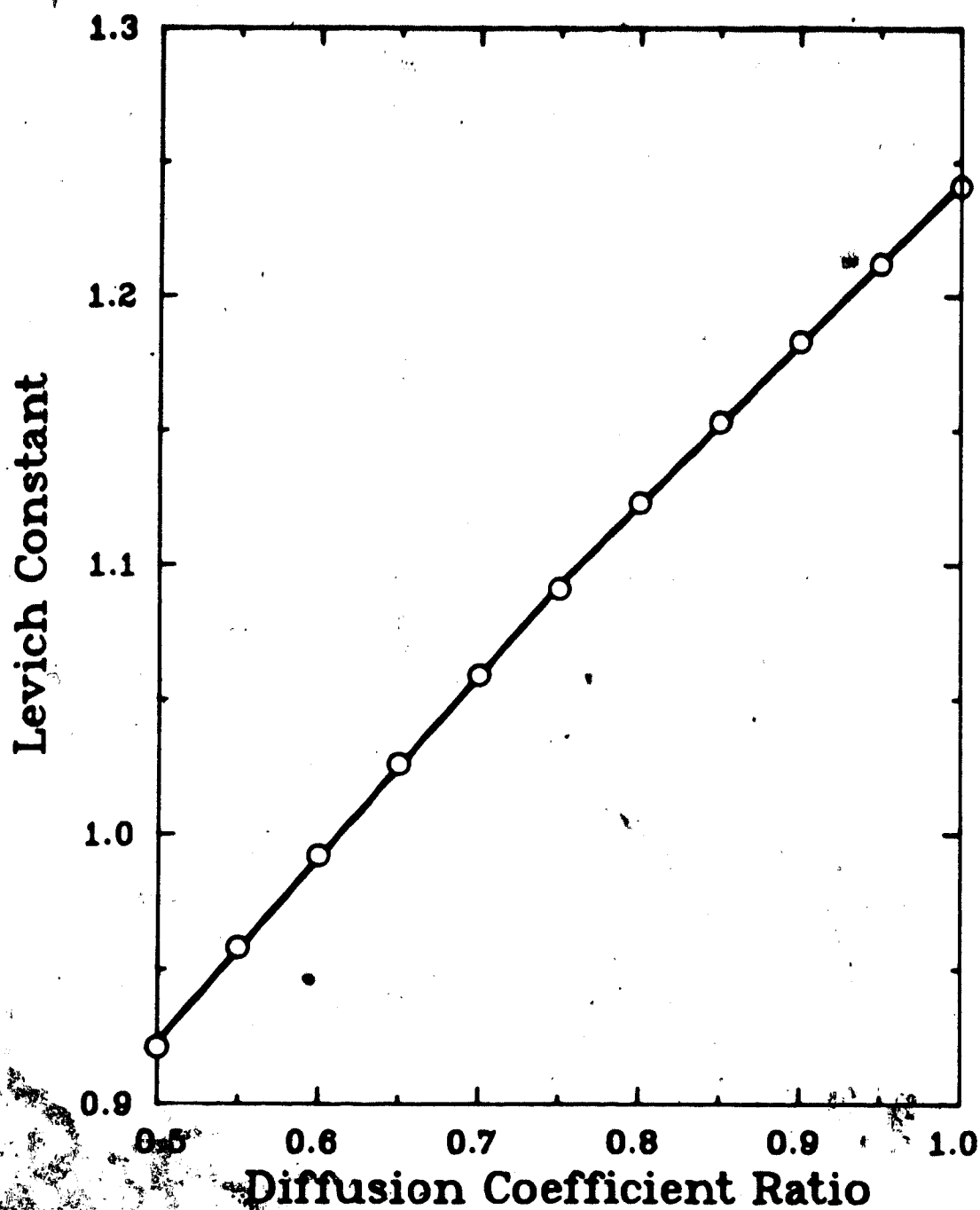
Figure 57. The Levich Constant as a Function of the
Diffusion Coefficient Ratio for the Interval
$0.5 \leq D_P/D_Q \leq 1.0$. The data and the equations
for the two line segments appear in Table 36.
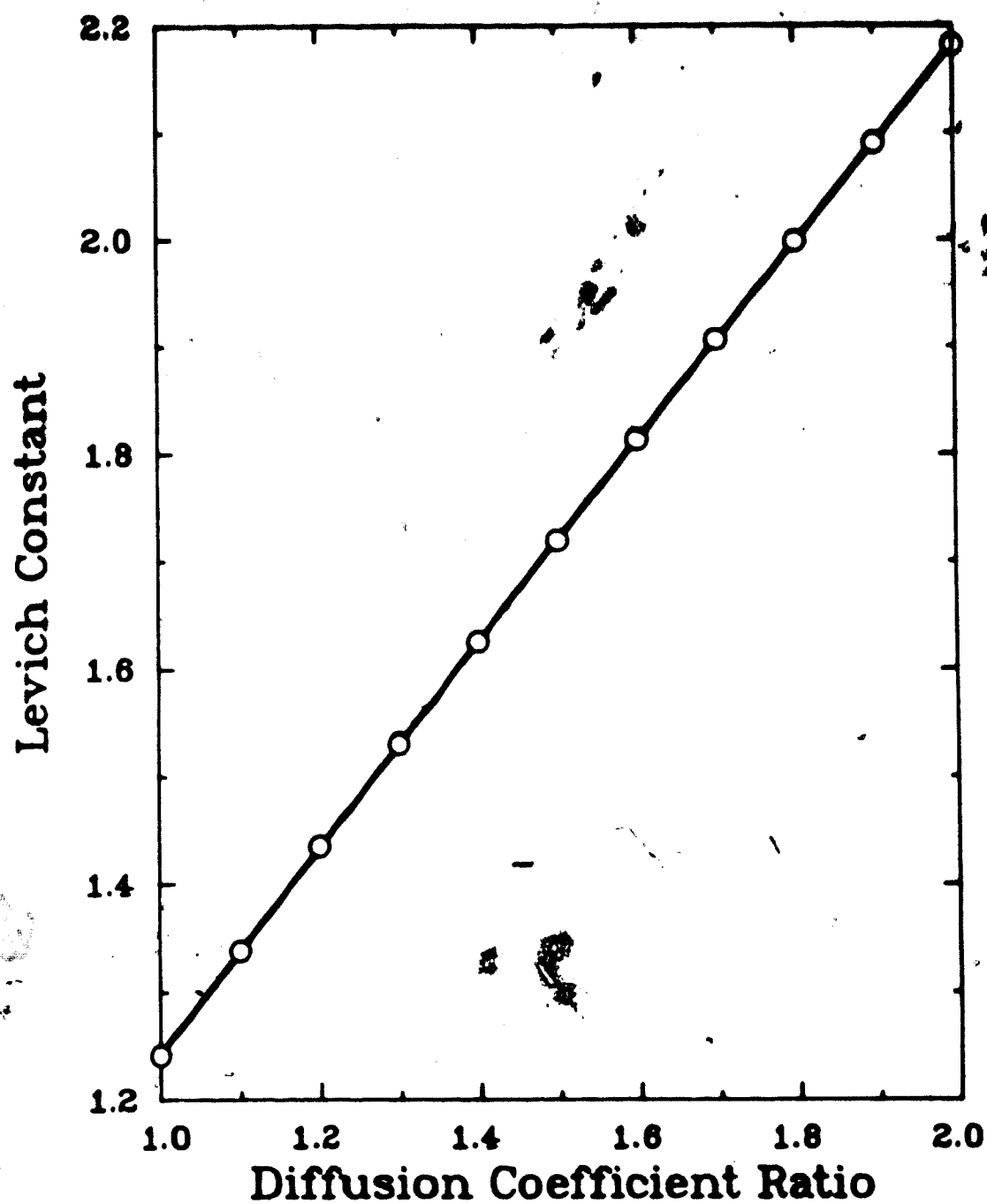
Figure 58. The Levich Constant as a Function of the
Diffusion Coefficient Ratio for the Interval
$1.0 \leq D_P/D_Q \leq 2.0$. The data and the equations
for the two line segments appear in Table 37.

$= 0.4458$ cm^2 and $v = 4.80 \times 10^{-3}$ cm^2/s, a value of (1).26 $\pm$ 0.03) $\times 10^{-5}$ cm^2/s was obtained. To calculate the diffusion coefficient of the cation radical, the expression for C_L in the range $0.50 < D_P/D_Q < 0.75$ was inserted in equation [71] to give

$$i_1 = (0.678(D_P/D_Q)^{1/3} + 0.584\ D_Q^{2/3})$$

$$\times\ FAD_Q^{2/3}\ v^{-1/6}\ \omega^{1/2}\ C_P(\infty) \qquad\qquad [72]$$

Using the result given in Table 35 for the two-electron reduction together with the values of A, v and D_P given above, equation [72] becomes

$$\frac{i_1}{\omega^{1/2}} = (0.1115/D_Q^{1/3} + 7.621 \times 10^3\ D_Q^{2/3}) = 9.623$$

$$D_Q = (1.158 \times 10^{-2} + 7.919 \times 10^2\ D_Q)^3$$

The cubic equation in D_Q was solved iteratively using a pocket calculator to give a value of $(1.92 \pm 0.03) \times 10^{-5}$ cm^2/s for the diffusion coefficient of the methyl viologen cation radical. The diffusion coefficients for the cation radicals of the other bipyridinium compounds studied were calculated in the manner just described. The data used in the calculations are given in Table 35 and the results obtained are summarized in Table 38.

Table 38. Diffusion Coefficients of Diquaternized Bipyridinium Dications and Cation Radicals in Acetonitrile (0.1 $\underline{M}$ TEAP).

Compound	Diffusion Coefficient[a]/10^{-5} cm^2/s		D_P/D_Q
	Dication (D_P)	Cation Radical (D_Q)	
MeV	1.26±0.03	1.92±0.03	0.66±0.03
HeV	1.13±0.01	1.53±0.02	0.74±0.02
CeV[b]	–	–	–
BzV	1.04±0.02	1.81±0.03	0.57±0.03
CxV	0.87±0.01	1.33±0.02	0.65±0.02
PhV	1.08±0.01	1.51±0.02	0.72±0.02
CyV	0.89±0.01	1.59±0.02	0.56±0.02
n-PrV	1.23±0.02	1.66±0.03	0.74±0.02
i-PrV	1.22±0.01	1.76±0.02	0.69±0.02
BuV	1.12±0.02	1.73±0.03	0.65±0.03
HxV	1.06±0.01	1.42±0.01	0.75±0.01
HpV	1.02±0.01	1.32±0.02	0.77±0.02
OcV	1.00±0.01	1.28±0.02	0.78±0.02
DiQ	1.22±0.05	1.93±0.05	0.63±0.05
TriQ	1.26±0.01	1.73±0.02	0.73±0.01
TetQ	1.24±0.02	1.94±0.03	0.64±0.02
DiP	1.01±0.02	–[c]	–[c]
TriP	0.91±0.02	–[c]	–[c]

a. Uncertainties based on 95% confidence limits for the slopes of the Levich plots.
b. Compound insoluble.
c. Electrode passivated by product of the two-electron reduction.

E. Experimental Confirmation of the Diffusion Coefficient of the Methyl Viologen Cation Radical

To check the validity of the value obtained for the diffusion coefficient of the methyl viologen cation radical, a more direct measurement was undertaken. A solution of the cation radical in acetonitrile (1×10^{-4} $\underline{M}$) was produced by electrolysis at constant potential as described in Chapter IV. The diffusion coefficient of $MeV^{+}\cdot$ was determined by measuring limiting current as a function of rotation speed for both the oxidation reaction $MeV^{+}\cdot \rightleftarrows MeV^{2+} + e^-$ ($E_D = 0.0$ V vs SCE) and the reduction reaction $MeV^{+}\cdot + e \rightleftarrows MeV^{\circ}$ ($E_D = -1.10$ V) at the GC RDE. The results obtained for five trials of the experiment are shown in Table 39. From the residual current observed for the reduction of MeV^{2+} at -0.65 V, it was apparent that the bulk electrolysis failed to achieve complete conversion of MV^{2+} to $MeV^{+}\cdot$. According to the half-life estimated from the decay curve for the electrolysis current, the electrolysis time ought to have been sufficient to ensure 99.9% conversion. The residual reduction current, corresponding to 2 to 5% of the original MeV^{2+}, probably resulted from the presence of traces of dioxygen in the purge gas. To compensate for

Table 39. Determination of the Diffusion Coefficient of the Methyl

Viologen Cation Radical.

[MeV^{2+}]	Residual[a]	MeV$^{+\bullet}$ Oxidation[b]		MeV$^{+\bullet}$ Reduction[c]	
mM	$\Delta i / \Delta \omega^{1/2}$	$\Delta i / \Delta \omega 1/2$	D	$\Delta i / \Delta \omega^{1/2}$	D
	$\mu A \ s^{1/2}$	$\mu A \ s^{1/2}$	$10^{-5} \ cm^2/s$	$\mu A \ s^{1/2}$	$10^{-5} \ cm^2/s$
0.1194	0.30	5.57	1.92	5.90	2.10
0.1194	0.20	5.52	1.90	5.62	1.95
0.1194	0.16	5.35	1.81	5.13	1.70
0.0992	0.12	4.52	1.84	4.18	1.88
0.0992	0.09	4.38	1.77	4.23	1.68
		Average	1.85		1.86
		s.d.	0.06		0.18
		95% CI	0.08		0.22

a. $E_D = -0.65$ V vs SCE.

b. $E_D = 0.00$ V.

c. $E_D = -1.10$ V.

incomplete conversion, the limiting current for MeV^{2+}

reduction at -0.65 V was measured as a function of

rotation speed. The results were subtracted from those

observed for $MeV^{+\cdot}$ reduction at -1.10 V and added to those

observed for $MeV^{+\cdot}$ oxidation at 0.0 V.

The diffusion coefficients obtained from the Levich

plots for the oxidation and reduction of $MeV^{+\cdot}$ are given

in Table 39. Although considerable scatter is present in

the results for the reduction, the averages of the results

are in good agreement. The overall average value is (1.86

± 0.12) × 10^{-5} cm^2/s. To provide a sound basis for

comparison, the determination of the diffusion coefficient

of $MeV^{+\cdot}$ using equation [72] was carried out at three

different concentrations. The results are shown in Table

40. The value obtained, (1.94 ± 0.06) × 10^{-5} cm^2/s, is in

reasonable agreement with that obtained from the

electrolysis experiment.

It was noted that the electrolysis reaction was not

chemically reversible. On admission of dioxygen to the

electrolysis cell, the blue color of the cation radical

slowly disappeared leaving behind a yellow solution rather

than the initial colorless solution. An electrolysis was

carried out using a blank solution but no color was

observed. The UV-visible absorbance spectrum of the

yellow solution remaining after air-oxidation was

Table 40. Reproducibility of the Diffusion Coefficients of the

Methyl Viologen Dication and Cation Radical.

$[MeV^{2+}]$	One-Electron Reduction		Two-Electron Reduction	
	$\Delta i / \Delta \omega^{1/2}$	$D_P{}^a$	$\Delta i / \Delta \omega^{1/2}$	$D_Q{}^b$
M	$\mu A \ s^{1/2}$	$10^{-5} \ cm^2/s$	$\mu A \ s^{1/2}$	$10^{-5} \ cm^2/s$
0.0992	3.55	1.29	7.77	1.95
0.1246	4.38	1.26	9.62	1.91
0.1916	6.93	1.31	15.10	1.95
	Average	1.29		1.94
	s.d.	0.02		0.02
	95% CI	0.06		0.06

a. Calculated from the Levich equation with $A = 0.4458 \ cm^2$ and $\nu = 4.80 \times 10^{-3} \ cm^2/s$.

b. Calculated from equation [72] using the value found for D_P at the same concentration.

recorded. The absorbance of the MeV^{2+} peak at 260 nm was only 80% of that expected given the original concentration. A broad peak at 396 nm with a shoulder at 474 nm was also observed.

A search of the literature uncovered reports from Sawyer's group on the quantitative formation of a bronze-colored, diamagnetic product when equimolar solutions of $MeV^{+\cdot}$ and O_2^{-} in DMF were mixed (154,155). The product was thought to be an alkyl peroxide formed by a radical-radical coupling at C_2 of the bipyridinium ring. The peroxide was not stable but decomposed rapidly to form a fairly complex mixture of products of which two were identified: 1-methyl-2-pyridone and the 1,1'-dimethyl-2-oxo-4,4'-bipyridinium dication. In view of its instability, it was not surprising that none of the spectral features reported for the peroxide (154) matched those observed for the yellow solution remaining after the electrolysis experiment. The reaction of O_2^{-} with $MeV^{+\cdot}$ could be responsible for the observed decomposition however. Although the reaction of O_2 with $MeV^{+\cdot}$ to form O_2^{-} is not thermodynamically favored in the absence of an acid (30), the subsequent reaction of O_2^{-} with another $MeV^{+\cdot}$ could change this. If the latter reaction initiates the decomposition of $MeV^{+\cdot}$, then the bulk of the decomposition would have taken place after the

electrolysis experiment was complete and dioxygen was admitted to the electrochemical cell. As residual dioxygen on the order of 5×10^{-7} $\underline{M}$ was present throughout the electrolysis, a certain amount of decomposition may have occurred over the course of the experiment. While it is not possible to estimate the extent to which this may have occurred, such decomposition may account for the lower value of the diffusion coefficient of $MeV^{+\cdot}$ observed in the bulk electrolysis experiment.

F. The Effect of the Differences in Diffusivities on the Values Obtained for k_1

Working curves for the kinetic experiments described in Chapter V were recalculated taking into account the diffusion coefficient ratios found in Table 38. These curves were used in conjunction with the experimental data to calculate new estimates for k_1. These values, denoted by k_1^*, are given in Table 41. For comparison, the values of k_1 obtained on the assumption of equal diffusivities are shown as well. Accounting for the difference in diffusivities leads to a 10 to 50% increase in the calculated value of k_1. The ratio k_1^*/k_1 shows no significant correlation with the diffusion coefficient ratio D_P/D_Q ($r = 0.022$) or with the value of k_1 ($r =$

Table 41. Effect of Differences in the Diffusivities of the Catalyst Species on the Values Obtained for k_1.

Compound	$D_P = D_Q$ k_1 $M^{-1}s^{-1}$	$D_P \neq D_Q$ k_1^* $M^{-1}s^{-1}$	k_1^*/k_1
MeV	$(1.40\pm0.05)\times10^6$	$(2.02\pm0.08)\times10^6$	1.44
HeV	$(1.24\pm0.03)\times10^6$	$(1.83\pm0.07)\times10^6$	1.48
CeV	$(1.10\pm0.14)\times10^6$	–	–
BzV	$(3.88\pm0.13)\times10^5$	$(4.46\pm0.15)\times10^5$	1.15
CxV	$(7.51\pm0.44)\times10^5$	$(9.90\pm0.49)\times10^4$	1.32
PhV	$(1.63\pm0.11)\times10^4$	$(1.96\pm0.15)\times10^4$	1.20
CyV	$(5.10\pm0.26)\times10^3$	$(7.35\pm0.36)\times10^3$	1.44
n-PrV	$(1.45\pm0.05)\times10^6$	$(1.79\pm0.17)\times10^6$	1.23
i-PrV	$(0.93\pm0.05)\times10^6$	$(1.29\pm0.06)\times10^6$	1.39
BuV	$(1.60\pm0.11)\times10^6$	$(2.47\pm0.22)\times10^6$	1.54
HxV	$(1.74\pm0.24)\times10^6$	$(2.58\pm0.12)\times10^6$	1.48
HpV	$(1.97\pm0.09)\times10^6$	$(2.39\pm0.38)\times10^6$	1.21
OcV	$(2.46\pm0.13)\times10^6$	$(2.90\pm0.15)\times10^6$	1.18
DiQ	$(5.04\pm0.31)\times10^5$	$(7.15\pm0.44)\times10^5$	1.42
TriQ	$(8.9\pm1.1)\times10^6$	$(1.56\pm0.09)\times10^7$	1.75
TetQ	$(1.98\pm0.16)\times10^8$	$(2.18\pm0.33)\times10^8$	1.10
DiP	$(2.43\pm0.33)\times10^6$	–	–
TriP	$(1.16\pm0.05)\times10^6$	–	–

-0.36). For the most part, the uncertainties associated with k_1^* are somewhat larger than those associated with k_1.

It should be noted that whereas the rate constants were determined in acetonitrile containing 1 $\underline{M}$ acetic acid, the diffusion coefficient ratios in Table 38 were measured in the absence of acid. (Current from the reduction of H^+ precluded the determination of the diffusion coefficients of the cation radicals in the presence of the acid.) In recalculating the rate constants, it has been assumed that the diffusion coefficient ratio is unchanged in the presence of the acid. In addition, the uncertainties of the ratios in Table 38, which are based on the 95% confidence intervals for the Levich slopes in Table 35, probably belie the accuracy with which these ratios are known. The ratios are based on limiting currents measured at four rotation speeds and at one concentration (ca. 1 × 10^{-4} $\underline{M}$). From the results obtained for three separate determinations of D_P and D_Q for methyl viologen at three different concentrations (Table 40), the ratio D_P/D_Q was calculated as 0.66 ± 0.06. These results suggest that uncertainties on the order of ±10% may be more appropriate for the diffusion coefficient ratios in Table 38. The ±10% uncertainty and the assumption associated with the use of

the diffusion coefficient ratios together with the $\pm 10\%$ uncertainty in k_1 associated with errors in dioxygen concentrations (see Chapter V) render the differences observed between k_1 and k_1^* less significant than the numbers in Table 41 might suggest. Overall errors in k_1 are on the order of $\pm 10\%$ whereas overall errors of $\pm 15-20\%$ are perhaps more appropriate for k_1^*.

Before closing this chapter, a few words are in order concerning the source of the differences in the diffusivities of bipyridinium dications and cation radicals. The stability of the cation radicals of diquaternized salts of 2,2'- and 4,4'-bipyridine is a consequence of the delocalization of the odd electron over the entire ring system (21). According to Homer et al. (22), some eighteen resonance structures can be drawn for the methyl viologen cation radical, none of which invoke charge separation. By contrast, the positive charges of the dication are localized around the ring nitrogens. Upon one-electron reduction, these two discrete positive charges are replaced by a single positive charge which, like the odd electron, is delocalized throughout the ring system. Substantial solvent and counterion reorganization can be expected to accompany this change and it is reasonable to assume that this reorganization would favor an increased diffusivity for the cation radical.

CHAPTER·VII

CORRELATION OF KINETIC RESULTS WITH THE CHEMICAL AND BIOLOGICAL PROPERTIES OF BIPYRIDINIUM COMPOUNDS

A. Introduction

In this chapter the results obtained for the rates of reaction of bipyridinium cation radicals with dioxygen are examined in a number of contexts. From the dependence of the rate constants on the half-wave potentials of the catalysts, conclusions are drawn concerning the nature of the homogeneous electron-transfer reaction. A comparison of the rate constants obtained in this work with those found by other workers using different techniques and different solvents follows. Finally, the kinetic results are compared to published data on the herbicidal activity of bipyridinium compounds. In this chapter discussion is confined almost exclusively to the results of Chapter V, which were calculated on the assumption of equal diffusivities for the oxidized and reduced forms of the bipyridinium compounds. Exceptions to this statement have been duly noted. While the effects of the differences in diffusivities observed in Chapter VI were significant relative to the estimated uncertainties in the values of

k_1, they are a little consequence with respect to the conclusions drawn in this chapter. Since it was not possible to evaluate the diffusion coefficient ratios for three of the compounds studied, a larger number of results are available when the diffusivities are assumed to be equal.

B. Calculation of the Rate Constant for the Equilibrium Exchange Reaction

Electron-transfer reactions in solution can be considered to comprise three successive steps (160). Using the $MeV^{+\cdot}/O_2$ reaction as an example:

$$MeV^{+\cdot} + O_2 \underset{k_{dif}}{\overset{k_{dif}}{\rightleftharpoons}} (MeV^{+\cdot}, O_2) \underset{k_{-1}^{Act}}{\overset{k_1^{Act}}{\rightleftharpoons}}$$

$$(MeV^{2+}, O_2^{-\cdot}) \underset{k_{dif}}{\overset{k_{dif}}{\rightleftharpoons}} MeV^{2+} + O_2^{-} \qquad [73]$$
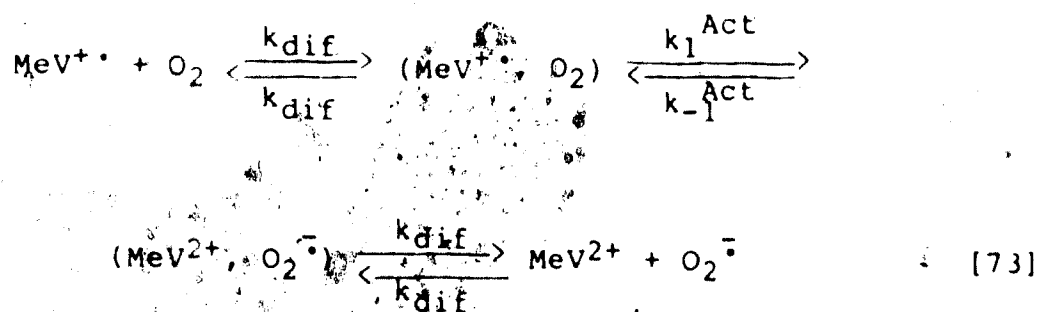
The quantities in parentheses represent the species in their reaction sites, k_1^{Act} and k_{-1}^{Act} are the activation-controlled rate constants and k_{dif} is the diffusion-limited rate constant. The observed forward rate constant k_1 is given by (161):

$$1/k_1 = 1/k_{dif} + 1/k_1^{Act} \qquad [74]$$

The diffusion-limited rate constant can be calculated from the Smoluchowski equation (161) as:

$$k_{dif} = 4\pi N_A \bar{D} d$$

where $\bar{D}$ is the average diffusion coefficient of the reactants, d is the distance between the reacting centers and N_A is Avogadro's number. From the results given in Tables 22 and 25, $\bar{D}$ for the $MeV^{+\cdot}/O_2$ reaction in acetonitrile is 4.8×10^{-5} cm^2/s. For dioxygen, the molecular radius has been calculated from the bond length and the van der Waals radius as 0.16 nm (30). Using the Stokes-Einstein equation and the diffusion coefficient ratio $D_{O_2}/D_{MeV2+} = 6.9$, the radius of the methyl viologen dication may be approximated as 1.1 nm. From these values and the Smoluchowski equation, k_{dif} is calculated as 5×10^{10} $M^{-1}s^{-1}$.

The activation-controlled rate constant for the forward electron transfer is given by (160):

$$\log k_1^{Act} = \log k_s^{sol} - \alpha^{sol}(E_{PQ}^\circ - E_{AB}^\circ)/0.059 \qquad [75]$$

where α^{sol} and k_s^{sol} are the transfer coefficient and the

equilibrium exchange rate constant of the homogeneous

electron-transfer reaction respectively. Equation [75]

predicts a linear relationship between log k_1 and the

difference in the standard potentials of the catalyst

(E_{PQ}^o) and the substrate (E_{AB}^o) couples. For the O_2/O_2^-

couple, Sawyer et al. give the formal reduction potential

$E^{o'}$ in acetonitrile containing 0.1 M TEAP as -0.87 V vs

aq. SCE (109). The half-wave potentials given in Tables

23 and 29 may be taken as valid estimates of the formal

potentials of the catalyst couples. (Hünig and co-workers

have studied a number of these compounds by polarography

in acetonitrile and have found the initial reduction waves

to be reversible without exception (122,140,141).)

Assuming that the difference in formal potentials equals

the difference in standard potentials and using the

measured values of k_1 from Tables 28 and 39, a plot of the

data was prepared according to equation [75]. The plot is

shown in Figure 59 and the data are given in Table 42.

The plot is linear over the entire range of compounds

studied and the slope, -8.7 ± 0.6 V^{-1}, is in good

agreement with the value expected for $\alpha^{sol} = 0.5$, that is,

8.5 V^{-1}. These results indicate that reaction [73] is

under activation control for all the compounds studied.

From the y-intercept of Figure 59, log k_s^{sol} equals 9.79 ±

0.29. Using the values of k_1 calculated in Chapter VI for
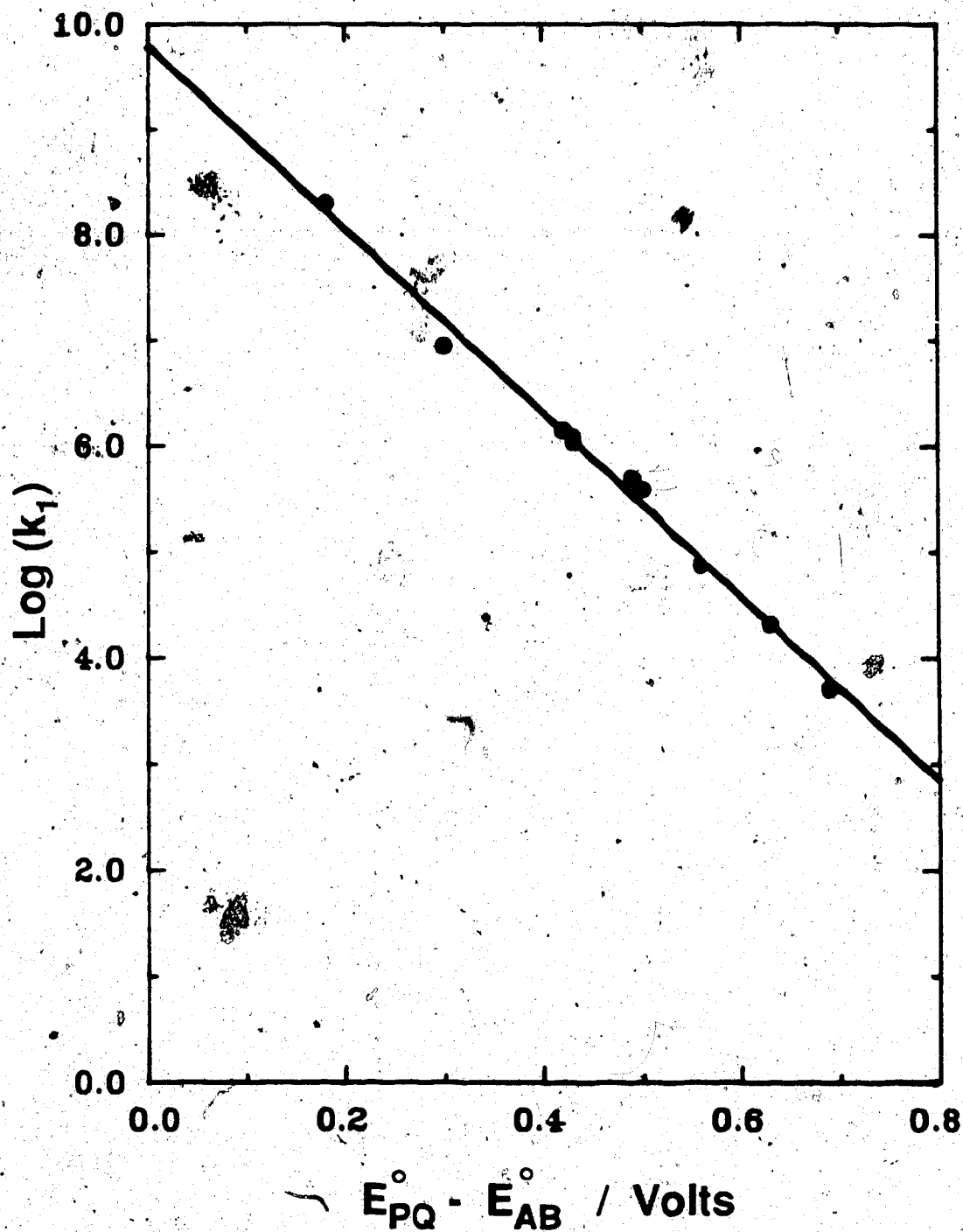
Figure 59. Log(k_1) versus the Standard Potential Difference
for the Reaction of Bipyridinium Cation Radicals
with Dioxygen in Acetonitrile. Data appear in
Table 42. Slope = -8.7 ± 0.6 V^{-1}; intercept =
9.8 ± 0.3; r = 0.995.

Table 42. Rate Constants for the Reaction of Bipyridinium Cation
Radicals with Dioxygen as a Function of Potential
Separation.

Compound	$-E_{1/2} = -E^{o\prime}_{PQ}$ V vs SCE	$E^{o\prime}_{PQ} - E^{o\prime}_{AB}$ V	$\log k_1$
MeV	0.45	0.42	6.15
HeV	0.44	0.43	6.09
CeV	0.44	0.43	6.04
BzV	0.37	0.50	5.59
CxV	0.31	0.56	4.88
PhV	0.24	0.63	4.21
CyV	0.18		3.71
DiQ	0.38	0.49	5.70
TriQ	0.57	0.30	6.95
TetQ	0.69	0.18	8.30

Note: $E^{o\prime}_{AB}$ for $O_2 + e^- \rightleftarrows O_2^{-}$ equals -0.87 V vs aq. SCE (109).

unequal catalyst diffusivities, a value of -8.7 ± 0.5 V^{-1} is obtained for the slope and 9.92 ± 0.26 for log k_s^{sol}.

It should be noted that the formal potentials used to calculate the standard potential difference $E_{PQ}^o - E_{AB}^o$ given in Figure 59 were determined under aprotic conditions. It is for this reason that the slope of the graph in Figure 59 is negative. Under aprotic conditions, reaction [73] proceeds in the opposite direction to that shown. The rate constant of the reverse reaction k_{-1} is inversely proportional to the rate constant k_1 which as actually measured.

C. Comparison with the Results of Other Kinetic Studies

As discussed in Chapter I, much of the previous work on the rates of reaction of bipyridinium cation radicals with dioxygen employed spectroscopic techniques such as pulse radiolysis (27,28) and laser photolysis (27) which are suited to the study of very fast reactions. In these techniques, ionizing radiation is used to generate one-electron reducing agents which react very rapidly (<10 μs) with bipyridinium dications to produce the corresponding cation radicals (27,28). The decay in the absorbance of the cation radicals in the presence of dioxygen is observed, typically for a few milliseconds, and the rate constant is calculated from the decay curve.

The rate constants for the reaction of a variety of bipyridinium cation radicals with dioxygen in aqueous solution have been determined by Farrington et al. using the technique of pulse radiolysis (28). The results obtained together with the comparable values measured in acetonitrile as part of the present work are shown in Table 43. The order of reactivity of the cation radicals is the same, but the pulse radiolysis values observed in aqueous solution are substantially higher. The ratio $k_{1,H_2O}/k_{1,AN}$ varies from 4.8 for the fastest reaction to 1048 for the slowest. Assuming that the estimates of k_{1,H_2O} and $k_{1,AN}$ are free of serious systematic error, it can be concluded that acetonitrile is a more strongly differentiating solvent, in terms of the reactivity of bipyridinium cation radicals toward dioxygen than is water. Since reaction rates in aqueous solution are approaching the diffusion limit, the observed rate constants contain significant contributions from diffusion according to equation [74]. It is for this reason that the rate constants measured in aqueous solution show considerably less variation than equation [75] predicts. In acetonitrile, the observed rates are determined entirely by activation, a process which is much more sensitive to the nature of the substituents of the bipyridinium cation radicals than is diffusion. (Diffusion coefficients for all the compounds in Table 43

Table 43. Comparison of Rate Constants Obtained by Pulse Radiolysis in Aqueous Solution with Those of This Work.

| Compound | Pulse Radiolysis in Aqueous Solution[a] | | Rotating Disk Electrode in Acetonitrile[b] | |
	k_1 / 10^8 $M^{-1}s^{-1}$	$\log k_1$	k_1 / 10^5 $M^{-1}s^{-1}$	$\log k_1$
MeV	8.0±0.3	8.90	14.0±0.5	6.15
HeV	3.6±0.2	8.56	12.4±0.3	6.09
BzV	_c	_c	3.88±0.13	5.59
PhV	0.22±0.01	7.34	0.16±0.01	4.32
DiQ	4.7±0.3	8.67	5.04±0.31	5 70
TriQ	8.4±0.6	8.92	89±11	6.95
TetQ	9.6±0.4	8.98	1980±160	8.30

a. Reference 28, pH 6.8, 18°C.

b. This work, 1.0 $\underline{M}$ HOAc, 0.1 $\underline{M}$ TEAP, 25°C.

c. Rapid dimerization of $BzV^{+\bullet}$ prevented the measurement of k_1.

lie in the range 1.0 to 1.2 $\times$ 10^{-5} cm^2/s.) The differentiating power of acetonitrile found in this context is not without precedent. The differentiation of mineral acid strengths that is observed in acetonitrile is well-known (162). In aqueous solution, these acids appear equally strong as a consequence of the limit on acid strength established by autoprotolysis. The diffusion limit exerts a kind of analogous limiting effect on the rates of fast electron-transfer reactions.

Further evidence of the sensitivity of the measurements made in acetonitrile can be found in the results for the alkyl-substituted viologens. These are plotted as a function of the number of carbon atoms in the alkyl chain in Figure 60. Reduction potentials measured for these compounds were identical within experimental error (see Table 23). The rate constants for the n-alkyl viologens showed a consistent trend toward larger values with increasing chain length. This can be rationalized in terms of better solvation of the product dication as the alkyl chain length increases. The substantial decrease in k$_1$ observed for isopropyl viologen is consistent with the location of the maximum unpaired spin density in the cation radical at the carbon atoms adjacent to the ring nitrogens (155). The greater steric hindrance suffered by these atoms account for the slower rate of reaction.

Rate constants obtained by Patterson et al. (27) for
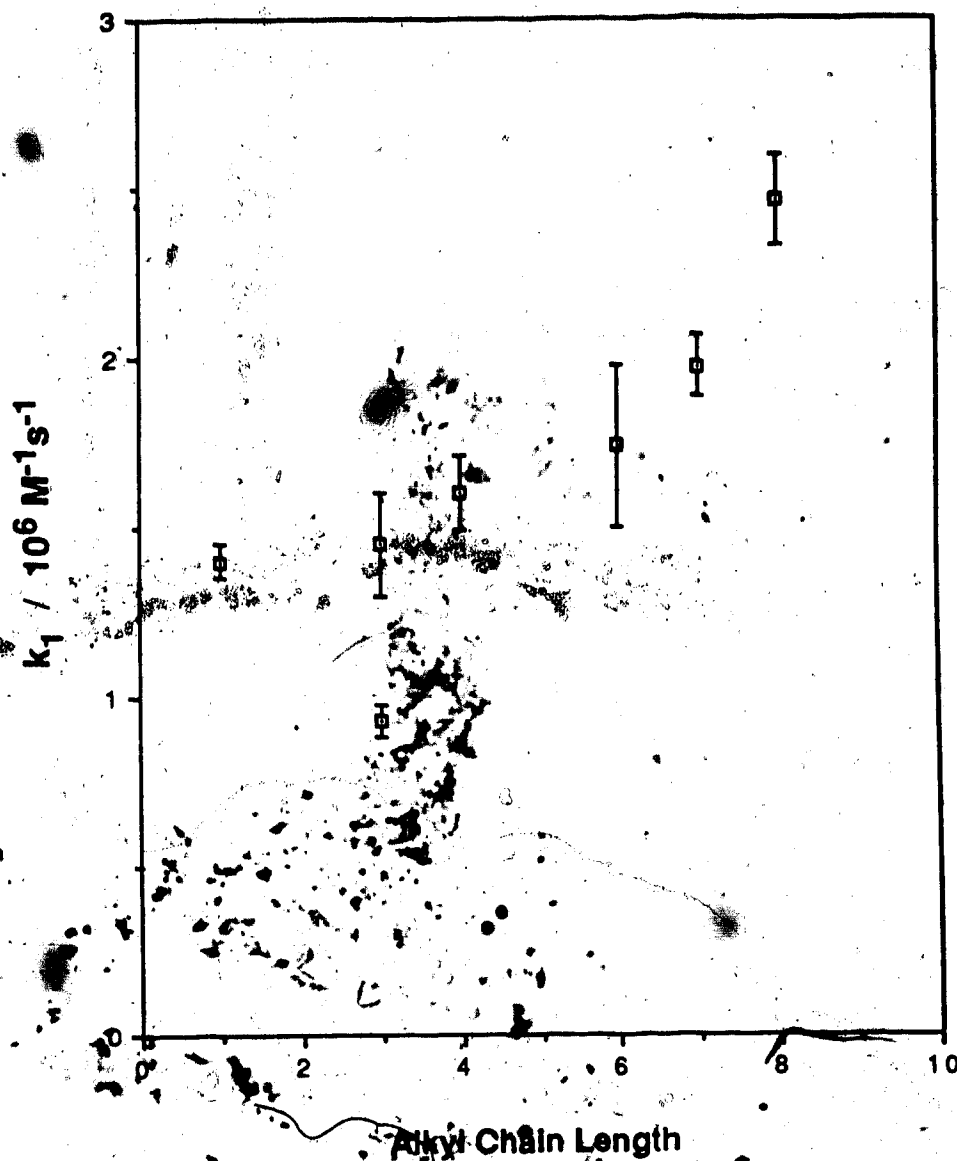
Figure 60. Rate of the Reaction of Alkyl Viologen Cation Radicals with Dioxygen in Acetonitrile as a Function of Alkyl Chain Length. The two entries at n = 3 correspond to n-propyl viologen (upper) and i-propyl viologen (lower).

the reaction of the methyl viologen cation radical with dioxygen in water and in a number of alcohols are shown in Table 44. With the exception of the value for water, the results are similar in magnitude to those found in acetonitrile and DMSO in the present work. Also shown in Table 44 are the viscosity and the dielectric constant for each of the solvents. The kinetic results resist attempts at correlation with these properties. Solvent viscosity would not be expected to directly affect the rate of electron-transfer reactions under activation control. The solvent dielectric constant has been invoked to explain the large difference between the results obtained in water and alcohols (27). No trend in the values of k_1 as a function of dielectric constant is found for the nonaqueous solvents of Table 44 however.

Finally, it is interesting to compare the results obtained in this work for rate constants and diffusion coefficients determined in acetonitrile and DMSO. From the results presented in Tables 22 and 34, the following ratios were calculated:

Compound	D_{DMSO}/D_{AN}	k_1^{DMSO}/k_1^{AN}
MeV	0.20	0.28
HeV	0.19	0.40
DiQ	0.19	0.33
O_2	0.28	—

Table 44. Rate Constants of the $MeV^{+\cdot}/O_2$ Reaction in Various Solvents at 25°C.

Solvent	η^a cP	ε^b	$k_1{}^c$ $10^6\ M^{-1}s^{-1}$
Methanol	0.543	32.6	3.3
Ethanol[f]	1.075	24.3	1.3
1-Propanol[f]	1.924	20.1	3.0
2-Propanol[f]	1.95[g]	18.3	0.87
Acetonitrile	0.343	38.8[d]	1.4[e]
Dimethylsulfoxide	1.95	45[d]	0.40[e]
Water	0.890	78.5	600

a. Viscosities from Reference 156 except where noted.

b. Dielectric constants from Reference 157 except where noted.

c. From Reference 27 except where noted.

d. From Reference 158.

e. This work.

f. Contained 5% water. Values for η and ε are for the pure solvents.

g. From Reference 159.

The viscosity ratio η_{AN}/η_{DMSO} equals 0.17. The diffusion coefficient ratios for the bipyridinium dications conform nicely to the Stokes-Einstein equation (163). That the ratio for dioxygen does not conform is likely due to its small size relative to the solvent molecules. As mentioned above, the rate constant ratio is not expected to be proportional to the viscosity ratio.

D. Correlation of the Kinetic Results with Herbicidal Activities

In one of the earliest papers on the subject, Homer et al. found a very strong correlation between the herbicidal activity of certain bipyridinium compounds and their standard reduction potentials in aqueous solution as measured by potentiometric titration with sodium dithionite (22). Their results are shown in Table 45 along with values of k_1 determined in acetonitrile (this work) and in aqueous solution (28). Herbicidal activities are given in terms of threshold concentrations, defined as the minimum concentration required to obtain a complete kill under a standardized set of experimental conditions. Threshold concentrations ranged from 1×10^{-5} to 5×10^{-3} M for the compounds studied. Correlation coefficients between the herbicidal activities and the various chemical properties are given in Table 45. The

Table 15. A Comparison of the Herbicidal Activities of Certain

Bipyridinium Compounds with Reduction Potentials and log k_1.

Compound	Aqueous Solution		Acetonitrile[c]		Herbicidal Activity	
	$-E^{o}$[a]	log k_1[b]	$-E_{1/2}$	log k_1	Mustard	Tomato
	V vs SCE		V vs SCE		-log T.C.	-log T.C.
MeV	0.69	8.90	0.45	6.15	3.52	4.12
HeV	0.65	8.56	0.44	6.09	4.00	4.46
CeV	0.67	–	0.44	6.04	–	4.04
DiQ	0.59	8.67	0.38	5.70	4.82	4.96
TriQ	0.79	8.92	0.57	6.95	2.30	2.52
r (Mustard)	+1.00	-0.73	+0.98	-0.98		
r (Tomato)	+0.98	-0.71	+0.99	-0.98		

a. Reference 22.

b. Reference 28.

c. This work.

strong correlation observed between threshold
concentrations and aqueous reduction potentials carries
over to the half-wave potentials measured in
acetonitrile. While herbicidal activities show a strong,
positive correlation with reduction potentials, they show
an equally strong, negative correlation with the values of
the rate constant k_1. Herbicidal activities are plotted
versus the logarithm of k_1 in Figure 61. Compounds whose
cation radicals reacted with dioxygen at a faster rate
were found to have larger threshold concentrations, and
therefore lower herbicidal activities. A similar negative
correlation, albeit a weaker one, was observed between
herbicidal activities and the values of k_1 measured in
water by pulse radiolysis.

The negative correlations were surprising in view of
the postulated mechanism. For the compounds studied, it
is the correlation with reduction potential that is more
significant in terms of rationalizing the observed
herbicidal activities. Using the standard reduction
potential and the threshold concentration for each
compound studied, Homer et al. employed the Nernst
equation to calculate the cation radical concentration
expected at the potential of the $NAD^+/NADH$ couple (0.38 V
vs NHE). The concentration was found to be approximately
constant (0.5 to 2.5 × 10^{-5} M) for the compounds studied
which suggests that thermodynamic factors control the
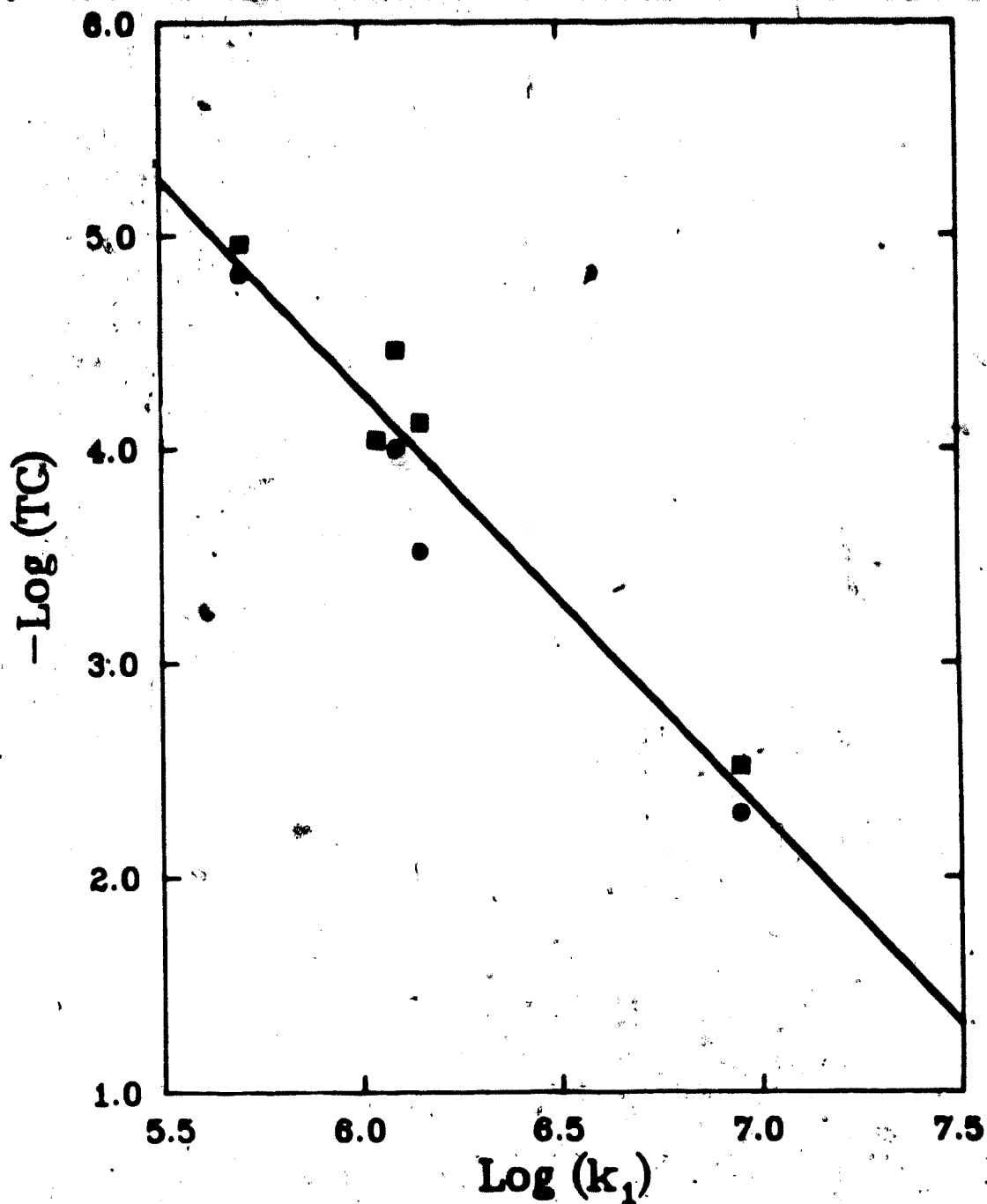
Figure 61. Comparison of the Herbicidal Activity of Bipyrid-
inium Compounds with the Reactivity of the Corre-
sponding Cation Radical Toward Dioxygen in Aceto-
nitrile. Data from Table 45. TC = threshhold
concentration (see text). ● Mustard, ■ Tomato.

herbicidal activity. Compounds whose cation radicals react more rapidly with dioxygen are also more difficult to reduce, and for the latter reason these are less toxic.

Homer et al. noted that such good results for the correlation of herbicidal activities with standard reduction potentials were not obtained in other plant species studied. (The results that were obtained for these other species were not published.) Some indication of the variability which may be encountered is given by the results of Summers for the di- and trimethylene-bridged salts of 1,10-phenanthroline (164). For diphen, the herbicidal activities (relative to diquat equals 1.0) toward linseed, buckwheat, mustard, and sugar beets were found to be 0.0, 0.0, 0.1, and 1.0 respectively. For triphen, the results were 0.1, 0.2, 0.3, and 1.0.

The positive correlation of herbicidal activities with reduction potentials holds for potentials less than or equal to that of diquat. According to White, compounds with more positive reduction potentials show decreasing herbicidal activity (23). Unfortunately there are no published data on the herbicidal activities of compounds in this potential range. In view of the relationship found to exist between half-wave potentials and log k_1, slower reaction rates can be expected at more positive potentials. While this offers a plausible explanation for the decreased activities that are reportedly observed, the

Lack of available data renders a quantitative test of this hypothesis impossible.

Data for herbicidal activities are available for the series of alkyl-substituted viologens. As mentioned previously, the half-wave potentials of these compounds in acetonitrile are virtually identical. Significant variations, however, are observed in their herbicidal activities. The results obtained by Ross et al. for duckweed (165) are plotted versus k_1 in Figure 62. A positive correlation exists but the correlation coefficient is not large (r = 0.35), and so the variation in k_1 does not account for much of the variation in observed herbicidal activities. In contrast to the half-wave potentials, the rate constant k_1 does provide a measure which is capable of some degree of discrimination among the various compounds.

Biological activities of chemical compounds are often complex functions of a number of factors and attempts to correlate such activities with any single chemical property are usually naive. Serious efforts to account for herbicidal activities need to consider a number of factors including such things as reduction potential, log k_1, solubility, and size of the molecule (166). In view of the species-to-species variability, a large amount of herbicidal data is required as well. The dearth of published information on the biological activity of
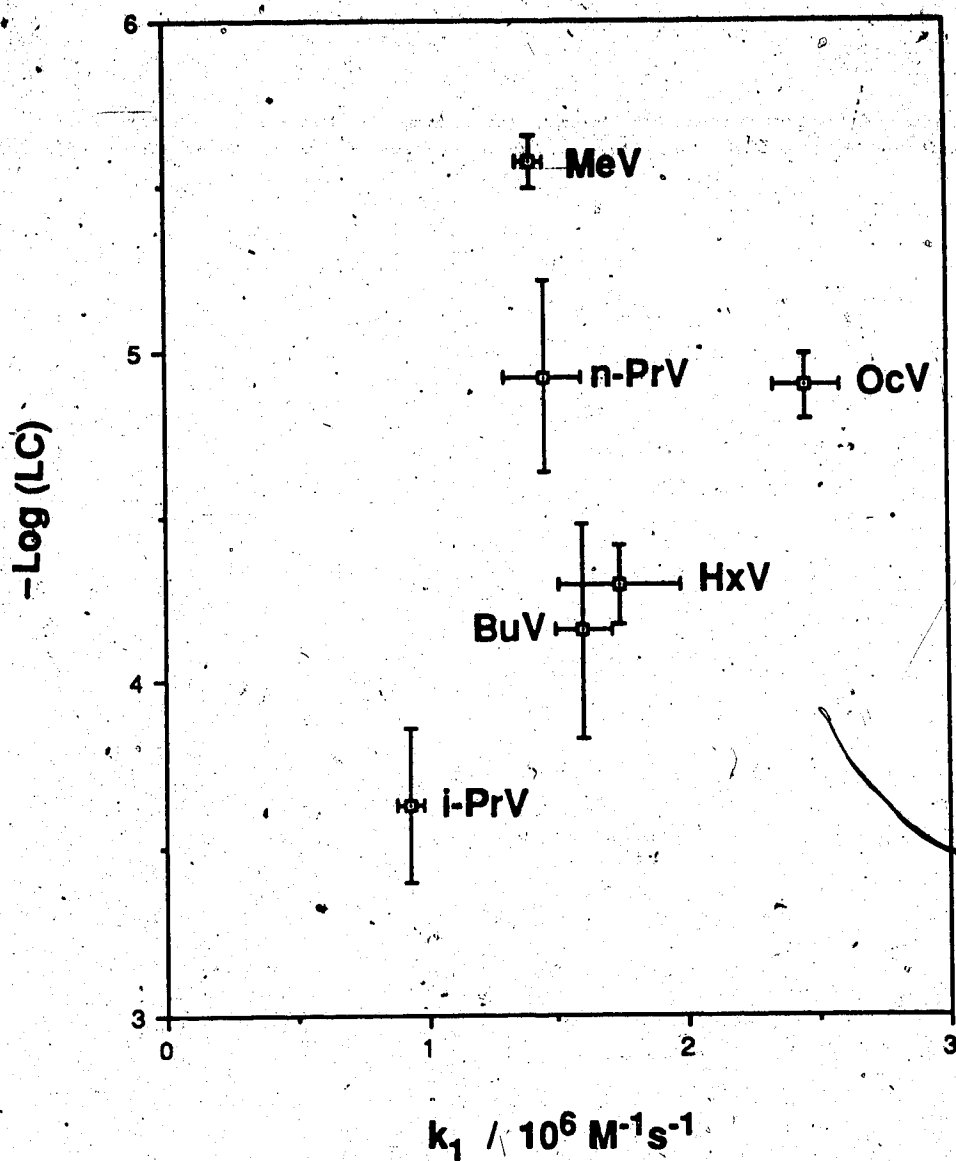
Figure 62. Comparison of the Herbicidal Activity of n-Alkyl
Viologens with the Rate of Reaction of their
Cation Radicals with Dioxygen in Acetonitrile.
Herbicidal activities from reference 165. LC =
lethal concentration (M). r = 0.35.

bipyridinium compounds is surprising in view of the considerable body of literature devoted to these compounds (-20,21). The value of the present work to the understanding of herbicidal activities lies in the demonstration that log k_1 is proportional to the half-wave potential for the bipyridinium dications. For electro-, chemically reversible bipyridinium compounds, the relationship can be expected to have predictive value, and so rate constants for such compounds can be estimated from the more easily measured half-wave potentials. The values obtained for k_1 may be of some utility in more elaborate analyses of the factors controlling the herbicidal activity of bipyridinium compounds.

CHAPTER VIII

SUMMARY AND CONCLUSIONS

Electron-transfer reactions involving dioxygen as the acceptor are of fundamental importance to life processes. Reactions of this type have been implicated in the toxic effects of a number of classes of chemical compounds. The objective of this work was to measure rate constants for the reaction of these mediators with dioxygen in solution.

In the first section, the differential equation describing the pseudo-first-order and second-order EC-catalytic mechanisms at the rotating disk electrode were solved numerically using a polynomial approximation technique. The results obtained were in good agreement with published approximate analytical solutions for various limiting cases. From currents measured at the RDE for the reduction of bipyridinium dications in the presence and absence of dioxygen, rate constants k_1 for the reaction of bipyridinium cation radicals with dioxygen in acidic acetonitrile and DMSO were determined. The numerical solution for the second-order EC-catalytic mechanism was used to relate observed currents to the rate

268

constants of the homogeneous reactions. Rate constants were obtained for the cation radicals of eighteen doubly quaternized derivatives, of 2,2' and 4,4'-bipyridine and 1,10-phenanthroline. The rate constants in acetonitrile ranged from 5×10^3 to 2×10^8 $M^{-1}s^{-1}$. The electrochemical technique proved to be well-suited to the determination of fast electron-transfer reactions involving dioxygen. Most of the information required, including dioxygen concentrations and diffusion coefficients for the reacting species, was obtained from currents measured at the RDE. From the results of the kinetic studies, the reaction rates were shown to be activation-controlled and the rate constant for the equilibrium exchange reaction of bipyridinium cation radicals and dioxygen in acetonitrile was calculated as $\log k_s^{sol}$ equals 9.8 ± 0.3.

From measurements of mass-transport-limited currents for the one- and two-electron reductions of bipyridinium dications, the diffusion coefficients of the corresponding cation radicals were determined. The calculations required the numerical solution of the differential equations describing current at the RDE for a consecutive electron transfer accompanied by a rapid, irreversible reproportionation. The diffusion coefficients of the bipyridinium cation radicals were found to be between 30

and 50 percent larger than those of the corresponding dications. For methyl viologen, this difference was confirmed by preparing a solution of the cation radical and measuring the diffusion coefficient according to the Levich equation. The estimates of the rate constants for the reaction of the cation radicals with dioxygen were increased by an average of 35 percent when the difference in the diffusion coefficients was taken into account.

The values of k_1 measured in acetonitrile were compared with published results obtained in aqueous solution by pulse radiolysis. While the order of reactivity was found to be the same in both solvents, the reactions in water were anywhere between five and one thousand times faster than the corresponding reactions in acetonitrile. Acetonitrile acted as a much more strongly differentiating solvent than did water. The rate constants measured in water spanned a factor of 40 whereas those measured for the same compounds in acetonitrile spanned four orders of magnitude. The difference was attributed to the levelling effect of diffusion processes on the observed rate constants in aqueous solution.

The results of the kinetic studies showed a strong negative correlation with published herbicidal activities measured for a number of the compounds in mustard and tomato plants. Compounds whose cation radicals react more

rapidly with dioxygen were poorer herbicides. It was concluded that for these compounds thermodynamic factors were more relevant to the herbicidal activities than were kinetic factors.

The values of k_1 measured in acetonitrile were found to be quite sensitive to changes in the nature of the substituents. Significant differences were even observed for the series of n-alkyl viologens whose substituents di███████ly one or two carbon atoms. Variations in k_1 did not account for much of the observed variation in the herbicidal activity of the alkyl viologens. The rate constants did provide a measure of discrimination among these compounds while their reduction potentials, which were virtually identical, did not.

In terms of future work, extension of the present techniques to the reaction of semiquinones with dioxygen appears promising. The relationship between observed catalytic currents and the rate of reaction of semiquinones with dioxygen is complicated by the competing process of disproportionation of the semiquinone. The excess acid required to drive the homogeneous oxidation also promotes the disproportionation. The hydroquinone produced by the disproportionation reaction is much less reactive toward dioxygen than is the semiquinone (167). Accounting for the disproportionation process in the

context of the EC-catalytic mechanism would permit kinetic
studies of a wider range of compounds including many of
those whose biological activity derives from redox
cycling.

REFERENCES

1. Kappus, H. and Sies, H., Experientia, **37**, 1233 (1981).

2. Borg, D.C. and Schaich, K.M., Israel J. Chem., **24**, 38 (1983).

3. Kappus, H., Biochem. Pharmacol., **35**, 1 (1986).

4. Lown, J.W., Acc. Chem. Res., **15**, 381 (1982).

5. Chesis, P.L., Levin, D.E., Smith, M.T., Ernster, L. and Ames, B.N., Proc. Natl. Acad. Sci., USA, **81**, 1696 (1984).

6. Smith, M.T., J. Toxicol. Environ. Health, <u>16</u>, 665 (1985).

7. Smith, M.T., Evans, C.G., Thor, H. and Orrenius, S. in "Oxidative Stress", H. Sies, ed., London: Academic Press, 1985, Ch. 5.

8. Lown, J.W., Molec. Cell. Biochem., **55**, 17 (1983).

9. Bus, J.S. and Gibson, J.E., in "Drug Metabolism and Drug Toxicity", J.R. Mitchell and M.G. Horning, eds., New York: Raven Press, 1984.

10. Clark, I.A. and Cowden, W.B., in "Oxidative Stress", H. Sies, ed., London: Academic Press, 1985, Ch. 7.

11. Lown, J.W., Chen, H.-H., Plambeck, J.A. and Acton, E.M., Biochem. Pharmacol., **31**, 575 (1982).

12. Peters, J.H., Gordon, G.R., Kashiwase, D., Lown,
    J.W., Yen, S.-F. and Plambeck, J.A., Biochem.
    Pharmacol., 35, 1309 (1986).

13. Rao, G.M., Lown, J.W. and Plambeck, J.A., J.
    Electrochem. Soc., 125, 534 (1978).

14. Rao, G.M., Lown, J.W. and Plambeck, J.A., J.
    Electrochem. Soc., 125, 540 (1978).

15. Svingen, B.A. and Powis, G., Arch. Biochem.
    Biophys., 209, 119 (1981).

16. Butler, J., Hoey, B.M. and Swallow, A.J., FEBS
    Lett., 182, 95 (1985).

17. Land, E.J., Mukherjee, T., Swallow, A.J. and Bruce,
    J.M., Br. J. Cancer, 51, 515 (1985).

18. Anne, A. and Moiroux, J., Nouv. J. Chim., 9, 83
    (1985).

19. Michaelis, L. and Hill, E.S., J. Gen. Physiol., 16,
    859 (1933).

20. Summers, L.A., "The Bipyridinium Herbicides", New
    York: Academic Press, 1980.

21. Bird, C.L. and Kuhn, A.T., Chem. Soc. Rev., 10, 49
    (1981).

22. Homer, R.F., Mees, G.C. and Tomlinson, T.E., J. Sci.
    Food Agric., 11, 309 (1960).

23. White, B.G., Proc. 10th Brit. Weed Control Conf., 3,
    997 (1971).

24. Thornely, R.N.F., Biochim. Biophys. Acta, 333, 487 (1974).

25. Evans, A.G., Dodson, N.K. and Rees, N.H., J. Chem. Soc., Perkin Trans. II, 1976, 859 (1976).

26. Evans, A.G., Alford, R.E. and Rees, N.H., J. Chem. Soc., Perkin Trans. II, 1977, 445 (1977).

27. Patterson, L.K., Small, R.D. and Scaiano, J.C., Radiat. Res., 72, 218 (1977).

28. Farrington, J.A., Ebert, M. and Land, E.J., J. Chem. Soc., Faraday Trans. L, 74, 665 (1978).

29. Rauwel, F. and Thévenot, D., J. Electroanal. Chem., 75, 579 (1977).

30. Andrieux, C.P., Hapiot, P. and Savéant, J.M., J. Electroanal. Chem., 189, 121 (1985).

31. Symons, M.C.R., Phil. Trans. R. Soc. Lond., B, 311, 451 (1985).

32. Kappus, H. in "Oxidative Stress", H. Sies, ed., London: Academic Press, 1985, Ch. 12.

33. Allen, A.O. and Bielski, B.H.J. in "Superoxide Dismutase", L. Oberley, ed., Boca Raton: CRC Press, 1982, Vol. 1, p. 125f.

34. Bielski, B.H.J., Phil. Trans. R. Soc. Lond., B, 311, 473 (1985).

35. Bielski, B.H.J. and Cabelli, D.E. in "Superoxide and Superoxide Dismutase in Chemistry, Biology and

Medicine", G. Rotilio, ed., Amsterdam: Elsevier, 1986, p. 3.

36. Walling, C., Acc. Chem. Res., 8, 125 (1975).

37. Popisil, Z., Coll. Czech. Chem. Commun., 18, 337 (1953).

38. Andrieux, C.P., Dumas-Bouchiat, J.M. and Savéant, J.M., J. Electroanal. Chem., 87, 39 (1978).

39. Zak, J. and Kuwana, T., J. Electroanal. Chem., 150, 645 (1983).

40. Kolthoff, I.M. and Parry, E.P., J. Am. Chem. Soc., 73, 3718 (1951).

41. Dimarco, D.M., Forshey, P.A. and Kuwana, T. in "Chemically Modified Surfaces in Catalysis and Electrocatalysis", ACS Symp. Ser. No. 192, Washington, D.C.: American Chemical Society, 1982, pp. 71-97.

42. Koutecky, J., Coll. Czech. Chem. Commun., 18, 311 (1953).

43. Smith, D.E., Anal. Chem., 35, 602 (1963).

44. Smith, D.E., Anal. Chem., 35, 610 (1963).

45. Bullock, K.R. and Smith, D.E., Anal. Chem., 46, 1567 (1974).

46. Haberland, D. and Landsberg, R., Ber. Bunsenges. Phys. Chem., 70, 724 (1966).

47. Brinkmann, A.A.A.M. and Los, J.M., J. Electroanal. Chem., **14**, 285 (1967).

48. Christie, J.H., J. Electroanal. Chem., **13**, 79 (1967).

49. Albery, W.J., Hitchman, M.L. and Ulstrup, J., Trans. Faraday Soc., **64**, 2831 (1968).

50. Klatt, L.N. and Blaedel, W.J., Anal. Chem., **40**, 512 (1968).

51. Winograd, N., Blount, H.N. and Kuwana, T., J. Phys. Chem., **73**, 3456 (1969).

52. Britton, W.E. and Fry, A.J., Anal. Chem., **47**, 95 (1975).

53. Dasgupta, S. and Ryan, M.D., J. Electroanal. Chem., **116**, 587 (1980).

54. Aoki, K., Tokuda, K. and Hiroaki, M., J. Electroanal. Chem., **76**, 217 (1977).

55. Lingane, P.J. and Christie, J.H., J. Electroanal. Chem., **13**, 227 (1967).

56. Kim, M.-H., and Birke, R.L., Anal. Chem., **55**, 522 (1983).

57. Fleischmann, M., Lasserre, F., Robinson, J. and Swan, D., J. Electroanal. Chem., **177**, 97 (1984).

58. Lanny Ng, S.L. and Cheh, H.Y., J. Electrochem. Soc., **132**, 93 (1985).

59. Zeng, J. and Osteryoung, R.A., Anal. Chem., **58**, 2766 (1986).

60. Hale, J.M., J. Electroanal. Chem., **8**, 332 (1964).

61. Blount, H.N., Winograd, N. and Kuwana, T., J. Phys. Chem., **74**, 3231 (1970).

62. Prater, K.B. and Bard, A.J., J. Electrochem. Soc., **117**, 1517 (1971).

63. Ryan, M.D. and Wilson, G.S., Anal. Chem., **47**, 885 (1975).

64. Ryan, M.D., Wei, J.-F., Feinberg, B.A. and Lau, Y.-K., Anal. Biochem., **96**, 326 (1979).

65. Andrieux, C.P., Dumas-Bouchiat, J.M. and Savéant, J.M., J. Electroanal. Chem., **87**, 55 (1978).

66. Andrieux, C.P., Blocman, C., Dumas-Bouchiat, J.M., M'Halla, F. and Savéant, J.M., J. Electroanal. Chem., **113**, 19 (1980).

67. Bowers, M.L. and Anson, F.C., J. Electroanal. Chem., **171**, 269 (1984).

68. Andrieux, C.P., Hapiot, P. and Savéant, J.M., J. Electroanal. Chem., **189**, 121 (1985).

69. Machado, R.M. and Chapman, T.W., J. Electrochem. Soc., **134**, 385 (1987).

70. Bowers, M.L., Anson, F.C. and Feldberg, S.W., J. Electroanal. Chem., **216**, 249 (1987).

71. Lund, H. and Simonet, J., J. Electroanal. Chem., **65**, 205 (1975).

72. Connors, T.F. and Rusling, J.F., J. Electrochem. Soc., **130**, 1120 (1983).

73. Mairanovsky, V.G., Angew. Chem., Int'l. Ed., **15**, 281 (1976).

74. Maia, H.L.S., Medeiros, M.J., Montenegro, M.I., Court, D. and Pletcher, D., J. Electroanal. Chem., **164**, 347 (1984).

75. Skinner, J.F., Glasel, A., Hsu, L. and Funt, B.L., J. Electrochem. Soc., **127**, 315 (1980).

76. Riddiford, A.C. in "Advances in Electrochemistry and Electrochemical Engineering", P. Delahay, ed., New York: Wiley Interscience, 1966, Vol. 4.

77. Opekar, F. and Beran, P., J. Electroanal. Chem., **69**, 1 (1976).

78. Filinovskii, V. Yu. and Pleskov, Yu. V. in "Comprehensive Treatise of Electrochemistry", E. Yeager et al. eds., New York: Plenum Press, 1984, Ch. 5.

79. Albery, W.J. and Hitchman, M.L., "Ring-Disk Electrodes", London: Oxford University Press, 1971.

80. Pleskov, Yu. V. and Filinoskii, V. Yu., "The Rotating Disk Electrode", New York: Consultants Bureau, 1976.

81. Levich, V.G., "Physiochemical Hydrodynamics", Englewood Cliffs, N.J.: Prentice-Hall, 1962.

82. Eddowes, M.J., J. Electroanal. Chem., **159**, 1 (1983).

83. Feldberg, S.W. in "Electroanalytical Chemistry", Vol. 3, A.J. Bard, ed., New York: Marcel Dekker, 1969.

84. Britz, D., "Digital Simulation in Electrochemistry", Berlin: Springer Verlag, 1981, p. 199.

85. Heinze, J., Angew. Chem. Int'l. Ed., **23**, 831 (1984).

86. Whiting, L.F. and Carr, P.W., J. Electroanal. Chem., **81**, 1 (1977).

87. Pons, S. in "Electroanalytical Chemistry", A.J. Bard, ed., Vol. 13, New York: Marcel Dekker, 1984, p. 115.

88. Yen, S.-C. and Chapman, T.W., J. Electrochem. Soc., **132**, 2149 (1985).

89. Matyska, B. and Duskova, D., Coll. Czech. Chem. Commun., **22**, 1747 (1957).

90. Savéant, J.M. and Vianello, E.M., Electrochim. Acta, **10**, 905 (1965).

91. Koryta, J., Coll. Czech. Chem. Commun., **20**, 1125 (1955).

92. Herrmann, J., Schmidt, H. and Vielstich, W., Z. Phys. Chem., Neue Folge, **139**, 83 (1984).

93. Andrieux, C.P., Dumas-Bouchiat, J.M., and Savéant, J.M., J. Electroanal. Chem., **113**, 1 (1980).

94. Andrieux, C.P., Blocman, C., Dumas-Bouchiat, J.M., M'Halla, F. and Savéant, J.M., J. Electroanal. Chem., **113**, 19 (1980).

95. Opekar, F. and Beran, P., J. Electroanal. Chem., **32**, 49 (1971).

96. Koutecky, J. and Levich, V.G., Zh. Fiz. Khim., **32**, 1565 (1958).

97. Villadsen, J.V. and Stewart, W.E., Chem. Eng. Sci., **22**, 1483 (1967).

98. Villadsen, J.V. and Michelsen, M.L., "Solution of Differential Equation Models by Polynomial Approximation", Englewood Cliffs, N.J.: Prentice-Hall, 1978.

99. Botha, J.F. and Pinder, G.F., "Fundamental Concepts in the Numerical Solution of Differential Equations", New York: Wiley, 1983.

100. Sparrow, E.M. and Gregg, J.L., J. Heat Transfer, **81C**, 249 (1959).

101. Gregory, D.P. and Riddiford, A.C., J. Chem. Soc., 3756 (1956).

102. Newman, J., J. Phys. Chem., **70**, 1327 (1966).

103. Feldberg, S.W., Bowers, M.L. and Anson, F.C., J. Electroanal. Chem., **215**, 11 (1986).

104. Hitchman, M.L., "Measurement of Dissolved Oxygen", New York: Wiley, 1978.

105. IUPAC Solubility Data Series, Vol. 7, "Oxygen and Ozone", R. Battino, ed., Oxford: Pergamon, 1981.

106. Baird, W.R. and Foley, R.T., J. Chem. Eng. Data, 17, 355 (1972).

107. Dymond, J.H., J. Phys. Chem., 71, 1829 (1967).

108. Battino, R., Rettich, T.R. and Tominaga, T., J. Phys. Chem. Ref. Data, 12, 163 (1983).

109. Sawyer, D.T., Chiericato, G., Angelis, C.T., Nanni, E.J. and Tsuchiya, T., Anal. Chem., 54, 1720 (1982).

110. Kolthoff, I.M. and Coetzee, J.F., J. Am. Chem. Soc., 79, 6110 (1957).

111. Butler, J.N., J. Electroanal. Chem., 14, 89 (1967).

112. Coetzee, J.F. in "Recommended Methods for Solvent Purification", J.F. Coetzee, ed., IUPAC, 1982.

113. Dimroth, O. and Heene, R., Ber., 54, 2934 (1921).

114. Bonczos, J., et al., Ger. Offen., 1,926,535 (1970); Chem. Abs. 72: 55272g (1970).

115. Nielsen, A.T., Moore, D.W., Muha, G.M. and Berry, K.H., J. Org. Chem., 29, 2175 (1964).

116. Dimroth, O. and Frister, F., Ber., 55, 3693 (1922).

117. Kazarinova, N.F., Solomko, K.A. and Kotelenets, M.N., Chem. Abs. 67: 2975d.

118. Vogel, A.I., J. Chem. Soc., 1948, 644 (1948).

119. Emmert, B. and Roh, N., Ber, **58**, 503 (1925).

120. Krumholz, P., J. Am. Chem. Soc., **73**, 3487 (1951).

121. Downes, J.E., J. Chem. Soc., **1967C**, 1491 (1967).

122. Hünig, S. and Schenk, W., Liebigs. Ann. Chem., **1979**, 727 (1979).

123. Homer, R.F. and Tomlinson, T.E., J. Chem. Soc., **1960**, 2498 (1960).

124. Hünig, S., Gross, J., Lier, E.F. and Quast, H., Liebigs. Ann. Chem., **1973**, 339 (1973).

125. Summers, L.A., Tetrahedron, **24**, 5433 (1968).

126. Armour, M.A., Browne, L.M. and Weir, G.L., "Hazardous Chemicals Information and Disposal Guide", 1982.

127. Schilt, A.A., "Perchloric Acid and Perchlorates", G. Frederick Smith Chemical Co., 1979.

128. Walter, M. and Ramaley, L., Anal. Chem., **45**, 165 (1973).

129. Kolthoff, I.M. and Coetzee, J.F., J. Am. Chem. Soc., **79**, 870 (1957).

130. Bauer, D. and Beck J.-P., J. Electroanal. Chem., **40**, 233 (1972).

131. Hoare, J.P, in "Encyclopedia of Electrochemistry of the Elements", Vol. 2, A.J. Bard, ed., New York: Marcel Dekker, 1974.

132. Schiffrin, D.J. in "Electrochemistry, A. Specialist Periodical Report", Vol. 8, D. Pletcher, ed., London: Royal Society of Chemistry, 1983.

133. Tarasevich, M.R., Sadkowski, A. and Yeager, E. in "Comprehensive Treatise of Electrochemistry", Vol. 7, B.E. Conway et al., eds., New York: Plenum Press, 1983.

134. Jain, P.S. and Lal, S., Electrochim. Acta, **27**, 759 (1982).

135. Lorenzola, T.A., Lopez, B.A. and Giordano, M.C., J. Electrochem. Soc., **130**, 1359 (1983).

136. Cofré, P. and Sawyer, D.T., Anal. Chem., **58**, 1057 (1986).

137. Johnson, E.L., Pool, K.H. and Hamm, R.E., Anal. Chem., **38**, 183 (1966).

138. Christian, S.D., Lane, E.H. and Garland, F., J. Chem. Ed., **51**, 475 (1974).

139. Christian, S.D. and Tucker, E.E., J. Chem. Ed., **61**, 788 (1984).

140. Hünig, S., Gross, J. and Schenk, W., Liebigs. Ann. Chem., **1973**, 324 (1973).

141. Hünig, S., Gross, J. Lier, E.F. and Quast, H., Liebigs. Ann. Chem., **1973**, 339 (1973).

142. Winograd, N. and Kuwana, T., J. Am. Chem. Soc., **93**, 4343 (1971).

143. Gruver, G.A. and Kuwana, T., J. Electroanal. Chem., **36**, 85 (1972).

144. Bewick, A., Serve, D. and Joslin, T.A., J. Electroanal. Chem., **154**, 81 (1983).

145. Andrieux, C.P. and Saveant, J.M., J. Electroanal. Chem., **28**, 339 (1970).

146. Ruzic, I. and Smith, D.E., J. Electroanal. Chem., **58**, 145 (1975).

147. Ruzic, I., Schwall, R.J. and Smith, D.E., Croat. Chem. Acta, **48**, 651 (1976).

148. Armstrong, N.R., Vanderborgh, N.E. and Quinn, R.K., J. Phys. Chem., **80**, 2740 (1976).

149. Eddowes, M.J. and Grätzel, M., J. Electroanal. Chem., **163**, 31 (1984).

150. Miller, S.L. and Orleman, E.F., J. Am. Chem. Soc., **75**, 2001 (1953).

151. Andrieux, C.P., Hapiot, P. and Saveant, J.M., J. Electroanal. Chem., **172**, 49 (1984).

152. Andrieux, C.P., Hapiot, P. and Saveant, J.M., J. Electroanal. Chem., **186**, 237 (1985).

153. Caban, R. and Chapman, T.W., Chem. Eng. Sci., **36**, 849 (1981) cited in reference 82.

154. Nanni, Jr., E.J., Angelis, C.T., Dickson, J. and Sawyer, D.T., J. Am. Chem. Soc., **103**, 4268 (1981).

155. Roberto, Jr., J.L. and Sawyer, D.T., Israel J.
     Chem., **23**, 430 (1983).

156. Stokes, R.H. and Mills, R., "Viscosity of
     Electrolytes and Related Properties", Oxford:
     Pergamon Press, 1965.

157. CRC Handbook of Chemistry and Physics, R.C. Weast,
     ed., 66th ed., Boca Raton, FL: CRC Press, 1985.

158. Merck Index, M. Windholz, ed., 10th ed., Rahway,
     NJ: Merck & Co., Inc., 1983.

159. International Critical Tables, E.W. Washburn, ed.,
     Vol. 7, New York: McGraw-Hill, 1930.

160. Andrieux, C.P., Blocman, C., Dumas-Bouchiat, J.M.
     and Saveant, J.M., J. Am. Chem. Soc., **101**, 3431
     (1979).

161. Kojima, H. and Bard, A.J., J. Am. Chem. Soc., **97**,
     6317 (1975).

162. Laitinen, H.A. and Harris, W.E., "Chemical
     Analysis", New York: McGraw-Hill, 1975.

163. Plambeck, J.A., "Electroanalytical Chemistry", New
     York: John Wiley, 1982.

164. Summers, L.A., Nature, **215**, 1410 (1967).

165. Ross, J.H., Lim, L.O. and Krieger, R.I., Drug Chem.
     Toxicol., **2**, 193 (1979).

166. Summers, L.A., Adv. Pestic. Sci. Plenary Lect. Symp. Pap. Int. Congr. Pestic. Chem., 4th, 1978 (Publ. 1979), 2, 244, H. Geissbuehler, ed., Oxford: Pergamon, 1979.

167. Ingraham, L.L. and Meyer, D.L., "Biochemistry of Dioxygen", New York: Plenum, 1985.

168. Hünig, S. and Schenk, W., Liebigs Ann. Chem., **1979**, 1523 (1979).

169. Van Dam, H.T. and Ponjeé, J.J., J. Electrochem. Soc., **121**, 1555 (1974).

170. Khaskin, B.A., Sablina, I.V., Melinkov, N.N., and Supin, G.S., Zh. Obshch. Khim., **42**, 2061 (1972).

171. Kawata, T., Yamamoto, M., Yamana, M., Tajima, M., and Nakano, T., Japan J. Appl. Phys., **14**, 725 (1975).

APPENDIX I

APPLICATION OF THE ORTHOGONAL COLLOCATION TECHNIQUE TO .THE

CONVECTIVE-DIFFUSION EQUATION FOR THE

ROTATING DISK ELECTRODE (RDE)

A. Introduction

This section describes the numerical approximation

technique employed to solve the differential equations

describing the pseudo-first- and second-order EC-catalytic

mechanisms at the RDE. By way of introduction to the

orthogonal collocation technique, the solution to the

differential equation describing mass-transport to the RDE

(the Levich equation) will be described in some detail.

We begin by considering an electrochemical reaction:

$$P \pm ne^- \rightleftharpoons Q \qquad\qquad [A-1]$$
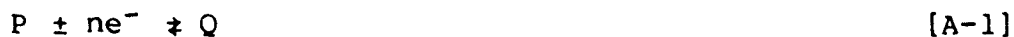
taking place at the surface of an RDE. The rate of the

reaction is assumed to be sufficiently large that the

current flow through the electrode is determined by the

rate of mass transfer from the bulk solution. The

variation of the concentration of species P with time at

any point in solution is given by (81):

$$\frac{\partial c_P}{\partial t} = D_P \frac{\partial^2 c_P}{\partial z^2} - v_z \frac{\partial c_P}{\partial z} \qquad \text{[A-2]}$$

where c_P = concentration of species P, D_P = diffusion coefficient of P, z = distance normal to the electrode, and v_z = axial velocity of the solution. The axial velocity near the electrode surface is approximated by (81):

$$v_z = -0.510 \; \omega^{3/2} \; \nu^{-1/2} \; z^2 \qquad \text{[A-3]}$$

where ω = angular velocity of the electrode and ν = kinematic viscosity. In the steady state, $\partial c / \partial t = 0$ and equation [A-2] becomes:

$$D_P \frac{d^2 c_P}{dz^2} - v_z \frac{dc_P}{dz} = 0 \qquad \text{[A-4]}$$

A similar equation can be written for the product species Q:

$$D_Q \frac{d^2 c_Q}{dz^2} - v_z \frac{dc_Q}{dz} = 0 \qquad \text{[A-5]}$$

The boundary conditions defining the problem are as follows. At z = 0:

$$D_P \left(\frac{dc_P}{dz}\right)_{z=0} + D_Q \left(\frac{dc_Q}{dz}\right)_{z=0} = 0 \qquad \text{[A-6]}$$

$$c_P(0)/c_Q(0) = \exp((nF/RT)(E^\circ - E)) \qquad \text{[A-7]}$$

At $z = \infty$: $c_P(\infty) = $ bulk concentration of P

$$c_Q(\infty) = 0$$

Equation [A-6] describes the flux balance which must exist at the electrode surface. Equation [A-7] expresses the surface concentration ratio in terms of the Nernst equation. For the mass-transport-limited case, equation [A-7] is replaced by $c_P(0) = 0$.

To endow the solution to the problem with general applicability, it is customary to redefine the problem in terms of dimensionless concentration and distance variables denoted here and throughout the body of the thesis by upper-case C and Z respectively. Concentrations are normalized with respect to the bulk concentration of P, $c_P(\infty)$:

$$C_P(z) = c_P(z)/c_P(\infty)$$

$$C_Q(z) = c_Q(z)/c_P(\infty)$$

Distance is normalized with respect to the transport boundary layer as given by Eddowes (82):

$$Z = z/z_T$$

where $z_T = 3.61 \cdot D_P^{1/3} \nu^{1/6} \omega^{-1/2}$. The interval z_T corresponds to twice the transport boundary layer thickness as defined by Levich (81). The solution to the problem is sought over the restricted interval $0 < Z < 1$.

Substituting the dimensionless variables and incorporating the expression for axial velocity transforms the equations describing the boundary value problem to:

$$\bar{D}_P \frac{d^2 C_P}{dZ^2} + 23.997 \, Z^2 \frac{dC_P}{dZ} = 0 \qquad \qquad [A-9]$$

$$\bar{D}_Q \frac{d^2 C_Q}{dZ^2} + 23.997 \, Z^2 \frac{dC_Q}{dZ} = 0 \qquad \qquad [A-10]$$

At $Z = 0$, $\bar{D}_P \frac{dC_P}{dZ} + \bar{D}_Q \frac{dC_Q}{dZ} = 0$

$$C_P(0)/C_Q(0) = \exp\{(nF/RT)(E^\circ - E)\}$$

At $Z = 1$, $C_P(1) = 1$

$$C_Q(1) = 0.$$

The dimensionless diffusion coefficients $\bar{D}_P$ and $\bar{D}_Q$ result from normalizing D_P and D_Q with respect to the larger of the two.

The solution to the above equations describes the variation of C_P and C_Q as a function of distance throughout the transport boundary layer. From the solution one can derive the familiar Levich equation describing current at the RDE.

B. Introduction to Orthogonal Collocation

Orthogonal collocation is one of a general class of approximation techniques known as methods of weighted residuals. It originated with Villadsen and Stewart (97) and has been applied to various problems in chemical engineering. The technique was introduced nto electrochemistry by Whiting and Carr (86). It has since been applied to a variety of electrochemical kinetic problems (87).

To understand the orthogonal collocation technique, consider the mass-transport equation for species P, equation [A-9]. To this ordinary differential equation in Z, we can write a trial solution in the form of a polynomial of degree N,

$$C_P(Z) = \sum_{j=0}^{N} a_j Z^j$$

valid over the interval $0 < Z < 1$. A collocation
technique results when the coefficients a_j of the trial
solution are determined by requiring that the solution fit
the differential equation at N+1 points distributed
through the interval and including the boundaries (98).

The accuracy and computational efficiency of
collocation techniques are strongly dependent on the
choice of the collocation points. Villadsen and Michelsen
have shown that an optimal collocation technique results
when the collocation points are chosen as the roots of a
set of orthogonal polynomials known as Jacobi polynomials
(98). These polynomials are defined over the interval $0 <$
$x < 1$ by the orthogonality relationship:

$$\int_0^1 x^\beta (1-x)^\alpha P_n^{(\alpha, \beta)}(x) \, P_m^{(\alpha, \beta)}(x) \, dx = 0$$

The mathematical basis of orthogonal collocation is set
forth in the book by Villadsen and Michelsen (98) and that
by Botha and Pinder (99).

C.   Transformation of the Boundary Value Problem to a Set of Linear Equations in Z

Given an orthogonal polynomial of degree N with N real roots Z_i, $i = 1$ to N, over the interval $0 < Z > 1$, we can express the solution to equation [A-9] at each of the roots as

$$C_p(Z_i) = \sum_{j=0}^{N+1} a_j (Z_i)^j \qquad [A-11]$$

Equation [A-11] is differentiated to give

$$\left. \frac{dC_p}{dZ} \right|_{Z=Z_i} = \sum_{j=1}^{N+1} j \, a_j (Z_i)^{j-1}$$

$$\left. \frac{d^2C_p}{dZ^2} \right|_{Z=Z_i} = \sum_{j=2}^{N+1} j(j-1) \, a_j (Z_j)^{j-2}$$

By substituting these expressions into [A-9] and evaluating the resulting equation at each of the N roots (known as the interior collocation points), we obtain a set of N equations in N+2 unknowns a_j, $j = 0$ to N+1. A similar set of N equations in N+2 unknowns b_j is obtained for species Q. The boundary conditions at $Z = 0$ and $Z = 1$ provide the four remaining equations required to complete the system. Thus the boundary value problem can be transformed to a set of simultaneous linear equations.

Instead of explicitly solving for the coefficients of the approximation polynomials a_i and b_i, it is usual to solve for the values of the ordinate at the collocation points, i.e. for $C_P(z_i)$ and $C_Q(z_i)$. This device simplifies formulation of the problem in cases where the solution or one of its derivatives is desired at some value(s) of Z. In the case of the RDE we are primarily interested in the flux of species P at the electrode surface and therefore wish to evaluate the quantity

$$\frac{dC_P}{dZ}\bigg|_{Z=0}$$

In general, the coefficients of the approximation polynomials are not directly of interest. Given $C_P(z_i)$ and $C_Q(z_i)$ together with the collocation points, the coefficients can be recovered, if necessary, by Lagrangian interpolation.

The spatial derivatives are expressed as a function of the concentrations at the collocation points by:

$$\frac{dC_P}{dZ}\bigg|_{Z=Z_i} = \sum_{j=0}^{N+1} A_{ij}\, C_P(z_j)$$

$$\frac{d^2 C_P}{dz^2} \Bigg|_{Z=Z_i} = \sum_{j=0}^{N+1} B_{ij} C_P(Z_j).$$

The coefficients A_{ij} and B_{ij} depend only on the degree N chosen for the orthogonal polynomial. These coefficients, along with the roots of a degree N Jacobi polynomial, are readily computed using published subroutines (87,98).

The system of simultaneous equations describing the boundary value problem in terms of the concentrations of species P and Q at the collocation points is given below. The boundary conditions at Z = 1 have been incorporated directly into the equations.

$$\sum_{j=0}^{N} (\bar{D}_P B_{ij} + 23.997\ Z_i^2 A_{ij})\ C_P(Z_j) =$$

$$- (\bar{D}_P B_{ij} + 23.997\ Z_i^2 A_{i,N+1}) \qquad\qquad [A-12]$$

$$\sum_{j=0}^{N} (\bar{D}_Q B_{ij} + 23.997\ Z_i^2 A_{ij})\ C_Q(Z_j) = 0 \qquad\qquad [A-13]$$

for i = 1 to N.

The boundary conditions at Z = 0 are

$$\sum_{j=0}^{N} A_{0,j}(\bar{D}_P\, C_P(Z_j) + \bar{D}_Q\, C_Q(Z_j)) = -\vec{D}_P A_{0,N+1}$$

$$C_P(0)/C_Q(0) = \exp\{(nF/RT)(E^\circ - E)\}$$

For the mass-transport-limited case, the ratio $C_P(0)/C_Q(0)$ is set to some arbitrarily small value such as 10^{-6}.

D. Solving for the Levich Equation

The program LEVICH was written to generate and solve the preceding system of equations. A listing of the program together with details concerning the implementation appears in Appendix II. The results obtained for concentrations at the collocation points are shown in Table A-1.

Current flow through an electrode is described by a combination of Fick's first law of diffusion and Faraday's law as

$$i = nFAD\,\frac{dc_P}{dz}\Big|_{z=0} \tag{A-14}$$

Table A-1. Concentrations at the Collocation Points for the Mass-
Transport-Limited Current at the RDE.

z	c_P	c_Q
0.000	1.000×10^{-6}	1.000
1.986×10^{-2}	4.448×10^{-2}	9.555×10^{-1}
1.017×10^{-1}	2.272×10^{-1}	7.728×10^{-1}
2.372×10^{-1}	5.176×10^{-1}	4.824×10^{-1}
4.083×10^{-1}	8.071×10^{-1}	1.929×10^{-1}
5.917×10^{-1}	9.607×10^{-1}	3.925×10^{-2}
7.628×10^{-1}	9.960×10^{-1}	3.984×10^{-3}
8.983×10^{-1}	9.997×10^{-1}	2.709×10^{-4}
9.801×10^{-1}	1.000	1.022×10^{-5}
1.000	1.000	0.000

Results obtained with $N = 8$, $D_P = D_Q$, $D/v = 0$, and $C_P(0)/C_Q(0) = 10^{-6}$.

The normalized concentration gradient at the electrode surface is calculated from the values for the concentration of P at the collocation points as

$$\frac{dC_P}{dz}\bigg|_{z=0} = \sum_{j=0}^{N+1} A_{0,j}\, C_P(z_j) \qquad\qquad [A-15]$$

Equation [A-14] is transformed into the Levich equation by recognizing that

$$\frac{dc_P}{dz}\bigg|_{z=0} = \frac{c_P(\infty)}{z_T}\,\frac{dC_P}{dz}\bigg|_{z=0} \qquad\qquad [A-16]$$

Substituting [A-16] into [A-14] and including the expression for z_T gives

$$i = \left[0.27704\,\frac{dC_P}{dz}\bigg|_{z=0}\right] nFAD^{2/3}\, v^{-1/6}\, \omega^{1/2}\, c_P(\infty)$$

The quantity in square brackets corresponds to the constant in the Levich equation. Results obtained by orthogonal collocation as a function of N are given in Table A-2. They are in good agreement with Levich's value of 0.62 for N > 4. For N > 8 the results are in excellent agreement with the value 0.62048 obtained by Sparrow and

Table A-2. The Levich Constant as a Function of the Degree of the

Approximation Polynomial.

N	Levich Constant
2	0.584824
4	0.622849
6	0.620373
8	0.620471
10	0.620467
12	0.620467

Gregg who used numerical integration to solve the
analogous heat transfer problem (100).

As mentioned above, the coefficients of the
approximation polynomials are easily calculated. The
coefficients for the N = 8 solution are given in Table
A-3. The coefficients were used to generate the
concentration profiles for species P and Q shown in Figure
A-1.

E. A Refinement to the Calculation - The Extended Axial
    Velocity Equation

The expression for axial velocity given by equation
[A-3] is an approximation valid only very near the
electrode surface, that is for $z < 1$. It is the first
term of the Cochrane equation, a power series describing
axial flow toward a rotating disk as a function of
distance normal to the disk (76,81). Riddiford has
pointed out that higher terms make a significant
contribution (76,101). An extended axial velocity
equation with coefficients as cited in reference 76 is
given by

$$v_z = -(\omega v)^{1/2}[0.51023\ (\tfrac{\omega}{v})z^2 - \tfrac{1}{3}\ (\tfrac{\omega}{v})^{3/2}z^3$$

Table A-3. Coefficients of the Approximation Polynomials for the Mass-Transport-Limited Case. Results obtained by orthogonal collocation with N = 8.

Degree	Species P	Species Q
0	1.0000×10^{-7}	1.0000
1	2.2396	-2.2396
2	7.0733×10^{-2}	-7.0734×10^{-2}
3	-1.6764	1.6764
4	9.5961	-9.5961
5	-5.6848×10^{1}	5.6848×10^{1}
6	1.2053×10^{2}	-1.2053×10^{2}
7	-1.1950×10^{2}	1.1950×10^{2}
8	5.7454×10^{1}	-5.7454×10^{1}
9	-1.0870×10^{1}	1.0870×10^{1}
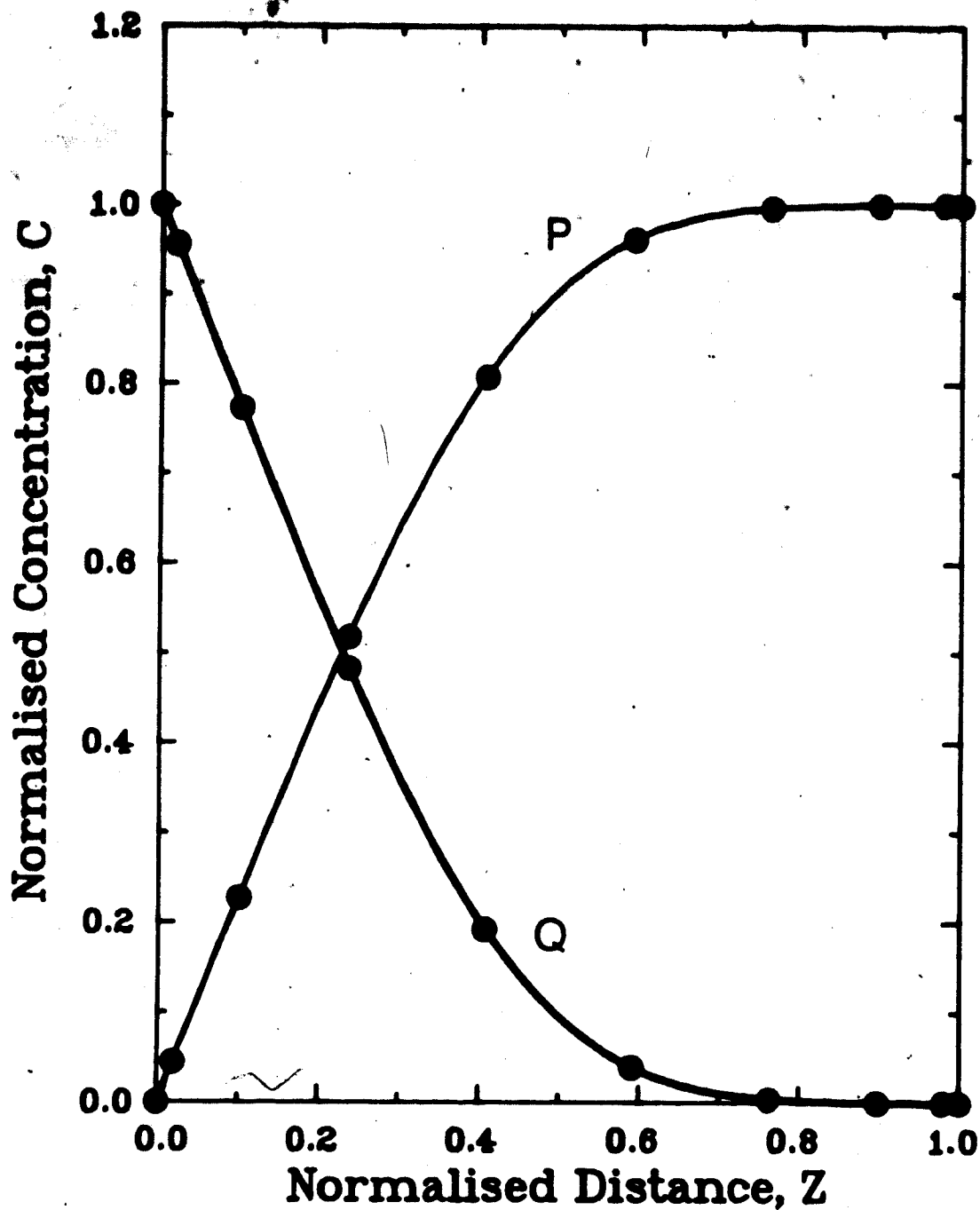
Figure A-1. Concentration Profiles for the Mass-Transport-Limited Current at the Rotating Disk Electrode. For the electrode reaction $P \pm ne^- \rightleftharpoons Q$ with $D_P = D_Q$. The circles locate the collocation points for $N = 8$.

$$+ \frac{0.61592}{6} \left(\frac{\omega}{\nu}\right)^2 z^4] \qquad\qquad (A-17)$$

Normalizing this equation and using it in place of (A-3) in the derivation of (A-9) gives

$$\bar{D}_P \frac{d^2 C_P}{dz^2} - 47.030[-0.51023 + 1.2032 \ Sc^{-1/3}z$$

$$- 1.3375 \ Sc^{-2/3}z^2]z^2 \frac{dC_P}{dz} = 0.$$

Use of the extended equation introduces an additional parameter, the Schmidt number Sc which is defined as Sc = ν/D_P. Values of Sc are generally in the range 50 to 2000 for aqueous and non-aqueous electrolytes. Use of only the first term of equation (A-17) is equivalent to assuming Sc = ∞.

The constant in the Levich equation C_L depends to a modest extent on the value of Sc. Gregory and Riddiford employed graphical integration to determine the dependence and expressed their results as (101):

$$C_L = 0.554/(0.8934 + 0.316 \ Sc^{-0.36}).$$

A decade later, Newman solved the problem analytially (102):

$$C_L = 0.62048/(1 + 0.2980\ Sc^{-1/3} + 0.14514\ Sc^{-2/3})$$

The extended axial velocity equation was included in the program LEVICH and C_L was determined as a function of Sc. The results are shown in Table A-4 along with values calculated using the above two equations. Agreement is excellent throughout. The collocation results are in especially good agreement with Newman's equation. Table A-4 also shows results obtained from a recent explicit finite-difference solution of the transient response of the RDE (103). This program accommodated the first 95 terms of the Cochrane equation, the number apparently required for convergence to 1 part in 10^6 for Sc ~ 10. Results for more realistic values of Sc, such as those shown in Table A-3, were obtained with 8 terms. The concern with additional terms beyond the third is probably warranted in view of the variability associated with the finite difference results.

While additional terms are easily incorporated in numerical solutions, those beyond the first contribute little of value to the overall result. Figure A-2 shows axial velocity as a function of distance Z calculated using equation [A-3] and equation [A-17] with Sc = 1000. Neglect of the higher terms leads to a substantial

Table A-4. The Levich Constant as a Function of the Schmidt Number Sc.

Sc	Collocation[a]	Finite Difference[b]	Newman[c]	Riddiford[d]
100	0.57961	0.57912-0.57925	0.57938	0.58095
500	0.59675	-	0.59670	0.59754
1000	0.60171	0.60181-0.60195	0.60168	0.60238
∞	0.62047	0.62065-0.62091	0.62048	0.62010

a. This work. $N = 8$, $D_P = D_Q$.

b. Reference 103. Exact value obtained depends on time and distance intervals used for the numerical approximation.

c. Reference 102. Analytical solution.

d. Reference 101. Graphical integration.
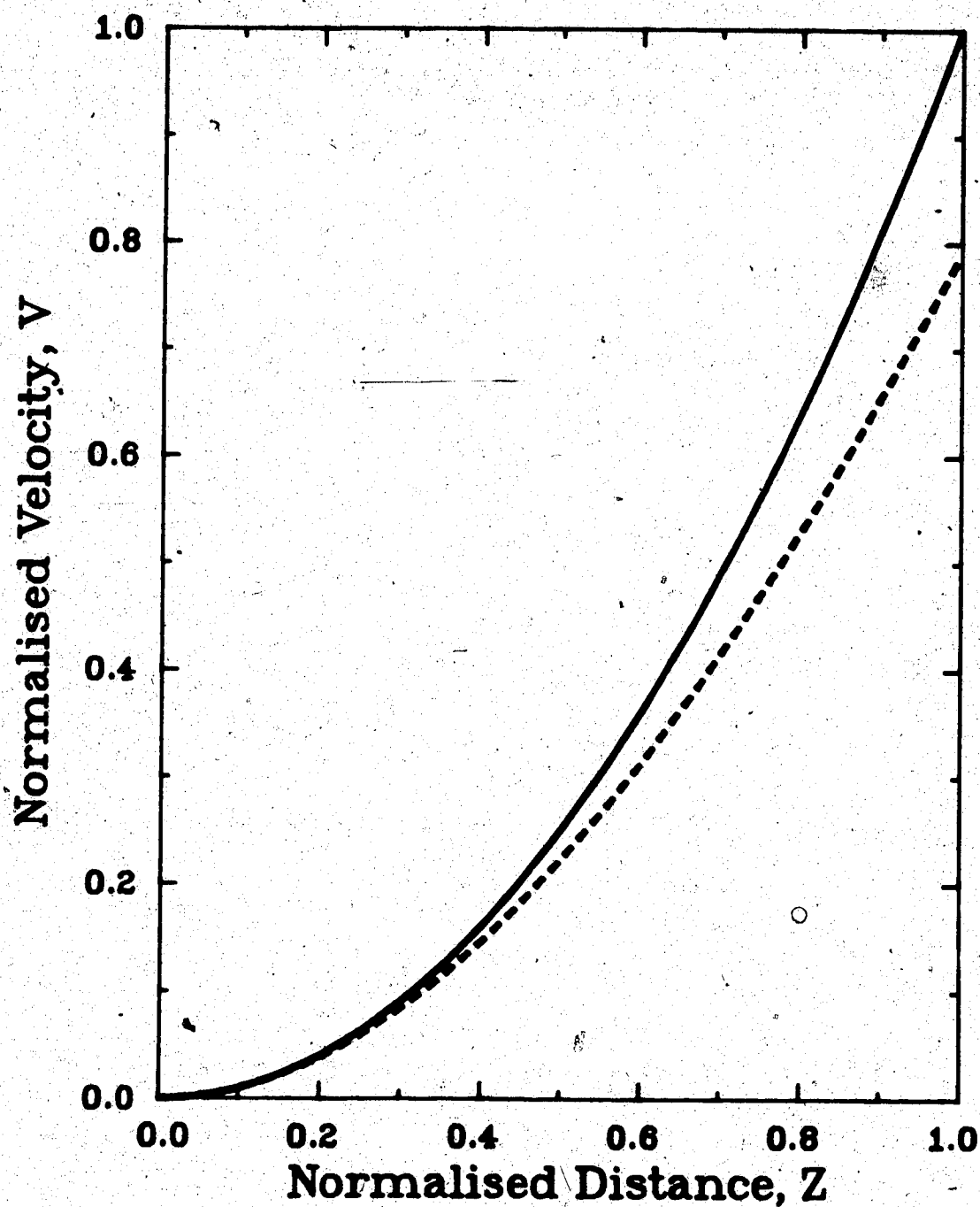
Figure A-2. Simple and Extended Axial Velocity Equations.
_____ Equation [A-3] (Simple); _ _ _ _ _
Equation [A-17] (Extended). Velocities have
been normalized with respect to equation [A-3].

overestimate of v_z for $Z > 0.5$. The error introduced into
the convection term in equation [A-9] is quite minor since
dC/dZ approaches zero in this region (see Figure A-1).
Levich has pointed out that neglect of the second and
higher terms of the Cochrane equation may be a virtue in
that it tends to compensate for the neglect of electrode
edge effects in the formulation of the problem (81).
Inclusion of higher terms is probably only justifiable if
edge effects are considered as well.

In the case of the EC-catalytic mechanism, the higher
terms are of even less import. The effect of the
homogeneous reaction is to increase the concentration
gradients near the electrode surface and thus to extend
the region over which dC/dZ is approximately zero. Due to
the parabolic dependence of v_z on Z, the entire convective
term becomes quite negligible. This is the basis of
Savéant's approximate numerical solution for the second-
order EC-catalytic mechanism (93) as discussed in Chapter
III.

APPENDIX II
PROGRAM LISTINGS

Included in this appendix are the programs and subroutines used to implement the numerical solutions to the boundary value problems discussed in Chapters III and VI and Appendix I. The programs were written in PDP-11 FORTRAN IV (Digital Equipment Corporation (DEC), Maynard, MA). They include:

Program Name	Function
LEVICH	Solution for the mass-transport-limited current at the RDE.
RDECR1	Solution for the psuedo-first-order EC-catalytic mechanism at the RDE.
ECR1WC	Working curves for the same.
RDECR2	Solution for the second-order EC-catalytic mechanism at the RDE.
ECR2WC	Working curves for the same.
RDECR3	Numerical solution for the second-order EC-catalytic mechanism at the RDE for large $\bar{k}\gamma$ (using the spline technique).
ECR3WC	Working curves for the same.
CETRP2	Consecutive electron-transfer with reproportionation.

The program listings are followed by listings of the
subroutines contained in the library file DGSPLB.OBJ. Not
included are listings of the subroutines contained in the
library file MATLIB.OBJ. These subroutines implement
standard mathematical operations and were taken from the
PDP-11 FORTRAN IV Scientific Subroutines Package. (Source
code for the same subroutines is publicly available as
part of the IBM Scientific Subroutines Package.)
Concerning PDP-11 FORTRAN IV, the only decidedly non-
standard feature is the $ format descriptor which is used
to suppress the carriage return character at the end of an
output record.

Programs were compiled and executed under the RT-11
SJ (V02-02C) operating system on a DEC PDP-11/03
minicomputer with 64 kbyte of memory and equipped with a
KEV11 Extended Arithmetic Chip. As a benchmark for
comparing execution times given in the body of the thesis
with those which can be expected on other machines, the
following values were recorded for the time required to
invert single precision matrices:

Dimension	Execution Time (s)
10 × 10	1.6
15 × 15	4.6
20 × 20	9.8
30 × 30	31.8
40 × 40	73.3

The matrix inversions were performed on matrices filled with randomly generated numbers using subroutine MINV of the Scientific Subroutines Package. This subroutine uses the Gauss-Jordan method with full row and column pivoting and it also calculates the determinant.

Concerning the use of the programs which follow, satisfactory results in terms of both accuracy and execution time were obtained for the EC-catalytic mechanism using collocation polynomials of degree 8 and a convergence criterion of 1×10^{-8}. The only exceptions to this rule occurred for the spline programs RDECR3 and ECR3WC. For large values of $\bar{k}_\gamma$ (greater than approximately 1000), the program occasionally failed to converge to 1 part in 10^8 and so a convergence criterion of 1×10^{-7} was used instead. Diffusion coefficients are normalized within the program and so may be entered in either dimensioned or dimensionless form.

Listings of two utility programs are also included in this appendix. The program KPRCAL uses Lagrangian interpolation to calculate kinetic parameters given a tabulated working curve and the appropriate experimentally measured currents. The program CONPRO uses Lagrangian interpolation to recover the coefficients of the approximation polynomials given a list of the

concentrations at the collocation points. The

approximation polynomials are then used to generate

concentration profiles over any desired interval.

```
C
C
C      Title:  Mass-Transport-Limited Current to the RDE.
C              Numerical Solution by Orthogonal Collocation.
C
C      Author:  J. Nolan                         Date:  03-Dec-86
C
C      Source File:  LEVICH.SNG       Object File:  LEVICH.SOB
C
       PROGRAM LEVICH
C
C      Purpose:
C
C          This program uses orthogonal collocation to obtain
C      the steady-state solution to the differential equations
C      describing mass transport to the RDE. Formulation of the
C      boundary value problem is based on Eddowes' treatment
C      (J. Electroanal Chem., Vol. 159, p.1, 1983).  Implementation
C      mentation of the orthogonal collocation technique follows
C      J. Villadsen and M.L. Michelsen, "Solution of Differential
C      Equation Models by Polynomial Approximation", Englewood
C      Cliffs, N.J.: Prentice-Hall, Inc., 1978.
C
C      Modifications:
C
C      1.  Included date and version number on printout (V01-B,
C          28-Jun-88).
C
C      External References:
C
C           Fn/Sr              Src File        Obj File
C
C      Subroutine GENAB        GENAB.SNG       DGSPLB.OBJ
C      Subroutine RDECDE       RDECDE.SNG      DGSPLB.OBJ
C      Subroutine CONSL1       CONSL1.SNG      DGSPLB.OBJ
C      Subroutine CSCGP        CSCGP.SNG       DGSPLB.OBJ
C      Subroutine DATE         N/A             FORLIB.OBJ
C
C      Variable Declarations:
C
       IMPLICIT REAL*4 (A-H,O-Z)
       LOGICAL*1 DATARR(9)
       DIMENSION ROOTS(20),CONCS(36),AMAT(20,20),BMAT(20,20),
     &           BOUND(36),CMAT(36,36)
       EQUIVALENCE (CONCS(1),BOUND(1))
C
C          Input:
C
C          N - Order of the collocation polynomial (N<=18).
C          NR - Number of simultaneous equations (=2*N).
C          DBARP - Normalized diffusion coefficient of species P.
C          DBARQ - Normalized diffusion coefficient of species Q.
C          DVRAT - Ratio of the larger diffusion coefficient to
C               the kinematic viscosity (=1/Sc).
C          CRATIO - Concentration ratio (P/Q) at Z = 0.
C
C          Output:
C
C          DATARR - System date (DD-MMM-YY).
C          ROOTS - Roots of the collocation polynomial.
C          AMAT,BMAT - Discretization matrices containing the
```

```
C              coefficients for the first and second derivatives
C              of the concentration profile.
C        CMAT - Matrix containing the system of simultaneous
C              equations generated.
C        BOUND - Vector containing the boundary conditions.
C        CONCS - Vector containing the concentrations at the
C              collocation points. (Equivalence'd to BOUND.)
C        CPO,CQO - Surface concentrations of species P and Q
C              respectively.
C        GRAD - Surface concentration gradient.
C        CLEV- Levich constant.
C
C     Logical Units Referenced:
C
C        5 = Terminal Input
C        7 = Terminal Output
C
C     Data Statements:
C
      DATA CTBL /3.609614/
      ND=20
      NE=36
C
C        ND=20 corresponds to the derivative array dimensions.
C        NE=36 corresponds to the simultaneous equation array
C              dimensions.
C
C     Executable Code
C
C     Print header and prompt for degree of collocation polynomial.
C
      CALL DATE(DATARR)
C
      WRITE(7,100) (DATARR(I),I=1,9)
      WRITE(7,110)
      READ(5,200) N
      NR=2*N
C
C     Prompt for transport parameters.
C
   10 WRITE(7,120)
      READ(5,210) DP
      WRITE(7,125)
      READ(5,210) DQ
      WRITE(7,130)
      READ(5,210) DVRAT
      WRITE(7,140)
      READ(5,210) CRATIO
C
C     Normalize diffusion coefficients with respect to the
C     larger of the two.
C
      DBARP=1.
      DBARQ=DQ/DP
      IF(DQ.LE.DP) GOTO 20
          DBARP=1./DBARQ
          DBARQ=1.
C
C     Evaluate coefficients of discretization matrices A and B.
C
```

```
 20   CALL GENAB(N,ND,ROOTS,AMAT,BMAT)
C
C       Generate matrix of simultaneous equations for the concen-
C       trations of species P and Q at the collocation points.
C
      CALL RDECDE(N,ND,NE,ROOTS,AMAT,BMAT,DVRAT,DBARP,DBARQ,
     &             CRATIO,CTBL,CMAT,BOUND)
C
C       Solve for concentrations at the collocation points.
C
      CALL CONSL1(N,NE,NR,CMAT,CONCS)
C
C       Calculate concentration gradient of species P at Z = 0.
C
      CALL CSCGP(N,ND,NE,DBARP,DBARQ,CRATIO,AMAT,CONCS,CPO,GRAD)
C
C
C       Print out collocation points and corresponding concentrations.
C
      WRITE(7,150)
      CQO=CPO/CRATIO
      WRITE(7,160) 0.,CPO,CQO
      WRITE(7,160) (ROOTS(I+1),CONCS(I),CONCS(I+N), I=1,N)
      WRITE(7,160) 1.,1.,0.
C
      CLEV=1./3.
      CLEV=DBARP**CLEV
      CLEV=CLEV/CTBL
      CLEV=CLEV*GRAD
C
      WRITE(7,170) GRAD
      WRITE(7,180) CLEV
C
C       Loop to repeat for set of values.
C
      WRITE(7,190)
      READ(5,220) ILOOP
      IF (ILOOP .EQ. 0) GOTO 30
          WRITE(7,100) (DATARR(I),I=1,9)
          GOTO 10
 30   CONTINUE
      STOP
C
C       Format Statements
C
 100  FORMAT('0',13X,'***Mass-Transport-Limited Current at the RDE
     &***',/,/,15X,'Numerical Solution by Orthogonal Collocation',
     &/,/,' Version V01-B',50X,9A1,/)
 110  FORMAT(' ','Enter degree of collocation polynomial (I2).  ',$)
 120  FORMAT(' ','Enter diffusion coefficient for species P.  ',$)
 125  FORMAT(' ','Enter diffusion coefficient for species Q.  ',$)
 130  FORMAT(' ','Enter D/v ratio.  ',$)
 140  FORMAT(' ','Enter value of surface concentration ratio.  ',$)
 150  FORMAT('0','Concentration Profile at the Collocation Points',
     &/,/,8X,'Z',12X,'Conc. P',9X,'Conc. Q',/,/)
 160  FORMAT(3(1PE15.6,1X),/)
 170  FORMAT('0','Concentration Gradient at the Disk Surface:  ',
     &1PE15.6)
 180  FORMAT('0','Levich Constant:  ',1PE15.6,/)
 190  FORMAT('0','Enter 1 to repeat, 0 to terminate.  ',$)
```

```
200 FORMAT(12)
210 FORMAT(G15.8)
220 FORMAT(I1)  .

C      END
```

```
C
C
C      Title:   Pseudo-First-Order EC-Catalytic Mechanism at the RDE.
C                  Numerical Solution by Orthogonal Collocation.
C
C      Author:   J. Nolan                      Date:   15-Dec-86
C
C      Source File:  RDECR1.SNG      Object File:   RDECR1.SOB
C
       PROGRAM RDECR1
C
C      Purpose:
C
C           This program uses orthogonal collocation to obtain
C      the solution to the differential equations describing the
C      pseudo-first-order EC-catalytic mechanism at the rotating
C      disk electrode.  Formulation of the boundary value problem
C      is based on Eddowes' treatment of the mass-transport- limited
C      case (J. Electroanal Chem., Vol. 159, p.1, 1983).  Imple-
C      mentation of the orthogonal collocation technique follows
C      J. Villadsen and M.L. Michelsen, "Solution of Differential
C      Equation Models by Polynomial Approximation", Englewood
C      Cliffs, N.J.: Prentice-Hall, Inc., 1978.
C           The program returns the concentration profiles of the
C      catalyst species P and Q as well as the dimensionless current
C      ratio R normalized to the case where k equals zero.  It
C      incorporates the extended axial velocity equation and prov-
C      ision is made for inequalities in the diffusion coefficients
C      of P and Q.
C
C      Modifications:
C
C      1.   Included date and version number on printout. (V01-B,
C           28-Jun-87)
C      2.   Input parameters and calculated results sent to file
C           attached to L. U. 4. (V01-C, 15-Sept-87)
C
C      External References:
C
C           Fn/Sr           Src File          Obj File
C
C      Subroutine GENAB      GENAB.SNG         DGSPLB.OBJ
C      Subroutine RDECDE     RDECDE.SNG        DGSPLB.OBJ
C      Subroutine CONSL1     CONSL1.SNG        DGSPLB.OBJ
C      Subroutine CSCGP      CSCGP.SNG         DGSPLB.OBJ
C      Subroutine DATE       N/A               FORLIB.OBJ
C      Function AMAX1        N/A               FORLIB.OBJ
C
C      Variable Declarations:
C
       IMPLICIT REAL*4 (A-H,O-Z)
       LOGICAL*1 DATARR(9)
       DIMENSION ROOTS(26),CONCS(48),AMAT(26,26),BMAT(26,26),
      &          BOUND(48),CMAT(48,48)
       EQUIVALENCE (CONCS(1),BOUND(1))
C
C      Input:
C
C      N - Order of the collocation polynomial (N<=24).
C      NR - Number of simultaneous equations (=2*N).
C      DBARP - Normalized diffusion coefficient of species P.
```

```
C          DBARQ - Normalized diffusion coefficient of species
C          DVRAT - Ratio of the larger diffusion coefficient to
C                  the kinematic viscosity (=1/Sc).
C          CRATIO - Concentration ratio (P/Q) at Z = 0 (
C                  at 1.E-06).
C          PARKIN - Kinetic parameter.
C          CTBL - Transport boundary layer coefficient
C
C          Output:
C
C          DATARR - System date (DD-MMM-
C          ROOTS - Roots of the collocation polynomial.
C          AMAT,BMAT - Discretization matrices containing the
C                  coefficients for the first and second derivatives
C                  of the concentration profile.
C          CMAT - Matrix containing the system of simultaneous
C                  equations generated.
C          BOUND - Vector containing boundary conditions.
C          CONCS - Vector containing concentrations at the
C                  collocation points. (Equivalence'd to BOUND.)
C          CP0,CQ0 - Surface concentrations of species P and Q
C                  respectively.
C          GRAD0 - Surface concentration gradient for PARKIN = 0.
C          GRATIO - Surface concentration ratio normalised to
C                  GRAD0.
C
C          Logical Units Referenced:
C
C          4 = File Output
C          5 = Terminal Input
C          7 = Terminal Output
C
C          Data Statements:
C
      DATA CRATIO,CTBL0 /1.E-06,3.609
      ND=26
      NE=48
C
C          ND=26 corresponds to the derivative array dimensions.
C          NE=48 corresponds to the simultaneous equation array
C                  dimensions.
C
C          Executable Code
C
C          Print header and prompt for degree of collocation polynomial.
C
      CALL DATE(DATARR)
      WRITE(7,100) (DATARR(I),I=1,9)
      WRITE(4,100) (DATARR(I),I=1,9)
C
      WRITE(7,110)
      READ(5,200) N
      NR=2*N
C
C          Prompt for transport parameters.
C
      WRITE(7,120)
      READ(5,210) DP
      WRITE(7,125)
      READ(5,210) DQ
```

```
      WRITE(7,130)
      READ(5,210) DVRAT
C
C     Echo input parameters on L.U. 4.
C
      WRITE(4,110)
      WRITE(4,230) N
      WRITE(4,120)
      WRITE(4,240) DP
      WRITE(4,125)
      WRITE(4,240) DQ
      WRITE(4,130)
      WRITE(4,240) DVRAT
C
C     Normalize diffusion coefficients with respect to the
C     larger of the two.
C
      DMAX=AMAX1(DP,DQ)
      DBARP=DP/DMAX
      DBARQ=DQ/DMAX
C
C     Evaluate coefficients of discretization matrices A and B.
C
    5 CALL GENAB(N,ND,ROOTS,AMAT,BMAT)
C
C     Initialize loop flag.  PARKIN = 0 for first time through
C     in order to calculate GRAD0.
C
      II=1
      PARKIN=0.
      CTBL=CTBL0
      GOTO 20
C
C     Prompt for the kinetic parameter and transport-boundary-
C     layer coefficient.  (Skip on first pass.)
C
   10 WRITE(7,135)
      READ(5,210) PARKIN
      WRITE(7,140)
      READ(5,210) CTBL
      IF(CTBL.LE.0.) CTBL=CTBL0
C
      WRITE(4,135)
      WRITE(4,240) PARKIN
      WRITE(4,140)
      WRITE(4,240) CTBL
C
C     Generate matrix of simultaneous equations for the concen-
C     trations of species P and Q at the collocation points.
C
   20 CALL RDECDE(N,ND,NE,ROOTS,AMAT,BMAT,DVRAT,DBARP,DBARQ,
     &            CRATIO,CTBL,CMAT,BOUND)
C
C     Include the kinetic term in the system of equations.
C
      TERM=PARKIN*CTBL**2
C
      DO 30 I=1,N
         IN=I+N
         CMAT(I,IN)=CMAT(I,IN)+(TERM/DBARP)
```

```
          CMAT(IN,IN)=CMAT(IN,IN)-(TERM/DBARQ)
 30   CONTINUE
C
C     Solve for concentrations at the collocation points.
C
      CALL CONSL1(N,NE,NR,CMAT,CONCS)
C
C     Calculate concentration gradient of species P at Z = 0.
C
      CALL CSCGP(N,ND,NE,DBARP,DBARQ,CRATIO,AMAT,CONCS,CPO,GRAD)
C
C     Clear loop flag and set GRADO on first pass.
C
      IF (I1 .EQ. 0) GOTO 40
         GRADO=GRAD
         I1=0
         GOTO 10
C
C     Print out collocation points and corresponding concentrations.
C
 40   WRITE(7,150)
      CQO=CPO/CRATIO
      WRITE(7,160) 0.,CPO,CQO
      WRITE(7,160) (ROOTS(I+1),CONCS(I),CONCS(I+N), I=1,N)
      WRITE(7,160) 1.,1.,0.
C
      GRATIO=GRADO/GRAD*CTBL/CTBLO
C
      WRITE(7,170) GRAD
      WRITE(7,180) GRATIO
C
C     Echo on L.U. 4.
C
      WRITE(4,150)
      WRITE(4,160) 0.,CPO,CQO
      WRITE(4,160) (ROOTS(I+1),CONCS(I),CONCS(I+N), I=1,N)
      WRITE(4,160) 1.,1.,0.
      WRITE(4,170) GRAD
      WRITE(4,180) GRATIO
C
C     Loop to repeat for next value of PARKIN.
C
      WRITE(7,190)
      READ(5,220) ILOOP
      IF (ILOOP .EQ. 0) GOTO 60
         GOTO 10
 60   CONTINUE
      STOP
C
C     Format Statements
C
 100  FORMAT('0',13X,'***Pseudo-First-Order EC Catalytic Mechanism
     &***',/,23X,'at the Rotating Disk Electrode',/,/,16X,
     &'Numerical Solution by Orthogonal Collocation',/,/,
     &' Version V01-C',50X,9A1,//)
 110  FORMAT(' ','Enter degree of collocation polynomial (I2).   ',$)
 120  FORMAT(' ','Enter diffusion coefficient for species P.   ',$)
 125  FORMAT(' ','Enter diffusion coefficient for species Q.   ',$)
 130  FORMAT(' ','Enter D/v ratio.   ',$)
 135  FORMAT(' ','Enter value of kinetic parameter.   ',$)
```

```
140 FORMAT(' ','Enter transport boundary coefficient. ',$)
150 FORMAT(' ','Concentrations at the Collocation Points:',
   &/,/,10X,'Z',12X,'Conc. P',9X,'Conc. Q',/)
160 FORMAT(3(1PE16.6))
170 FORMAT('0','Concentration Gradient at the Disk Surface: ',
   &1PE15.6)
180 FORMAT('0','Current Ratio:  ',1PE15.6,/)
190 FORMAT(' ','Enter 1 to repeat, 0 to terminate. ',$)
200 FORMAT(I2)
210 FORMAT(G15.6)
220 FORMAT(I1)
230 FORMAT(' ',I2)
240 FORMAT(' ',1PG15.6)
C
    END
```

```
C
C
C      Title:  Pseudo-First-Order EC-Catalytic Mechanism at the RDE.
C              Working Curves by Orthogonal Collocation.
C
C      Author:  J. Nolan                        Date:  15-Dec-86
C
C      Source File:  ECR1WC.SNG     Object File:  ECR1WC.SOB
C
       PROGRAM ECR1WC
C
C      Purpose:
C
C           This program calculates working curves (i.e. current
C      ratio R as a function of the log of the kinetic parameter)
C      for the pseudo-first-order EC-catalytic mechanism at the RDE.
C      R is calculated by the orthogonal collocation technique using
C      the extended axial velocity equation.  Provision is made for
C      inequalities in the diffusion coefficients of the three
C      species involved.  Transport boundary optimisation is avail-
C      able as an option.  It is useful for large values of the
C      kinetic parameter.
C
C      Modifications:
C
C      1.  Included date and version number on printout (V01-B,
C          28-Jun-87).
C
C      External References:
C
C          Fn/Sr            Src File        Obj File
C
C      Subroutine GENAB     GENAB.SNG       DGSPLB.OBJ
C      Subroutine OCECR1    OCECR1.SNG      DGSPLB.OBJ
C      Subroutine DATE      N/A             FORLIB.OBJ
C      Function ABS,AMAX1   N/A             FORLIB.OBJ
C
C      Variable Declarations:
C
       IMPLICIT REAL*4 (A-H,O-Z)
       DIMENSION ROOTS(26),AMAT(26,26),BMAT(26,26)
       REAL*4 LKHI,LKLO,LKINC,LK,K
       LOGICAL*1 DATARR(9)
C
C          N - Order of the collocation polynomial (N<=24).
C          NR - Number of simultaneous equations (=2*N).
C          DBARP - Normalized diffusion coefficient of species P.
C          DBARQ - Normalized diffusion coefficient of species Q.
C          DVRAT - Ratio of the larger diffusion coefficient to
C                  the kinematic viscosity (=1/Sc).
C          CRATIO - Concentration ratio (P/Q) at Z = 0 (fixed
C                   at 1.E-06).
C          CTBL - Transport boundary layer coefficient.
C
C          Output:
C
C          DATARR - System date (DD-MMM-YY).
C          GRAD - Surface concentration gradient.
C          K - Kinetic parameter
C          LK - LOG10 of K
C          ROC - Current ratio normalized to k = 0.
```

```
C
C      Logical Units Referenced:
C
C          4 = Data File
C          5 = Terminal Input
C          6 = Terminal Output
C
C      Data Statements
C
       DATA CRATIO,CTBL0 /1.E-06,3.6096/
       ND=26
C
C      Executable Code
C
C      Print header.
C
       CALL DATE(DATARR)
       WRITE(7,100) (DATARR(I),I=1,9)
       WRITE(4,100) (DATARR(I),I=1,9)
C
C      Prompt for working curve parameters.
C
       WRITE(7,110)
       READ(5,200) N
       WRITE(7,120)
       READ(5,210) DP
       WRITE(7,130)
       READ(5,210) DQ
       WRITE(7,140)
       READ(5,210) DVRAT
       WRITE(7,150)
       READ(5,240) NCTBL
C
C      Prompt for calculation loop parameters.
C
       WRITE(7,160)
       READ(5,210) LKLO
       WRITE(7,170)
       READ(5,210) LKHI,
       WRITE(7,180)
       READ(5,210) LKINC
C
C      List parameters in data file.
C
       WRITE(4,110)
       WRITE(4,220) N
       WRITE(4,120)
       WRITE(4,230) DP
       WRITE(4,130)
       WRITE(4,230) DQ
       WRITE(4,140)
       WRITE(4,230) DVRAT
       WRITE(4,150)
       WRITE(4,220) NCTBL
C
C      Normalize with respect to the larger diffusion coefficient.
C
       DMAX=AMAX1(DP,DQ)
       DBARP=DP/DMAX
       DBARQ=DQ/DMAX
```

```
C
C      Calculate factor matrices and determine GRAD0.
C
       CTBL=CTBL0
       CALL GENAB(N,ND,ROOTS,AMAT,BMAT)
       CALL OCECR1(N,ND,ROOTS,AMAT,BMAT,O.,DVRAT,DBARP,DBARQ,
      &              CTBL,CRATIO,GRAD)
       GRAD0=GRAD/CTBL
C
C      Initialise calculation loop.
C
       IUP=INT(ABS(LKHI-LKLO)/LKINC+0.5)+1
       IF (LKLO .GT. LKHI) LKINC=-1.*ABS(LKINC)
C
       WRITE(7,185)
       WRITE(4,185)
C
       DO 20 I=1,IUP
          LK=LKLO+FLOAT(I-1)*LKINC
          K=10.**LK
          IF(NCTBL.EQ.0) GOTO 10
             CTBL1=8./DSQRT(K)
             IF (CTBL1.LT.CTBL0) CTBL=CTBL1
   10     CALL OCECR1(N,ND,ROOTS,AMAT,BMAT,K,DVRAT,DBARP,DBARQ,
      &            CTBL,CRATIO,GRAD)
          ROC=CTBL*GRAD0/GRAD
          WRITE(7,190) LK,ROC
          WRITE(4,190) LK,ROC
   20  CONTINUE
C
       STOP
C
C       Format Statements
C
  100  FORMAT('0',13X,'***Pseudo-First-Order EC-Catalytic Mechanism
      &***',/,23X,'at the Rotating Disk Electrode',/,/,18X,'Working
      & Curves by Orthogonal Collocation',/,/,' Version V01-B',50X,
      &9A1,/)
  110  FORMAT(' ','Enter degree of collocation polynomial (I2).  ',$)
  120  FORMAT(' ','Enter diffusion coefficient for species P.  ',$)
  130  FORMAT(' ','Enter diffusion coefficient for species Q.  ',$)
  140  FORMAT(' ','Enter D/v ratio.  ',$)
  150  FORMAT(' ','Transport boundary layer optimisation (0/1)?  ',$)
  160  FORMAT(' ','Enter initial value for LOG10(K).  ',$)
  170  FORMAT(' ','Enter final value for LOG10(K).  ',$)
  180  FORMAT(' ','Enter increment value for LOG10(K).  ',$)
  185  FORMAT(' ',5X,'Log(K)',8X,'Current Ratio',/)
  190  FORMAT(2(1PE16.6))
  200  FORMAT(I2)
  210  FORMAT(G15.6)
  220  FORMAT(' ',I2)
  230  FORMAT(' ',1PG15.6)
  240  FORMAT(I1)
C
       END
```

9

```
C
C
C     Title:  Second-Order EC-Catalytic Mechanism at the RDE.
C             Numerical Solution by Orthogonal Collocation.
C
C     Author:  J. Nolan                          Date:  04-Jan-87
C
C     Source File:  RDECR2.SNG        Object File:  RDECR2.SOB
C
      PROGRAM RDECR2
C
C     Purpose:
C
C          This program uses orthogonal collocation to obtain
C     the steady-state solution to the differential equations
C     describing the second-order EC-catalytic mechanism at
C     the RDE.  Formulation of the boundary value problem is
C     based on Eddowes' treatment of the mass-transport-limited
C     case (J. Electroanal Chem., Vol. 159, p.1, 1983).  Imple-
C     mentation of the orthogonal collocation technique follows
C     J. Villadsen and M.L. Michelsen, "Solution of Differential
C     Equation Models by Polynomial Approximation", Englewood
C     Cliffs, N.J.: Prentice-Hall, Inc., 1978.
C          The program returns concentration profiles of the three
C     species involved as well as the dimensionless current ratio
C*    R, which is normalized to the case where k equals 0. Simple
C     iteration is used to solve the set of nonlinear equations
C     describing the mechanism.  To conserve storage and to speed
C     execution, the equations describing the substrate A are
C     handled independently from those describing the catalyst
C     species P and Q.
C
C     Modifications:
C
C     1.  Included date and version number on printout (V01-B,
C         28-Jun-87).
C     2.  Input parameters and calculated results sent to file
C         attached to L. U. 4 (V01-C, 09-Sept-87)
C
C     External References:
C
C         Fn/Sr            Src File         Obj File
C
C     Subroutine GENAB     GENAB.SNG        DGSPLB.OBJ
C     Subroutine RDECDE    RDECDE.SNG       DGSPLB.OBJ
C     Subroutine HSRCDE    HSRCDE.SNG       DGSPLB.OBJ
C     Subroutine CSCGP     CSCGP.SNG        DGSPLB.OBJ
C     Subroutine SCNCA     SCNCA.SNG        DGSPLB.OBJ
C     Subroutine ARRAY     ARRAY.FOR        MATLIB.OBJ
C     Subroutine SIMQ      SIMQ.FOR         MATLIB.OBJ
C     Subroutine DATE      N/A              FORLIB.OBJ
C     Function AMAX1       N/A              FORLIB.OBJ
C
C     Variable Declarations:
C
      IMPLICIT REAL*4 (A-H,O-Z)
      LOGICAL*1 DATARR(9)
      DIMENSION ROOTS(20),AMAT(20,20),BMAT(20,20),PCNCS(36),
     &          CNCS(36),CMAT(36,36),DMAT(1296),PCNCSA(18),
     &          CNCSA(18),CMATA(18,18),DMATA(324),BOUND(36),
     &          BOUNDA(18),CONCS1(36)
```

```
C
C       Input:
C
C
C       N - Order of the collocation polynomial (N<=18).
C       NR - Number of simultaneous equations.
C       CRATIO - Surface concentration ratio (P/Q).
C       DBARP - Normalized diffusion coefficient of species P.
C       DBARQ - Normalized diffusion coefficient of species Q.
C       DBARA - Normalized diffusion coefficient of species A.
C       DVRAT - Ratio of the largest diffusion coefficient to
C               the kinematic viscosity (=1/Sc).
C       CBARA - Concentration of species A normalized to that
C               of P.
C       PARKIN - Kinetic parameter.
C       CTBL - Transport boundary layer coefficient.
C       SSQRCM - Convergence criterion, defined as the sum of
C               the squares of the corrections between successive
C               iterations.
C
C       Output:
C
C       DATARR - System date (DD-MMM-YY).
C       ROOTS - Roots of the collocation polynomial.
C       AMAT,BMAT - Discretization matrices containing the
C               coefficients for the first and second derivatives
C               of the concentration profile.
C       CMAT - Matrix containing the system of simultaneous
C               equations for species P and Q.
C       DMAT - Packed vector equivalent of CMAT.
C       CNCS - Vector containing concentrations of species P
C               and Q at the collocation points.
C       CMATA,DMATA,CNCSA - Corresponding arrays for species A.
C       BOUND,BOUNDA - Vectors containing constant terms for the
C               respective systems of equations.
C       CONCS1 - Initial concentrations of P and Q from the mass-
C               transport limited case.
C       CP0,CQ0,CA0 - Concentrations of the respective species
C               at Z = 0.
C       GRAD.- Surface concentration gradient of species P.
C       GRAD0 - Surface concentration gradient for PARKIN = 0.
C       NITS - Number of iterations required for convergence.
C       ROC - Current ratio.
C       CAT -Catalytic efficiency.
C
C       Logical Units Referenced:
C
C               4 = File Output
C               5 = Terminal Input
C               7 = Terminal Output
C
C       Data Statements
C
        DATA CRATIO,CTBL /1.E-06,3.6096/
        ND=20
        NE=36
        NF=18
        THIRD=1./3.
C
C       Executable Code
C
```

```
C       Print header and prompt for parameters.
C
        CALL DATE(DATARR)
        WRITE(7,100) (DATARR(I),I=1,9)
        WRITE(4,100) (DATARR(I),I=1,9)
C
        WRITE(7,110)
        READ(5,200) N
        WRITE(7,115)
        READ(5,210) DP
        WRITE(7,120)
        READ(5,210) DQ
        WRITE(7,130)
        READ(5,210) DVRAT
C
C       Echo parameters on L.U. 4.
C
        WRITE(4,110)
        WRITE(4,230) N
        WRITE(4,115)
        WRITE(4,240) DP
        WRITE(4,120)
        WRITE(4,240) DQ
        WRITE(4,130)
        WRITE(4,240) DVRAT
C
C       Normalize with respect to the largest diffusion coefficient.
C
        DMAXO=AMAX1(DP,DQ)
        DBARP=DP/DMAXO
        DBARQ=DQ/DMAXO
        NR=2*N
C
C       Generate matrix of simultaneous equations for the concen-
C       trations of species P and Q at the collocation points.
C
        CALL GENAB(N,ND,ROOTS,AMAT,BMAT)
C
        CALL RDECDE(N,ND,NE,ROOTS,AMAT,BMAT,DVRAT,DBARP,DBARQ,CRATIO,
     &              CTBL,CMAT,CONCS1)
C
C       Solve for concentrations at the collocation points for the
C       case where k = 0.
C
        CALL ARRAY(2,NR,NR,NE,NE,DMAT,CMAT)
        CALL SIMQ(DMAT,CONCS1,NR,KS)
        IF (KS.EQ.1) GOTO 99
C
C       Calculate concentration gradient (of species P) at Z = 0.
C
        CALL CSCGP(N,ND,NE,DBARP,DBARQ,CRATIO,AMAT,CONCS1,CPO,GRAD)
        GRADO=GRAD
C
C       Prompt for kinetic parameter, normalized concentration,
C       diffusion coefficient of species A, etc.
C
   10   WRITE(7,140)
        READ(5,210) PARKIN
        WRITE(7,150)
        READ(5,210) CBARA
```

```
      WRITE(7,160)
      READ(5,210) DA
      WRITE(7,170)
      READ(5,210) SSQRCM
C
C     Echo on L.U. 4.
C
      WRITE(4,140)
      WRITE(4,240) PARKIN
      WRITE(4,150)
      WRITE(4,240) CBARA
      WRITE(4,160)
      WRITE(4,240) DA
      WRITE(4,170)
      WRITE(4,240) SSQRCM
C
C     Re-normalize with respect to the largest diffusion
C     coefficient.
C
      DMAX=AMAX1(DP,DQ,DA)
      DBARP=DP/DMAX
      DBARQ=DQ/DMAX
      DBARA=DA/DMAX
      DMAX13=(DMAX/DMAX0)**THIRD
      DRAT23=((DP/DA)**THIRD)**2
C
      NITS=1
C
C     Set previous A concentrations equal to the bulk concentration
C     as a first approximation.  Set previous P and Q concentrations
C     to those found for k = 0.
C
      DO 20 I=1,N
          IN=I+N
          PCNCS(I)=CONCS1(I)
          PCNCS(IN)=CONCS1(IN)
          PCNCSA(I)=CBARA
  20  CONTINUE
C
C     Regenerate the discretized transport equations for species
C     P and Q and generate those for the substrate.
C
      CALL RDECDE(N,ND,NE,ROOTS,AMAT,BMAT,DVRAT,DBARP,DBARQ,CRATIO,
     &           CTBL,CMAT,BOUND)
      CALL HSRCDE(N,ND,NF,ROOTS,AMAT,BMAT,DVRAT,DBARA,CBARA,CTBL,
     &           CMATA,BOUNDA)
C
C     Generate the packed vector equivalents.  This is the starting
C     point for the iterative solution of the nonlinear system of
C     equations.
C
  30  CALL ARRAY(2,NR,NR,NE,NE,DMAT,CMAT)
      CALL ARRAY(2,N,N,NF,NF,DMATA,CMATA)
C
      DO 33 I=1,N
          IN=I+N
          CNCS(I)=BOUND(I)
          CNCS(IN)=BOUND(IN)
          CNCSA(I)=BOUNDA(I)
  33  CONTINUE
```

```fortran
C
C       Include the kinetic terms.
C
        CONST=PARKIN*CTBL**2
C
        DO 35 I=1,N
            II=(I-1)*N+I
            IIN=(I+N-1)*NR+I
            ININ=IIN+N
            TERM=CONST*PCNCSA(I)
            DMAT(IIN)=DMAT(IIN)+TERM/DBARP
            DMAT(ININ)=DMAT(ININ)-TERM/DBARQ
            DMATA(II)=DMATA(II)-CONST*PCNCS(I+N)/DBARA
  35    CONTINUE
C
C       Solve for concentrations at the collocation points.
C
        CALL SIMQ(DMAT,CNCS,NR,KS)
        IF (KS.EQ.1) GOTO 99
        CALL SIMQ(DMATA,CNCSA,N,KS)
        IF (KS.EQ.1) GOTO 99
C
C       Determine the sum of the squared corrections and save
C       current concentrations.
C
        SSQRC=0.
        DO 40 I=1,N
            IN=I+N
            SSQRC=SSQRC+(PCNCSA(I)-CNCSA(I))**2
            PCNCSA(I)=CNCSA(I)
            SSQRC=SSQRC+(PCNCS(I)-CNCS(I))**2
            PCNCS(I)=CNCS(I)
            SSQRC=SSQRC+(PCNCS(IN)-CNCS(IN))**2
            PCNCS(IN)=CNCS(IN)
  40    CONTINUE
C
        IF (SSQRC.LE.SSQRCM) GO TO 45
            NITS=NITS+1
            GOTO 30
C
C       Calculate current ratio and catalytic efficiency.
C
  45    CALL CSCGP(N,ND,NE,DBARP,DBARQ,CRATIO,AMAT,CNCS,CPO,GRAD)
        CQO=CPO/CRATIO
        CALL SCNCA(N,ND,NF,AMAT,CBARA,CNCSA,CAO)
        ROC=(GRADO/GRAD)*DMAX13
        CAT=DRAT23*(1./ROC-1.)/CBARA
C
C       Print results along with final concentrations.  Echo on
C       L.U. 4.
C
        WRITE(7,180) NITS
        WRITE(7,185) 0.,CPO,CQO,CAO
        WRITE(7,185) (ROOTS(I+1),CNCS(I),CNCS(N+I),CNCSA(I),
     &               I=1,N)
        WRITE(7,185) 1.,1.,0.,CBARA
        WRITE(7,190) GRAD,ROC,CAT
C
        WRITE(4,180) NITS
        WRITE(4,185) 0.,CPO,CQO,CAO
```

```
      WRITE(4,185) (ROOTS(I+1),CNCS(I),CNCS(N+I),CNCSA(I),
     &              I=1,N)
      WRITE(4,185) 1.,1.,0.,CBARA
      WRITE(4,190) GRAD,ROC,CAT
C
C     Loop to repeat for next value of PARKIN, CBARA and/or
C     CBARA.
C
      WRITE(7,195)
      READ(5,220) ILOOP
      IF (ILOOP .EQ. 0) GOTO 60
          GOTO 10
60    CONTINUE
      STOP
C
C     Error exit for singular matrices.
C
99    WRITE(7,999)
      STOP
C
C     Format Statements
C
100   FORMAT('0',16X,'***Second-Order EC-Catalytic Mechanism***',
     &/,23X,'at the Rotating Disk Electrode',/,/,16X,'Numerical
     & Solution by Orthogonal Collocation',/,/,' Version V01-C',
     &50X,9A1,/)
110   FORMAT(' ','Enter degree of collocation polynomial (I2). ',$)
115   FORMAT(' ','Enter diffusion coefficient for species P. ',$)
120   FORMAT(' ','Enter diffusion coefficient for species Q. ',$)
130   FORMAT(' ','Enter D/v ratio.  ',$)
140   FORMAT(' ','Enter value of kinetic parameter.  ',$)
      FORMAT(' ','Enter normalized concentration of species A. ',$)
      FORMAT(' ','Enter diffusion coefficient for species A. ',$)
      FORMAT(' ','Enter convergence criterion.  ',$)
      FORMAT('0','Number of Iterations:',I3,/,/,8X,'Root',11X,
     &'Conc. P',9X,'Conc. Q',9X,'Conc. A',/)
185   FORMAT(4(1PE16.6))
190   FORMAT('0','Concentration Gradient at the Disk Surface: ',
     &1PE15.6,/,/,' Current Ratio:  ',1PE15.6,/,/,
     &' Catalytic Efficiency:  ',1PE15.6,/)
195   FORMAT('0','Enter 1 to repeat, 0 to terminate.  ',$)
200   FORMAT(I2)
210   FORMAT(G15.6)
220   FORMAT(I1)
230   FORMAT(' ',I2)
240   FORMAT(' ',1PG15.6)
999   FORMAT('0','Singular matrix encountered...execution ends.',/)
C
      END
```

```
C
C
C     Title:  ***Second Order EC-Catalytic Mechanism at the RDE***
C                  Working Curves by Orthogonal Collocation
C
C     Author:  J. Nolan                        Date:  07-Jan-87
C
C     Source File:  ECR2WC.SNG     Object File:  ECR2WC.SOB
C
      PROGRAM ECR2WC
C
C     Purpose:
C
C          This program calculates working curves (i.e. current
C     ratio R as a function of the log of the kinetic parameter)
C     for the second-order EC-catalytic mechanism at the RDE.  R is
C     calculated by the orthogonal collocation technique using the
C     extended axial velocity equation.  Provision is made for
C     inequalities in the diffusion coefficients of the three
C     species involved.
C
C     Modifications:
C
C     1.  Included date and version number on printout (V01-B,
C         28-Jun-87).
C
C     External References:
C
C         Fn/Sr            Src File          Obj File
C
C     Subroutine GENAB     GENAB.SNG        .DGSPLB.OBJ
C     Subroutine RDECDE    RDECDE.SNG        DGSPLB.OBJ
C     Subroutine HSRCDE    HSRCDE.SNG        DGSPLB.OBJ
C     Subroutine CSCGP     CSCGP.SNG         DGSPLB.OBJ
C     Subroutine OCECR2    OCECR2.SNG        DGSPLB.OBJ
C     Subroutine DATE      N/A               FORLIB.OBJ
C     Function AMAX1,ABS    N/A               FORLIB.OBJ
C
C     Variable Declarations:
C
      IMPLICIT REAL*4 (A-H,O-Z)
      LOGICAL*1 DATARR(9)
      DIMENSION ROOTS(20),AMAT(20,20),BMAT(20,20),CMAT(36,36),
     *          CMATA(18,18),BOUND(36),BOUNDA(18),CNCS(36)
      REAL*4 LKHI,LKLO,LKINC,LK
C
C          N      - Order of the collocation polynomial (N<=18).
C          ROOTS  - Roots of the collocation polynomial.
C          AMAT,BMAT - Discretization matrices containing the
C                   coefficients for the first and second derivatives
C                   of the concentration profile.
C          GRADO  - Surface concentration gradient when k = 0.
C          DBARP  - Normalized diffusion coefficient of species P.
C          DBARQ  - Normalized diffusion coefficient of species Q.
C          DBARA  - Normalized diffusion coefficient of species A.
C          DVRAT  - Ratio of the largest diffusion coefficient to
C                   the kinematic viscosity (=1/Sc).
C          CBARA  - Concentration of species A normalized to that of
C                   species P ( = Excess Factor).
C          PARKIN - Kinetic parameter
C          LKLO, LKHI - Range of Log(kinetic parameter).
```

```
C      CRATIO - Surface concentration ratio (P/Q).
C      CTBL - Transport boundary layer coefficient.
C      SSQRCM - Convergence criterion.
C
C      Output:
C
C      DATARR - System date (DD-MMM-YY).
C      CMAT,CMATA - Matrices containing the systems of trans-
C           port equations for species P, Q and A.
C      BOUND,BOUNDA - Vectors containing the constant terms
C           for above systems.
C      CNCS - Concentrations of P and Q at the collocation
C           points.
C      GRAD - Surface concentration gradient.
C      LK - LOG10(Kinetic parameter).
C      ROC - Current ratio.
C      CAT - Catalytic efficiency.
C
C   Logical Units Referenced:
C
C      4 = Data File
C      5 = Terminal Input
C      7 = Terminal Output
C
C   Data Statements
C
      DATA CRATIO,CTBL /1.E-06,3.6096/
      ND=20
      NE=36
      NF=18
C
C      Executable Code
C
C      Print header.
C
      CALL        (DATARR)
      WRITE(7,100) (DATARR(I),I=1,9)
      WRITE(4,100) (DATARR(I),I=1,9)
C
C      Prompt for program parameters.
C
      WRITE(7,110)
      READ(5,200) N
      WRITE(7,115)
      READ(5,210) DP
      WRITE(7,120)
      READ(5,210) DQ
      WRITE(7,125)
      READ(5,210) DA
      WRITE(7,130)
      READ(5,210) CBARA
      WRITE(7,135)
      READ(5,210) DVRAT
      WRITE(7,140)
      READ(5,210) SSQRCM
C
C      Prompt for calculation loop parameters.
C
      WRITE(7,145)
      READ(5,210) LKLO
```

```
      WRITE(7,150)
      READ(5,210) LKHI
      WRITE(7,160)
      READ(5,210) LKINC
C
C     List parameters in data file.
C
      WRITE(4,110)
      WRITE(4,230) N
      WRITE(4,115)
      WRITE(4,220) DP
      WRITE(4,120)
      WRITE(4,220) DQ
      WRITE(4,125)
      WRITE(4,220) DA
      WRITE(4,130)
      WRITE(4,220) CBARA
      WRITE(4,135)
      WRITE(4,220) DVRAT
      WRITE(4,140)
      WRITE(4,220) SSQRCM
C
C     Normalize diffusion coefficients with respect to the largest.
C
      DMAX=AMAX1(DP,DQ,DA)
      DBARP=DP/DMAX
      DBARQ=DQ/DMAX
      DBARA=DA/DMAX
C
C     Calculate factor matrices and determine GRADO.
C
      CALL GENAB(N,ND,ROOTS,AMAT,BMAT)
      CALL RDECDE(N,ND,NE,ROOTS,AMAT,BMAT,DVRAT,DBARP,DBARQ,CRATIO,
     &            CTBL,CMAT,BOUND)
      CALL HSRCDE(N,ND,NF,ROOTS,AMAT,BMAT,DVRAT,DBARA,CBARA,CTBL,
     &            CMATA,BOUNDA)
      CALL OCECR2(N,0.,DBARP,DBARQ,DBARA,CBARA,SSQRCM,CMAT,BOUND,
     &            CMATA,BOUNDA,NITS,CNCS)
      CALL CSCGP(N,ND,NE,DBARP,DBARQ,CRATIO,AMAT,CNCS,CPO,GRADO)
C
C     Initialise calculation loop and print headings.
C
      IUP=INT(ABS(LKHI-LKLO)/LKINC+0.5)+1
      IF (LKLO .GT. LKHI) LKINC=-1.*ABS(LKINC)
C
      WRITE(7,170)
      WRITE(4,170)
C
C     Generate the working curve.
C
      DO 10 I=1,IUP
          LK=LKLO+FLOAT(I-1)*LKINC
          PARKIN=10.**LK
          CALL OCECR2(N,PARKIN,DBARP,DBARQ,DBARA,CBARA,SSQRCM,
     &            CMAT,BOUND,CMATA,BOUNDA,NITS,CNCS)
          CALL CSCGP(N,ND,NE,DBARP,DBARQ,CRATIO,AMAT,CNCS,CPO,GRAD)
          ROC=GRADO/GRAD
          CAT=(1./ROC-1.)/CBARA
          WRITE(7,180) LK,ROC,CAT,NITS
          WRITE(4,180) LK,ROC,CAT,NITS
```

```
   10  CONTINUE
C
       STOP
C
C      Format Statements
C
  100  FORMAT('0',16X,'***Second-Order EC-Catalytic Mechanism***',
      &/,23X,'at the Rotating Disk Electrode',/,/,18X,'Working
      & Curves by Orthogonal Collocation',/,/,' Version V01-B',
      &50X,9A1)
  110  FORMAT('0','Enter degree of collocation polynomial (I2).  ',$)
  115  FORMAT(' ','Enter diffusion coefficient for species P.  ',$)
  120  FORMAT(' ','Enter diffusion coefficient for species Q.  ',$)
  125  FORMAT(' ','Enter diffusion coefficient for species A:  ',$)
  130  FORMAT(' ','Enter normalized concentration of species A.  ',$)
  135  FORMAT(' ','Enter D/v ratio.  ',$)
  140  FORMAT(' ','Enter convergence criterion.  ',$)
  145  FORMAT(' ','Enter initial value for LOG10(K).  ',$)
  150  FORMAT(' ','Enter final value for LOG10(K).  ',$)
  160  FORMAT(' ','Enter increment value for LOG10(K).  ',$)
  170  FORMAT(/,7X,'Log(k)',6X,'Current Ratio',2X,
      & 'Cat. Efficiency',2X,'Nits',/)
  180  FORMAT(3(1PE16.6),I6)
  200  FORMAT(I2)
  210  FORMAT(G15.6)
  220  FORMAT(' ',1PG15.6)
  230  FORMAT(' ',I2)
C
       END
```

```
C
C      Title:     Second Order EC-Catalytic Mechanism at the RDE.
C                 Numerical Solution by Global Spline Collocation.
C
C      Author:  J. Nolan                        Date:  11-Mar-87
C
C      Source File:  RDECR3.SNG        Object File:  RDECR3.SOB
C
       PROGRAM RDECR3
C
C      Purpose:
C
C          This program uses global spline collocation to obtain
C      the steady-state solution to the differential equations
C      describing the second-order EC-catalytic mechanism at
C      the RDE.   Formulation of the boundary value problem is
C      based on Eddowes treatment of the mass-transport-limited
C      case (J. Electroanal Chem., Vol. 159, p.1, 1983).  Imple-
C      mentation of the orthogonal collocation technique follows
C      J. Villadsen and M.L. Michelsen, "Solution of Differential
C      Equation Models by Polynomial Approximation", Englewood
C      Cliffs, N.J.: Prentice-Hall, Inc., 1978.
C          The program returns concentration profiles of the three
C      species involved as well as the dimensionless current ratio
C      R, which is normalized to the case where k equals 0. Simple
C      iteration is used to solve the set of nonlinear equations
C      describing the mechanism.  To conserve storage and to speed
C      execution, the equations describing the substrate A are
C      handled independently from those describing the catalyst
C      species P and Q.
C
C      Modifications:
C
C      1.   Included date and version number on printout (V01-B,
C           28-Jun-87).
C      2.   Input parameters and calculated results sent to file
C           attached to L. U. 4 (V01-C, 10-Sept-87)
C
C      External References:
C
C           Fn/Sr              Src File         Obj File
C
C      Subroutine GENAB        GENAB.SNG        DGSPLB.OBJ
C      Subroutine RDCDSP       RDCDSP.SNG       DGSPLB.OBJ
C      Subroutine HSCDSP       HSCDSP.SNG       DGSPLB.OBJ
C      Subroutine KTCDSP       KTCDSP.SNG       DGSPLB.OBJ
C      Subroutine ARRAY        ARRAY.FOR        MATLIB.OBJ
C      Subroutine SIMQ         SIMQ.FOR         MATLIB.OBJ
C      Subroutine DATE         N/A              FORLIB.OBJ
C      Function AMAX1          N/A              FORLIB.OBJ
C
C      Variable Declarations:
C
       IMPLICIT REAL*4 (A-H,O-Z)
       LOGICAL*1 DATARR(9)
       DIMENSION ROOTS(16),AMAT(16,16),BMAT(16,16),PCNCS(60),
      &          CNCS(60),CMAT(60,60),BOUND(60),CONCS1(60),CNCSA(30),
      &          PCNCSA(30),CMATA(30,30),BOUNDA(30),COLPTS(30)
       EQUIVALENCE (CNCS(1),BOUND(1)),(CNCSA(1),BOUNDA(1))
C
```

```
C      Input:
C
C
C         N - Order of the collocation polynomial (N<=14).
C         NR - Number of simultaneous equations.
C         CRATIO - Surface concentration ratio (P/Q).
C         DBARP - Normalized diffusion coefficient of species P.
C         DBARQ - Normalized diffusion coefficient of species Q.
C         DBARA - Normalized diffusion coefficient of species A.
C         DVRAT - Ratio of the largest diffusion coefficient to
C               the kinematic viscosity (=1/Sc).
C         CBARA - Concentration of species A normalized to that
C               of P.
C         PARKIN - Kinetic parameter.
C         CTBL - Transport boundary layer coefficient.
C         SPLPT - Spline point.
C         SSQRCM - Convergence criterion, defined as the sum of
C               the squares of the corrections between successive
C               iterations.
C
C      Output:
C
C         DATARR - Current system date (DD-MMM-YY).
C         ROOTS - Roots of the collocation polynomial.
C         AMAT,BMAT - Discretization matrices containing the
C               coefficients for the first and second derivatives
C               of the concentration profile.
C         CMAT - Matrix containing the system of simultaneous
C               equations for species P and Q.
C         CNCS - Vector containing concentrations of species P
C               and Q at the collocation points.
C         CMATA,CNCSA - Corresponding arrays for species A.
C         BOUND,BOUNDA - Vectors containing constant terms for the
C               respective systems of equations.
C         CONCS1 - Initial concentrations of P and Q from the mass-
C               transport-limited case.
C         GRAD - Surface concentration gradient of species P.
C         GRAD0 - Surface concentration gradient for PARKIN = 0.
C         NITS - Number of iterations required for convergence.
C         ROC - Current ratio.
C         CAT - Catalytic efficiency.
C
C      Logical Units Referenced:
C
C         4 = File Output
C         5 = Terminal Input
C         7 = Terminal Output
C
C      Data Statements
C
DATA CRATIO,CTBL /1.E-06,3.6096/
ND=16
NE=60
NF=30
THIRD=1./3.
C
C      Executable Code
C
C      Print header and prompt for parameters.
C
CALL DATE(DATARR)
```

```
      WRITE(7,100) (DATARR(I),I=1,9)
      WRITE(4,100) (DATARR(I),I=1,
C
      WRITE(7,110)
      READ(5,200) N
      WRITE(7,115)
      READ(5,210) DP
      WRITE(7,120)
      READ(5,210) DQ
      WRITE(7,130)
      READ(5,210) DVRAT
      WRITE(7,135)
      READ(5,210) SPLPT
C
C       Echo on L.U. 4.
C
      WRITE(4,110)
      WRITE(4,230) N
      WRITE(4,115)
      WRITE(4,240) DP
      WRITE(4,120)
      WRITE(4,240) DQ
      WRITE(4,130)
      WRITE(4,240) DVRAT
      WRITE(4,135)
      WRITE(4,240) SPLPT
C
      CSPLPT=1.-SPLPT
C
C
C       Normalize with respect to the largest diffusion coefficient.
C
      DMAX0=AMAX1(DP,DQ)
      DBARP=DP/DMAX0
      DBARQ=DQ/DMAX0
      NR=4*N+4
      NR2=NR/2
      N1=N+1
      N2=N+2
C
C
C       Generate matrix of simultaneous equations for the concen-
C       trations of species P and Q at the collocation points.
C
      CALL GENAB(N,ND,ROOTS,AMAT,BMAT)
C
      CALL RDCDSP(N,ND,NE,ROOTS,AMAT,BMAT,DVRAT,DBARP,DBARQ,CRATIO,
     &           CTBL,SPLPT,CMAT,CONCS1)
C
C       Solve for concentrations at the collocation points for the
C       case where k = 0.
C
      CALL ARRAY(2,NR,NR,NE,NE,CMAT,CMAT)
      CALL SIMQ(CMAT,CONCS1,NR,KS)
      IF (KS.EQ.1) GOTO 99
C
C       Calculate concentration gradient (of species P) at Z = 0.
C
      GRAD0=0.
      DO 5 J=1,N2
          GRAD0=GRAD0+AMAT(1,J)*CONCS1(J)
    5 CONTINUE
```

```
      GRADO=GRADO/SPLPT
C
C     Prompt for kinetic parameter, normalized concentration,
C     diffusion coefficient of species A, etc.
C
 10   WRITE(7,140)
      READ(5,210) PARKIN
      WRITE(7,150)
      READ(5,210) CBARA
      WRITE(7,160)
      READ(5,210) DA
      WRITE(7,170)
      READ(5,210) SSQRCM
C
C     Echo on L.U. 4.
C
      WRITE(4,140)
      WRITE(4,240) PARKIN
      WRITE(4,150)
      WRITE(4,240) CBARA
      WRITE(4,160)
      WRITE(4,240) DA
      WRITE(4,170)
      WRITE(4,240) SSQRCM
C
C     Re-normalize with respect to the largest diffusion coefficient
C
      DMAX=AMAX1(DP,DQ,DA)
      DBARP=DP/DMAX
      DBARQ=DQ/DMAX
      DBARA=DA/DMAX
      DMAX13=(DMAX/DMAX0)**THIRD
      DRAT23=((DP/DA)**THIRD)**2
C
      NITS=1
C
C     Set previous A concentrations equal to the bulk concentration
C     as a first approximation.  Set previous P and Q concentrations
C     to those found for k = 0.
C
      DO 20 I=1,NR2
          IN=I+NR2
          PCNCS(I)=CONCS1(I)
          PCNCS(IN)=CONCS1(IN)
          PCNCSA(I)=CBARA
 20   CONTINUE
C
C     Regenerate the discretized transport equations for species
C     P and Q and generate those for the substrate.  This is the
C     starting point for the iterative solution of the system of
C     nonlinear equations.
C
 30   CALL RDCDSP(N,ND,NE,ROOTS,AMAT,BMAT,DVRAT,DBARP,DBARQ,CRATIO,
     &            CTBL,SPLPT,CMAT,BOUND)
      CALL HSCDSP(N,ND,NF,ROOTS,AMAT,BMAT,DVRAT,DBARA,CBARA,CTBL,
     &            SPLPT,CMATA,BOUNDA)
C
C     Include the kinetic terms.
C
      CALL KTCDSP(N,NE,NF,PARKIN,DBARP,DBARQ,DBARA,CTBL,SPLPT,
```

```
     &                    PCNCSA,PCNCS,CMATA,CMAT)
C
C        Solve for concentrations at the collocation points.
C
      CALL ARRAY(2,NR,NR,NE,NE,CMAT,CMAT)
      CALL SIMQ(CMAT,CNCS,NR,KS)
      IF (KS.EQ.1) GOTO 99
      CALL ARRAY(2,NR2,NR2,NF,NF,CMATA,CMATA)
      CALL SIMQ(CMATA,CNCSA,NR2,KS)
      IF (KS.EQ.1) GOTO 99
C
C        Determine the sum of the squared corrections and save
C        current concentrations.
C
      SSQRC=0.
      DO 40 I=1,NR2
           IN=I+NR2
           SSQRC=SSQRC+(PCNCSA(I)-CNCSA(I))**2
           PCNCSA(I)=CNCSA(I)
           SSQRC=SSQRC+(PCNCS(I)-CNCS(I))**2
           PCNCS(I)=CNCS(I)
           SSQRC=SSQRC+(PCNCS(IN)-CNCS(IN))**2
           PCNCS(IN)=CNCS(IN)
   40 CONTINUE
C
      IF (SSQRC.LE.SSQRCM) GOTO 45
           NITS=NITS+1
           GOTO 30
C
   45 DO 50 I=1,N1
           IN=I+N1
           COLPTS(I)=ROOTS(I)*SPLPT
           COLPTS(IN)=SPLPT+ROOTS(I)*CSPLPT
   50 CONTINUE
C
C        Calculate current ratio and catalytic efficiency.
C
      GRAD=0.
      DO 55 J=1,N2
           GRAD=GRAD+AMAT(1,J)*CNCS(J)
   55 CONTINUE
      GRAD=GRAD/SPLPT
      ROC=(GRAD0/GRAD)*DMAX13
      CAT=DRAT23*(1./ROC-1.)/CBARA
C
C        Print results along with final concentrations.  Echo on
C        on L.U. 4.
C
      WRITE(7,180) NITS
      WRITE(7,185) (COLPTS(I),CNCS(I),CNCS(I+NR2),CNCSA(I),
     &              I=1,NR2)
      WRITE(7,185) 1.,1.,0.,CBARA
      WRITE(7,190) GRAD,ROC,CAT
C
      WRITE(4,180) NITS
      WRITE(4,185) (COLPTS(I),CNCS(I),CNCS(I+NR2),CNCSA(I),
     &              I=1,NR2)
      WRITE(4,185) 1.,1.,0.,CBARA
      WRITE(4,190) GRAD,ROC,CAT
```

```
C     Loop to repeat for next value of PARKIN, CBARA and/or
C     DBARA.
C
      WRITE(7,195)
      READ(5,220) ILOOP
      IF (ILOOP .EQ. 0) GOTO 60
           GOTO 10
  60  CONTINUE
      STOP
C
C  .  Error exit for singular matrices.
C
  99  WRITE(7,999)
      STOP
C
C     Format Statements
C
 100  FORMAT('0',16X,'***Second-Order EC-Catalytic Mechanism***',/,
     &23X,'at the Rotating Disk Electrode',/,/,14X,'Numerical
     & Solution by Global Spline Collocation',/,/,/,' Version V01-C',
     &50X,9A1,/)
 110  FORMAT(' ','Enter degree of collocation polynomial (I2).   ',$)
 115  FORMAT(' ','Enter diffusion coefficient for species P.  ',$)
 120  FORMAT(' ','Enter diffusion coefficient for species Q.  ',$)
 130  FORMAT(' ','Enter D/v ratio.. ',$)
 135  FORMAT(' ','Enter spline point.  ',$)
 140  FORMAT(' ','Enter value of kinetic parameter.  ',$)
 150  FORMAT(' ','Enter normalized concentration of species A.  ',$)
 160  FORMAT(' ','Enter diffusion coefficient for species A.  ',$)
 170  FORMAT(' ','Enter convergence criterion.  ',$)
 180  FORMAT('0','Number of Iterations:',I3,/,/,8X,'Root',11X,
     &' Conc. P',9X,'Conc. Q',9X,'Conc. A',/)
 185  FORMAT(4(1PE16.6))
 190  FORMAT('0','Concentration Gradient at the Disk Surface: ',
     &1PE15.6,/,/,' Current Ratio:  ',1PE15.6,/,/,
     &' Catalytic Efficiency:  ',1PE15.6,/)
 195  FORMAT(' ','Enter 1 to repeat, 0 to terminate.  ',$)
 200  FORMAT(I2)
 210  FORMAT(G15.6)
 220  FORMAT(I1)
 230  FORMAT(' ',I2)
 240  FORMAT(' ',1PG15.6)
 999  FORMAT('0','Singular matrix encountered...execution ends.',/)
C
      END
```

```
C
C
C    Title: ***Second-Order EC-Catalytic Mechanism at the RDE***
C                Working Curves by Global Spline Collocation
C
C    Author: J. Nolan                        Date:  12-Mar-87
C
C    Source File:  ECR3WC.SNG      Object File:  ECR3WC.SOB
C
      PROGRAM ECR3WC
C
C    Purpose:
C
C          This program calculates working curves (i.e. current
C      ratio as a function of the log of the kinetic parameter)
C      for the second-order EC-Catalytic mechanism at the RDE.
C      Global spline collocation is used to solve the boundary-
C      value problem.  The program incorporates the extended axial
C      velocity equation and provision is made for inequalities
C      among the diffusion coefficients of the three species
C      involved.
C
C    Modifications:
C
C    1.  Included date and version number on printout (V01-B,
C        26-Jun-88).
C
C    External References:
C
C           Fn/Sr            Src File          Obj File
C
C      Subroutine GENAB     GENAB.SNG         DGSPLB.OBJ
C      Subroutine GSECR3    GSECR3.SNG        DGSPLB.OBJ
C      Subroutine DATE      N/A               FORLIB.OBJ
C      Function AMAX1,ABS    N/A               FORLIB.OBJ
C
C    Variable Declarations:
C
      IMPLICIT REAL*4 (A-H,O-Z)
      LOGICAL*1 DATARR(9)
      DIMENSION ROOTS(16),AMAT(16,16),BMAT(16,16)
      REAL*4 LKHI,LKLO,LKINC,LK
C
C          N - Order of the collocation polynomial (N<=14).
C          ROOTS - Roots of the collocation polynomial.
C          AMAT,BMAT - Discretization matrices containing the
C                coefficients for the first and second derivatives
C                of the concentration profile.
C          GRAD0 - Surface concentration gradient when k = 0.
C          DBARP - Normalized diffusion coefficient of species P.
C          DBARQ - Normalized diffusion coefficient of species Q.
C          DBARA - Normalized diffusion coefficient of species A.
C          DVRAT - Ratio of the largest diffusion coefficient to
C                the kinematic viscosity (=1/Sc).
C          CBARA - Concentration of species A normalized to that of
C                species P ( = Excess Factor).
C          PARKIN - Kinetic parameter.
C          LKLO, LKHI - Range of log(kinetic parameter).
C          CRATIO - Surface concentration ratio (P/Q).
C          CTBL - Transport boundary layer coefficient.
```

```
C          Output:
C
C          DATARR - System date (DD-MMM-YY).
C          GRAD - Surface concentration gradient.
C          LK - LOG10(Kinetic parameter).
C          ROC - Current ratio.
C          CAT - Catalytic efficiency.
C
C       Logical Units Referenced:
C
C          4 = Data File
C          5 = Terminal Input
C          7 = Terminal Output
C
C       Data Statements
C
       DATA CRATIO /1.E-06/
       ND=16
C
C       Executable Code
C
C       Print header.
C
       CALL DATE(DATARR)
       WRITE(7,100) (DATARR(I),I=1,9)
       WRITE(4,100) (DATARR(I),I=1,9)
C
C       Prompt for program parameters.
C
       WRITE(7,110)
       READ(5,200) N
       WRITE(7,115)
       READ(5,210) DP
       WRITE(7,120)
       READ(5,210) DQ
       WRITE(7,125)
       READ(5,210) DA
       WRITE(7,130)
       READ(5,210) CBARA
       WRITE(7,135)
       READ(5,210) DVRAT
       WRITE(7,140)
       READ(5,210) SSQRCM
C
C       Prompt for calculation loop parameters.
C
       WRITE(7,145)
       READ(5,210) LKLO
       WRITE(7,150)
       READ(5,210) LKHI
       WRITE(7,160)
       READ(5,210) LKINC
C
C       List parameters in the data file.
C
       WRITE(4,110)
       WRITE(4,230) N
       WRITE(4,115)
       WRITE(4,220) DP
       WRITE(4,120)
```

```fortran
      WRITE(4,220) DQ
      WRITE(4,125)
      WRITE(4,220) DA
      WRITE(4,130)
      WRITE(4,220) CBARA
      WRITE(4,135)
      WRITE(4,220) DVRAT
      WRITE(4,140)
      WRITE(4,220) SSQRCM
C
C     Normalize diffusion coefficients with respect to the largest.
C
      DMAX=AMAX1(DP,DQ,DA)
      DBARP=DP/DMAX
      DBARQ=DQ/DMAX
      DBARA=DA/DMAX
C
C     Calculate factor matrices and determine GRAD0.
C
      CALL GENAB(N,ND,ROOTS,AMAT,BMAT)
C
      CALL GSECR3(N,ND,ROOTS,AMAT,BMAT,DVRAT,DBARP,DBARQ,CRATIO,
     &           DBARA,CBARA,SSQRCM,0.,NITS,GRAD0)
C
C     Initialise calculation loop.
C
      IUP=INT(ABS(LKHI-LKLO)/LKINC+0.5)+1
      IF (LKLO .GT. LKHI) LKINC=-1.*ABS(LKINC)
C
      WRITE(7,170)
      WRITE(4,170)
C
      DO 10 I=1,IUP
          LK=LKLO+FLOAT(I-1)*LKINC
          PARKIN=10.**LK
          CALL GSECR3(N,ND,ROOTS,AMAT,BMAT,DVRAT,DBARP,DBARQ,
     &           CRATIO,DBARA,CBARA,SSQRCM,PARKIN,NITS,GRAD)
          ROC=GRAD0/GRAD
          CAT=(1./ROC-1.)/CBARA
          WRITE(7,180) LK,ROC,CAT,NITS
          WRITE(4,180) LK,ROC,CAT,NITS
   10 CONTINUE
C
      STOP
C
C     Format Statements
C
  100 FORMAT('0',16X,'***Second-Order EC-Catalytic Mechanism***',/,
     &23X,'at the Rotating Disk Electrode',/,/,16X,'Working Curves
     & by Global Spline Collocation',/,/,' Version V01-B',50X,
     &9A1,/)
  110 FORMAT('0','Enter degree of collocation polynomial (I2).  ',$)
  115 FORMAT(' ','Enter diffusion coefficient for species P.  ',$)
  120 FORMAT(' ','Enter diffusion coefficient for species Q.  ',$)
  125 FORMAT(' ','Enter diffusion coefficient for species A.  ',$)
  130 FORMAT(' ','Enter normalized concentration of species A.  ',$)
  135 FORMAT(' ','Enter D/v ratio.  ',$)
  140 FORMAT(' ','Enter convergence criterion.  ',$)
  145 FORMAT(' ','Enter initial value for LOG10(K).  ',$)
  150 FORMAT(' ','Enter final value for LOG10(K).  ',$)
```

```
160   FORMAT(' ','Enter increment value for LOG10(K).  ',$)
170   FORMAT(/,7X,'Log(k)',6X,'Current Ratio',2X,
     & 'Cat. Efficiency',2X,'Nits',/)
180   FORMAT(3(1PE16.6),I6)
200   FORMAT(I2)
210   FORMAT(G15.6)
220   FORMAT(' ',1PG15.6)
230   FORMAT(' ',I2)
C
      END
```

```
C     Title:   Consecutive Electron Transfer with Reproportionation.
C              Numerical Solution by Orthogonal Collocation.
C
C     Author:  J. Nolan                          Date:   01-Jun-88
C
C     Source File:  CETRP2.FOR       Object File:  CETRP2.OBJ
C
C     PROGRAM CETRP2
C
C     Purpose:
C
C          This program uses orthogonal collocation to obtain the
C     solution to the differential equations describing consecutive
C     electron transfer accompanied by an irreversible reproportion-
C     ation at the rotating disk electrode.  Formulation of the
C     problem follows Eddowes (J. Electroanal. Chem., Vol. 159,
C     p.1, 1983).  Implementation of the orthogonal collocation
C     technique follows J. Villadsen and M.L. Michelsen, "Solution
C     of Differential Equation Models by Polynomial Approximation",
C     Englewood Cliffs, N.J.: Prentice-Hall, Inc., 1978.
C          The program returns concentration profiles of the three
C     species involved as well as the concentration gradients at the
C     electrode surface.  Newton-Raphson iteration is employed to
C     solve the nonlinear system of equations describing the
C     mechanism.  The weighting factor GAMMA controls the tendency
C     the program to oscillate about the desired solution at larger
C     values of kinetic parameter (>10).  A value of around 0.25
C     seems to work reasonably well.
C
C     Modifications:  None.
C
C     External References:
C
C          Fn/Sr              Src File         Obj File
C
C     Subroutine GENAB        GENAB.SNG        DGSPLB.OBJ
C     Subroutine SCGRD1       SCGRD1.FOR       DGSPLB.OBJ
C     Subroutine ARRAY        ARRAY.FOR        MATLIB.OBJ
C     Subroutine GMPRD        GMPRD.FOR        MATLIB.OBJ
C     Subroutine GMSUB        GMSUB.FOR        MATLIB.OBJ
C     Subroutine SIMQ         SIMQ.FOR         MATLIB.OBJ
C     Subroutine DATE         N/A              FORLIB.OBJ
C     Function AMAX1          N/A              FORLIB.OBJ
C
C     Variable Declarations:
C
      IMPLICIT REAL*4 (A-H,O-Z)
      DIMENSION ROOTS(26),AMAT(26,26),BMAT(26,26),PCONCS(72),
     &          CONCS(72),BOUND(72),PMAT(24,24),QMAT(24,24),
     &          RMAT(24,72),RJCBMX(576),PMATV(576),QMATV(576),
     &          RMATV(1728)
      EQUIVALENCE (PMAT(1,1),PMATV(1)),(QMAT(1,1),QMATV(1)),
     &            (RMAT(1,1),RMATV(1))
      LOGICAL*1 DATARR(9)
C
C     Input:
C
C     N - Order of the collocation polynomial (N<=24).
C     NR - Number of simultaneous equations.
```

```
C        DBARP - Normalized diffusion coefficient of species P.
C        DBARQ - Normalized diffusion coefficient of species Q.
C        DBARR - Normalized diffusion coefficient of species R.
C        PARKIN - Kinetic parameter.
C        CTBL - Transport boundary layer coefficient.
C        CKTCOF - Kinetic term coefficient.
C        SSQRCM - Convergence criterion, defined as the sum of
C             the squares of the corrections between successive
C             iterations.
C        GAMMA - Damping factor.
C
C     Output:
C
C        DATARR - Array containing the current date (DD-MMM-YY).
C        ROOTS - Roots of the collocation polynomial.
C        AMAT,BMAT - Discretization matrices containing the
C             coefficients for the first and second derivatives
C             of the concentration profile.
C        PMAT - Matrix containing the coefficients of the system
C             of simultaneous equations for species P.
C        QMAT - Matrix containing the coefficients of the system
C             of simultaneous equations for species Q.
C        RMAT - Matrix containing the coefficients of the system
C             of simultaneous equations for species R.
C        CONCS - Vector containing concentrations of species P, Q,
C             and R at the collocation points.
C        BOUND - Vector containing constant terms for the system
C             of equations describing P, Q and R.
C        PCONCS - Previous concentrations of P, Q and R.
C        RJCBMX - Scratch matrix used to hold Jacobians.
C        CR0 - Concentrations of species R at Z = 0.
C        GRADP - Surface concentration gradient of species P (=0).
C        GRADQ - Surface concentration gradient of species Q.
C        GRADR - Surface concentration gradient of species R.
C        NITS - Number of iterations required for convergence.
C
C     Logical Units Referenced:
C
C        4 = Data File Output
C        5 = Terminal Input
C        7 = Terminal Output
C
C     Data Statements
C
      DATA CTBLO /3.6096/
      ND=26
      NE=24
      NF=72
      CTBL=CTBLO
C
C     Executable Code
C
C     Print header and prompt for parameters.
C
      CALL DATE(DATARR)
      WRITE(7,100) (DATARR(I),I=1,9)
C
      WRITE(7,110)
      READ(5,200) N
C
```

```
      WRITE(7,115)
      READ(5,210) DP
      WRITE(7,120)
      READ(5,210) DQ
      WRITE(7,130)
      READ(5,210) DR
      WRITE(7,160)
      READ(5,210) SSQRCM
C
C     Normalize with respect to the largest diffusion coefficient.
C
      DMAX=AMAX1(DP,DQ,DR)
      DBARP=DP/DMAX
      DBARQ=DQ/DMAX
      DBARR=DR/DMAX
C
C     Generate matrix of simultaneous equations for the concen-
C     trations of species P, Q and R at the collocation points.
C
      CALL GENAB(N,ND,ROOTS,AMAT,BMAT)
C
      NR=3*N
      NT=N+2
      CTBL3=0.51023*CTBL**3
C
      DO 10 I=1,N
         I1=I+1
         IN=I+N
         AXVEL=CTBL3*ROOTS(I1)**2
         AXVELP=AXVEL/DBARP
         AXVELQ=AXVEL/DBARQ
         AXVELR=AXVEL/DBARR
         BOUND(I)=-BMAT(I1,NT)-AXVELP*AMAT(I1,NT)
         BOUND(IN)=0.
         TEMP=(BMAT(I1,1)+AXVELR*AMAT(I1,1))/AMAT(1,1)/DBARR
         BOUND(IN+N)=TEMP*DBARP*AMAT(1,NT)
         CONCS(I)=BOUND(I)
         DO 10 J=1,N
            J1=J+1
            JN=J+N
            JNN=JN+N
            TEMP1=TEMP*AMAT(1,J1)
            PMAT(I,J)=AXVELP*AMAT(I1,J1)+BMAT(I1,J1)
            QMAT(I,J)=AXVELQ*AMAT(I1,J1)+BMAT(I1,J1)
            RMAT(I,JNN)=AXVELR*AMAT(I1,J1)+BMAT(I1,J1)
            RMAT(I,J)=-DBARP*TEMP1
            RMAT(I,JN)=-DBARQ*TEMP1
            RMAT(I,JNN)=RMAT(I,JNN)-TEMP1*DBARR
10    CONTINUE
C
C     Calculate concentrations at the collocation points in the
C     absence of a homogeneous reaction as a first approximation.
C
      CALL ARRAY(2,N,N,NE,NE,RJCBMX,PMAT)
      CALL SIMQ(RJCBMX,CONCS,N,KS)
      IF(KS.EQ.1) GOTO 99
C
      DO 15 I=1,N
         IN=I+N
         CONCS(IN)=0.
```

```
            CONCS(IN+N)=1.-CONCS(I)
   15  CONTINUE
C
C      Pack coefficient matrices.
C
       CALL ARRAY(2,N,N,NE,NE,PMATV,PMAT)
       CALL ARRAY(2,N,N,NE,NE,QMATV,QMAT)
       CALL ARRAY(2,N,NR,NE,NF,RMATV,RMAT)
C
C      Input kinetic parameter and damping factor.
C
   20  NITS=1
       WRITE(7,140)
       READ(5,210) PARKIN
       WRITE(7,145)
       READ(5,210) GAMMA
       WRITE(7,150)
       READ(5,220) IPRINT
       CKTCOF=PARKIN*CTBL**2
C
C      Save previously determined concentrations and load boundary
C      vectors.  This is the starting point for the iteration.
C
   25  DO 30 I=1,NR
            PCONCS(I)=CONCS(I)
   30  CONTINUE
C
C      Compute residual vector (stored in CONCS).
C
       N1=N+1
       N2=N1+N
       CALL GMPRD(RMAT,PCONCS,CONCS,N,N,1)
       CALL GMSUB(CONCS,BOUND,CONCS,N,1)
       CALL GMPRD(QMAT,PCONCS(N1),CONCS(N1),N,N,1)
       CALL GMSUB(CONCS(N1),BOUND(N1),CONCS(N1),N,1)
       CALL GMPRD(RMAT,PCONCS,CONCS(N2),N,NR,1)
       CALL GMSUB(CONCS(N2),BOUND(N2),CONCS(N2),N,1)
C
C      Include the kinetic terms.
C
       DO 35 I=1,N
            IN=I+N
            TERM=CKTCOF*PCONCS(I)*PCONCS(IN+N)
            CONCS(I)=CONCS(I)-TERM/DBARP
            CONCS(IN)=CONCS(IN)+2.*TERM/DBARQ
            CONCS(IN+N)=CONCS(IN+N)-TERM/DBARR
   35  CONTINUE
C
C      Compute Jacobian for species P.
C
       NX2=N*2
       NN=N+N
       DO 40 I=1,NN
            RJCBMX(I)=PMATV(I)
   40  CONTINUE
C
       DO 45 I=1,N
            II=(I-1)*N+I
            RJCBMX(II)=RJCBMX(II)-CKTCOF*PCONCS(NX2+I)/DBARP
   45  CONTINUE
```

```
C
C       Compute correction terms.
C
        CALL SIMQ(RJCBMX,CONCS(1),N,KS)
        IF(KS.EQ.1) GOTO 99
C
C       Repeat for species Q.
C
        DO 50 I=1,NN
            RJCBMX(I)=QMATV(I)
  50    CONTINUE
C
        CALL SIMQ(RJCBMX,CONCS(N1),N,KS)
        IF(KS.EQ.1) GOTO 99
C
C       And for species R.
C
        IOFF=2*NN
        DO 60 I=1,NN
            RJCBMX(I)=RMATV(IOFF+I)
  60    CONTINUE
C
        DO 65 I=1,N
            II=(I-1)*N+I
            RJCBMX(II)=RJCBMX(II)-CKTCOF*PCONCS(I)/DBARR
  65    CONTINUE
C
        CALL SIMQ(RJCBMX,CONCS(N2),N,KS)
        IF(KS.EQ.1) GOTO 99
C
C       Calculate new estimates for concentrations and determine
C       the sum of the squared corrections.
C
        SSQRC=0.
        DO 70 I=1,NR
            SSQRC=SSQRC+CONCS(I)**2
            CONCS(I)=PCONCS(I)-CONCS(I)
            CONCS(I)=CONCS(I)+GAMMA*PCONCS(I)-GAMMA*CONCS(I)
  70    CONTINUE
C
        IF(IPRINT.NE.1) GOTO 72
        WRITE(7,180) NITS
        WRITE(7,185) (ROOTS(I+1),CONCS(I),CONCS(I+N),CONCS(I+NX2),
     &                I=1,N)
C
  72    IF (SSQRC.LE.SSQRCM) GO TO 75
            NITS=NITS+1
            GOTO 25
C
C       Calculate surface concentration gradients.
C
  75    CALL SCGRD1(N,ND,NF,DBARP,DBARQ,DBARR,AMAT,CONCS,GRADP,
     &              GRADQ,GRADR,CR0)
C
C       Print results along with final concentrations.
C
        WRITE(7,180) NITS
        WRITE(7,185) 0.,0.,0.,CR0
        WRITE(7,185) (ROOTS(I+1),CONCS(I),CONCS(I+N),CONCS(I+NX2),
     &                I=1,N)
```

```fortran
      WRITE(7,185) 1.,1.,0.,0.
      WRITE(4,185) 0.,0.,0.,CRO
      WRITE(4,185) (ROOTS(I+1),CONCS(I),CONCS(I+N),CONCS(I+NX2),
     &             I=1,N)
      WRITE(4,185) 1.,1.,0.,0.
      WRITE(7,190) GRADP
      WRITE(7,191) GRADQ
      WRITE(7,192) GRADR
C
C     Loop to repeat program.
C
      WRITE(7,195)
      READ(5,220) ILOOP
      IF ('ILOOP .EQ. 0) GOTO 80
          GOTO 20
  80  CONTINUE
      STOP
C
C     Error exit for singular matrices.
C
  99  WRITE(7,999)
      STOP
C
C     Format Statements
C
 100  FORMAT('0',10X,'Consecutive Electron Transfer with Repro
     &portionation',/,/,26X,'at the Steady State RDE',/,/,
     &' Version V03-A',50X,9A1,/)
 110  FORMAT(' ','Enter degree of collocation polynomial (I2).   ',$)
 115  FORMAT(' ','Enter diffusion coefficient for species P.    ',$)
 120  FORMAT(' ','Enter diffusion coefficient for species Q.    ',$)
 130  FORMAT(' ','Enter diffusion coefficient for species R.    ',$)
 140  FORMAT(' ','Enter value of kinetic parameter.    ',$)
 145  FORMAT(' ','Enter value of weighting factor.    ',$)
 150  FORMAT(' ','Enter 1 for extended output.    ',$)
 160  FORMAT(' ','Enter convergence criterion.    ',$)
 180  FORMAT('0','Number of Iterations:',I6,/,/,7X,'Root',11X,
     &' Conc. P',9X,'Conc. Q',9X,'Conc. R',/)
 185  FORMAT(4(1PE15.6,1X))
 190  FORMAT('0','Surface Concentration Gradient of Species P:  ',
     &1PE15.6)
 191  FORMAT('0','Surface Concentration Gradient of Species Q:  ',
     &1PE15.6)
 192  FORMAT('0','Surface Concentration Gradient of Species R:  ',
     &1PE15.6)
 195  FORMAT('0','Enter 1 to repeat, 0 to terminate.   ',$)
 200  FORMAT(I2)
 210  FORMAT(G15.8)
 220  FORMAT(I1)
 999  FORMAT('0','Singular matrix encountered...execution ends.',/)
C
      END
```

```
C
C
C      Title:  Concentration Profiles for the RDE.
C
C      Author:  J. Nolan                          Date: 22-Nov-86
C
C      Source File: CONPRO.SNG      Object File: CONPRO.OBJ
C
       PROGRAM CONPRO
C
C      Purpose:
C
C           This program recovers the coefficients of the approxi-
C      mation polynomial relating concentration to distance given
C      a set of collocation points and the corresponding concen-
C      trations.  It then uses these coefficients to generate a
C      concentration profile over a specified interval.
C
C      Modifications:  None.
C
C      External References:
C
C          Fn/Sr              Src File        Obj Fi
C
C      Subroutine ARRAY     ARRAY.FOR         MATLIB.OBJ
C      Subroutine SIMQ      SIMQ.FOR          MATLIB.OBJ
C      Subroutine PVAL      PVAL.FOR          MATLIB.OBJ
C      Subroutine ASSIGN    N/A               FORLIB.OBJ
C
C      Variable Declarations:
C
       IMPLICIT REAL*4 (A-H,O-Z)
       DIMENSION ROOTS(20),CCNCS(20   ),COEFFS(20,3),CVCT(3),
     &           QMAT(20,20),TMAT(20,20)
       EQUIVALENCE (COEFFS(1,1),CCNCS(1,1))
C
C          Input:
C
C          NCNPR - Number of concentration profiles.
C          NROOTS - Number of collocation points.
C          ROOTS - Vector containing collocation points.
C          CCNCS - Concentrations at the collocation points.
C          XLO - Lower bound for concentration profile.
C          XHI - Higher bound for concentration profile.
C          XINC - Step size for concentration profile.
C          NPTS - Number of points for concentration profile.
C
C          Output:
C
C          QMAT - Polynomial factor matrix.
C          COEFFS - Coefficients of the approximation polynomial
C                   (equivalenced to CCNCS).
C          TMAT - Scratch matrix.
C          CVCT - Concentrations of species at distance X.
C
C      Logical Units Referenced:
C
C          3 = File Input
C          4 = Plot File
C          5 = Terminal Input
C          6 = Terminal Output
```

```
C
C
C       Executable Code
C
C       Open data file and read collocation points and corres-
C       ponding concentrations.
C
        WRITE (7,100)
        CALL ASSIGN(3,'DK1:A',-1)
        WRITE (7,110)
        READ (5,200) NCNPR
C
        NROOTS=0
        ND=20
C
        DO 10 I=1,ND
             READ(3,210,END=20) ROOTS(I),(CCNCS(I,J),J=1,NCNPR)
             NROOTS=NROOTS+1
   10   CONTINUE
C
C       Open plot file.
C
   20   WRITE (7,120)
        CALL ASSIGN(4,'DK1:A',-1)
C
C       Generate factor matrix.
C
        DO 30 I=1,NROOTS
             QMAT(I,1)=1.D0
             DO 30 J=2,NROOTS
                  QMAT(I,J)=QMAT(I,J-1)*ROOTS(I)
   30   CONTINUE
C
C       Calculate and list the coefficients of approximation
C       polynomials.
C
        DO 40 ICNPR=1,NCNPR
             CALL ARRAY(2,NROOTS,NROOTS,ND,ND,TMAT,QMAT)
             CALL MQ(TMAT,CCNCS(1,ICNPR),NROOTS,KS)
             IF (KS.EQ. 1) GOTO 99
   40   CONTINUE
C
        WRITE (7,130)
        DO 45 I=1,NROOTS
             WRITE (7,220) I-1,(COEFFS(I,J),J=1,NCNPR)
   45   CONTINUE
C
C       Input limits for the evaluated concentration profile.
C
        WRITE(7,140)
        READ(5,230) XLO
        WRITE(7,150)
        READ(5,230) XHI
        WRITE(7,160)
        READ(5,230) XINC
C
C       Initialise calculation loop.
C
        NPTS=INT(ABS(XHI-XLO)/XINC+0.5)+1
        IF(XLO.GT.XHI) XINC=-1.*ABS(XINC)
C
```

```
      WRITE(7,170)
C
      DO 60 I=1,NPTS
          X=XLO+(FLOAT(I-1))*XINC
          DO 50 J=1,NCNPR
              CALL PVAL(CVCT(J),X,COEFFS(1,J),NROOTS)
50        CONTINUE
          WRITE(7,210) X,(CVCT(J),J=1,NCNPR)
          WRITE(4,210) X,(CVCT(J),J=1,NCNPR)
60    CONTINUE
C
      STOP
C
99    WRITE(7,180)
      STOP
C
C     Format Statements.
C
100   FORMAT('0',5X,'***RDE Concentration Profiles***',/,/,
     & ' Enter the input datafile name.    ',$)
110   FORMAT(' ','Enter the number of species.    ',$)
120   FORMAT(' ','Enter the output datafile name.    ',$)
130   FORMAT(' ','Coefficients of the approximation polynomials
     & are:',/)
140   FORMAT('0','Enter the lower bound of the concentration
     & profile.    ',$)
150   FORMAT(' ','Enter the upper bound of the concentration
     & profile.    ',$)
160   FORMAT(' ','Enter the increment size.    ',$)
170   FORMAT('0','Concentration profiles as a function of distance
     & are:',/)
180   FORMAT('0','Singular factor matrix encountered...execution
     & terminated.')
200   FORMAT(I2)
210   FORMAT(4(1PE16.6))
220   FORMAT(I5,3(1PE15.6,1X))
230   FORMAT(G15.8)
C
      END
```

```
C
C
C     Title:  Kinetic Parameter Calculation Program
C
C     Author:  J. Nolan                        Date:  16-Dec-86
C
C     Source File:  KPRCAL.FOR,     Object File:  KPRCAL.OBJ
C
      PROGRAM KPRCAL
C
C     Purpose:
C
C         This program determines kinetic parameters for second-
C     order EC catalytic reactions given experimental data and
C     the appropriate working curve (i.e., current ratios as a
C     function of kinetic parameter).  The approximate kinetic
C     parameter is located by a binary search and a refined esti-
C     mate is obtained by Lagrangian interpolation.
C
C     Modifications:
C
C     Added filename prompts and program repeat loop  (06-Jan-87)
C     Altered display format and error handling  (19-Sep-87)
C     Modified program repeat loop and added date and version
C     number (V01-C) to output.  (26-May-88)
C
C     External References:
C
C         Fn/Sr           Src File          Obj File
C
C     Function ABS        N/A               FORLIB.OBJ
C     Subroutine DATE     N/A               FORLIB.OBJ
C     Subroutine ASSIGN   N/A               FORLIB.OBJ
C     Subroutine CLOSE    N/A               FORLIB.OBJ
C     Subroutine BINSEA   BINSEA.FOR        BINSEA.OBJ
C     Subroutine ARRAY    ARRAY.FOR         MATLIB.OBJ
C     Subroutine SIMQ     SIMQ.FOR          MATLIB.OBJ
C     Subroutine PVAL     PVAL.FOR          MATLIB.OBJ
C
C     Variable Declarations:
C
      DIMENSION RVALS(1000),FMAT(4,4),COEFFS(4)
      LOGICAL*1 DATARR(9)
C
C         Input:
C
C     RVALS - Current ratios for working curve.
C     Y0,Y1 - First and last entries for kinetic parameter
C             on working curve.
C     NWCP - Number of points  on working curve.
C     YINCR - Kinetic parameter step size.
C     N - Degree of interpolation polynomial.
C     W - Rotation speed in rpm.
C     CLSST - Roundoff criterion.
C     FMAT - Factor matrix for Lagrangian interpolation.
C
C         Output:
C
C     DATARR - Current date (DD-MMM-YY).
C     OMEGAL - Log (base 10) of angular velocity.
C     INRST - Index of nearest point on working curve.
```

```
C      COEFFS - Coefficients of interpolation polynomial.
C      RLOGKP - Log (base 10) of kinetic parameter.
C      RKP - Kinetic parameter.
C
C      Logical Units Referenced:
C
C          3 = Working Curve Data
C          4 = Experimental Data
C          5 = Terminal Input
C          6 = Terminal Output
C
C      Executable Code
C
C      Program header and prompt for working curve file name.
C
       CALL DATE(DATARR)
       WRITE(7,100) (DATARR(I),I=1,9)
C
     5 WRITE(7,105)
       CALL ASSIGN(3,'DK1:A',-1)
C
       NWCP=1
       READ(3,200) Y0,RVALS(1)
       DO 10 I=2,1000
           READ(3,200,END=20) Y1,RVALS(I)
           NWCP=NWCP+1
    10 CONTINUE
C
    20 YINCR=ABS((Y1-Y0)/FLOAT(NWCP-1))
       CLSST=0.25*YINCR
C
C      Beginning of calculation loop.  Input data.
C
    25 WRITE(7,110)
       CALL ASSIGN(4,'DK1:A',-1)
C
       WRITE(7,115)
C
    30 READ(4,210,END=70) W,C0,C1
       R=C0/C1
C
C      Find index of nearest R value on working curve.
C
       CALL BINSEA(R,RVALS,INRST,NWCP)
C
C      Print message and go to next point if current ratio is out
C      of the range over which valid interpolation may be carried
C      out.
C
       IF (INRST.LT.3) GOTO 98
       IF ((INRST+2).GT.NWCP) GOTO 98
C
C      Compute base index for polynomial interpolation.  (If R
C      value falls about midway between two points on working
C      curve four points are used for interpolation.  Otherwise
C      three are used.)
C
       N=3
       IBASE=INRST-1
       IF(ABS(R-RVALS(INRST)).LE.CLSST) GOTO 40
```

```
          N=4
          IF(R.LT.RVALS(INRST)) GOTO 40
                IBASE=IBASE-1
C
C     Compute factor matrix.  Note that the interpolation is
C     carried out relative to the kinetic parameter corresponding
C     to IBASE.
C
  40   DO 50 I=1,N
          COEFFS(I)=FLOAT(I-1)*YINCR
          FMAT(I,1)=1.
          TEMP=RVALS(IBASE+I-1)
          DO 50 J=2,N
                FMAT(I,J)=FMAT(I,J-1)*TEMP
  50   CONTINUE
C
C     Solve for polynomial coefficients.
C
       IF(N.EQ.4) GOTO 60
          CALL ARRAY(2,N,N,4,A,FMAT,FMAT)
C
  60   CALL SIMQ(FMAT,COEFFS,N,KS)
       IF(KS.EQ.1) GOTO 99
C
C     Compute the value of log (KP) corresponding to R.
C
       CALL PVAL(YOFFST,R,COEFFS,N)
       RLOGKP=Y0+FLOAT(IBASE-1)*YINCR+YOFFST
C
C     Calculate remaining parameters and print.
C
       OMEGAL=ALOG10(0.1047198*W)
       RKP=10.**RLOGKP
       WRITE(7,120) W,R,OMEGAL,RLOGKP,RKP
       GOTO 30
C
  70   CALL CLOSE(4)
       WRITE(7,150)
       READ(5,220) ILOOP
C
       WRITE(7,160)
       GOTO (90,80,25) ILOOP+1
C
  80   CALL CLOSE(3)
       GOTO 5
C
  90   STOP
C
C     Error messages.
C
  98   WRITE(7,130) W,R
       GOTO 30
C
  99   WRITE(7,140) W,R
       GOTO 30
C
C     Format Statements
C
 100   FORMAT(' ',19X,'***Kinetic Parameter Evaluation***',/,
      &        ' Version V01-C',50X,9A1,/,/)
```

```
105 FORMAT(' ','Enter working curve file name.  ',$)
110 FORMAT(' ','Enter input data file name.  ',$)
115 FORMAT(' ',5X,'W',10X,'R',13X,'Log(w)',9X,'Log K.P.',10X,
   &'K.P.',/)
120 FORMAT(' ',F8.1,4(1PE16.8))
130 FORMAT(' ',F8.1,1PE16.8,2X,'Current ratio out of range.')
140 FORMAT(' ',F8.1,1PE16.8,2X,'Singular matrix encountered.')
150 FORMAT('0','Enter 0 to stop, 1 for new working curve, 2 for new
   & data.  ',$)
160 FORMAT(' ')
200 FORMAT(2E16.8)
210 FORMAT(3G15.8)
220 FORMAT(I1)
C
      END
C
C     Title:  Binary Search Routine
C
C     Author:  J. Nolan                    Date:  16-Dec-86
C
C     Source File: BINSEA.FOR       Object File:  BINSEA.OBJ
C
      SUBROUTINE BINSEA(X,XLIST,INDEX,LLEN)
C
C     Purpose:
C
C         This routine searches a list sorted in either ascending
C     or descending order.  It returns the index of the nearest
C     match to the search term.  If the list does not encompass
C     the search term an index of -1 is returned.
C
C     Modifications: None.
C
C     External References:
C
C         Fn/Sr              Src File          Obj File
C
C     Function SIGN, INT N/A                    FORLIB.OBJ
C
C     Variable Declarations:
C
      DIMENSION XLIST(1)
C
C         Input:
C
C         X - Search term.
C         XLIST - List to be searched.
C         LLEN - Length of list.
C
C         Output:
C
C         INDEX - Index of search term.
C
C     Executable Code
C
      INDEX=-1
      ISIGN=INT(SIGN(1.,XLIST(LLEN)-XLIST(1)))
      ITOP=LLEN
      IBOT=1
C
```

```fortran
C        Reverse assignments if list is descending order.
C
      IF(ISIGN.EQ.1.) GOTO 10
         ITOP=1
         IBOT=LLEN
C
C        Return if search term not in range of list.
C
      IF(X.GT.XLIST(ITOP)) RETURN
      IF(X.LT.XLIST(IBOT)) RETURN
C
 15   IF(IABS(ITOP-IBOT).LE.1) GOTO 30
      IMID=(ITOP+IBOT)/2
C
      IF(X-XLIST(IMID)) 20,25,25
 20   ITOP=IMID
      GOTO 15
 25   IBOT=IMID
      GOTO 15
C
C        Determine which index is closest to target value.
C
 30   INDEX=IBOT
      NXTIND=ISIGN+INDEX
      XCLOSE=XLIST(NXTIND)-XLIST(INDEX)
      XCLOSE=ABS((X-XLIST(INDEX))/XCLOSE)
      IF(XCLOSE.GT.0.5) INDEX=NXTIND
      RETURN
C
      END
```

```
C
C    Title:    Orthogonal Collocation--Calculation of the
C              Concentrations at the Collocation Points.
C
C    Author:  J. Nolan                        Date:   22-Sep-86
C
C    Source File:  CONSL1.SNG       Object File:  DGSPLB.OBJ
C
     SUBROUTINE CONSL1(N,NE,NR,CMAT,BOUND)
C
C    Purpose:
C
C         This routine solves the system of linear equations
C    describing concentrations at the collocation points.
C
C    Modifications:  None.
C
C    External References:
C
C         Fn/Sr            Src File          Obj File
C
C    Subroutine SIMQ      SIMQ.FOR          MATLIB.OBJ
C    Subroutine ARRAY     ARRAY.FOR         MATLIB.OBJ
C
C    Variable Declarations:
C
     IMPLICIT REAL*4 (A-H,O-Z)
     DIMENSION BOUND(NE),CMAT(NE,NE)
C
C        Input:
C
C         N - Order of the collocation polynomial.
C         NR - Number of simultaneous equations.
C         NE - Dimension of arrays in calling program.
C         CMAT - Matrix containing the system of simultaneous
C              equations generated.
C         BOUND - Vector containing boundary conditions.
C
C        Output:
C
C         CMAT - Matrix containing the remnants of the Gaussian
C              elimination procedure of subroutine SIMQ.
C         BOUND - Vector containing concentrations at the colloc-
C              ation points.
C
C    Executable Code
C
C    Solve for concentrations at the collocation points.
C
     CALL ARRAY(2,NR,NR,NE,NE,CMAT,CMAT)
C
     CALL SIMQ(CMAT,BOUND,NR,KS)
C
C    If KS = 1, CMAT is singular.
C
     IF (KS .EQ. 1) GOTO 99
C
     RETURN
C
C    Error exit for singular matrices.
```

```
C
 99   WRITE(7,100)
      STOP
C
100   FORMAT('0','Execution terminated...singular matrix encountered
     &  in Subroutine CONSL1.',/,/)
C
      END
```

```
C
C
C       Title:  Orthogonal Collocation--Calculation of the Surface
C                     Concentration Gradient of Species P.
C
C       Author:  J. Nolan                        Date:  20-Oct-86
C
C       Source File:  CSCGP.SNG        Object File:  DGSPL8.OBJ
C
        SUBROUTINE CSCGP(N,ND,NE,DBARP,DBARQ,CRATIO,AMAT,CONCS,CPO,
     &             GRAD)
C
C       Purpose:
C
C           This routine calculates the surface concentration and
C       surface concentration gradient of species P given the
C       concentrations of species P and Q at the interior collocation
C       points.
C
C       Modifications:  None.
C
C       Variable Declarations:
C
        IMPLICIT REAL*4 (A-H,O-Z)
        DIMENSION AMAT(ND,ND),CONCS(NE)
C
C       Input:
C
C           N - Order of the collocation polynomial.
C           ND,NE - Correspond to the array dimensions in the
C                   calling program.
C           CRATIO - Concentration ratio (P/Q) at Z = 0.
C           DBARP - Normalized diffusion coefficient of species P.
C           DBARQ - Normalized diffusion coefficient of species Q.
C           CONCS - Concentrations of P and Q at the N interior
C                   collocation points.
C           AMAT - Coefficient matrix for the first derivative
C                   of concentration with respect to distance.
C
C       Output:
C
C           CPO - Concentration of species P at Z = 0.
C           GRAD - Concentration gradient of species P at Z = 0.
C
C       Executable Code
C
C       Calculate the surface concentration.
C
        NT=N+2
        CPO=0.
        DO 10 J=1,N
            J1=J+1
            JN=J+N
            CPO=CPO+AMAT(1,J1)*(DBARP*CONCS(J)+DBARQ*CONCS(JN))
  10    CONTINUE
        CPO=CPO+AMAT(1,NT)*DBARP
        CPO=-CRATIO*CPO/(AMAT(1,1)*(CRATIO*DBARP+DBARQ))
        CP1=1.
C
C
C       Calculate the concentration gradient.
C
```

```
      GRAD=0.
      DO 20 J=1,N
         J1=J+1
         GRAD=GRAD+AMAT(1,J1)*CONCS(J)
20    CONTINUE
      GRAD=GRAD+AMAT(1,1)*CP0+AMAT(1,NT)*CP1
C
      RETURN
C
      END
```

```
C
C
C        Title:   Orthogonal Collocation--Differentiation and
C                       Gaussian Quadrature Weights.
C
C        Authors: -
C
C           Villadsen, J. and Michelsen, M.L., "Solution of
C        Differential Equation Models by Polynomial Approximation",
C        Englewood Cliffs, N.J.:  Prentice-Hall, Inc., 1978, pp.
C        133f., 419.
C
C        Source File:  DFOPR.SNG         Object File:  DGSPLB.OBJ
C
         SUBROUTINE DFOPR(ND,N,N0,N1,I,ID,DIF1,DIF2,DIF3,ROOT,VECT)
C
C        Purpose:
C           Subroutine evaluates discretization matrices and Gaussian
C        quadrature weights normalized to sum 1.
C
C        Modifications:  None.
C
C        External References:  None.
C
C        Variable Declarations:
C
         IMPLICIT REAL*4 (A-H,O-Z)
         DIMENSION DIF1(ND),DIF2(ND),DIF3(ND),ROOT(ND),VECT(ND)
C
C           Input:
C
C              ND - Dimension of output vectors.
C              N  - Degree of Jacobi polynomial.
C              N0 - X = 0 included? (Y=1, N=0).
C              N1 - X = 1 included? (Y=1, N=0).
C              ID - Indicator
C                   = 1 :  Discretization matrix for Y(1) (X)
C                   = 2 :  Discretization matrix for Y(2) (X)
C                   = 3 :  Gaussian quadrature weights
C              AL,BE - Values of alpha and beta.
C              ROOT - Vector containing the N+N0+N1 zeros of
C                     the node polynomial.
C              DIF1, DIF2, DIF3 - Vectors containing the first,
C                     second and third derivatives of the node
C                     polynomial.
C
C           Output:
C
C              VECT - Computed vector of weights.
C
C        Executable Code
C
         NT=N+N0+N1
         IF (ID .EQ. 3) GOTO 10
         DO 20 J=1,NT
         IF (J .NE. I) GOTO 21
         IF (ID .NE. 1) GOTO 5
         VECT(I)=DIF2(I)/DIF1(I)/2.
         GOTO 20
   5     VECT(I)=DIF3(I)/DIF1(I)/3.
         GOTO 20
```

```
21   Y=ROOT(I)-ROOT(J)
     VECT(J)=DIF1(I)/DIF1(J)/Y
     IF (ID .EQ. 2) VECT(J)=VECT(J)*(DIF2(I)/DIF1(I)-2./Y)
20   CONTINUE
     GOTO 50
10   Y=0.
     DO 25 J=1,NT
     X=ROOT(J)
     AX=X*(1.-X)
     IF (NO .EQ. 0) AX=AX/X/X
     IF (N1 .EQ. 0) AX=AX/(1.-X)/(1.-X)
     VECT(J)=AX/DIF1(J)**2
25   Y=Y+VECT(J)
     DO 60 J=1,NT
60   VECT(J)=VECT(J)/Y
C
50   RETURN
     END
```

```
C
C
C      Title:   Orthogonal Collocation--Computation of the
C                 Discretization Matrices A and B.
C
C      Author:  J. Nolan                    Date:   10-Jul-86
C
C      Source File:  GENAB.SNG        Object File:  DGSPLB.OBJ
C
       SUBROUTINE GENAB(N,ND,ROOTS,AMAT,BMAT)
C
C      Purpose:
C
C          This routine generates the coefficient matrices for
C      the first and second derivatives of concentration with
C      respect to distance.  Derivatives are evaluated at each
C      of roots of the collocation polynomial of degree N as well
C      as at the points 0 and 1.
C
C      Modifications:
C
C      1.  Redimensioned for N<=26 (V01-B,01-Jun-88).
C
C      External References:
C
C         Fn/Sr            Src File        Obj File
C
C      Subroutine JCOBI     JCOBI.SNG       DGSPLB.OBJ
C      Subroutine DFOPR     DFOPR.SNG       DGSPLB.OBJ
C
C      Variable Declarations:
C
       IMPLICIT REAL*4 (A-H,O-Z)
       DIMENSION ROOTS(ND),AMAT(ND,ND),BMAT(ND,ND)
       DIMENSION DIF1(26),DIF2(26),DIF3(26),WORKV(26)
C
C        Input:
C
C        N - Order of the collocation polynomial.
C        ND - Array dimensions.
C
C        Output:
C
C        ROOTS - Roots of the collocation polynomial.
C        DIF1,DIF2,DIF3 - Vectors containing the first, second
C                 and third derivatives of the node polynomial at
C                 the collocation points.
C        AMAT,BMAT - Discretization matrices containing the
C                 coefficients for the first and second derivatives
C                 of the concentration profile.
C
C      Data Statements:
C
       DATA AL,BE,NO,N1 /0.,0.,1,1/
C
C        AL=BE=0 means Legendre polynomials evaluated by JCOBI.
C        NO=N1=1 means X = 0 and X = 1 are included as inter-
C                 polation points.
C
C      Executable Code
C
```

```
C       Calculate roots and derivatives of Legendre polynomial of
C       degrée N.
C
      CALL JCOBI(NQ,N,NO,N1,AL,BE,DIF1,DIF2,DIF3,ROOTS)
C
C       Evaluate coefficients of discretization matrices A and B.
C
      NT=N+NO+N1
      DO 20 I=1,NT
          CALL DFOPR(ND,N,NO,N1,I,1,DIF1,DIF2,DIF3,ROOTS,WORKV)
          DO 10 J=1,NT
              AMAT(I,J)=WORKV(J)
   10     CONTINUE
          CALL DFOPR(ND,N,NO,N1,I,2,DIF1,DIF2,DIF3,ROOTS,WORKV)
          DO 20 J=1,NT
              BMAT(I,J)=WORKV(J)
   20 CONTINUE
C
      RETURN
C
      END
```

```
C
C      Title:    Second Order EC-Catalytic Mechanism at the RDE.
C                Numerical Solution by Global Spline Collocation.
C
C      Author:   J. Nolan                        Date:   12-Mar-87
C
C      Source File:  GSECR3.SNG      Object File:  DGSPLB.OBJ
C
       SUBROUTINE GSECR3(N,ND,ROOTS,AMAT,BMAT,DVRAT,DBARP,DBARQ,
      &            CRATIO,DBARA,CBARA,SSQRCM,PARKIN,NITS,GRAD)
C
C      Purpose:
C
C           This routine uses global spline collocation to obtain
C      the steady-state solution to the differential equations
C      describing the second-order EC-Catalytic mechanism at the
C      RDE.  Formulation of the boundary value problem is based
C      on Eddowes' treatment of the mass-transport-limited case
C      (J. Electroanal Chem., Vol. 159, p.1, 1983).  Implement-
C      ation of the orthogonal collocation technique follows
C      J. Villadsen and M.L. Michelsen, "Solution of Differential
C      Equation Models by Polynomial Approximation", Englewood
C      Cliffs, N.J.: Prentice-Hall, Inc., 1978.
C           The program returns the surface concentration gradient
C      of species P as well as the number of iterations required
C      for convergence.  Note that the spline point is re-evaluated
C      at the end of the run using the calculated value of GRAD.
C      This spline point is used when this routine is next called.
C
C      Modifications:
C
C      1.  Revised calculation of spline point (V01-B,26-Jun-88).
C
C      External References:
C
C          Fn/Sr           Src File         Obj File
C
C      Subroutine RDCDSP    RDCDSP.SNG       DGSPLB.OBJ
C      Subroutine HSCDSP    HSCDSP.SNG       DGSPLB.OBJ
C      Subroutine KTCDSP    KTCDSP.SNG       DGSPLB.OBJ
C      Subroutine ARRAY     ARRAY.FOR        MATLIB.OBJ
C      Subroutine SIMQ      SIMQ.FOR         MATLIB.OBJ
C      Function AMAX1       N/A              FORLIB.OBJ
C
C      Variable Declarations:
C
       IMPLICIT REAL*4 (A-H,O-Z)
       DIMENSION ROOTS(ND),AMAT(ND,ND),BMAT(ND,ND),PCNCS(60),
      &          CNCS(60),CMAT(60,60),BOUND(60),PCNCSA(30),
      &          CNCSA(30),CMATA(30,30),BOUNDA(30)
       EQUIVALENCE (CNCS(1),BOUND(1)),(CNCSA(1),BOUNDA(1))
C
C      Input:
C
C          N - Order of the collocation polynomial (N<=14).
C          NR - Number of simultaneous equations.
C          CRATIO - Surface concentration ratio (P/Q).
C          DBARP - Normalized diffusion coefficient of species P.
C          DBARQ - Normalized diffusion coefficient of species Q.
C          DBARA - Normalized diffusion coefficient of species A.
```

```
C        DVRAT - Ratio of the largest diffusion coefficient to
C                the kinematic viscosity (=1/Sc).
C        CBARA - Concentration of species A normalized to that
C                of P.
C        PARKIN - Kinetic parameter.
C        CTBL - Transport boundary layer coefficient.
C        SPLPT - Spline point.
C        SSQRCM - Convergence criterion, defined as the sum of
C                the squares of the corrections between successive
C                iterations.
C        ROOTS - Roots of the collocation polynomial.
C        AMAT,BMAT - Discretization matrices containing the
C                coefficients for the first and second derivatives
C                of the concentration profile.
C
C     Output:
C
C        GRAD - Surface concentration gradient of species P.
C               (with respect to the spline point).
C        NITS - Number of iterations required for convergence.
C
C     Data Statements
C
      DATA CTBL,SPLPT0,SPLPT /3.6096,0.5,0.5/
      DATA PCNCSA,PCNCS /30*0.,60*0./
      NE=60
      NF=30
C
C     Executable Code
C
      NITS=1
      N2=N+2
      NR=4*N+4
      NR2=NR/2
C
      IF (PARKIN.EQ.0.) SPLPT=0.5
C
C     Generate the discretized transport equations for catalyst
C     couple as well as those for the substrate.  This is the
C     starting point for the iterative solution.
C
   10 CALL RDCDSP(N,ND,NE,ROOTS,AMAT,BMAT,DVRAT,DBARP,DBARQ,CRATIO,
     &            CTBL,SPLPT,CMAT,BOUND)
      CALL HSCDSP(N,ND,NF,ROOTS,AMAT,BMAT,DVRAT,DBARA,CBARA,CTBL,
     &            SPLPT,CMATA,BOUNDA)
C
C     Include the kinetic terms.
C
      CALL KTCDSP(N,NE,NF,PARKIN,DBARP,DBARQ,DBARA,CTBL,SPLPT,
     &            PCNCSA,PCNCS,CMATA,CMAT)
C
C     Solve for concentrations at the collocation points.
C
      CALL ARRAY(2,NR,NR,NE,NE,CMAT,CMAT)
      CALL SIMQ(CMAT,CNCS,NR,KS)
      IF (KS.EQ.1) GOTO 99
      CALL ARRAY(2,NR2,NR2,NF,NF,CMATA,CMATA)
      CALL SIMQ(CMATA,CNCSA,NR2,KS)
      IF (KS.EQ.1) GOTO 99
C
```

```
C       Determine the sum of the squared corrections and save
C       current concentrations.
C
        SSQRC=0.
        DO 20 I=1,NR2
            IN=I+NR2
C           SSQRC=SSQRC+(PCNCSA(I)-CNCSA(I))**2
            PCNCSA(I)=CNCSA(I)
            SSQRC=SSQRC+(PCNCS(I)-CNCS(I))**2
            PCNCS(I)=CNCS(I)
            SSQRC=SSQRC+(PCNCS(IN)-CNCS(IN))**2
            PCNCS(IN)=CNCS(IN)
 20     CONTINUE
C
        IF (SSQRC.LE.SSQRCM) GOTO 30
            NITS=NITS+1
            GOTO 10
C
C       Calculate concentration gradient of species P at Z = 0.
C
 30     GRAD=0.
        DO 40 J=1,N2
            GRAD=GRAD+AMAT(1,J)*CNCS(J)
 40     CONTINUE
        GRAD=GRAD/SPLPT
C
C       Update spline point.
C
        SPLPT=4./GRAD
        IF (SPLPT.GT.SPLPT0) SPLPT=SPLPT0
C
        RETURN
C
C       Error exit for singular matrices.
C
 99     WRITE(7,999)
        STOP
C
C       Format Statements
C
999     FORMAT('0','Singular matrix encountered in subroutine
      & GSECR3.',/,/)
C
        END
```

```
C
C
C      Title:  Second-Order EC-Catalytic Mechanism at the RDE.
C                  Transport Equations for the Substrate
C                         by Spline Collocation.
C
C      Author:   J. Nolan                    Date:   11-Mar-87
C
C      Source File:  HSCDSP.SNG        Object File:  DGSPLB.OBJ
C
       SUBROUTINE HSCDSP(N,ND,NE,ROOTS,AMAT,BMAT,DVRAT,DBARA,CBARA,
      &              CTBL,SPLPT,CMATA,BOUNDA)
C
C      Purpose:
C
C           This routine generates the system of equations des-
C      cribing the transport of the substrate species A as part of
C      the spline collocation solution of the second-order EC-
C      catalytic mechanism at the RDE.  The interval over which
C      the problem is defined is divided into two sub-intervals
C      at the spline point SPLPT.
C
C      Modifications:   None.
C
C      Variable Declarations:
C
       IMPLICIT REAL*4 (A-H,O-Z)
       DIMENSION ROOTS(ND),AMAT(ND,ND),BMAT(ND,ND),BOUNDA(NE),
      &           CMATA(NE,NE)
C
C          Input:
C
C          N - Order of the collocation polynomial.
C          ND,NE - Correspond to the array dimensions in the
C                  calling program.
C          ROOTS - Collocation points.
C          AMAT,BMAT - Discretization matrices containing the
C                  coefficients for the first and second deriv-
C                  atives of the concentration profile.
C          DVRAT - Ratio of diffusion coefficient (of species P)
C                  to kinematic viscosity.
C          DBARA - Diffusion coefficient of species A normalized
C                  to that of species P.
C          CBARA - Concentration of species A normalized to that
C                  of species P.
C          CTBL - Transport boundary layer coefficient.
C          SPLPT - Spline point.
C
C          Output:
C
C          CMATA - Coefficients for the system of equations
C                  describing the transport of species A.
C          BOUNDA - Vector containing corresponding constant terms.
C
C      Define statement function for axial velocity and parameters
C      for same.
C
       AXVEL(X,C1,C2)=CTBL3*(5.1023E-01+X*(C1+C2*X))*X**2
C
       DVR3A=1./3.
       DVR3A=(DVRAT*DBARA)**DVR3A
```

```
      C1A=-1.2032*DVR34
      C2A=1.3375*DVR34**2
      CTBL3=CTBL**3
C
      N1=N+1
      N2=N+2
      NR=2*N+2
      CSPLPT=1.-SPLPT
C
C     Zero simultaneous equation matrix.
C
      DO 10 I=1,NR
          DO 10 J=1,NR
              CMATA(I,J)=0.
  10  CONTINUE
C
C     Compute coefficients for first sub-interval.
C
      DO 20 I=1,N
          I1=I+1
          BOUNDA(I)=0.
          ROOT=ROOTS(I1)*SPLPT
          AXVELA=SPLPT*AXVEL(ROOT,C1A,C2A)/DBARA
          DO 20 J=1,N2
              CMATA(I,J)=BMAT(I1,J)+AXVELA*AMAT(I1,J)
  20  CONTINUE
C
C     Ditto for second sub-interval.
C
      DO 30 I=1,N
          I1=I+1
          I2=I+N
          ROOT=ROOTS(I1)*CSPLPT+SPLPT
          AXVELA=CSPLPT*AXVEL(ROOT,C1A,C2A)/DBARA
          BOUNDA(I2)=-CBARA*(BMAT(I1,N2)+AXVELA*AMAT(I1,N2))
          DO 30 J=1,N1
              J2=J+N1
              CMATA(I2,J2)=BMAT(I1,J)+AXVELA*AMAT(I1,J)
  30  CONTINUE
C
C     Continuity/condition for dA/dZ at the spline point.
C
      NA1=2*N+1
      IASP=N+2
      FACTR=SPLPT/CSPLPT
      BOUNDA(NA1)=AMAT(1,N2)*FACTR*CBARA
C
      DO 40 J1=1,N+1
          J2=IASP+J1-1
          CMATA(NA1,J1)=AMAT(N2,J1)
          CMATA(NA1,J2)=-AMAT(1,J1)*FACTR
  40  CONTINUE
C
      CMATA(NA1,IASP)=CMATA(NA1,IASP)+AMAT(N2,N2)
C
C     Boundary condition at Z = 0.
C
      NA1=NA1+1
      DO 50 J=1,N2
          CMATA(NA1,J)=AMAT(1,J)
```

```
   50   CONTINUE
C
      BOUNDA(NA1)=0.
C
      RETURN
C
      END
```

```
C
C
C     Title:   Second-Order EC-Catalytic Mechanism at the RDE.
C              Transport Equations for the Substrate.
C
C     Author:  J. Nolan                        Date:  25-Oct-86
C
C     Source File:  HSRCDE.SNG      Object File:  DGSPLB.OBJ
C
      SUBROUTINE HSRCDE(N,ND,NE,ROOTS,AMAT,BMAT,DVRAT,DBARA,CBARA,
     &                  CTBL,CMATA,BOUNDA)
C
C     Purpose:
C
C          This routine generates the system of equations
C     describing the transport of substrate species A.  It
C     incorporates the extended form of the axial velocity
C     equation.
C
C     Modifications:  None.
C
C     Variable Declarations:
C
      IMPLICIT REAL*4 (A-H,O-Z)
      DIMENSION ROOTS(ND),AMAT(ND,ND),BMAT(ND,ND),BOUNDA(NE),
     &          CMATA(NE,NE)
C
C         Input:
C
C         N - Order of the collocation polynomial.
C         NT - Number of collocation points (=N+2).
C         ND,NE - Correspond to the array dimensions in the
C                 calling program.
C         ROOTS - Collocation points.
C         AMAT,BMAT - Discretization matrices containing the
C                 coefficients for the first and second deriv-
C                 atives of the concentration profile.
C         DVRAT - Ratio of diffusion coefficient (of species P)
C                 to kinematic viscosity.
C         DBARA - Diffusion coefficient of species A normalized
C                 to that of species P.
C         CBARA - Concentration of species A normalized to that
C                 of species P.
C         CTBL - Transport boundary layer coefficient.
C
C         Output:
C
C         CMATA - Coefficients for the system of equations
C                 describing the transport of species A.
C         BOUNDA - Vector containing corresponding constant terms.
C
C     Define statement function for axial velocity and parameters
C     for same.
C
      AXVEL(X,C1,C2)=CTBL3*(5.1023E-01+X*(C1+C2*X))*X**2
C
      DVR3A=1./3.
      DVR3A=(DVRAT*DBARA)**DVR3A
      C1A=-1.2032*DVR3A
      C2A=1.3375*DVR3A**2
      CTBL3=CTBL**3
```

```
C
      NT=N+2
C
C     Generate the discretized transport equations for species A
C     at the collocation points.
C
      DO 10 I=1,N
         I1=I+1
         AXVELA=AXVEL(ROOTS(I1),C1A,C2A)/DBARA
         B1=(BMAT(I1,1)+AXVELA*AMAT(I1,1))/AMAT(1,1)
         B2=BMAT(I1,NT)+AXVELA*AMAT(I1,NT)
         BOUNDA(I)=(B1*AMAT(1,NT)-B2)*CBARA
         DO 10 J=1,N
            J1=J+1
            CMATA(I,J)=BMAT(I1,J1)+AXVELA*AMAT(I1,J1)-
     &               B1*AMAT(1,J1)
 10   CONTINUE
C
      RETURN
C
      END
```

```
C
C
C      Title:  Roots and Derivatives of Jacobi Polynomials
C      Authors:
C
C          Villadsen, J. and Michelsen, M.L., "Solution of
C      Differential Equation Models by Polynomial Approximation",
C      Englewood Cliffs, N.J.:  Prentice-Hall, Inc., 1978, pp.
C      131f., 418.
C
C      Source File:  JCOBI.SNG        Object File:  DGSPLB.OBJ
C
       SUBROUTINE JCOBI(ND,N,N0,N1,AL,BE,DIF1,DIF2,DIF3,ROOT)
C
C      Purpose:
C          Evaluation of roots and derivatives of Jacobi poly-
C      nomials P(N) (AL,BE).  Machine accuracy 7 D.
C
C      Modifications:  None.
C
C      External References:  None.
C
C      Variable Declarations:
C
       IMPLICIT REAL*4 (A-H,O-Z)
       DIMENSION DIF1(ND),DIF2(ND),DIF3(ND),ROOT(ND)
C
C          Input:
C
C      ND - Dimension of output vectors.
C      N  - Degree of Jacobi polynomial.
C      N0 - X = 0 included? (Y=1, N=0).
C      N1 - X = 1 included? (Y=1, N=0).
C      AL,BE - Values of alpha and beta.
C
C      Output:
C
C      ROOT - Vector containing the N+N0+N1 zeros of
C             the node polynomial.
C      DIF1, DIF2, DIF3 - Vectors containing the first,
C             second and third derivatives of the node
C             polynomial.
C
C      Executable Code
C
C          First, evaluation of coefficients in recursion formulas.
C      Recursion coefficients are stored in DIF1 and DIF2.
       AB=AL+BE
       AD=BE-AL
       AP=BE*AL
       DIF1(1)=(AD/(AB+2.)+1)/2.
       DIF2(1)=0.
       IF (N .LT. 2) GOTO 15
       DO 10 I=2,N
       Z1=I-1
       Z=AB+2.*Z1
       DIF1(I)=(AB*AD/Z/(Z+2.)+1)/2.
       IF (I .NE. 2) GOTO 11
       DIF2(I)=(AB+AP+Z1)/Z/Z/(Z+1.)
```

```
        GOTO 10
 11     Z=Z*Z
        Y=Z1*(AB+Z1)
        Y=Y*(AP+Y)
        DIF2(I)=Y/Z/(Z-1.)
 10     CONTINUE
C
C
C       Root determination by Newton method with suppression of
C       previously determined roots.
C
 15     X=0
        DO 20 I=1,N
 25     XD=0.
        XN=1.
        XD1=0.
        XN1=0.
        DO 30 J=1,N
        XP=(DIF1(J)-X)*XN-DIF2(J)*XD
        XP1=(DIF1(J)-X)*XN1-DIF2(J)*XD1-XN
        XD=XN
        XD1=XN1
        XN=XP
 30     XN1=XP1
        ZC=1.
        Z=XN/XN1
        IF (I .EQ. 1) GOTO 21
        DO 22 J=2,I
 22     ZC=ZC-Z/(X-ROOT(J-1))
 21     Z=Z/ZC
        X=X-Z
        IF (ABS(Z) .GT. 1.E-06) GOTO 25
        ROOT(I)=X
        X=X+0.0001
 20     CONTINUE
C
C
C       Add eventual interpolation points as X=0 and/or X=1.
C
        NT=N+NO+N1
        IF (NO .EQ. 0) GOTO 35
        DO 31 I=1,N
        J=N+1-I
 31     ROOT(J+1)=ROOT(J)
        ROOT(1)=0.
 35     IF (N1 .EQ. 1) ROOT(NT)=1.
C
C
C       Now evaluate derivatives of polynomial.
C
        DO 40 I=1,NT
        X=ROOT(I)
        DIF1(I)=1.
        DIF2(I)=0.
        DIF3(I)=0.
        DO 40 J=1,NT
        IF (J .EQ. I) GOTO 40
        Y=X-ROOT(J)
        DIF3(I)=Y*DIF3(I)+3*DIF2(I)
        DIF2(I)=Y*DIF2(I)+2*DIF1(I)
        DIF1(I)=Y*DIF1(I)
 40     CONTINUE
C
```

RETURN
END

```
C
C
C      Title:   Second-Order EC-Catalytic Mechanism at the RDE.
C                 Calculation of the Kinetic Terms for the
C                     Spline Collocation Solution.
C
C      Author:   J. Nolan
C                                              Date:   12-Mar-87
C      Source File:  KTCDSP.SNG          Object File:  DGSPLB.OBJ
C
       SUBROUTINE KTCDSP(N,NE,NF,PARKIN,DBARP,DBARQ,DBARA,CTBL,
      &               SPLPT,PCNCSA,PCNCS,CMATA,CMAT)
C
C      Purpose:
C
C           This routine calculates the kinetic terms appropriate
C      to a second-order catalytic reaction at an RDE and incorpor-
C      ates them in the systems of transport equations generated by
C      the subroutines RDCDSP and HSCDSP.
C
C      Modifications:   None.
C
C      Variable Declarations:
C
       IMPLICIT REAL*4 (A-H,O-Z)
       DIMENSION PCNCSA(NF),CMATA(NF,NF),PCNCS(NE),CMAT(NE,NE)
C
C           Input:
C
C           N - Order of the collocation polynomial.
C           NE,NF - Correspond to the array dimensions in the
C                   calling program.
C           PARKIN - Kinetic parameter.
C           DBARP,DBARQ,DBARA - Normalized diffusion coefficients
C                   for the respective species.
C           CTBL - Transport boundary layer coefficient.
C           SPLPT - Spline point.
C           PCNCS,PCNCSA - Previous concentrations of species P, Q
C                   and A.
C           CMAT,CMATA - Matrices containing coefficients for trans-
C                   port equations of catalyst couple and substrate.
C
C           Output:
C
C           CMAT,CMATA - Matrices including kinetic terms.
C
       N2=N+2
       CSPLPT=1.-SPLPT
C
       IQOFF=2*N+1
       JQOFF=3*N+4
       FACTR1=PARKIN*(CTBL*SPLPT)**2
       FACTR2=PARKIN*(CTBL*CSPLPT)**2
C
       DO 10 IP1=1,N
           IP2=IP1+N
           IQ1=IP1+IQOFF
           IQ2=IQ1+N
           JQ1=IP1+IQOFF+2
           JQ2=IP1+JQOFF
```

```
C
          TERM=FACTR1*PCNCSA(IP1+1)
          CMAT(IP1,JQ1)=CMAT(IP1,JQ1)+TERM/DBARP
          CMAT(IQ1,JQ1)=CMAT(IQ1,JQ1)-TERM/DBARQ
C
          TERM=FACTR2*PCNCSA(IP1+N2)
          CMAT(IP2,JQ2)=CMAT(IP2,JQ2)+TERM/DBARP
          CMAT(IQ2,JQ2)=CMAT(IQ2,JQ2)-TERM/DBARQ
C
          TERM=FACTR1*PCNCS(JQ1)
          CMATA(IP1,IP1+1)=CMATA(IP1,IP1+1)-TERM/DBARA
C
          TERM=FACTR2*PCNCS(JQOFF+IP1)
          CMATA(IP2,IP1+N2)=CMATA(IP2,IP1+N2)-TERM/DBARA
C
   10     CONTINUE
C
          RETURN
C
          END
```

```
C
C
C
C      Title:   Pseudo-First-Order EC-Catalytic Mechanism at the RDE.
C                 Numerical Solution by Orthogonal Collocation.
C
C      Author:  J. Nolan                          Date:  15-Dec-86
C
C      Source File:  OCECR1.SNG        Object File:  DGSPLB.OBJ
C
       SUBROUTINE OCECR1(N,ND,ROOTS,AMAT,BMAT,PARKIN,DVRAT,DBARP,
      &               DBARQ,CTBL,CRATIO,GRAD)
C
C      Purpose:
C
C           This subroutine uses orthogonal collocation to obtain
C      the steady-state solution to the differential equations
C      describing the pseudo-first-order EC-catalytic mechanism at
C      the RDE.  Formulation of the boundary value problem is
C      based on Eddowes' treatment of the mass-transport-limited
C      case (J. Electroanal Chem., Vol. 159, p.1, 1983).  Imple-
C      mentation of the orthogonal collocation technique follows
C      J. Villadsen and M.L. Michelsen, "Solution of Differential
C      Equation Models by Polynomial Approximation", Englewood
C      Cliffs, N.J.: Prentice-Hall, Inc., 1978.
C           The routine returns the surface concentration gradient
C      given a value for the kinetic parameter.  Note that the
C      A and B matrices must be supplied by the calling program.
C
C      Modifications:  None.
C
C      External References:
C
C          Fn/Sr             Src File         Obj File
C
C      Subroutine RDECDE     RDECDE.SNG      DGSPLB.OBJ
C      Subroutine CONSL1     CONSL1.SNG      DGSPLB.OBJ
C      Subroutine CSCGP      CSCGP.SNG       DGSPLB.OBJ
C
C      Variable Declarations:
C
       IMPLICIT REAL*4 (A-H,O-Z)
       DIMENSION ROOTS(ND),AMAT(ND,ND),BMAT(ND,ND),
      &          CONCS(48),BOUND(48),CMAT(48,48)
       EQUIVALENCE (CONCS(1),BOUND(1))
C
C          Input:
C
C          N - Order of the collocation polynomial (N<=24).
C          NR - Number of simultaneous equations (=2*N).
C          DBARP - Normalized diffusion coefficient of species P.
C          DBARQ - Normalized diffusion coefficient of species Q.
C          DVRAT - Ratio of the diffusion coefficient to kinematic
C                  viscosity (=1/Sc).
C          CRATIO - Concentration ratio (P/Q) at Z = 0.
C          PARKIN - Kinetic parameter.
C          CTBL - Transport boundary layer coefficient.
C
C          Output:
C
C          CMAT - Matrix containing the system of simultaneous
C                  equations generated.
```

```
C          BOUND - Vector containing boundary conditions.
C          CONCS -- Vector containing concentrations at the
C               collocation points. (Equivalence'd to BOUND.).
C          GRAD - Surface concentration gradient.
C
C     Data Statements:
C
      NE=48
      NR=2*N
C
C          (NE=48 corresponds to the simultaneous equation array
C               dimensions.)
C
C     Executable Code
C
C     Generate matrix of simultaneous equations for the concen-
C     trations of species P and Q at the collocation points.
C
      CALL RDECDE(N,ND,NE,ROOTS,AMAT,BMAT,DVRAT,DBARP,DBARQ,
     &          CRATIO,CTBL,CMAT,BOUND)
C
C     Include the kinetic term in the system of equations.
C
      TERM=PARKIN*CTBL**2
C
      DO 10 I=1,N.
          IN=I+N
          CMAT(I,IN)=CMAT(I,IN)+(TERM/DBARP)
          CMAT(IN,IN)=CMAT(IN,IN)-(TERM/DBARQ)
   10 CONTINUE
C
C     Solve for concentrations at the collocation points.
C
      CALL CONSL1(N,NE,NR,CMAT,CONCS)
C
C     Calculate concentration gradient of species P at Z = 0.
C
      CALL CSCGP(N,ND,NE,DBARP,DBARQ,CRATIO,AMAT,CONCS,CP0,GRAD)
C
      RETURN
C
      END
```

```
C
C
C       Title:   Second-Order EC-Catalytic Mechanism at the RDE.
C                Numerical Solution by Orthogonal Collocation.
C
C       Author:   J. Nolan                              Date:   07-Jan-87
C
C       Source File:   OCECR2.SNG         Object File:   DGSPLB.OBJ
C
        SUBROUTINE OCECR2(N,PARKIN,DBARP,DBARQ,DBARA,CBARA,SSQRCM,
       &              CMAT,BOUND,CMATA,BOUNDA,NITS,CNCS)
C
C       Purpose:
C
C            This subroutine uses orthogonal collocation to obtain
C       the steady-state solution to the differential equations
C       describing the second-order EC-catalytic mechanism at
C       the RDE.  Formulation of the boundary value problem is
C       based on Eddowes' treatment of the mass-transport-limited
C       case (J. Electroanal Chem., Vol. 159, p.1, 1983).  Imple-
C       mentation of the orthogonal collocation technique follows
C       J. Villadsen and M.L. Michelsen, "Solution of Differential
C       Equation Models by Polynomial Approximation", Englewood
C       Cliffs, N.J.: Prentice-Hall, Inc., 1978.
C            The subroutine returns the concentrations of the parti-
C       ating species at the collocation points given values for
C       for the kinetic parameter, the bulk concentration of sub-
C       strate species A and the normalized diffusion coefficients
C       species P, Q and A.  Simple iteration is used to solve the
C       nonlinear set of equations describing the mechanism.  To
C       conserve storage and to speed execution, the equations for
C       the substrate are handled independently of those for the
C       catalyst couple.
C            Note that, with the exception of the first call, the
C       concentrations found in the preceding call are used as the
C       starting point for the iterative procedure.
C
C       Modifications:   None.
C
C       External References:
C
C           Fn/Sr             Src File         Obj File
C
C       Subroutine ARRAY      ARRAY.FOR        MATLIB.OBJ
C       Subroutine SIMQ       SIMQ.FOR         MATLIB.OBJ
C
C       Variable Declarations:
C
        IMPLICIT REAL*4 (A-H,O-Z)
        DIMENSION CNCS(36),CMAT(36,36),DMAT(1296),CNCSA(18),
       &          CMATA(18,18),DMATA(324),BOUND(36),BOUNDA(18),
       &          PCNCS(36),PCNCSA(18)
C
C       Input:
C
C       N - Order of the collocation polynomial (N<=18).
C       PARKIN - Kinetic parameter.
C       DBARP - Normalized diffusion coefficient of species P.
C       DBARQ - Normalized diffusion coefficient of species Q.
C       DBARA - Normalized diffusion coefficient of species A.
C       CBARA - Concentration of species A normalized to that
```

```
C          of P.
C          SSQRCM - Convergence criterion, defined as the sum of
C                  the squares of the corrections between succesive
C                  iterations.
C          CTBL - Transport boundary coefficient (fixed at 3.6096).
C          CMAT,CMATA - Matrices containing the system of simul-
C                  taneous equations for species P, Q and A.
C          BOUND,BOUNDA - Vectors containing constant terms for
C                  the systems of linear equations.
C
C       Output:
C
C          DMAT,DMATA - Packed vector equivalents of CMAT,CMATA.
C          CNCS - Vector containing concentrations of species P
C                  and Q at the collocation points.
C          NITS - Number of iterations required.
C
C       Data Statements:
C
       DATA  CTBL,PCNCS,PCNCSA /3.6096,36*0.,18*0./
C
C       Executable Code
C
       NR=2*N
       NITS=1
       NE=36
       NF=18
C
C
C       Regenerate the packed coefficient matrices and the boundary
C       vectors.
C
   10  CALL ARRAY(2,NR,NR,NE,NE,DMAT,CMAT)
       CALL ARRAY(2,N,N,NF,NF,DMATA,CMATA)
C
       DO 20 I=1,N
           IN=I+N
           CNCS(I)=BOUND(I)
           CNCS(IN)=BOUND(IN)
           CNCSA(I)=BOUNDA(I)
   20  CONTINUE
C
C       Include the kinetic terms.
C
       CONST=PARKIN*CTBL**2
C
       DO 30 I=1,N
           II=(I-1)*N+I
           IIN=(I+N-1)*NR+I
           ININ=IIN+N
           TERM=CONST*PCNCSA(I)
           DMAT(IIN)=DMAT(IIN)+TERM/DBARP
           DMAT(ININ)=DMAT(ININ)-TERM/DBARQ
           DMATA(II)=DMATA(II)-CONST*PCNCS(I+N)/DBARA
   30  CONTINUE
C
C       Solve for concentrations at the collocation points.
C
       CALL SIMQ(DMAT,CNCS,NR,KS)
       IF (KS.EQ.1) GOTO 99
       CALL SIMQ(DMATA,CNCSA,N,KS)
```

```
      IF (KS.EQ.1) GOTO 99
C
C     Determine the      of the squared corrections and save
C     current concentrations.
C
      SSQRC=0.
      DO 40 I=1,N
          IN=I+N
          SSQRC=SSQRC+(PCNCSA(I)-CNCSA(I))**2
          PCNCSA(I)=CNCSA(I)
          SSQRC=SSQRC+(PCNCS(I)-CNCS(I))**2
          PCNCS(I)=CNCS(I)
          SSQRC=SSQRC+(PCNCS(IN)-CNCS(IN))**2
          PCNCS(IN)=CNCS(IN)
   40 CONTINUE
C
      IF (SSQRC.LE.SSQRCM) GO TO 50
          NITS=NITS+1
          GOTO 10
C
   50 RETURN
C
   99 WRITE(7,999)
      STOP
C
  999 FORMAT('0','Singular matrix encountered in subroutine OCECR2
     &.',/)
      END
```

```
C
C
C      Title:   Second-Order EC-Catalytic Mechanism at the RDE.
C               Transport Equations for the Catalyst Couple
C                         by Spline Collocation.
C
C      Author:  J. Nolan                        Date:  11-Mar-87
C
C      Source File: RDCDSP.SNG      Object File:  DGSPLB.OBJ
C
       SUBROUTINE RDCDSP(N,ND,NE,ROOTS,AMAT,BMAT,DVRAT,DBARP,DBARQ,
      &            CRATIO,CTBL,SPLPT,CMAT,BOUND)
C
C      Purpose:
C
C           This routine generates the system of simultaneous
C      equations corresponding to the spline collocation solution
C      of the convective-diffusion equations for a redox couple
C      at a rotating disk electrode.  The interval over which
C      the problem is defined is subdivided into two intervals
C      at the spline point SPLPT.
C
C      Modifications:  None.
C
C      Variable Declarations:
C
       IMPLICIT REAL*4 (A-H,O-Z)
       DIMENSION ROOTS(ND),AMAT(ND,ND),BMAT(ND,ND),BOUND(NE),
      &          CMAT(NE,NE)
C
C          Input:
C
C
C          N - Order of the collocation polynomial.
C          NR - Number of simultaneous equations (=4*N+4)
C          ND,NE - Correspond to the array dimensions in the
C               calling program.
C          ROOTS - Collocation points.
C          AMAT,BMAT - Discretization matrices containing the
C               coefficients for the first and second deriv-
C               atives of the concentration profile.
C          CRATIO - Concentration ratio (P/Q) at X = 0.
C          DVRAT - Ratio of diffusion coefficient to kinematic
C               viscosity.
C          DBARP - Normalized diffusion coefficient of species P.
C          DBARQ - Normalized diffusion coefficient of species Q.
C          CTBL - Transport boundary coefficient.
C          SPLPT - Spline point.
C
C          Output:
C
C          CMAT - Matrix containing the system of simultaneous
C               equations generated in terms of unknown conc-
C               entrations at the collocation points.
C          BOUND - Vector containing constants corresponding to
C               the boundary at Z=1.
C
C      Define statement function for axial velocity and parameters
C      for same.
C
       AXVEL(X,C1,C2)=CTBL3*(5.1023E-01+X*(C1+C2*X))*X**2
C
```

```
      DVR3P=1./3.
      DVR3Q=(DVRAT*DBARQ)**DVR3P
      DVR3P=(DVRAT*DBARP)**DVR3P
      C1P=-1.2032*DVR3P
      C2P=1.3375*DVR3P**2
      C1Q=-1.2032*DVR3Q
      C2Q=1.3375*DVR3Q**2
      CTBL3=CTBL**3
C
      N1=N+1
      N2=N+2
      NR=4*N+4
      CSPLPT=1.-SPLPT
C
C
C     Zero simultaneous equation matrix.
C
      DO 10 I=1,NR
          DO 10 J=1,NR
              CMAT(I,J)=0.
 10   CONTINUE
C
C
C     Compute coefficients for first sub-interval.
C
      IOFF=2*N+1
      DO 20 IP=1,N
          I1=IP+1
          IQ=IP+IOFF
          BOUND(IP)=0.
          BOUND(IQ)=0.
          ROOT=ROOTS(I1)*SPLPT
          AXVELP=SPLPT*AXVEL(ROOT,C1P,C2P)/DBARP
          AXVELQ=SPLPT*AXVEL(ROOT,C1Q,C2Q)/DBARQ
          DO 20 JP=1,N2
              JQ=JP+IOFF+1
              CMAT(IP,JP)=BMAT(I1,JP)+AXVELP*AMAT(I1,JP)
              CMAT(IQ,JQ)=BMAT(I1,JP)+AXVELQ*AMAT(I1,JP)
 20   CONTINUE
C
C
C     Ditto for second sub-interval.
C
      IOFF=3*N+1
      DO 30 I=1,N
          I1=I+1
          IP=I+N
          IQ=I+IOFF
          ROOT=ROOTS(I1)*CSPLPT+SPLPT
          AXVELP=CSPLPT*AXVEL(ROOT,C1P,C2P)/DBARP
          AXVELQ=CSPLPT*AXVEL(ROOT,C1Q,C2Q)/DBARQ
          BOUND(IP)=-BMAT(I1,N2)-AXVELP*AMAT(I1,N2)
          BOUND(IQ)=0.
          DO 30 J=1,N1
              JP=J+N1
              JQ=IOFF+J+2
              CMAT(IP,JP)=BMAT(I1,J)+AXVELP*AMAT(I1,J)
              CMAT(IQ,JQ)=BMAT(I1,J)+AXVELQ*AMAT(I1,J)
 30   CONTINUE
C
C
C     Continuity conditions for dP/dZ and dQ/dZ at the spline point.
C
      NP1=2*N+1
```

```
      IPSP=N+2
      FACTR=SPLPT/CSPLPT
      BOUND(NP1)=AMAT(1,N2)*FACTR
C
      NQ1=4*N+2
      IQSP=3*N+4
      IQ0=2*N+3
      BOUND(NQ1)=0.
C
      DO 40 JP1=1,N+1
          JP2=IPSP+JP1-1
          JQ1=IQ0+JP1-1
          JQ2=IQSP+JP1-1
          CMAT(NP1,JP1)=AMAT(N2,JP1)
          CMAT(NP1,JP2)=-AMAT(1,JP1)*FACTR
          CMAT(NQ1,JQ1)=AMAT(N2,JP1)
          CMAT(NQ1,JQ2)=-AMAT(1,JP1)*FACTR
  40  CONTINUE
C
      CMAT(NP1,IPSP)=CMAT(NP1,IPSP)+AMAT(N2,N2)
      CMAT(NQ1,IQSP)=CMAT(NQ1,IQSP)+AMAT(N2,N2)
C
C     Boundary conditions at Z = 0.
C
      NPQ1=4*N+3
      CMAT(NPQ1,1)=1.
      CMAT(NPQ1,IQ0)=-CRATIO
      BOUND(NPQ1)=0.
C
      NPQ1=NPQ1+1
      DO 50 JP=1,N2
          JQ=IQ0+JP-1
          CMAT(NPQ1,JP)=AMAT(1,JP)*DBARP
          CMAT(NPQ1,JQ)=AMAT(1,JP)*DBARQ
  50  CONTINUE
C
      BOUND(NPQ1)=0.
C
      RETURN
      END
```

```
C
C
C     Title:  Transport Equations for a Redox Couple at the RDE.
C             Numerical Solution by Orthogonal Collocation.
C
C     Author:  J. Nolan                           Date:  06-Oct-86
C
C     Source File:  RDECDE.SNG        Object File:  DGSPLB.OBJ

      SUBROUTINE RDECDE(N,ND,NE,ROOTS,AMAT,BMAT,DVRAT,DBARP,DBARQ,
     &             CRATIO,CTBL,TMAT,BOUND)
C
C     Purpose:
C
C          This routine generates the system of simultaneous
C     equations corresponding to the orthogonal collocation
C     solution of the convective-diffusion equation for a single
C     redox couple at a rotating disk electrode.  It incorporates
C     the extended form of the equation for axial velocity and
C     provision is made for inequalities in the diffusion
C     coefficients of the two members of the couple.  The interval
C     over which the boundary value problem is defined can be
C     varied through the parameter CTBL.
C
C     Modifications:  None.
C
C     Variable Declarations:

      IMPLICIT REAL*4 (A-H,O-Z)
      DIMENSION ROOTS(ND),AMAT(ND,ND),BMAT(ND,ND),BOUND(NE),
     &             TMAT(NE,NE)
C
C     Input:
C
C
C     N - Order of the collocation polynomial.
C     NT - Number of collocation points (=N+2).
C     NR - Number of simultaneous equations (=2N).
C     ND,NE - Correspond to the array dimensions in the
C             calling program.
C     ROOTS - Collocation points.
C     AMAT,BMAT - Discretization matrices containing the
C             coefficients for the first and second deriv-
C             atives of the concentration profile.
C     CRATIO - Concentration ratio (P/Q) at X = 0.
C     DVRAT - Ratio of diffusion coefficient to kinematic
C             viscosity.
C     DBARP - Normalized diffusion coefficient of species P.
C     DBARQ - Normalized diffusion coefficient of species Q.
C     CTBL - Transport boundary coefficient.
C
C     Output:
C
C     TMAT - Matrix containing the system of simultaneous
C             equations generated in terms of unknown conc-
C             entrations at the collocation points.
C     BOUND - Vector containing constants corresponding to
C             the boundary at X=1.
C
C     Define statement function for axial velocity and parameters
C     for same.
C
```

```
      AXVEL(X,C1,C2)=CTBL3*(5.1023E-01+X*(C1+C2*X))*X**2
C
      DVR3P=1./3.
      DVR3Q=(DVRAT*DBARQ)**DVR3P
      DVR3P=(DVRAT*DBARP)**DVR3P
      C1P=-1.2032*DVR3P
      C2P=1.3375*DVR3P**2
      C1Q=-1.2032*DVR3Q
      C2Q=1.3375*DVR3Q**2
      CTBL3=CTBL**3
C
C
C     Generate a system of 2N simultaneous equations in terms
C     of the 2N concentrations of species P and Q at the collo-
C     cation points.  The equations describing the boundary
C     conditions at Z = 0 (flux balance and P/Q concentration
C     ratio) have been included thereby eliminating the variables
C     representing the unknown concentrations of P and Q at Z = 0.
C
      B0=AMAT(1,1)*(CRATIO*DBARP+DBARQ)
      NT=N+2
C
      DO 10 I=1,N
         I1=I+1
         IN=I+N
         AXVELP=AXVEL(ROOTS(I1),C1P,C2P)/DBARP
         AXVELQ=AXVEL(ROOTS(I1),C1Q,C2Q)/DBARQ
         B1P=(BMAT(I1,1)+AXVELP*AMAT(I1,1))*CRATIO/B0
         BOUND(I)=B1P*DBARP*AMAT(1,NT)-(BMAT(I1,NT)+AXVELP*AMAT
     &            (I1,NT))
         B1Q=(BMAT(I1,1)+AXVELQ*AMAT(I1,1))/B0
         BOUND(IN)=B1Q*DBARP*AMAT(1,NT)
         DO 10 J=1,N
            J1=J+1
            JN=J+N
            B2P=B1P*AMAT(1,J1)
            TMAT(I,J)=AXVELP*AMAT(I1,J1)+BMAT(I1,J1)-DBARP*B2P
            TMAT(I,JN)=-DBARQ*B2P
            B2Q=B1Q*AMAT(1,J1)
            TMAT(IN,J)=-B2Q*DBARP
            TMAT(IN,JN)=AXVELQ*AMAT(I1,J1)+BMAT(I1,J1)-DBARQ*B2Q
10    CONTINUE
C
      RETURN
      END
```

```
C
C
C      Title:  Consecutive Electron Transfer with Reproportionation.
C              Calculation of Surface Concentration Gradients.
C
C      Author:  J. Nolan                        Date:  28-May-88
C
C      Source File:  SCGRD1.SNG        Object File:  DGSPLB.OBJ
C
       SUBROUTINE SCGRD1(N,ND,NE,DBARP,DBARQ,DBARR,AMAT,CONCS,GRADP,
      &            GRADQ,GRADR,CRO)
C
C      Purpose:
C
C          This routine calculates the surface concentration of
C      species R and the surface concentration gradients of species
C      P, Q and R given their concentrations at the interior collo-
C      cation points.
C
C      Modifications:  None.
C
C      Variable Declarations:
C
       IMPLICIT REAL*4 (A-H,O-Z)
       DIMENSION AMAT(ND,ND),CONCS(NE)
C
C          Input:
C
C
C          N - Order of the collocation polynomial.
C          ND,NE - Correspond to the array dimensions in the
C                  calling program.
C          DBARP - Normalized diffusion coefficient of species P.
C          DBARQ - Normalized diffusion coefficient of species Q.
C          DBARR - Normalized diffusion coefficient of species R.
C          CONCS - Concentrations of P, Q and R at the N interior
C                  collocation points.
C          AMAT - Coefficient matrix for the first derivative
C                  of concentration with respect to distance.
C
C          Output:
C
C          CRO - Concentration of species R at Z = 0.
C          GRADP - Concentration gradient of species P at Z = 0.
C          GRADQ - Concentration gradient of species Q at Z = 0.
C          GRADR - Concentration gradient of species R at Z = 0.
C
C      Executable Code
C
C      Calculate the surface concentration of species R.
C
       NT=N+2
       CRO=0.
       DO 10 J=1,N
          J1=J+1
          JN=J+N
          JNN=JN+N
          CRO=CRO+AMAT(1,J1)*(DBARP*CONCS(J)+DBARQ*CONCS(JN)+
      &          DBARR*CONCS(JNN))
   10  CONTINUE
       CRO=(-CRO-AMAT(1,NT)*DBARP)/DBARR/AMAT(1,1)
C
```

```
C      Calculate the surface concentration gradients.
C
       GRADP=0.
       GRADQ=0.
       GRADR=CR0*AMAT(1,1)
       DO 20 J=1,N
           J1=J+1
           JN=J+N
           JNN=JN+N
           GRADP=GRADP+AMAT(1,J1)*CONCS(J)
           GRADQ=GRADQ+AMAT(1,J1)*CONCS(JN)
           GRADR=GRADR+AMAT(1,J1)*CONCS(JNN)
  20   CONTINUE
C
       GRADP=GRADP+AMAT(1,NT)
C
       RETURN
C
       END
```

```
C
C
C     Title:  Second-Order EC-Catalytic Mechanism at the RDE.
C             Surface Concentration of the Substrate.
C
C     Author:  J. Nolan                    Date:  26-Feb-87
C
C     Source File:  SCNCA.SNG      Object File:  DGSPLB.OBJ
C
      SUBROUTINE SCNCA(N,ND,NF,AMAT,CBARA,CONCSA,CAO)
C
C     Purpose:
C
C        This routine evaluate the surface concentrations for
C     the substrate given its concentrations at the interior
C     collocation points.
C
C     Modifications:  None.
C
C     Variable Declarations:
C
      IMPLICIT REAL*4 (A-H,O-Z)
      DIMENSION AMAT(ND,ND),CONCSA(NF)
C
C     Input:
C
C        AMAT  - Discretization matrix for first derivative of
C                the collocation polynomial.
C        CBARA - Concentration of A at Z = 1 (Excess factor).
C        CNCSA - Concentration of A at collocation points.
C
C     Output:
C
C        CAO  - Concentration of A at Z = 0.
C
C     Executable Code
C
      CAO=0.D0
      DO 10 J=1,N
         J1=J+1
         CAO=CAO+AMAT(1,J1)*CONCSA(J)
 10   CONTINUE
      CAO=(-AMAT(1,N+2)*CBARA-CAO)/AMAT(1,1)
C
      RETURN
C
      END
```

```fortran
C
C
C     Title:  Second-Order EC-Catalytic Mechanism at the RDE.
C        Surface Concentrations of the Catalyst Species P and Q.
C
C     Author:  J. Nolan,                      Date: 26-Feb-87
C
C     Source File:  SCNCPQ.SNG      Object File:  DGSPLB.OBJ
C
      SUBROUTINE SCNCPQ(N,ND,NE,AMAT,DBARP,DBARQ,CRATIO,CONCS,
     &                  CPO,CQO)
C
C     Purpose:
C
C        This routine evaluate the surface concentrations for
C     species P and Q given their concentrations at the interior
C     collocation points.
C
C     Modifications:  None.
C
C     Variable Declarations:
C
      IMPLICIT REAL*4 (A-H,O-Z)
      DIMENSION AMAT(ND,ND),CONCS(NE)
C
C     Input:
C
C        AMAT - Discretization matrix for first derivative of
C           collocation polynomial.
C        DBARP,DBARQ - Dimensionless diffusion coefficients
C           for P and Q.
C        CRATIO - Concentration ratio of P and Q at Z = 0.
C        CNCS - Concentrations of P and Q at the collocation
C           points.
C
C     Output:
C
C        CPO,CQO - Concentrations of P and Q at Z = 0.
C
C     Executable Code
C
      NT=N+2
      CPO=0.D0
      DO 10 J=1,N
         J1=J+1
         JN=J+N
         CPO=CPO+AMAT(1,J1)*(DBARP*CONCS(J)+DBARQ*CONCS(JN))
   10 CONTINUE
      CPO=CPO+AMAT(1,NT)*DBARP
      CPO=-CRATIO*CPO/(AMAT(1,1)*(CRATIO*DBARP+DBARQ))
C
      CQO=CPO/CRATIO
C
      RETURN
C
      END
```